

University of Groningen

Type VII collagen in the intraocular environment

Wullink, Bart

IMPORTANT NOTE: You are advised to consult the publisher's version (publisher's PDF) if you wish to cite from it. Please check the document version below.

Document Version

Publisher's PDF, also known as Version of record

Publication date:

2019

[Link to publication in University of Groningen/UMCG research database](#)

Citation for published version (APA):

Wullink, B. (2019). *Type VII collagen in the intraocular environment*. Rijksuniversiteit Groningen.

Copyright

Other than for strictly personal use, it is not permitted to download or to forward/distribute the text or part of it without the consent of the author(s) and/or copyright holder(s), unless the work is under an open content license (like Creative Commons).

The publication may also be distributed here under the terms of Article 25fa of the Dutch Copyright Act, indicated by the "Taverne" license. More information can be found on the University of Groningen website: <https://www.rug.nl/library/open-access/self-archiving-pure/taverne-amendment>.

Take-down policy

If you believe that this document breaches copyright please contact us providing details, and we will remove access to the work immediately and investigate your claim.

Downloaded from the University of Groningen/UMCG research database (Pure): <http://www.rug.nl/research/portal>. For technical reasons the number of authors shown on this cover page is limited to 10 maximum.

Type VII collagen

in the intraocular environment



Bart Wullink

COLOPHON

Layout and cover design: Design Your Thesis, www.designyourthesis.com
Printing: Ridderprint B.V., www.ridderprint.nl
ISBN: 978-94-6375-414-9

Printed on recycled paper

Cover: Type VII collagen molecules, schematically depicted as hooked shapes in varying thickness, are dispersed (but arranged) to form an eye.

The printing of this thesis was financially supported by the the Prof. Mulder Stichting, the Graduate School of Medical Sciences, the Kolff Institute, the University of Groningen, Stichting Blindenhulp, Rotterdamse Stichting Blindenbelangen.

Copyright © 2019 by Bart Wullink. All rights reserved. Any unauthorized reprint or use of this material is prohibited. No part of this thesis may be reproduced, stored or transmitted in any form or by any means, without written permission of the author or, when appropriate, of the publishers of the publications.



rijksuniversiteit
 groningen

Type VII collagen in the intraocular environment

Proefschrift

ter verkrijging van de graad van doctor aan de
Rijksuniversiteit Groningen
op gezag van de
rector magnificus prof. dr. E. Sterken
en volgens besluit van het College voor Promoties.

De openbare verdediging zal plaatsvinden op

maandag 8 juli 2019 om 9.00 uur

door

Bart Wullink

geboren op 2 oktober 1980
te Ermelo

Promotor

Prof. dr. J.M.M. Hooymans

Copromotores

Dr. L.I. Los

Dr. T.G. van Kooten

Dr. H.H. Pas

Beoordelingscommissie

Prof. dr. R.A. Bank

Prof. dr. M.J. Jager

Prof. dr. S.M. Imhof

ABBREVIATIONS

3H	triple helix collagen domain
aa	amino acid
ACD	anterior chamber depth
AEC	3-amino-9-ethylcarbazole
AF	anchoring fibril(s)
BM(s)	basement membrane(s)
BSA	bovine serum albumin
CA	corpora amylacea
CD-31	endothelial cell marker
COL7A1	gene encoding for Col VII
Col VII	type VII collagen
D	diopter
DAPI	2-(4-Amidinophenyl)-6-indolecarbamidine dihydrochloride
DDEB	dominant dystrophic epidermolysis bullosa
EB	epidermolysis bullosa
EBS	epidermolysis bullosa simplex
FITC	fluorescein isothiocyanate
FN3	fibronectin domain 3
GCL	ganglion cell layer
GFAP	glial fibrillary acidic protein
ILM	inner limiting membrane
IPL	inner plexiform layer
INL	inner nuclear layer
iTEM	immuno TEM
JEB	junctional epidermolysis bullosa
kDa	kilodalton
LM	light microscopy
mRNA	messenger RNA
NC	negative control

NC-1	non-collagenous domain 1
NFL	nerve fiber layer
NPE	non-pigmented epithelium (of ciliary body)
OCT	optical coherence tomography
OD	oculus dexter (right eye)
ONL	outer nuclear layer
OPL	outer plexiform layer
Optos	ultra-widefield scanning laser ophthalmoscope
OS	oculus sinister (left eye)
OU	oculo uterique (both eyes)
PAS	periodic acid-Schiff
PB(S)	phosphate buffer(ed saline)
PE	pigmented epithelium (of ciliary body)
PKP	penetrating keratoplasty
PR	photoreceptors
RAMPO	rabbit-anti-mouse peroxidase
RDEB	recessive dystrophic epidermolysis bullosa
RPE	retinal pigmented epithelium
SARPO	swineanti-rabbit peroxidase
SMA	smooth muscle actin
Sup Info	supporting information
T8100	glycol methacrylate resin
TBS	Tris buffered saline
TEM	transmission electron microscopy
TRITC	tetramethyl rhodamine isothiocyanate
TTBS	TBS containing 0.05% Tween-20
vb	vitreous body
vWFA	von Willebrand factor type A
WOD	Wet op Orgaandonatie
UMCG	University Medical Center Groningen

TABLE OF CONTENTS

Chapter 1	General introduction	9
Chapter 2	Type VII collagen expression in the human vitreoretinal interface, corpora amylacea and inner retinal layers	31
Chapter 3	Type VII Collagen in the Human Accommodation System: Expression in Ciliary Body, Zonules, and Lens Capsule	65
Chapter 4	Type VII Collagen in the Ocular Vasculature	93
Chapter 5	Recessive Dystrophic Epidermolysis Bullosa: type VII collagen deficiency is not associated with intraocular defects	129
Chapter 6	General Discussion	159
Chapter 7	Summary	191
Chapter 8	Nederlandse samenvatting (Dutch summary)	197
	Dankwoord (Acknowledgements)	203
	Curriculum vitae	209



1

Chapter 1

General introduction

This thesis is about fundamental and observational investigations on type VII collagen (Col VII) expression in human ocular tissues. Predominantly immunohistochemical data are presented in such a way, that these data can be used and interpreted by its readers, including clinicians. In order to optimize the data presentation, it is appropriate to provide selected background information on the biomolecular aspects of collagens, in particular Col VII. The molecular aspects of this particular collagen molecule are described in relation to the binding properties of the various antibodies to the collagen in tissues and the lysates of those tissues.

1.0 COLLAGENS

1.1 Collagens are ubiquitous and versatile proteins

Collagens are the bulk construction molecules of the human body: they provide the 3D framework for our tissues and organs, and make up about 30% of the human dry weight. Collagens may serve as a tissue glue, but also perform biochemical signaling and organizing functions within the extracellular matrix. Collagens derive from procollagens, which are made in the endoplasmic reticulum, transported to the Golgi, and from there are secreted into the extracellular matrix. To date, 29 types of collagen have been described in man, each with different functional characteristics. The versatility in function of a collagen is not only derived from its molecular composition, but also its supramolecular assembly. The differences in molecular composition of a collagen type dictate how it functions, and thus where it is located/needed.¹ For example, the hierarchy of collagens in tendons and muscle warrants tissue strength and flexibility, while the inclusion of minerals provides stiffness to bones. In cornea, the collagen structural hierarchy allows not only for strength, but also transparency.

1.2 The general composition of a collagens

The hallmark of the collagens (as a protein group) lies in their amino acid sequence; they all consist of a repeating amino acid motif Glycin-X-Y, where X and Y may be any amino acid, but are often proline and hydroxyproline, respectively. These sequences thus form a helical polymer: the α -chain. Typically, three α -chains will combine into a larger structure, a right-handed triple helix, by gyrating around one another while maintaining their glycine amino acid residues at their core; the collagen molecule (**Figure 1**).

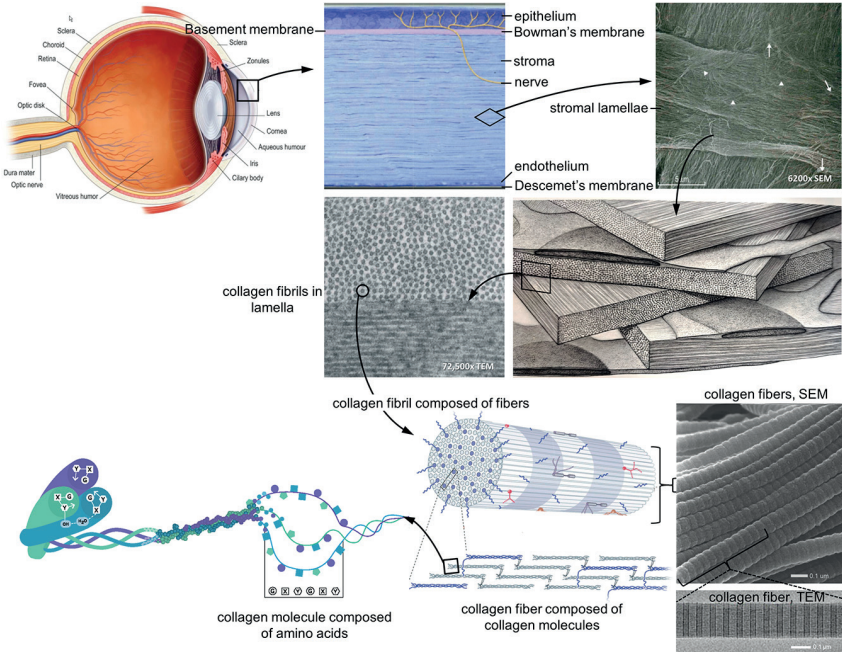


FIGURE 1. Collagen fibrils as aggregates of collagen fibers, and their visualization by electron microscopy. Schematic, Scanning (SEM) and transmission (TEM) electron microscopic representations of corneal collagen fibrils to their ultimate amino acid composition. *Adapted from Adler's Physiology of the eye, 11th edition, Elsevier Saunders, 2011 & Hogan et al. Histology of the human eye, Saunders, 1971.*

Beside this triple helix, there are also non-collagenous parts to a whole collagen molecule, such as a carboxy and amino terminal domain. The various parts of a collagen molecule may allow for interaction with adjacent collagens of the same type. In some collagen types this interaction may result in fiber formation, while in others it may lead to aggregation into larger structures: the fibrils. Alternatively, networks may be formed by some collagen types.

1.3 α -Chain variance provides diversity within collagen fibers: the isoform

The three α -chains that form the triple helix may be identical (forming a homotrimeric collagen molecule) while in others, the α -chains may have differences in their amino-acid sequences (heterotrimer). Heterotrimers provide a collagen type with additional types, or isoforms, that may have additional biological functionalities.

2.0 BASEMENT MEMBRANES

2.1 Basement membranes: an example of collagen isoform variation

Basement membranes (BMs) are the acellular protein 'sheets' that delineate tissue boundaries. These specialized extracellular matrix protein complexes provide an adhesive scaffold for the cells of epithelia, endothelia, and parenchymal cells, hereby separating such cells from surrounding mesenchyme/connective tissue. Such compartmentalization allows for different organs to be formed, but also for guided morphogenesis and tissue repair. Because of the varying protein composition of BMs, BMs are able to influence their adjacent tissues by mediating cell signaling events, and alter cellular behavior through their tissue-specific composition and structure. For example, the BM of blood vessels is needed for ongoing stability and elasticity of the blood vessels, while the lens capsule -essentially a basement membrane- reshapes the lens after each accommodation. Although the retinal BM (inner limiting membrane, ILM) separates the stromal vitreous from neuroretinal epithelium, it appears not to be essential post-partum since the stromal vitreous and ILM may be removed in vitrectomy without serious consequences.^{2, 3, 4} The basement membrane zone of the skin and cornea is, amongst other things, designed to withstand the mechanical forces received from the environment. The dermal-epidermal BM does so by the aid of a multitude of proteins, one of which is the subject of this thesis: Col VII.

2.2 Variation of α -chain combinations dictates BM composition per tissue

The tissue-specific composition of a BM is derived from the 178 distinct BM proteins that may associate around a network of type IV collagen heterotrimers.^{4, 5} The Col IV network is regarded as the foundation of all BMs, but this network may also vary in composition per tissue. There are six different Col IV α -chains that may contribute to the network. But although 3 α -chains are needed for a stable Col IV molecule, not all α -chain combinations occur. There are typical heterodimer combinations throughout the body, of which the typical chain combinations are $[\alpha1_2 + \alpha2]$, $[\alpha3 + \alpha4 + \alpha5]$, and $[\alpha5_2 + \alpha6]$ (**Figure 2**).⁶

In ocular BMs, the chain combinations that are mainly found are $\alpha1$ with $\alpha2$ chains, such as in retinal blood vessels and the lens capsule. The inner basement membrane of the retinal Müller cells (inner limiting membrane), however, contains mainly $\alpha3$ - $\alpha4$ - $\alpha5$ chain combinations.^{7, 8} The adult human corneal epithelial BM contains $\alpha3$ - $\alpha5$ chains at its central area, whereas the limbal BM contains mainly $\alpha1$ - $\alpha2$ and $\alpha5$ chains. The latter example suggests a 'horizontal' isoform differentiation within a tissue. The Descemet's

membrane was reported to have a 'vertical' isoform differentiation, with $\alpha 1$ - $\alpha 2$ in its stromal face, and $\alpha 3$ - $\alpha 5$ on its endothelial face.⁹ There may even be an isoform differentiation of a tissue in time, since infant central corneal epithelial BM changed from $\alpha 1$ - $\alpha 2$ chain to $\alpha 3$ - $\alpha 4$ chain dominance after age 3 years.¹⁰ At their Descemet's membrane, $\alpha 1$ - $\alpha 6$ chains were mainly found on the stromal and endothelial face, but remained only on the endothelial face upon reaching adulthood.¹⁰ Apart from Col IV, other BM associated proteins may also vary per tissue/organ: specific isoforms exist of the fundamental components laminin, nidogen and perlecan. Such proteins are often restricted temporally and spatially in their expression, in correspondence to the needs of the tissue.¹¹

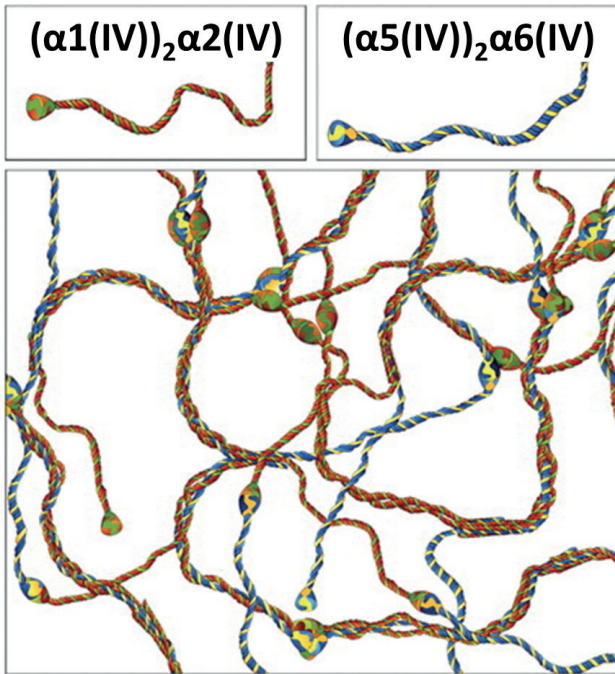


FIGURE 2. Formation of the type IV collagen network at the dermo-epidermal basement membrane zone. The isoforms $\alpha 1$ with $\alpha 2$, and $\alpha 5$ with $\alpha 6$ require end-to-end interactions between their C-terminal globular NC1 domains (*pinheads*) and interactions through their tails (N-terminal 7S domains). The lateral aggregation and twisting of these collagenous domains provide a tightly entangled collagen IV-network. *Adapted from Behrens DT, Villone D, Koch M, et al, J Biol Chem. 2012; 287:18700-18709.*

3.0 TYPE VII COLLAGEN

3.1 Type VII collagen is a BM associated anchoring protein

An example of a spatially restricted BM-associated protein is Col VII. This anchoring protein was demonstrated underneath several BMs, but is not thought to exist as a common component of BM zones. It is most renowned for its expression at the largest of human organs: the skin. At the dermal-epidermal BM, this particular collagen forms anchoring fibrils: structures which secure the epidermis to the underlying stroma. The anchorage ability of these fibrils is a characteristic that is unique to Col VII, and a result of the collagen's aggregation into flexible loops.

3.2 Anchoring fibrils contain aggregated Col VII molecules

Shortly after the first isolation of Col VII from choriarnion by Bentz et al. (1983),¹² its first biochemical characteristics were reported. In contrast to most collagens, Col VII appeared not to aggregate longitudinally into a head-to-tail aggregated fibril (such as Col I; **Figure 1**). Therefore, it was not classified as a member of the *Fibril forming* collagen group (indicating typical long polymers), but instead as a *basement membrane associated* collagen, as part of the *non-fibrillar* collagen group. This latter classification is factually a misnomer, since Col VII does aggregate into fibrils, albeit through lateral aggregation. The precursor of Col VII, Type VII procollagen, was found to be a homotrimer (3 identical α -chains), flanked by two non-collagenous domains: a large NC-1 and a small NC-2 globular domain.

3.3 Anchoring fibrils are mostly loop shaped due to their affinity for BMs

The characteristics of these two globular domains, next to a flexible triple-helical domain, allow for Col VII to assume a looped shape. After a Col VII monomeric molecule is synthesized, it gets secreted into the extracellular milieu, the NC-2 domain is proteolytically cleaved, and the molecule is called 'mature'.^{13, 14} In the ECM, two Col VII molecules form antiparallel dimers; their α -chains overlap at their NC-2 terminal ends, while the large NC-1 globules stick out at the other end (**Figure 2**). The two NC-1 domains of the Col VII molecule have affinity for two specific basement membrane components, Col IV and laminin-332.^{15- 17} Therefore, both NC-1 domains of a Col VII dimer may connect to these basement membrane components, so that most dimers form the typical U-shape (**Figure 2**), at least in skin.¹⁸ When the complex supramolecular

process of lateral aggregation (and often looping) is completed, Col VII fibrils may have become thick enough to be visually identified by electron microscopy (as a true anchoring fibril).¹⁹

3.4 Anchoring fibrils function by direct binding to or physical entrapment of adjacent proteins

Presently, the anchoring fibril is the only functional mode of Col VII that is proven to secure epithelia to their underlying stroma. The looped configuration of the anchoring fibril secures the epithelial BM to the stroma by physical entrapment of the underlying stromal fibrils (collagen types I and III, from the *Fibril forming* group). But the NC-1 domains of Col VII also exert some direct affinity for the large stromal fibrils, suggesting an additional connection mode.^{15,20} Indeed, some anchoring fibrils appear to have only one NC-1 domain of their dimer connected to the BM, while the other NC-1 domain connects to a stromal fiber instead of the BM (**Figure 3**).^{20,21} Such direct interaction of Col VII with such large fibers probably adds to the fastening of the BM to the stroma²⁰ as well, but also indicates that not all anchoring fibrils are compulsory loops.

3.5 An alternative to anchoring fibril looping: the anchoring plaque connection

Anchoring plaques were thought to be mediators in anchorage among such non-looped anchoring fibrils (i.e. junctions between two or more linear shaped AF).²² Such amorphous plaques were described extensively, also in other species.^{23, 24} They were believed to be physiologically significant, as additional connections between anchoring fibrils, to let these extend further down into the papillary dermis as a chain. Some authors noted that these plaques appeared most extensively in the cornea, but were also obvious in multiple other tissues containing anchoring fibrils.²⁴ In 1997, it was suggested that anchoring plaques were a mere embedding artefact, and the mentioning of anchoring plaques diminished.^{22, 25}

As can be appreciated from the current literature, there is still some debate whether the anchoring plaques exist or not, and whether Col VII connects solely to the lamina densa, or alternatively, might connect to stromal fibrils (i.e. through molecular binding) according to the proposed configuration of Villone et al. (2008) (**Figure 5**).²⁰ Interestingly however, schematic representations of anchoring fibril connections typically depict the Col VII molecules as laterally aggregated dimers. In representations such as **Figure 6**, the dimers are depicted in unaggregated condition, but that was only meant for increased simplicity. In fact, no literature exists (to our knowledge) that describes sparsely aggregated, or even unaggregated dimeric fibrils which may or may

not perform as true anchoring fibrils. Of course, such individual fibrils might be very difficult to discern, since aggregated fibrils may already prove elusive, as reported in literature. For example, Gipson et al. (1987) reported that the structure and composition of anchoring fibrils may be difficult to discern in routinely fixed corneas (half-strength Karnovsky fixative/glutaraldehyde/paraformaldehyde; immediately after dissection).²³ Anchoring fibrils were found to be more distinct in 24h organ-cultures, after fixation with osmium-tetroxide in collidine buffer.²⁶

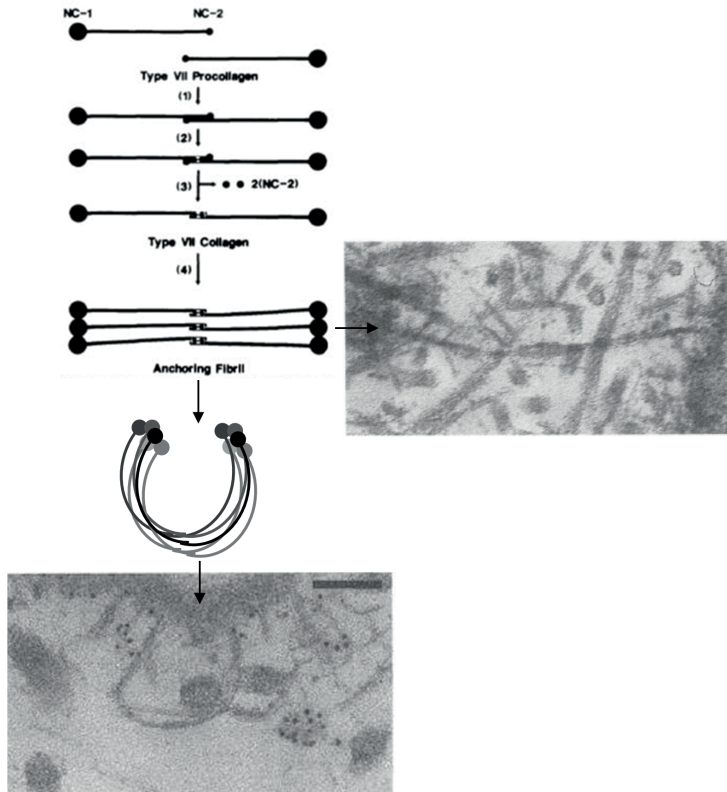


FIGURE 3. Schematic 2D representation and TEM imaging of anchoring fibril assembly. After lateral aggregation of assembled dimers, some of the NC-1 globules of the Col VII molecule will connect to the basement membrane forming a 'classic' looped anchoring fibril. Transmission electron microscopic visualization of such an anchoring fibril, at the bovine cornea basement membrane zone (*bottom*). In contrast, a linear anchoring fibril (*right*) may sometimes be appreciated, e.g. at the epidermal basement membrane zone of a human neonatal foreskin. Scale bar 100 nm. Adapted from Bachinger HP, et al. *J Biol Chem.* 1990; 265:10095-10101, and Lunstrum et al. *J Biol Chem.* 1987; 262:13706-13712.

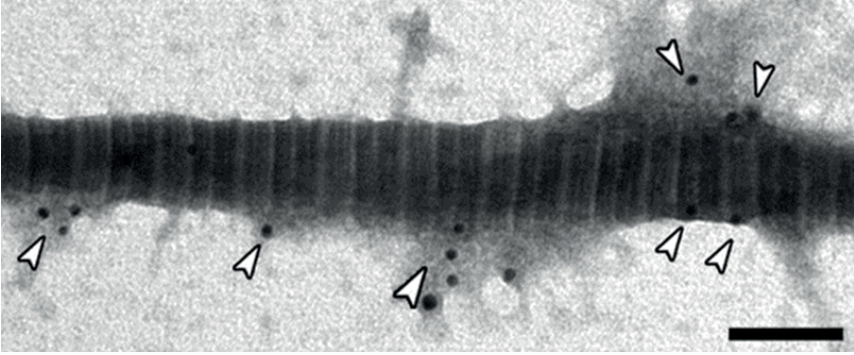


FIGURE 4. Anchoring fibrils are co-localized with type I collagen fibrils. Immunoelectron microscope image of a skin sample treated with gold labeled antibodies to collagen VII. At the sublamina densa, a large stromal type I collagen fibril is covered with anti-Col VII labeling (*white arrowheads*). Note the 'barcode' pattern of Col I due to its D-periodically banding. From Villone et al., *J Biol Chem.* 2008;283:24506-24513.

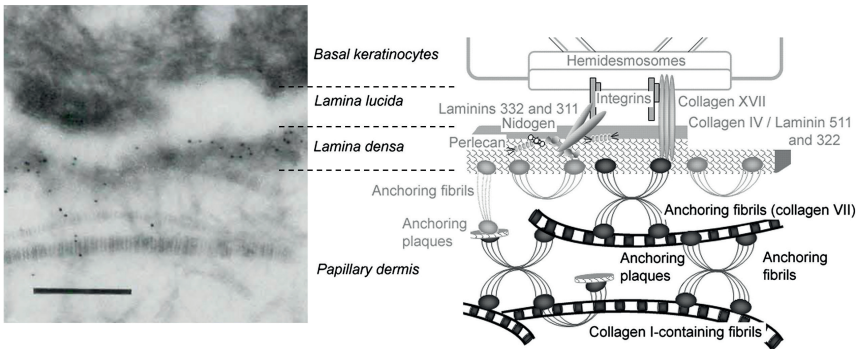


FIGURE 5. The organization of the anchoring complex of the dermal-epidermal junction zone; TEM (left) and 2D schematic (right). Many proteins have a role in stabilizing the dermo-epidermal connection. Anti-Col VII gold labels (*black dots in TEM figure*) localize at the lamina densa as well as at stromal collagen fibers. Schematic: classical looping anchoring fibrils are depicted in light grey, whereas proposed novel, covalently stabilized interactions are depicted in dark grey. Scale bar 200nm. Adapted from Villone et al., *J Biol Chem.* 2008; 283:24506-24513; and Hashimoto et al., *Br J Dermatol.* 1996; 134:336-339.

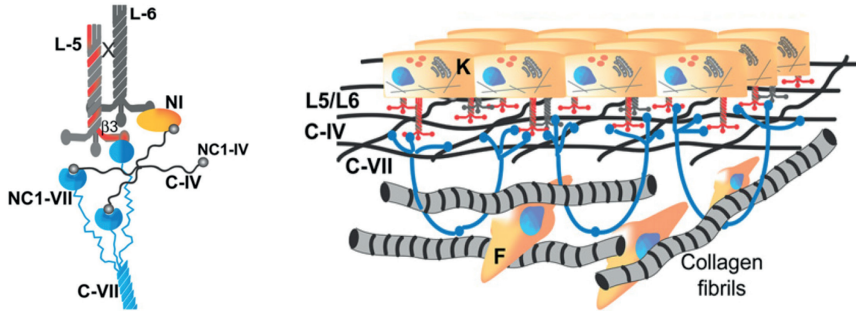


FIGURE 6. The organization of the anchoring complex of the dermal-epidermal junction zone; specific binding interactions and 3D schematic. (Left) Col VII binds with its NC1 domain (NC1-VII) to the NC1 domain of Col IV (NC1-IV) and the short arm of the $\beta 3$ chain of laminin 5 ($\beta 3$). (Right) basic keratinocytes (K) interact with the type IV collagen network (C-IV) through laminin-5 and -6 (L5/L6). Col VII connects to both laminin-5 and the Col IV network, hereby forming loops, but also interlaces with Col I fibrils derived from fibroblasts (F). Adapted from Brittingham et al., *Biochem Biophys Res Commun.* 2006; 343:692-699.

3.6 Anchoring fibrils are detected by visualization in TEM analysis

The gold standard of demonstrating anchoring fibrils has always been electron microscopy, either aided by immunogold labeling or without. As lateral aggregate, the anchoring fibril was discovered by electron microscopy²⁷⁻³⁷ long before the discovery of their main Col VII component by Sakai et al. (1986).³⁸ The ultrastructure of anchoring fibrils (in fixed tissues) indicated that each anchoring fibril was an unstaggered lateral aggregate of many molecules, although it was thought unlikely that the proximity of several helical domains would significantly stabilize an anchoring fibril in the absence intermolecular cross-links within the helical domains.²¹ To date, however, the idea that Col VII is the major (if not only) component of anchoring fibrils still holds.³⁸ An anchoring fibril was determined to be 780 nm long. Years later, the triple-helical domain of one Col VII monomer was determined to be 420 nm, which is the longest triple-helical region amongst vertebrate collagens (i.e. 1.5 times the length of a type I collagen α -chain).^{12,39} Each pair of Col VII molecules in a dimer thus has a 60 nm overlap at the carboxy terminal end of their α -chain.¹⁹ By transmission electron microscopy (TEM), the AF displayed variable diameters and degrees of curvature.²¹ The extreme degree of flexibility that the Col VII dimers exemplify in AF is not seen in other collagen molecules, including type IV collagen.²¹ Such deformability of anchoring fibrils in a network is thought to provide a mechanism to minimize the strain applied to the network by external forces and the resistance provided by fibrous stromal elements

entrapped by the network.²¹ Therefore, a BM 'sheet' with looping anchoring fibrils underneath which physically secure it to the underlying stroma may be compared to a biological Velcro.⁴⁰

3.7 Col VII detection is possible only after mRNA is transcribed from the COL7A1 gene

As in all protein synthesis, the encoding gene must first be transcribed into mRNA. The mRNA is then translated into an amino-acid sequence, which makes up a protein. Sometimes, cells may be capable of transcribing a certain mRNA, but are not stimulated by their environment to actually do so. Cells may, for example, be stimulated by the extracellular matrix to start synthesis at another time, when the protein is needed. Thus, demonstrating the presence of certain genes or even mRNA transcripts does not necessarily mean that cells actually express the corresponding protein product as well. Conversely, however, cells that lack gene transcripts (thus mRNA) are not capable of actual protein expression.

In addition, proteins from a single gene variant may also be translated into slightly different proteins by a process called alternate splicing. Alternative splicing means that a single gene may code for multiple proteins, because parts of such a gene (exons) may either be included or excluded in certain transcripts. This allows for non-identical mRNA transcripts and thus different amino-acid sequences and proteins. Consequently, the proteins that are translated from alternatively spliced mRNA may differ in their function.

The expression of the Col VII gene (COL7A1) and the protein product (Col VII) characteristics have been thoroughly examined. Col VII was shown to be made up of 2944 amino acid residues (aa); 1237aa at the NC-1 terminal domain, 1530aa at the triple helical collagenous part, 161aa at the carboxy terminal end, and a putative signal peptide of 16aa.^{39, 41, 42} When the amino acid sequences of human and mouse Col VII are compared, a relatively low degree of homology is seen in comparison to other collagens. Still, the organization of each domain in Col VII is conserved, especially in the triple helical part. This suggests that the functional flexibility of the molecule, dedicated to small interruptions in the triple helix such as the 'hinge' region, is essential for the anchoring function of fibrils, and therefore likely is conserved throughout the species.^{21, 41, 43, 44} Furthermore, only one genetic variant of Col VII and its encoding gene (COL7A1) are known to exist in healthy individuals. Sawamura et al. (2003) hypothesized whether COL7A1 could have alternative splice variants, since alternative splicing occurs frequently in genes that code for extracellular matrix proteins (including collagens)

which may have functional implications.⁴⁵ The possibility of one or more alternate splicing variants of COL7A1 may indeed not just be a theoretical one, since COL7A1 has a staggering 118 exons.⁴¹ Theoretically, there could exist another 6 isoforms in man, based on determined mRNA sequences (ncbi.nlm.nih.gov/gene/1294), but these transcripts or their proteins have never been demonstrated. Sawamura et al. (2003) found that expression of alternative transcripts of COL7A1 mRNA differed among several cell types, and that TGF- β (a potent inducer of COL7A1 expression and fibrosis) would promote such alternative splicing.⁴⁵

3.8 Detection of Col VII in tissue lysates by molecular weight determination and immunoreaction

Type VII procollagen is a molecule of very high molecular weight. Each procollagen molecule is composed of three homopolymer pro- α -chains. Biochemical studies predicted the molecular weights of the components of each the pro- α -chain by computer analysis of Col VII cDNA sequences: 133 kDa for the NC-1 globule, 145 kDa for the collagenous part, and 18 kDa for the small NC-2 globule.^{41, 46} Estimated and predicted molecular weights of Col VII and its enzyme-induced released components (NC-1, NC-1 and 3H) differed somewhat from the results obtained from SDS-PAGE migrations (145 kDa for NC-1; 170 kDa for triple helix; ~30 kDa for NC-2), especially the NC-2 domain.^{38, 47} The reason for such differences is poorly understood since glycosylation is very unlikely⁴⁰. This would mean that the predicted molecular weight would be about 295 kDa for a procollagen monomer, thus about 885 kDa for one complete homotrimeric procollagen molecule.³⁹ By electrophoresis migration, these values would theoretically be 345 kDa and 1035 kDa, respectively.

4.0 DISTRIBUTION OF COL VII IN HEALTH AND DISEASE

4.1 Distribution of Col VII: the cornea

By TEM, Kenyon and Maumee (1968) were able to visualize anchoring fibrils in the cornea, after which Gipson et al. (1987) could identify Col VII in anchoring fibrils by monoclonal antibody immunolocalization.^{23, 39, 48} Anchoring fibrils were shown to penetrate into the corneal stroma by 0.6 μm . The widths of the fibrils were measured to be up to 0.15 μm , but AF were not seen in cross sections thinner than 0.15 μm . This led to the believe that the circumference of AF must not be round but rather ribbon-shaped.²³ Alternatively, it was suggested that in cornea, most fibrils would run parallel to the basement membrane, and that only infrequently these fibrils would attach

at both sides to the BM. Additionally, it was suggested that the looping anchoring fibrils was more prevalent in the epidermis than in cornea, possibly because of the undulation of the epidermal BM as opposed to the cornea.²³ In infant corneas, the immunolocalization of Col VII by monoclonal antibodies in immunofluorescence was seen as a 'strands of beads' originating at the corneal epithelial basement membrane and running down towards the stroma. In adult corneas, such labeling was reduced to a thin line.²⁴ Despite successful Col VII labeling in immunofluorescence, Gipson et al. (1989) were unable to demonstrate AF in wounded cornea until 4 weeks of healing.⁴⁹ In the developing ocular surface, Col VII is also detected immunohistochemically before any cross-banded AF were discernable by TEM.⁵⁰

4.2 Distribution of Col VII: the retina

In a previous study of the vitreoretinal interface, our group evaluated the presence and distribution of several collagens by immunohistochemistry and real-time PCR, including Col VII. Locations of interest were the pre-equatorial area, the equator and posterior pole of donor retina samples, and retinectomy samples. The mRNA analysis of these retina samples confirmed the presence of COL7A1 mRNA. Both mono- and polyclonal antibodies labeled intracellular structures in the superficial retina especially at the posterior pole.⁵¹ This was an unexpected discovery, because Col VII is commonly labeled as an extracellular linear pattern underneath certain basement membranes. In these sections, the blood vessels of the retina were not labeled by the anti-Col VII antibodies.⁵¹ In a later study, our group found spontaneously immortalized retinal Müller cells not only to express COL7A1 mRNA, but also to synthesize the protein, Col VII. These cells would react to anti-Col VII antibodies in routine immunohistochemical culture stainings, and lysates of these cells showed Col VII presence by Western blots. Extracellular Col VII deposition, however, was not detected in cell cultures (within 48 hours).⁵² The role of Col VII at the superficial retina and Müller cell associated Col VII remains unknown.

4.3 Distribution of Col VII: pathology

In skin, Col VII is roughly estimated to comprise only 0.001% of the total collagen content.⁵³ Given the amount of residual non-collagenous proteins in skin, the proportion of Col VII relative to the total protein content will be even lower.⁵³ Still, this minute amount of Col VII is essential in stabilizing the dermal-epidermal connection, since a diminished amount of Col VII leads to less (or less functional) anchoring fibrils.^{23,38,54} Col VII deficiency leads to the bullous disorder 'dystrophic epidermolysis bullosa'.⁵⁵ In the recessive variant of dystrophic epidermolysis bullosa (RDEB), the anchoring fibrils are

absent, or otherwise dysfunctional, which results in repeated cutaneous blistering of the affected patients. Such blistering occurs after moments of mechanical friction of the skin, but is also reported to occur spontaneously. The ongoing blistering complicates wound healing, and facilitates bacterial infections of the wounds. Patients often succumb to the disease before age 35 years due to sepsis and aggressive squamous cell carcinoma. Due to the blistering of oral mucosa and strictures of the esophagus, malnutrition and vitamin/mineral deficiency are frequent. Extensive scarring of their extremities leaves patients with fused 'mitten' hands and feet. Their constant pain and itching drastically reduces their quality of life.⁵⁶ The involvement of their ocular tissues is evidenced by blistering and fibrosis of the exterior tissues, i.e. the cornea and conjunctiva. Again, the considerable scar formation leads to cicatricial complications, such as ocular surface disease, pannus and symblepharon.⁵⁷⁻⁶⁰ Additionally, some investigators have claimed that an association between keratoconus formation and Col VII deficiency might exist, since immunohistochemical analysis showed a diminished immunoreactivity for Col VII in such donor tissues.⁶¹⁻⁶³ The importance of minute basic quantities Col VII in skin and cornea is clear, although this raises more questions about the intraretinal depositions of Col VII discovered by Ponsioen et al.^{51,52} Still, in a RDEB mouse model, only 35% of the normal/physiological levels of Col VII was sufficient to mechanically stabilize their skins.⁶⁴ So, despite the apparent low concentration of (semi-quantitatively determined) Col VII in the human retina, there might be enough to provide an actual functional contribution.

4.4 The function of intraocular Col VII

To date, much is known about the characteristics of Col VII in dermal tissues such as skin and cornea, but there are still many questions that arise after viewing the literature. What is the function of intraocular Col VII? Why is it detectable in the retinal Müller cell cultures, but does not label as a linear deposition at the BM of those cells? Why does Col VII not delineate the BMs of other tissues besides skin? Some of these questions may be addressed by the amount of mechanical friction that is encountered in the corresponding tissues, since the amount of AF in skin apparently varies per region, probably reflecting the amount of mechanical friction applied there.^{65,66} Tidman et al. (1984) concluded that a mild frictional stimulus which fails to produce significant alterations in epidermal thickness can produce a marked increase in anchoring fibril frequency.⁶⁶ This indicates that tissues that normally contain Col VII (as AF) might harness more Col VII at areas of increased mechanical loading or friction. In the intraocular milieu, that might apply to the accommodation system, where mechanical loading occurs at the ciliary muscle, zonules and lens. According to Hilding (1954), mechanical forces are also transduced onto the neuroretina, by the vitreoretinal

adhesion mechanism.⁶⁷ Recently, it was suggested that systemic hypertension might already induce mechanical stress onto the retina, via the retinal vasculature, so in turn, eye movements alone might already invoke and transduce some amount of force onto the retina via a multitude of vitreoretinal attachment mechanisms.⁶⁸ Could the Col VII, demonstrated at the superficial retina, have some protective function by firmly attaching the retina to the stromal vitreous body? And could the Col VII that was demonstrated in the superficial retina, be absent in RDEB patients, who then experience epithelial-mesenchymal tissue detachments at their vitreoretinal interfaces?

5.0 AIMS AND OUTLINE OF THIS THESIS

In order to address these questions, this thesis should provide more insight into the characteristics of intraocular Col VII. Any intraocular anchorage mechanism is potentially relevant, since many intraocular pathologies are associated with tissue detachments. A better understanding of which side of a tissue border harbors an effective anchoring protein may lead to a better understanding of detachments or other defects. Similarly, the iatrogenic induction of intraocular detachments (e.g. ocriplasmin at the vitreoretinal interface) would theoretically be ineffective if vitreoretinal adhesion was indeed supported by (plasmin-insensitive) Col VII. Our main goal is therefore to elucidate more of the characteristics of intraocular Col VII, and possibly deduce its function in the intraocular milieu. Therefore, we investigate the vitreoretinal interface and superficial layers of the retina, first to immunolocate Col VII at such areas, confirming earlier observations. We then analyzed the accommodation system for Col VII expression and deposition, since we assume the mechanical loading is the most elaborate at this intraocular site. The intraocular basement membranes were immunohistochemically investigated, such as the lens capsule, the ILM, and the BM of retinal and choroidal blood vessels. In order to confirm our immunohistochemical results, and to elucidate more about the consequences of Col VII deficiency, we investigated RDEB patients both clinically (four patients) as well immunohistochemically (one donor).

Chapter 1 is the general introduction of this thesis, which provides its reader with several aspects that are combined in our studies. It hopes to explain which characteristics of collagens may be relevant in the interpretation of the results to come, and tries to trigger the reader to realize that an anchoring protein -already essential in minute amounts- is located intraocularly, but that roughly 20 years after its initial discovery, no significant intraocular findings are reported in Col VII deficient patients.

Chapter 2 continues the investigation on (vitreo)retinal Col VII depositions that were described by our group. We seek to confirm the earlier observations, and apply various immunochemical techniques in order to gain more insight in a possible anchoring function of Col VII at the epithelial-stromal interface. Moreover, we describe another (glial) cellular source of Col VII in the superficial retina.

Chapter 3 addresses the expression of COL7A1 and deposition of its protein product, Col VII, at the accommodation system, i.e. ciliary body, zonules and lens capsule. Concomitantly, we address the Col VII associated zonular origin and lens capsule insertion. Additionally, we validate and characterize our main anti-Col VII antibody by epitope mapping, and others by immunohistochemistry.

Chapter 4 reports on the discrepancy in literature on the presence of Col VII at blood vessels. Some authors have witnessed some anti-Col VII immunoreactions in their tissues of interest, while it is generally accepted that Col VII is not part of the vascular basement membrane zone. In light of the results that are discussed in chapter 3, we addressed this discrepancy by investigating the retinal vasculature and comparing it to blood vessels in other tissues.

Chapter 5 discusses the theoretical implications of the intraocular Col VII function, by assessing the consequences of intraocular Col VII dysfunction. RDEB patients were clinically investigated with modern techniques, and a pair of RDEB donor eyes was immunohistochemically analyzed. Special attention was paid to the existence of any intraocular tissue defects and/or detachments.

Chapter 6 summarizes the implications of the data from the previous chapters, and interprets these data in light of the current literature. It addresses the gap between the presence of Col VII -determined by immunohistochemical techniques- at various intraocular tissues on the one side, and the absence of notable anchoring fibrils on the other. Inconsistencies in the literature are put forward and compared to our own findings.

Chapter 7 and 8 provide readers with an English and Dutch synopsis of this thesis.

REFERENCES

- Bella J, Hulmes DJ. Fibrillar Collagens. *Subcell Biochem.* 2017; 82:457-490.
- Bächinger, HP, Mizuno, K, Vranka, J & Boudko, SP. Collagen formation and structure. In: *Comprehensive Natural Products II: Chemistry and Biology.* Vol. 5, Elsevier Ltd; 2010: 469-530.
- Urabe N, Naito I, Saito K, Yonezawa T, Sado Y, Yoshioka H, et al. Basement membrane type IV collagen molecules in the choroid plexus, pia mater and capillaries in the mouse brain. *Arch Histol Cytol.* 2002; 65:133-143.
- Binns D, Dimmer E, Huntley R, Barrell D, O'Donovan C, Apweiler R. QuickGO: a web-based tool for Gene Ontology searching. *Bioinformatics.* 2009; 25:3045-3046.
- Behrens DT, Villone D, Koch M, Brunner G, Sorokin L, Robenek H, et al. The epidermal basement membrane is a composite of separate laminin- or collagen IV-containing networks connected by aggregated perlecan, but not by nidogens. *J Biol Chem.* 2012; 287:18700-18709.
- Khoshnoodi J, Pedchenko V, Hudson BG. Mammalian collagen IV. *Microsc Res Tech.* 2008; 71:357-370.
- Fukuda K, Chikama T, Nakamura M, Nishida T. Differential distribution of subchains of the basement membrane components type IV collagen and laminin among the amniotic membrane, cornea, and conjunctiva. *Cornea.* 1999; 18:73-79.
- Uechi G, Sun Z, Schreiber EM, Halfter W, Balasubramani M. Proteomic view of basement membranes from human retinal blood vessels, inner limiting membranes, and lens capsules. *J Proteome Res.* 2014; 13:3693-3705.
- Ljubimov AV, Burgeson RE, Butkowski RJ, Michael AF, Sun TT, Kenney MC. Human corneal basement membrane heterogeneity: topographical differences in the expression of type IV collagen and laminin isoforms. *Lab Invest.* 1995; 72:461-473.
- Kabosova A, Azar DT, Bannikov GA, Campbell KP, Durbeej M, Ghohestani RF. Compositional differences between infant and adult human corneal basement membranes. *Invest Ophthalmol Vis Sci.* 2007; 48:4989-4999.
- Has C, Nyström A. Epidermal Basement Membrane in Health and Disease. *Curr Top Membr.* 2015; 76:117-170.
- Bentz H, Morris NP, Murray LW, Sakai LY, Hollister DW, Burgeson RE. Isolation and partial characterization of a new human collagen with an extended triple-helical structural domain. *Proc Natl Acad Sci USA.* 1983; 80:3168-3172.
- Chen YQ, Mauviel A, Ryyänen J, Sollberg S, Uitto J. Type VII collagen gene expression by human skin fibroblasts and keratinocytes in culture: influence of donor age and cytokine responses. *J Invest Dermatol.* 1994; 102:205-209.
- Amano S, Ogura Y, Akutsu N, Nishiyama T. Quantitative analysis of the synthesis and secretion of type VII collagen in cultured human dermal fibroblasts with a sensitive sandwich enzyme-linked immunoassay. *Exp Dermatol.* 2007; 16:151-155.
- Brittingham R, Uitto J, Fertala A. High-affinity binding of the NC1 domain of collagen VII to laminin 5 and collagen IV. *Biochem Biophys Res Commun.* 2006; 343:692-699.
- Chen M, Marinkovich MP, Jones JC, O'Toole EA, Li YY, Woodley DT. NC1 domain of type VII collagen binds to the beta3 chain of laminin 5 via a unique subdomain within the fibronectin-like repeats. *J Invest Dermatol.* 1999; 112:177-183.

17. Wegener H, Paulsen H, Seeger K. The cysteine-rich region of type VII collagen is a cystine knot with a new topology. *J Biol Chem.* 2014; 289:4861-4869.
18. Shimizu H, Ishiko A, Masunaga T, Kurihara Y, Sato M, Bruckner-Tuderman L. Most anchoring fibrils in human skin originate and terminate in the lamina densa. *Lab Invest.* 1997; 76:753-763.
19. Morris NP, Keene DR, Glanville RW, Bentz H, Burgeson RE. The tissue form of type VII collagen is an antiparallel dimer. *J Biol Chem.* 1986; 261:5638-5644.
20. Villone D, Fritsch A, Koch M, Bruckner-Tuderman L, Hansen U, Bruckner P. Supramolecular interactions in the dermo-epidermal junction zone: anchoring fibril-collagen VII tightly binds to banded collagen fibrils. *J Biol Chem.* 2008; 283:24506-24513.
21. Bächinger HP, Morris NP, Lunstrum GP, Keene DR, Rosenbaum LM, Compton LA. The relationship of the biophysical and biochemical characteristics of type VII collagen to the function of anchoring fibrils. *J Biol Chem.* 1990; 265:10095-10101.
22. Rousselle P, Keene DR, Ruggiero F, Champlaud MF, Rest M, Burgeson RE. Laminin 5 binds the NC-1 domain of type VII collagen. *J Cell Biol.* 1997; 138:719-728.
23. Gipson IK, Spurr-Michaud SJ, Tisdale AS. Anchoring fibrils form a complex network in human and rabbit cornea. *Invest Ophthalmol Vis Sci.* 1987; 28:212-220.
24. Burgeson RE. Type VII collagen. In: Mayne R, Burgeson RE, eds. *Structure and Function of Collagen Types.* Orlando, Academic Press; 1987:145-172.
25. Adachi E, Hopkinson I, Hayashi T. Basement-membrane stromal relationships: interactions between collagen fibrils and the lamina densa. *Int Rev Cytol.* 1997; 173:73-156.
26. Kelly DE. Fine structure of desmosomes, hemidesmosomes, and an adepidermal globular layer in developing newt epidermis. *J Cell Biol.* 1966; 28:51-72.
27. Brody I. The ultrastructure of the tonofibrils in the keratinization process of normal human epidermis. *J Ultrastruct Res.* 1960; 4:264-297.
28. Younes MS, Steele HD, Robertson EM, Bencosme SA. Correlative light and electron microscope study of the basement membrane of the human ectocervix. *Am J Obstet Gynaecol.* 1965; 92:163-171.
29. Palade GE, Farquhar MG. A special fibril of the dermis. *J Cell Biol.* 1965; 27:215-224.
30. Schroeder HE, Theilade J. Electron microscopy of normal human gingival epithelium. *J Periodontal Res.* 1966; 1:95-119.
31. Swanson JL, Helwig EB. Special fibrils of human dermis. *J Invest Dermatol.* 1968; 50:195-199.
32. Susi FR. Anchoring fibrils in the attachment of epithelium to connective tissue in oral mucous membranes. *J Dent Res.* 1969; 48:144-148.
33. Bruns RR. A symmetrical, extracellular fibril. *J Cell Biol.* 1969; 42:418-430.
34. Briggaman RA, Dalldorf FG, Wheeler CE Jr. Formation and origin of basal lamina and anchoring fibrils in adult human skin. *J Cell Biol.* 1971; 51:384-395.
35. Laguens R. Subepithelial fibrils associated with the basement membrane of human cervical epithelium. *J Ultrastruct Res.* 1972; 41:202-208.
36. Kawanami O, Ferrans VJ, Roberts WC, Crystal RG, Fulmer JD. Anchoring fibrils. A new connective tissue structure in fibrotic lung disease. *Am J Pathol.* 1978; 92:389-410.
37. Wasano K, Yamamoto T. Microthread-like filaments connecting the epithelial basal lamina with underlying fibrillar components of the connective tissue in the rat trachea. A real anchoring device? *Cell Tissue Res.* 1985; 239:485-495.

38. Sakai LY, Keene DR, Morris NP, Burgeson RE. Type VII collagen is a major structural component of anchoring fibrils. *J Cell Biol.* 1986; 103:1577-1586.
39. Lunstrum GP, Sakai LY, Keene DR, Morris NP, Burgeson RE. Large complex globular domains of type VII procollagen contribute to the structure of anchoring fibrils. *J Biol Chem.* 1986; 261:9042-9048.
40. Tolar J, Wagner JE. A biologic Velcro patch. *N Engl J Med.* 2015; 372:382-384.
41. Christiano AM, Greenspan DS, Lee S, Uitto J. Cloning of Human Type VII Collagen. Complete primary sequence of the alpha 1(VII) chain and identification of intragenic polymorphisms. *J Biol Chem.* 1994; 269:20256-20262.
42. Parente MG1, Chung LC, Ryyänen J, Woodley DT, Wynn KC, Bauer EA, et al. Human type VII collagen: cDNA cloning and chromosomal mapping of the gene. *Proc Natl Acad Sci USA.* 1991; 88:6931-6935.
43. Li K, Christiano AM, Copeland NG, Gilbert DJ, Chu ML, Jenkins NA, Uitto J. cDNA cloning and chromosomal mapping of the mouse type VII collagen gene (Col7a1): evidence for rapid evolutionary divergence of the gene. *Genomics.* 1993; 16:733-739.
44. Kivirikko S, Li K, Christiano AM, Uitto J. Cloning of mouse type VII collagen reveals evolutionary conservation of functional protein domains and genomic organization. *J Invest Dermatol.* 1996; 106:1300-1306.
45. Sawamura D, Goto M, Yasukawa K, Kon A, Akiyama M, Shimizu H. Identification of COL7A1 alternative splicing inserting 9 amino acid residues into the fibronectin type III linker domain. *J Invest Dermatol.* 2003; 120:942-948.
46. Greenspan DS. The carboxyl-terminal half of type VII collagen, including the non-collagenous NC-2 domain and intron/exon organization of the corresponding region of the COL7A1 gene. *Hum Mol Genet.* 1993; 2:273-278.
47. Burgeson RE. Type VII Collagen, Anchoring Fibrils, and Epidermolysis Bullosa. *J Invest Dermatol.* 1993; 101:252-255.
48. Kenyon KR, Maumenee AE. The histological and ultrastructural pathology of congenital hereditary corneal dystrophy: a case report. *Invest Ophthalmol.* 1968; 7:475-500.
49. Gipson IK, Spurr-Michaud S, Tisdale A, Keough M. Reassembly of the anchoring structures of the corneal epithelium during wound repair in the rabbit. *Invest Ophthalmol Vis Sci.* 1989; 30:425-434.
50. Tisdale AS, Spurr-Michaud SJ, Rodrigues M, Hackett J, Krachmer J, Gipson IK. Development of the anchoring structures of the epithelium in rabbit and human fetal corneas. *Invest Ophthalmol Vis Sci.* 1988; 29:727-736.
51. Ponsioen TL, van Luyn MJ, van der Worp RJ, van Meurs JC, Hooymans JM, Los LI. Collagen distribution in the human vitreoretinal interface. *Invest Ophthalmol Vis Sci.* 2008; 49:4089-4095.
52. Ponsioen TL, van Luyn MJ, van der Worp RJ, Pas HH, Hooymans JM, Los LI. Human retinal Müller cells synthesize collagens of the vitreous and vitreoretinal interface in vitro. *Mol Vis.* 2008; 14:652-660.
53. Bruckner-Tuderman L, Schnyder UW, Winterhalter KH, Bruckner P. Tissue form of type VII collagen from human skin and dermal fibroblasts in culture. *Eur J Biochem.* 1987; 165:607-611.
54. Keene DR, Sakai LY, Lunstrum GP, Morris NP, Burgeson RE. Type VII Collagen Forms an Extended Network of Anchoring Fibrils. *J Cell Biol.* 1987; 104:611-621.
55. Briggaman RA, Wheeler CE Jr. Epidermolysis bullosa dystrophica-recessive: a possible role of anchoring fibrils in the pathogenesis. *J Invest Dermatol.* 1975; 65:203-211.
56. Pfindner EG, Lucky AW. Dystrophic Epidermolysis Bullosa. In: Adam MP, Ardinger HH, Pagon RA,

- Wallace SE, Bean LJH, Stephens K, Amemiya A, eds. *SourceGeneReviews*® [Internet]. Seattle (WA): University of Washington, Seattle; 1993-2019.
57. Fine JD, Mellerio JE. Extracutaneous manifestations and complications of inherited epidermolysis bullosa: part II. Other organs. *J Am Acad Dermatol.* 2009; 61:387-402.
58. Smith KA, Jones SM, Nischal KK. Refractive and ocular motility findings in children with epidermolysis bullosa. *Am Orthopt J.* 2009; 59:76-83.
59. Jones SM, Smith KA, Jain M, Mellerio JE, Martinez A, Nischal KK. The Frequency of Signs of Meibomian Gland Dysfunction in Children with Epidermolysis Bullosa. *Ophthalmology.* 2016; 123:991-999.
60. Fine JD, Mellerio JE. Extracutaneous manifestations and complications of inherited epidermolysis bullosa: part I. Epithelial associated tissues. *J Am Acad Dermatol.* 2009; 61:367-384.
61. Zimmermann DR, Fischer RW, Winterhalter KH, Witmer R, Vaughan L. Comparative studies of collagens in normal and keratoconus corneas. *Exp Eye Res.* 1988; 46:431-442.
62. Kenney MC, Nesburn AB, Burgeson RE, Butkowski RJ, Ljubimov AV. Abnormalities of the extracellular matrix in keratoconus corneas. *Cornea.* 1997; 16:345-351.
63. Tuori AJ, Virtanen I, Aine E, Kalluri R, Miner JH, Uusitalo HM. The immunohistochemical composition of corneal basement membrane in keratoconus. *Curr Eye Res.* 1997; 16:792-801.
64. Poulsen ET, Runager K, Risør MW, Dyrland TF, Scavenius C, Karring H, Praetorius J. Comparison of two phenotypically distinct lattice corneal dystrophies caused by mutations in the transforming growth factor beta induced (TGFBI) gene. *Proteomics Clin Appl.* 2014; 8:168-177.
65. Banks WJ, Bale E, White FH. Morphometric studies of the epidermal-dermal junction in the rat ear: some effects of experimental friction on epidermis and anchoring fibrils. *J Anat.* 1984; 139:425-435.
66. Tidman MJ, Eady RA. Ultrastructural morphometry of normal human dermal-epidermal junction. The influence of age, sex, and body region on laminar and nonlaminar components. *J Invest Dermatol.* 1984; 83:448-453.
67. Hilding AC. Normal vitreous, its attachments and dynamics during ocular movement. *AMA Arch Ophthalmol.* 1954; 52:497-514.
68. Kinoshita H, Suzuma K, Maki T, Maekawa Y, Matsumoto M, Kusano M. Cyclic stretch and hypertension increase retinal succinate: potential mechanisms for exacerbation of ocular neovascularization by mechanical stress. *Invest Ophthalmol Vis Sci.* 2014; 55:4320-4326.



2

Chapter 2

Type VII Collagen expression in the human vitreoretinal interface, corpora amylacea and inner retinal layers

Bart Wullink^{1,2,*}

Hendri H Pas³

Roelofje J Van der Worp^{1,2,4}

Roel Kuijer^{2,4}

Leonoor I Los^{1,2}

¹ Department of Ophthalmology, University Medical Center Groningen, University of Groningen, Groningen, the Netherlands

² W.J. Kolff Institute, Graduate School of Medical Sciences, University of Groningen, Groningen, the Netherlands

³ Department of Dermatology, University Medical Center Groningen, University of Groningen, Groningen, the Netherlands

⁴ Department of Biomedical Engineering, University Medical Center Groningen, University of Groningen, Groningen, the Netherlands

ABSTRACT

Type VII collagen, as a major component of anchoring fibrils found at basement membrane zones, is crucial in anchoring epithelial tissue layers to their underlying stroma. Recently, type VII collagen was discovered in the inner human retina by means of immunohistochemistry, while proteomic investigations demonstrated type VII collagen at the vitreoretinal interface of chicken. Because of its potential anchoring function at the vitreoretinal interface, we further assessed the presence of type VII collagen at this site. We evaluated the vitreoretinal interface of human donor eyes by means of immunohistochemistry, confocal microscopy, immunoelectron microscopy, and Western blotting. Firstly, type VII collagen was detected alongside vitreous fibers at the vitreoretinal interface. Because of its known anchoring function, it is likely that type VII collagen is involved in vitreoretinal attachment. Secondly, type VII collagen was found within cytoplasmic vesicles of inner retinal cells. These cells resided most frequently in the ganglion cell layer and inner plexiform layer. Thirdly, type VII collagen was found in astrocytic cytoplasmic inclusions, known as corpora amylacea. The intraretinal presence of type VII collagen was confirmed by Western blotting of homogenized retinal preparations. These data add to the understanding of vitreoretinal attachment, which is important for a better comprehension of common vitreoretinal attachment pathologies.

INTRODUCTION

Type VII collagen (Col VII) is renowned as the major component of anchoring fibrils (AF).¹ AF are pliable, centrosymmetrically banded structures essential for the attachment of basement membranes to their underlying connective tissue matrix.² They are found as a network at the epithelial-mesenchymal border regions of various types of epithelia.¹⁻¹¹ Because of the deformability of the anchoring fibrils, both the strain applied to the network by external forces, and its resistance, provided by entrapped fibrous stromal elements, might be minimized.¹² In the outer eye, AF have been demonstrated to perform an anchoring role beneath the basement membrane of the cornea, limbus, and conjunctiva.¹³⁻¹⁶ In the inner eye, AF have never been described. Recently, however, Col VII expression was discovered in the inner human retina,^{17, 18} and inner limiting membrane (ILM) of chicken.¹⁹ These findings suggest a possible role for Col VII in vitreoretinal anchoring. The present study was undertaken to further characterize type VII collagen at the vitreoretinal interface. Our main purpose was to identify sites of Col VII expression in the normal human vitreoretinal interface. Any possible involvement of Col VII in vitreoretinal attachment should enhance our understanding of normal and pathological vitreoretinal adhesion mechanisms. Posterior vitreous detachment, for example, is a key factor involved in numerous ophthalmic pathologies, including the formation of macular holes, epiretinal membranes, rhegmatogenous retinal detachment, vitreoretinal traction syndromes, and other pathologies.²⁰ Furthermore, Col VII involvement would indicate that current enzymatic agents used for vitreoretinal separation might not target all necessary matrix components. Specific targeting should lead to less traumatic treatment: Current agents still result in adverse toxicity, lack of efficacy, or both.²⁰ We demonstrate that Col VII is an additional extracellular matrix component expressed at the vitreoretinal interface, possibly involved in vitreoretinal anchorage.

MATERIALS AND METHODS

Ethics Statement: Eyes were provided by the Euro Cornea Bank, Beverwijk (<http://www.eurotissuebank.nl/comeabank/>), the Netherlands. In the Netherlands, the usage of donor material is provided for by the Organ Donation Act (WOD: *Wet op de orgaandonatie*). In accordance with this law, donors provide written informed consent for donation, with an opt-out for the usage of leftover material for related scientific research. Specific requirements for the use in scientific research of leftover material originating from corneal grafting have been described in an additional document

formulated by the Ministry of Health, Welfare, and Sport, and the BIS foundation (Eurotransplant; Leiden, July 21, 1995; 6714.ht). The current research was carried out in accordance with all requirements stated in the WOD and the relevant documents. Approval of the local medical ethics committee was not required, since the data were analyzed anonymously.

A total of 28 human eyes from 25 donors (11 men and 14 women), with ages varying between 17 and 82 years (mean donor age 65.8 years), were used (**Sup info Table 1**). The eyes were without known ophthalmic disorders, although in two donors idiopathic epiretinal membranes were found during experiments. The eyes were analyzed immunohistochemically by means of light microscopy (LM), confocal microscopy, and transmission-electron microscopy (TEM). Homogenized retinal preparations were analyzed using Western blotting. For antibody specifications see Sup info Table 2. Within 48 hours post mortem, all of the eyes were either fixed, or processed for Western blotting.

Embedding in paraffin for light microscopy

Eyes were fixed by immersion in 2% paraformaldehyde (Polysciences Inc., Warrington, UK) in phosphate buffered saline (PBS) (pH 7.4). Two small holes were cut into the globe for better penetration of the fixative. By gently rotating the specimens during the washing, dehydration, and infiltration steps, the loss of vitreous was prevented. Ethanol (50-100%) and xylene were used as dehydrators, and paraffin embedding followed. Sections of 3-4 μm thickness were cut in the transverse (i.e., parallel to the longitudinal axis of the eye) and/or frontal planes (i.e., parallel to the equator of the eye) using a microtome (RM2265, Leica Microsystems, Heidelberg, Germany) and mounted on adhesive slides (Waldemar-Knittel, Braunschweig, Germany).

Embedding in Technovit 8100 for light microscopy

Eyes were fixed for 1 hour by means of immersion in 2% paraformaldehyde, in 0.1 M phosphate buffer (pH 7.4). Again, two holes were made, and the eyes were gently rotated. The specimens were fixed additionally, for a total of 4 hours, in 2% paraformaldehyde. Specimens were washed in a solution of 6.8% sucrose in phosphate buffer overnight, and then briefly in distilled water before being dehydrated in acetone (30-100%). Specimens were pre-infiltrated, infiltrated, and embedded in Technovit 8100 (T8100) (Heraeus Kulzer, Wehrheim, Germany), according to the instructions of the manufacturer. Sections of 3 μm thickness were cut using a rotary microtome (Jung, Heidelberg, Germany) for LM.

Immunohistochemical staining for LM: paraffin

Sections were deparaffinized with xylene followed by brief rehydration steps with ethanol (100-50%). After washing with deionized water, antigen retrieval was performed by incubating the sections with 0.01% type XXIV protease (Sigma, St. Louis, USA) in PBS for 30 minutes at room temperature. The sections were washed with PBS, and endogenous peroxidases were blocked by incubation in 0.1% H₂O₂ for 30 minutes. Next, sections were incubated in PBS with 2% bovine serum albumin (BSA) (Sanquin, Amsterdam, the Netherlands) and 5% serum for 10 minutes. Primary antibodies were diluted (1:500) in PBS with 1% BSA and added for 1 hour. The primary antibodies used were rabbit polyclonal anti-type VII collagen (Calbiochem, Darmstadt, Germany), mouse monoclonal anti-type VII collagen (LH7.2, Abcam, Cambridge, UK; clone 32, Chemicon, Temacula, California, USA), anti-gliab fibrillary protein (GFAP) (an astrocyte marker, Sigma), and anti-vimentin (a Müller cell marker, Dako, Glostrup, Denmark) (S2 Table). After washing, secondary antibodies, conjugated with horseradish peroxidase, diluted (1:500) in PBS, 1% BSA, and 2% human serum were added for 1 hour at room temperature. These secondary antibodies included rabbit-anti-mouse peroxidase (RAMPO) and swine-anti-rabbit peroxidase (SARPO) (Dako). Sections were stained using 3-amino-9-ethylcarbazole (AEC, Sigma) and counterstained with hematoxylin. Some serial sections were counterstained using periodic acid-Schiff's base according to a standard protocol.

Immunohistochemical staining for LM: T8100

The T8100 sections from all four eyes were pretreated with 0.05% trypsin (Gibco, Paisley, Scotland) in Tris buffer (pH 7.8) containing 0.1% CaCl₂, for 15 minutes at 37°C, for antigen retrieval. The sections were washed in phosphate buffer and incubated in 0.1 M citric acid pH 3.0 for 30 minutes at 37°C and washed. In order to block nonspecific binding of the primary antibodies, sections were incubated with PBS containing 2% BSA and 2% serum for 30 minutes at room temperature. The primary antibodies were diluted in phosphate buffer/1% BSA-c (Aurion, Wageningen, the Netherlands) (1:100). Sections were incubated in primary antibody initially for 2 hours at 37°C and then at room temperature overnight. Primary antibodies included the rabbit polyclonal and mouse monoclonals against Col VII. Sections were incubated in SARPO or RAMPO (1:500) in PBS with 1% BSA and 2% human serum for 1 hour. Sections were stained with 3-amino-9-ethylcarbazole and counterstained with hematoxylin. In control sections primary antibody was omitted.

Qualitative analysis of Col VII: light microscopy

Objective lens powers ranging from 20x to 100x were used for an analysis by LM of general and more detailed aspects of Col VII-labeled structures, and their relationship to retinal cells and layers.

Quantitative analysis of Col VII: light microscopy

Analysis of Col VII-labeled structures was done in different planes and included quantification, localization, and semi-quantitative size determination. Frontally cut sections were used for analyzing Col VII distribution at the equator in four quadrants (inferior-superior-temporal-nasal) by two authors (BW, RJW) independently, at 400x magnification. Sections of one eye did not contain sufficient retina tissue and were excluded. Numbers of Col VII-labeled spots were quantified per retinal layer. Transversally cut sections were used for analyzing distributions in anterior, equator, and posterior regions. The retinal sections were masked except for an open window at these regions, 3 mm in diameter. Two authors (LIL, RJW) analyzed the retina within these windows and quantified Col VII spots at 400x magnification.

Confocal microscopy

Sections from paraffin-embedded eyes and retinal whole mounts were used for double staining Col VII/GFAP experiments. In order to block nonspecific binding of the primary antibodies, sections were incubated with PBS containing 2% fatty acid free BSA (Sigma), for 30 minutes. The sections were incubated with primary antibodies (anti-Col VII rabbit polyclonal, 1:100; anti-GFAP mouse monoclonal, Sigma, 1:100) in 1%BSA/PBS, for 1 hour. Then, sections were incubated in rabbit anti-mouse tetramethyl rhodamine isothiocyanate (TRITC, Sigma, 1:500) and swine anti-rabbit fluorescein isothiocyanate (FITC, Dako, 1:500) for 45 minutes. Nuclei were visualized with (1:5000) 4', 6'-diamino-2-phenylindole solution (DAPI, Sigma). All steps were performed at room temperature. Whole retina preparations were fixed (2% paraformaldehyde, 20 minutes), incubated in 1% Triton X-100/dH₂O (10 minutes) and washed extensively to remove loose retinal pigment epithelia fragments. These preparations were then incubated in 3% H₂O₂/PBS for three days to reduce autofluorescence of the remaining pigment epithelium and 5%/PBS blocking buffer for 24 hours. Two primary antibody combinations were used, for increased probative value: (1) anti-Col VII rabbit polyclonal (1:200) and anti-GFAP mouse monoclonal (1:200), followed by the above mentioned secondary antibodies and DAPI, (2) anti-Col VII monoclonal (1:100) and anti-GFAP polyclonal (1:100), followed by the secondary antibodies donkey anti-mouse Red-X (Jackson, Suffolk, UK, 1:100) and donkey anti-rabbit FITC (Jackson, 1:100) and DAPI. All incubations

were performed for 24 hours, all steps were performed at 4°C. In control samples, the primary antibodies were omitted. Visualization was done in a Leica TCS Sp2 confocal microscope, using Leica imaging software (LAS AF, LCS). The primary polyclonal anti-Col VII antibody specificity was tested on single-stained normal and Col VII deficient skin paraffin sections, which underwent the same procedures as described above.

Pre-embedding in epon

For ILM analysis, pieces of both posterior and anterior retina were dissected and fixed in 2% paraformaldehyde for 2 hours. These pieces were washed in 0.1% NaBH₄ with 6.8% sucrose in phosphate buffer. Blocking was done overnight, using 5% BSA and 5% goat serum. Specimens were incubated in primary polyclonal antibody (1:100) overnight. They were washed and incubated in secondary gold-labeled antibody (Gold Colloid 2nm, British Biocell International, Cardiff, UK, 1:200) overnight. The samples were washed, fixed in 2% glutaraldehyde for 30 minutes, washed in 0.1 M cacodylate buffer, and contrasted using 1% osmium tetroxide. Then a silver enhancement step was performed (R-gent enhancer kit protocol, 1:1, Aurion) for 5 minutes, at room temperature. After washing, the samples were dehydrated in ethanol (50%-100%) and propylene oxide, and then mounted in epon. In retina control sections, the primary antibodies were omitted. The primary antibody specificity was tested on cornea samples which underwent the same procedure as described above. All steps were performed at 4°C. Sections of 100 nm were cut using an ultramicrotome (Ultracut type 701, Reichert-Jung, Austria) and placed on copper grids (150 mesh). Sections were incubated in uranyl acetate, methanol, and Pb/NaOH, respectively, for 2 minutes each. Analysis was done using a CM100 BioTwin TEM (Philips, Eindhoven, the Netherlands) and iTEM software (ResAlta Research Technologies, Golden, CO, USA).

Post-embedding in T8100

Sections of 100 nm were cut and mounted on grids. They underwent the same procedures as described for light microscopy. Then, after incubation of the primary polyclonal anti-Col VII antibody (1:100) for 1 hour at 37°C, samples were incubated in secondary gold-labeled antibody (Gold Colloid 5nm, British Biocell International, 1:200) for 1 hour at room temperature. Samples were fixed in 2% glutaraldehyde for 2 minutes after which silver enhancement (kit protocol 1:1) was performed for 10 minutes. Samples were contrasted by methylcellulose-uranyl acetate (9:1) for 15 minutes at 4°C and analyzed (CM100).

Western blot

Retinae were dissected and homogenized by pipetting for 10 minutes without any additives and divided into four groups (A, B, C, D). The supernatants were tested for collagenous content by establishing their susceptibility to digestion by bacterial type VII collagenase (high purity grade, Sigma).²¹ In groups A and B, no collagenase was added. In groups C and D, collagenase was added to supernatants in 30 units/ml and 60 units/ml concentrations, respectively. Samples of groups B through D were incubated at 37°C for 120 minutes. Previously, the absence of nonspecific proteases in the collagenase batch had been confirmed.²² Because the non-collagenous terminal domains of Col VII are known to be susceptible to pepsin, pepsin digestion was performed on fresh retinal supernatant for 1 hour at 37°C at a final concentration of 1 mg/ml. Polyacrylamide SDS electrophoresis was executed in conformity with Laemmli's technique²³ as described,¹⁷ using 5% slab gels and a 72 mm wide 2D gel comb in a Bio-Rad Mini Protean II electrophoresis apparatus (Bio-Rad, Hercules, CA, USA). Afterwards, the gel was blotted to nitrocellulose paper using a Mini Protean II blotting unit (Bio-Rad) with 22 mM Tris, 0.05% SDS, 168 mM glycine, and 20% methanol as a transfer buffer. Then, the blot was blocked for 1 hour in TBS-buffer (20 mM Tris-HCl and 500 mM NaCl; pH 7.5) containing 3% BSA. Primary rabbit polyclonal antibody diluted 1:500 in TBS was added to the blot. After incubation overnight, the blot was washed with TBS containing 0.05% Tween-20 (TTBS). Secondary mouse-anti-rabbit antibody diluted 1:1000 in TBS was added. After 1 hour of incubation, the blot was washed with TTBS and incubated with alkaline phosphatase conjugated tertiary goat-anti-mouse antibody diluted 1:500 in TTBS for another hour. After washing with TTBS and alkaline phosphatase buffer (100 mM Tris-HCl, 100 mM NaCl, and 5 mM MgCl₂, pH 9.5), the blot was developed with nitro blue tetrazolium and 5-bromo-4-chloro-3-indolyl phosphate in alkaline phosphatase buffer. Incubation and washing steps were performed at room temperature.

RESULTS

Immunohistochemistry by light microscopy

Qualitative aspects of corpora amylacea

By LM, anti-Col VII labeling was most obvious in cytoplasmic inclusions within astrocytic processes, known as corpora amylacea (CA). All CA were periodic acid-Schiff-positive (PAS) due to their glycoproteinaceous contents (**Figure 1**). The overlap between PAS-

and Col VII-positivity seemed absolute. All anti-Col VII antibodies labeled CA similarly. CA were mainly located at the posterior pole. Their numbers diminished towards the pre-equatorial and anterior areas (**Table 1**). Some CA also reacted with anti-GFAP and anti-vimentin antibodies (**Sup info Fig 1**). Negative control sections showed no labeling (**Figure 1**).

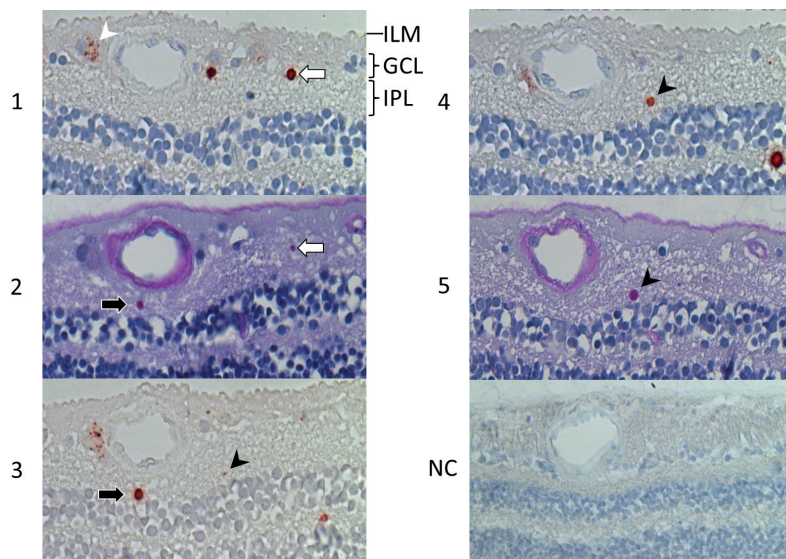


FIGURE 1. Retinal type VII collagen distribution. Immunohistochemical analysis at the vitreoretinal junction of a paraffin-embedded, serially sectioned (thickness 3-4 μm) human donor eye evaluated by light microscopy. Anti-type VII collagen labeling with monoclonal LH7.2 (sections **1, 3 & 4**) and periodic acid-Schiff (sections **2 & 5**). Type VII collagen is present in astrocytic corpora amylacea. At least three corpora amylacea were sliced in this series, consecutively visualized in sections 1-2 (white arrows), sections 2-3 (black arrows) and sections 3-5 (black arrowheads). Corpora amylacea reside in the ganglion cell layer and inner plexiform layer (IPL). Type VII collagen is also present in small vesicles, clustered near large nuclei in the inner retina (white arrowhead). The vesicles reside outside the nucleus, and within the cytoplasm (sections 1, 2 & 3 compared). The cytoplasm of the type VII collagen yielding cell type seems more extensive than that of most other cells residing in the ganglion cell layer (GCL). Furthermore, their nuclei are larger and appear less dense in PAS (or hematoxylin) stains. The inner limiting membrane (ILM) does not label visibly for type VII collagen. Negative control section (NC) shows no labeling. Magnification x200.

TABLE 1. Distribution of Col VII-labeled corpora amylacea.

		eye 1	eye 2	eye 3	eye 4	total	total %
Age		29	56	70	74		
Gender		m	m	m	f		
Region	anterior	15	0	1	6	22	14.6
	equator	12	2	15	19	48	31.8
	posterior	29	3	14	35	81	53.6
	total	56	5	30	60	151	100
Layer	internal limiting membrane	0	0	0	1	1	0.7
	nerve fiber layer	2	0	0	4	6	4.0
	ganglion cell layer	3	2	0	17	22	14.6
	inner plexiform layer	44	3	26	35	108	71.5
	inner nuclear layer	7	0	4	3	14	9.3
	outer plexiform layer	0	0	0	0	0	0
	outer nuclear layer	0	0	0	0	0	0
	total	56	5	30	60	151	100#
Size	small	39	1	18	43	101	66.9
	medium	15	4	12	13	44	29.1
	large	2	0	0	4	6	4.0
	total	56	5	30	60	151	100

Numbers (n) of type VII collagen labeled corpora amylacea in human retina, as analyzed in transverse Technovit sections.[#]Percentages rounded up to whole numbers. The most common corpus amylaceum is relatively small and located in the posterior retina in the inner plexiform layer. There are considerable inter-donor variations. No clear age-related characteristics are obvious.

Quantitative analysis of corpora amylacea

The quantitative analysis and distribution patterns were analyzed in transverse sections. The size of ganglion cell nuclei was used for semi-quantitative comparison of the CA. CA with the size of a ganglion cell nucleus were termed “medium” size. If they were obviously smaller than ganglion cell nuclei, they were termed “small.” If they were obviously larger than ganglion cell nuclei, they were termed “large.” In nearly two-thirds of the cases (67%), the CA were smaller than ganglion cell nuclei. Only a few were designated as “large,” measuring up to three times the size of a ganglion cell nucleus, mainly in the nerve fiber layer (data not shown). Overall, CA were mainly distributed in the inner plexiform layer (72%) and the posterior region (54%) (Table 1). Distribution of the (Col VII-labeled) CA appears to differ both inter-ocularly and intra-ocularly. For

example, transverse sections of eyes "1," "2," and "3," combined, contained about 96% of all the Col VII-labeled spots, whereas eye "1" only contained about 4%. Our sample size is too small to be able to indicate possible causes of these inter-individual differences. Therefore, the results have been arranged conveniently (**Table 1**).

Clustered small vesicles

Col VII expression was observed in small, clustered vesicles within cells that resided in the ganglion cell layer and, to lesser extent, in the inner plexiform layer. In comparison to most ganglion cells, these vesicle-associated cells were shown to have large nuclei, with low nuclear hematoxylin staining densities (**Figure 1**). Furthermore, their PAS-stained cytoplasm appeared voluminous, in which the widely dispersed vesicles were probably confined to. Rarely, some non-dispersed vesicles were detected in the outer nuclear layer. These vesicles resided at (or close to) the cell nucleus (**Sup info Figure 2**). The vesicles stained weakly with periodic acid-Schiff (**Figure 1**). They were not labeled by anti-vimentin antibodies (data not shown). In some donor samples, the vesicle-associated cells were numerous (**Figure 2**).

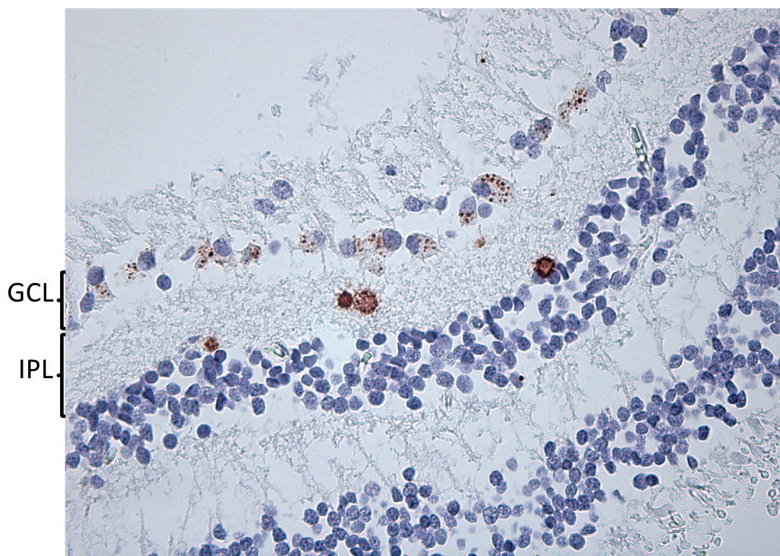


FIGURE 2. Immunohistochemical analysis at the vitreoretinal junction of a paraffin-embedded section. Anti-type VII collagen labeling with monoclonal LH7.2. This donor sample contains a lot of cells within the ganglion cell layer (GCL) that have Col VII-positive vesicles in their cytoplasm. Four corpora amylacea reside in the inner plexiform layer (IPL). Magnification x400.

Inner limiting membrane

By LM, the donor eyes included in this study did not show conclusive Col VII expression at the ILM itself. In two donor eyes, an epiretinal membrane was observed, which did express detectable Col VII levels.

Confocal microscopy

On confocal microscopy, Col VII-positive vesicles were intensely labeled and located within the cytoplasm, at variable distances from the cell nucleus, and without apparent polarization (**Figure 3**). The vesicle-associated cells resided mainly in the ganglion cell layer and inner plexiform layer (Sup info Video 1). In most donor samples, Col VII and GFAP-positive vesicles colocalized within clusters besides filamentous labeling of the

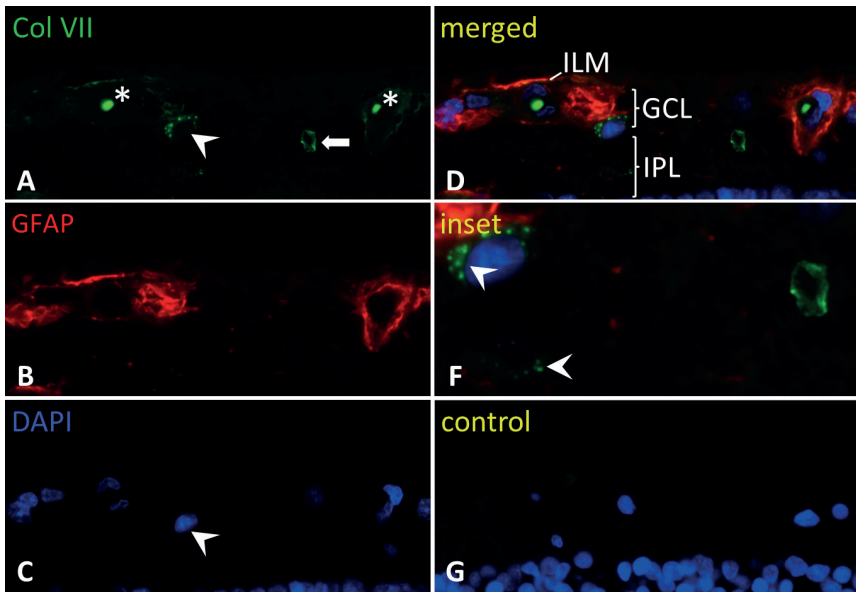


FIGURE 3. Confocal microscopy image of retinal section. (A-C) Type VII collagen-positive vesicles (LH7.2; green) are seen around cell nuclei (*white arrowhead*; DAPI blue) in the inner plexiform layer (IPL). Within the lumen of blood vessels, autofluorescent erythrocytes (*) are seen. Filamentous GFAP (polyclonal; red) labeling within the nerve fiber layer and around blood vessels. They can be discriminated from the corpus amylaceum (*white arrow*) in terms of fluorescence intensity, size and location. (D, F) The inner limiting membrane (ILM) directly above the left blood vessel shows some focal positivity for type VII collagen labeling in the merged channels compilation. (G) A control section does not show any Col VII or GFAP labeling. GCL ganglion cell layer. Magnification x400; *inset* x960.

nerve fiber layer (**Figure 4**). Filamentous labeling was increased around blood vessels. Some donor samples lacked GFAP-positivity in the Col VII-positive vesicle clusters (**Figure 3**). Others had GFAP/Col-VII-positive CA and vesicles, but lacked filamentous labeling (**Figure 5**) Retinal control sections showed no labeling (**Figure 3**). Skin sections served as positive (normal skin) and negative control (rEBD skin). The primary polyclonal antibody specifically stained the dermal-epidermal basement membrane from a healthy donor sample, in contrast to that of a Col VII deficient donor sample (**Sup info Figure 4**).

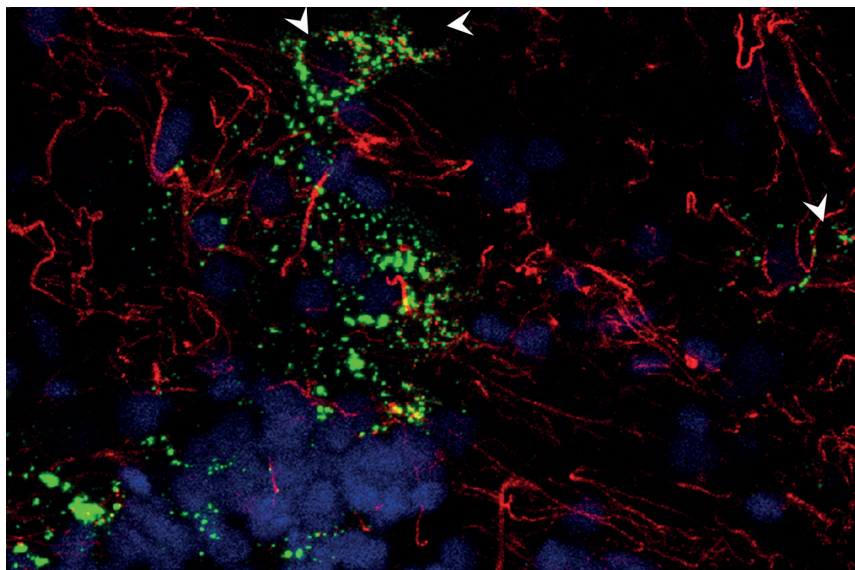


FIGURE 4. Confocal microscopy image of retinal wholemount. Type VII collagen-positive vesicles (LH7.2; green) colocalize with GFAP-positive vesicles (polyclonal; red) around cells (*white arrowheads*, note that their nuclei are not included in this section). In this donor sample, filamentous GFAP labeling is observed in the nerve fiber layer. This overlay projection is of the nerve fiber layer down to the inner plexiform layer. Most Col VII vesicles are located at the junction of ganglion cell layer and inner plexiform layer. Although GFAP positive filaments meander around nuclei, the GFAP vesicles can be distinguished from sectioned filaments. Magnification x630.

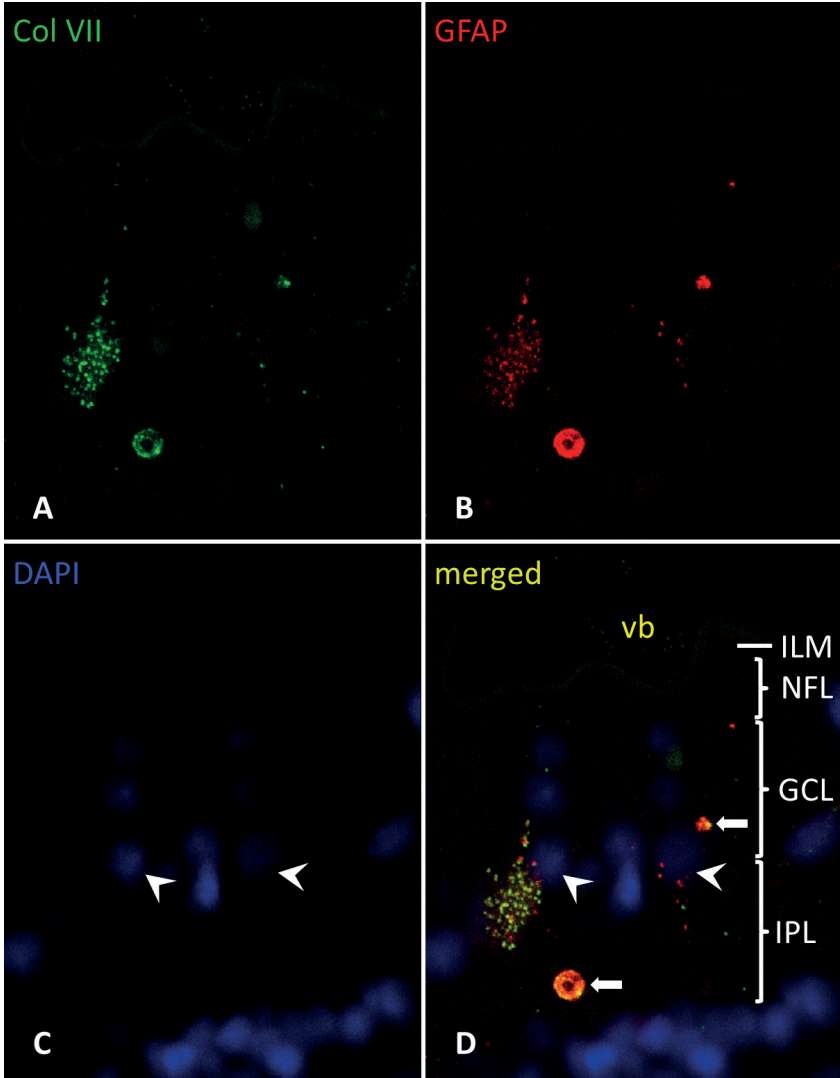


FIGURE 5. Colocalization of type VII collagen and GFAP within vesicle clusters and corpora amylacea. Image of the inner retina, paraffin section. Type VII collagen labeling (**A**, polyclonal; green) colocalizes with that of GFAP (**B**, monoclonal; red). (**C**, **D**) The vesicle cluster around one nucleus (*left white arrowhead*) contains both Col VII- and GFAP-positive vesicles, while another cluster (*right white arrowhead*) has few Col VII-positive vesicles. Most vesicles contain both type VII collagen and GFAP and label yellowish, but others contain either Col VII or GFAP. In this donor sample, no filamentous GFAP labeling is detected (by monoclonal antibodies) at the nerve fiber layer (NFL). Two corpora amylacea can be seen, both labeled dually (*white arrows*). ILM inner limiting membrane, GCL ganglion cell layer, IPL inner plexiform layer, vb vitreous body. Magnification x400.

Transmission electron microscopy

Col VII was detected in both posterior and anterior retinal ILM, with good specificity, in T8100 and epon embedded samples. The ILM contained gold labeling not only on the vitreous side (**Figure 6A- C**), but also in deeper parts of the ILM itself. Mostly, concomitant deep and superficial gold labeling was observed (**Figure 6A, C**). Gold labeling was also located alongside numerous vitreous fibers. There seemed to be no increase in gold labeling in the trajectory underneath their insertions in the ILM. There was no obvious variation in gold labeling toward the posterior pole, despite the increase in ILM thickness. Classical arcade shaped AF were not distinguished. Positive

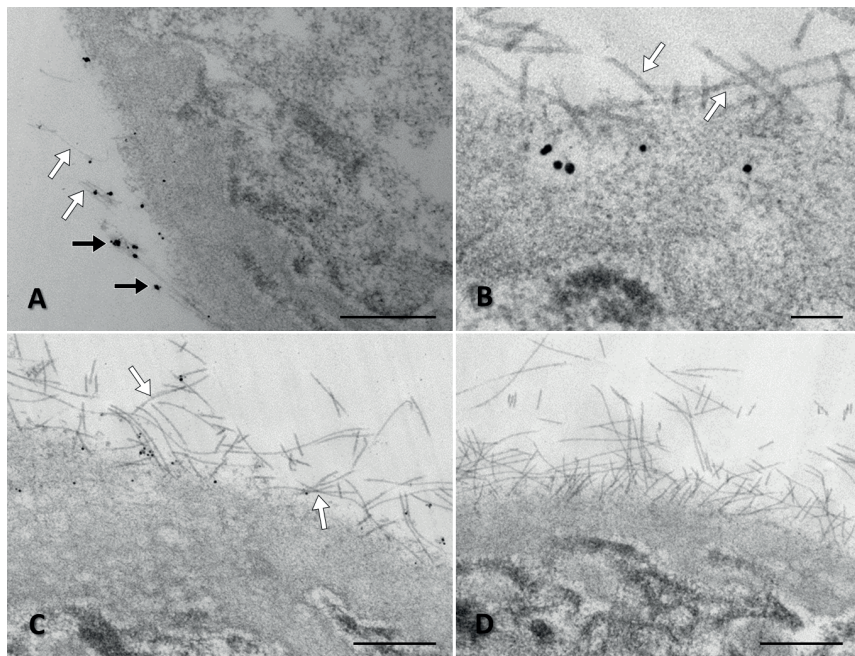


FIGURE 6. Type VII collagen is visualized at the vitreoretinal interface by immuno-TEM (epon). Immuno-electron microscopic image of the inner limiting membrane of a human retina. (**A-C**) Immunogold-labeled polyclonal antibody directed against type VII collagen (*black arrows*) is found in the direct vicinity of vitreous fibrils (*white arrows*) at the vitreoretinal interface. Some gold labeling is also situated within the inner limiting membrane (*ILM*). (**A**) Anterior retina, showing sparse, clustered labeling. Vitreous collagen fibrils join the retina. (**B**) The posterior retina has frequent gold labeling at a depth of 150-200 nm in the inner limiting membrane. (**C**) Posterior retina, gold labeling for type VII collagen is mostly at the retinal side of the vitreous fibrils. Müller cell endfeet (*M*) remain unlabeled. vb vitreous body. (**D**) Negative control of posterior retina shows no labeling. Scale bars A 500 nm; B 100 nm; C and D 500 nm.

control cornea samples showed gold labels on AF at the basement membrane zone. The gold labeling was intense and very specific, when using the polyclonal antibody (**Sup info Figure 5**). Both the Müller cell endfeet and the negative controls showed no labeling (**Figure 6D**), but had some background staining from silver enhancement. In the T8100 specimens, CA contained diffusely dispersed immunogold labeling (**Figure 7**). In contrast to the corneal basement membrane, no fibrillar shapes could be distinguished within CA. Furthermore, the vesicles (and the associated cells) could not be identified, due to absent gold labeling at their appropriate locations.

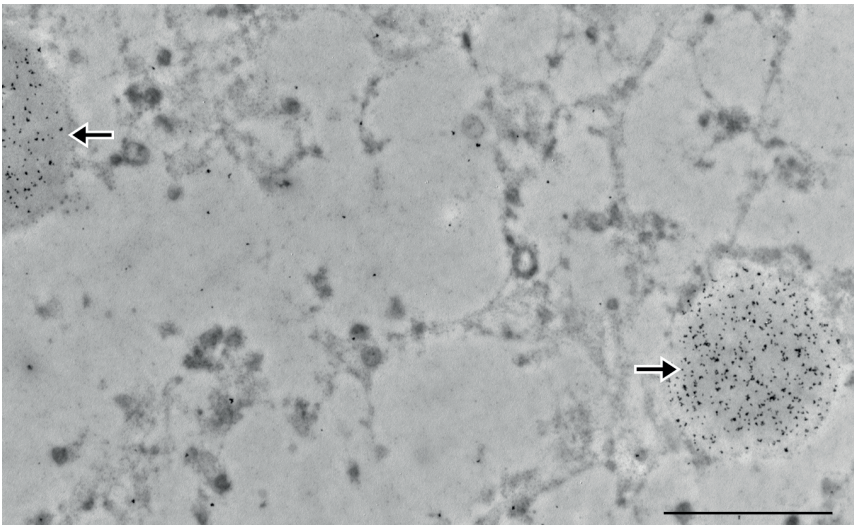


FIGURE 7. Type VII collagen is visualized within corpora amylacea (T8100). Immuno-electron microscopic image of the inner plexiform layer of a human retina. Immunogold-labeled polyclonal antibody directed against type VII collagen labels two corpora amylacea (*arrows*) diffusely. Within the corpora amylacea, there is no evidence of fibrillar collagen or banding. Some background labeling is present. Scale bar 5 μm .

Western blot

The immunoblotting showed a specific band at 290 kDa (**Figure 8A**). After two hours of incubation in collagenase (30 units/ml), the 290 kDa band disappeared completely due to digestion. Meanwhile, a 145 kDa band of degradation products was formed (**Figure 8C**). Without collagenase addition, the 290 kDa band faded in two hours (**Figure 8B**) due to auto-digestion. After two hours of incubation in collagenase (60 units/ml), all bands had disappeared (group D; data not shown). The use of an LH7.2 monoclonal

antibody resulted in the appearance of a 320 kDa band in addition to the 290 kDa and 145 kDa bands (**Sup info Figure 6**). The 320 kDa band probably corresponds to type VII procollagen. After pepsin digestion, all bands had disappeared (**Sup info Figure 7**).

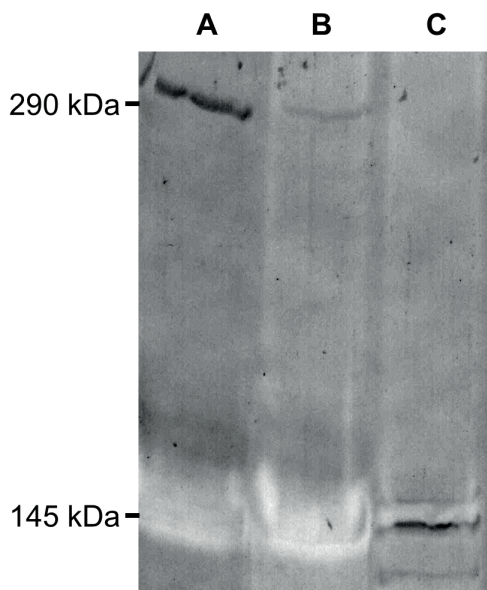


FIGURE 8. Western blot confirms type VII collagen content in retinal substrates. Western blot stained for type VII collagen. A 290 kDa band appeared in samples (directly) placed in reducing agent buffer (group/lane **A**). Omitting the use of reducing agents resulted in fading of the 290 kDa band (group/lane **B**). When samples were incubated in 30 units/ml collagenase, the 290 kDa band disappeared completely, while a 145 kDa band appeared (group/lane **C**).

DISCUSSION

Corpora amylacea

The Col VII positive “spots” previously described by Ponsioen et al.,¹⁷ were found to correspond to CA. CA are smooth (or granular) structures that occur in round or oval forms, measuring 1 to 50 μm in diameter.²⁴⁻²⁷ Ocular CA are found in the inner retinal layers (i.e. nerve fiber layer through inner nuclear layer) and optic nerve.²⁷⁻²⁹ Here, they

reside most frequently in astrocytes, or occasionally within neuritic processes, but also exist as extracellular deposits. They are thought to be of mitochondrial origin.³⁰ Since astrocytes, and their processes, are closely associated with retinal ganglion cells^{28, 31} and contain GFAP³² and vimentin³³, our qualitative and quantitative CA characteristics correlate with earlier investigations.^{28, 34} We expect that during normal ageing (or neurodegeneration) some Col VII molecules (or epitopes) lose their function and are therefore phagocytized by astrocytes and stored in CA. In correspondence to similar protein accumulations within CA,³⁵ this would benefit retinal neuroprotection. Otherwise, obsolete proteins could aggravate the immune system, leading to neuronal damage.^{26, 33, 37}

Vesicles

The Col VII-labeled vesicles, which Ponsioen termed “dots”,¹⁷ reside in a cell type with decreased nuclear density. Low densities may arise when the nuclear euchromatin is increased, indicating active gene transcription. Since the Col VII-labeled vesicles were also labeled by anti-GFAP antibodies during CA quantification experiments in paraffin, we suspected these Col VII/GFAP-labeled vesicles to reside in activated astrocytes. Additionally, the distribution of these vesicle-associated cells is comparable with that of astrocytes. Both predominantly reside in the nerve fiber layer and ganglion cell layer,^{32, 38} although astrocytes can migrate to other layers where vesicles were found, e.g. the inner plexiform layer and outer nuclear layer. Alternatively, ganglion cells are a candidate cell type, based on the predominant ganglion cell layer distribution of the vesicle-associated cells. The presence of Col VII in idiopathic epiretinal membranes would be consistent with either cell type, since both astrocytes and ganglion cell neurites can be present in these membranes.^{39, 40} The Col VII positive vesicles might reflect Col VII synthesis, phagocytosis, or both. At present, our data is not robust enough to differentiate between these possibilities.

Vitreoretinal interface

Immunogold labeling suggests low concentrations of Col VII in comparison to other collagens, as in skin.⁴¹ Small quantities of Col VII may be clinically relevant, since absence or malfunction of Col VII leads to severe blistering in the skin. The vitreoretinal Col VII distribution suggests interactions with vitreous collagen fibers, therefore probably performing a role in vitreoretinal attachment. We visualized the NC1 domains of Col VII inside the ILM, although AF were not seen. *In vivo*^{11, 14, 15, 42-44} and *in vitro*^{6, 12} investigations acknowledge difficulties in visualizing AF, despite apparent Col VII labeling. Some authors have advocated that only one end of the skin AF inserts into

the basement membrane,⁴⁵ while others state that lateral aggregation might not be necessary for a functional role.⁴⁶ In skin, laterally aggregated AF can entrap stromal matrix components by looping back into the lamina densa.^{1, 8, 9, 47, 48} It is conceivable that the lateral aggregation is not compulsory for a functional role. Furthermore, in rat trachea, the AF that are actually entrapping underlying fibers are few, which would indicate that their arcade shape might not provide the sole anchoring modus.⁴⁶ Generally, the dermal AF density seems to correlate with the frictional exposure of the tissue, suggesting a function in stabilizing the epithelial-stromal border.² Despite this important function, Col VII constitutes only 0.001% of the total skin tissue collagens.⁴¹ In the inner eye, we expect this proportion and thus the number of AF (if present) to be even lower, given the challenge of adequate immunolabeling. Moreover, AF numbers vary widely both among individuals and within the same subject.⁴⁹ Furthermore, epitope recognition by anti-Col VII antibodies can be influenced, even in cell cultures, as illustrated by a study using different fixation techniques.¹ For these reasons and concomitant technical difficulties,² demonstrating Col VII or visualizing AF can be a challenge in itself.⁴⁶

Limitations

Our study demonstrates vitreoretinal Col VII depositions, without the obvious AF formations found at dermal and corneal basement membrane zones.^{2, 14} The lack of evident AF can be considered as a limitation of our study, although a low AF density and alternative functional Col VII formations⁵⁰ would sufficiently explain this. Our dataset is too small to draw conclusions about age-related influences, such as the numbers of CA containing Col VII, or the weakening of the vitreoretinal interface because of degenerating adhesive molecules that could give rise to age-related vitreous degeneration and posterior vitreous detachment. In contrast to whole mounts and paraffin samples, no vesicles were labeled in the T8100 and epon samples. The glycol methacrylate T8100 was elected for maintaining good tissue morphology, but at the possible expense of labeling sensitivity. Firstly, glycol methacrylate cannot be removed completely. Therefore, slides are etched in order to retrieve antigens. Secondly, because of its hydrophobic nature, residual T8100 can hinder antigen-antibody complex formation. In epon samples, the lack of vesicular labeling could be explained by limited antibody penetration.

CONCLUSION

We detected Col VII expression 1.) in corpora amylacea, 2.) within intracellular vesicles, of an undisclosed cell type residing in the ganglion cell layer and inner plexiform layer, and 3.) at the inner limiting membrane. At these sites, no anchoring fibrils could be visualized.

Acknowledgements

We would like to thank Professor RA Bank from the Department of Medical Biology, University Medical Center Groningen, for his critical appraisal and the Euro Cornea Bank for supplying donor eyes.

SUPPORTING INFORMATION

SUPPORTING INFORMATION TABLE 1. Donor materials.

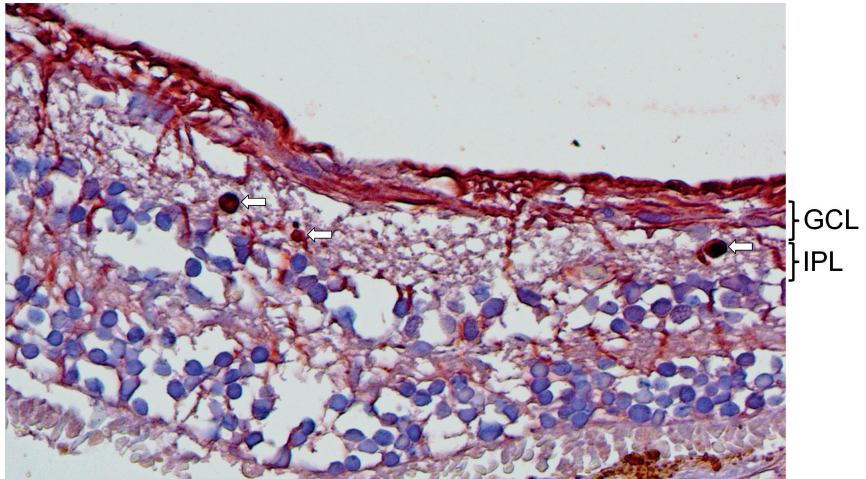
Assay	Age	Gender	Cause of Death	Comorbidity	Embedded	Side
Counting CA & Cornea AF	74	f	lung embolia	carcinoma	T8100 post embedding	Left
	29	m	brain tumor		T8100 post embedding	Left
	70	m	respiratory failure	COPD	T8100 post embedding	Left
Counting CA & ILM AF	56	m	myocardial infarction	TS trauma, heart surgery	T8100 post embedding	Both
ILM AF	77	m	recurrent atrial fibrillation		T8100 post embedding	Right
	78	f	myocardial infarction, asystolia		T8100 post embedding	Right
	<i>n = 7</i>					
ILM Analysis by TEM	68	m	malignancy, mesothelioma	Grawitz tumor	Epon pre embedding	Right
	17	f	head trauma		Epon pre embedding	Right
	71	f	circulational,		Epon pre embedding	Both
	48	f	liver cirrhosis	alcohol abuse	Epon pre embedding	Left
	82	m	head trauma		Epon pre embedding	Left
	81	m	bladder malignancy		Epon pre embedding	Left
	<i>n = 7</i>					
Fluorescence & IHC	67	f	hepatic encephalopathy	alcohol abuse	paraffin	Left
	73	f	malignancy, brain metastasis		paraffin	Left
	80	f	malignancy		paraffin	Both
	64	f	respiratory		paraffin	Right
Fluorescence	70	f	lung malignancy		wholemout	Left
	79	f	pneumonia	pharynx malignancy	wholemout	Left
	81	m	heart		wholemout	Left
	57	f	malignancy		wholemout	Left
	<i>n = 9</i>					
Western Blot	74	m	malignancy		pooled	Left
	70	f	circulational		pooled	Left
	66	m	trauma		pooled	Left
	<i>n = 3</i>					

Twenty-eight donor eyes without known ophthalmic disorders were used for our experiments. Experiment type and donor characteristics are listed.

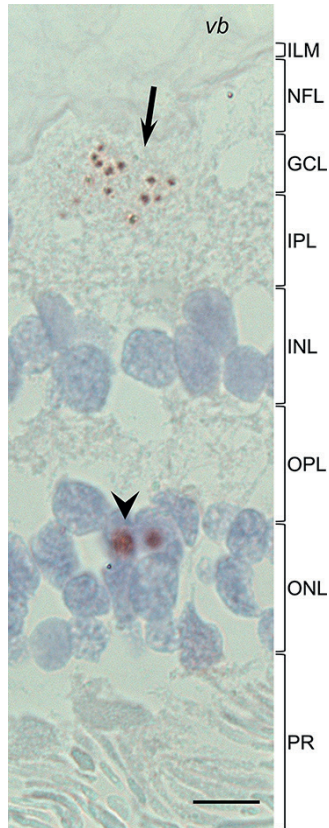
SUPPORTING INFORMATION TABLE 2. Antibodies.

Primary antibody	Clonality	Host	Isotype	Company	Catalogus no.	Antibody Registry	Immunogen
Anti-Collagen, type VII	Polyclonal	Rabbit	IgG	Cabiochem (Merck/ Millipore)	234192	AB_211739	purified, human placenta collagen type VII
Anti-Collagen, type VII [LH7.2]	Monoclonal	Mouse	IgG1	Abcam	ab6312	AB_305415	Full length native protein (purified) (Human). Insoluble fractions prepared from neonatal foreskin epidermal cells.
Anti-Collagen, type VII [H-32]	Monoclonal	Mouse	IgG1	Chemicon (Merck/ Millipore)	MAB2500	AB_94355	Recognizes human and bovine Type VII Collagen.
Anti-GFAP [G-A-5]	Monoclonal	Mouse	IgG1	Sigma-Aldrich	G3893	AB_477010	GFAP from pig spinal cord
Anti-GFAP	Polyclonal	Rabbit	IgG	Abcam	ab7260	AB_305808	GFAP from myelin associated material from bovine spinal cord
Anti-Vimentin [Vim 3B4]	Monoclonal	Mouse	IgG2a kappa	Dako	M7020	AB_2304493	Vimentin isolated from bovine eye lens
Secondary antibody							
Rabbit anti-Goat HRP				Dako			
Rabbit anti-Mouse HRP				Dako			
Swine anti-Rabbit HRP				Dako			
Swine anti-Rabbit FITC		1:500		Dako			
Rabbit anti-Mouse TRITC		1:500		Sigma			
Donkey anti-mouse	Polyclonal	1:100	Whole IgG	Jackson	715-295-150	AB_2340831	
Donkey anti-rabbit	Polyclonal	1:100	Whole IgG	Jackson	711-295-152	AB_2340613	
Gold Colloid 2nm		1:200		British Biocell International			
Gold Colloid 5nm		1:200		British Biocell International			
essentially fatty acid free BSA				Sigma-Aldrich			

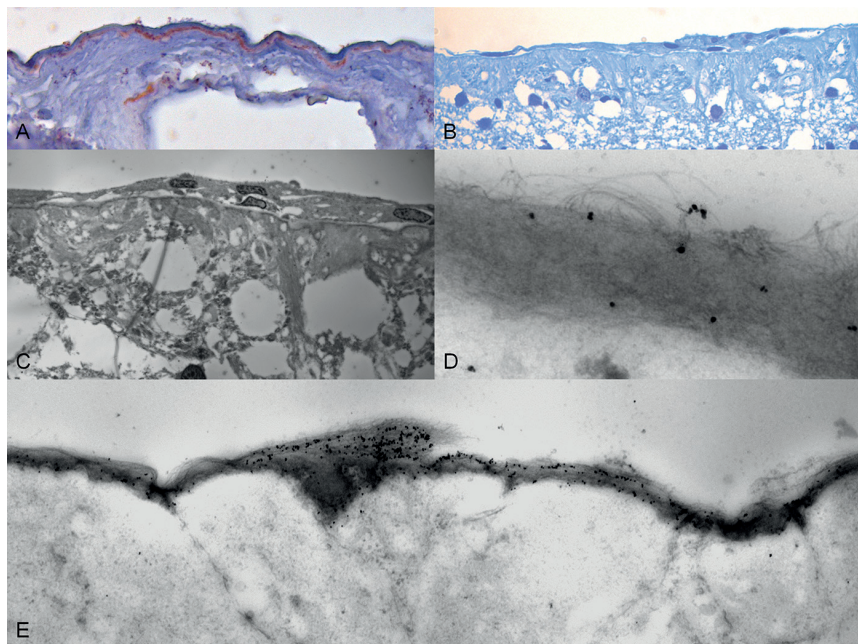
Overview of antibody characteristics.



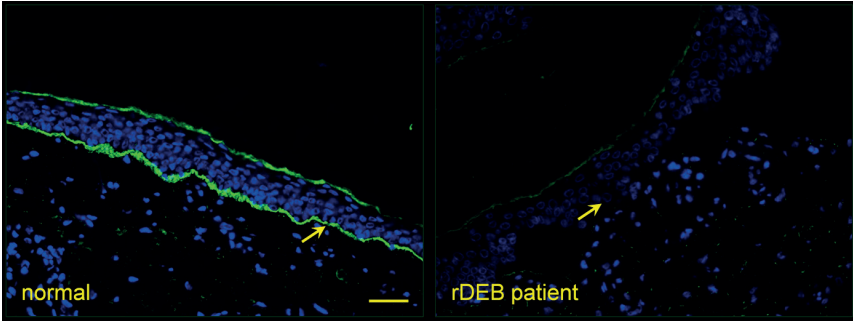
SUPPORTING INFORMATION FIGURE 1. Retinal vimentin distribution. Immunohistochemical analysis at the vitreoretinal junction of a paraffin-embedded section. Monoclonal anti-vimentin labeling is seen in Müller cells, but also in corpora amylacea of the inner plexiform layer (*IPL*) (*white arrows*). *GCL* ganglion cell layer. Magnification x20.



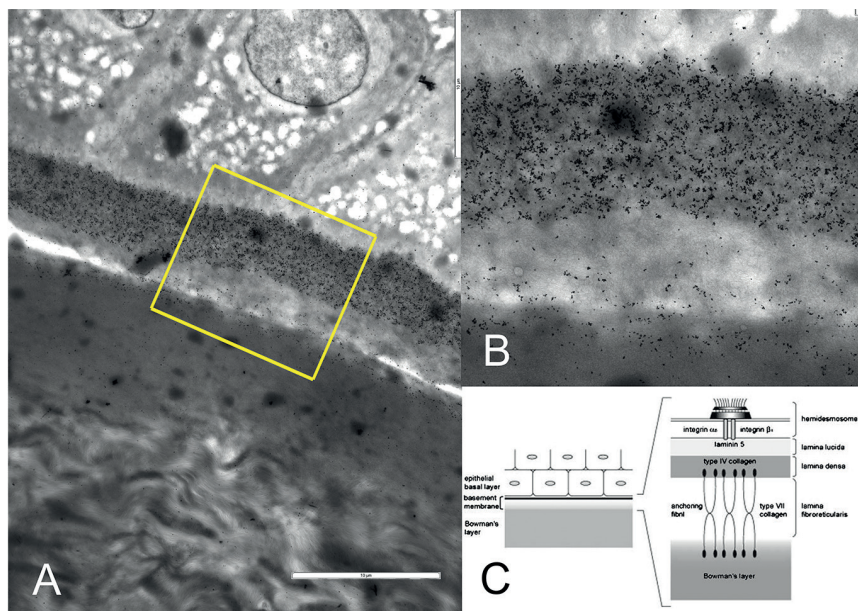
Supporting information Figure 2. Retinal type VII collagen distribution: inner plexiform layer vs. outer nuclear layer. Immunohistochemical analysis at the vitreoretinal junction of a paraffin-embedded, serially sectioned human donor eye evaluated by LM peroxidase staining. Polyclonal anti-type VII collagen labeling is seen in close vicinity to the nucleus in the outer nuclear layer (*arrowhead*), while reactivity is seen dispersed in the cytoplasm in the nerve fiber layer (*arrow*). *ILM* inner limiting membrane, *NFL* nerve fiber layer, *GCL* ganglion cell layer, *IPL* inner plexiform layer, *INL* inner nuclear layer, *OPL* outer plexiform layer, *ONL* outer nuclear layer *PR* photoreceptors, *vb* vitreous body. Scale bar 500 nm.



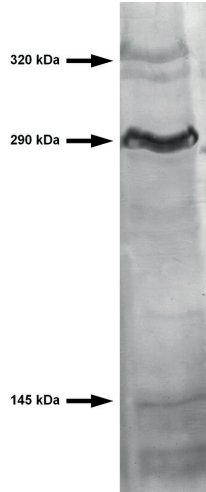
Supporting information Figure 3. Type VII collagen expression in (human) epiretinal membrane. (A) Immunohistochemical staining of a 73-year-old female retina, polyclonal anti-collagen type VII on paraffin sections. A dense epiretinal membrane is seen, as a dark blue layer containing cells. Between the epiretinal membrane and the ILM, type VII collagen labeling is seen (red). Labeling seems to be strongest directly underneath the cells. T8100 section of a 77-year-old male. (B) Hematoxylin, light microscopy. (C- E) Electron microscopy (post-embedded, polyclonal anti-Col VII antibody). (C) Overview of E. (D) Gold labels are found within the epiretinal membrane. Arcing fibers reminiscent of anchoring fibrils associate with the gold-labeled antibodies. (E) Intense gold labeling is seen without apparent arced fibers on lower magnification.



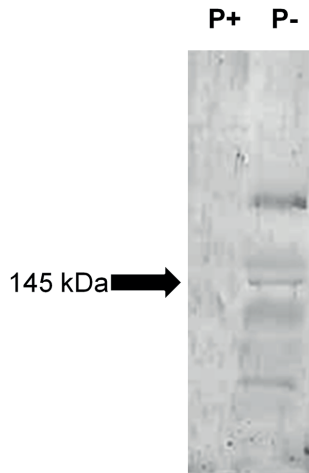
Supporting information Figure 4. Antibody specificity test: immunofluorescence staining intensities in skin of healthy control and recessive Epidermolysis Bullosa Dystrofica (rDEB) patient. Arrows point to type VII collagen deposition at the basement membrane zone. In contrast to the healthy control, the rDEB patient's type VII collagen deficient skin shows no immunofluorescence when tested with the polyclonal antibody. Please note that the remaining fluorescence in the rDEB is due autofluorescence of the stratum corneum. Scale bar 100 μm .



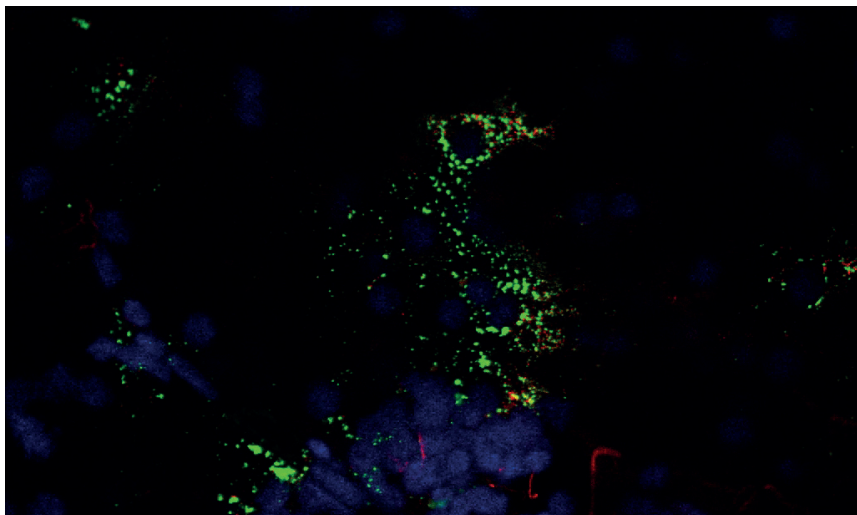
Supporting information Figure 5. Human Bowman's membrane of cornea, immunogold-labeled for type VII collagen. T8100, immuno-electron microscopic image. Polyclonal antibody directed against NC-1 domain of type VII collagen. **(A)** Intense immunogold-labeled lamina densa. Because of the arced shapes of the type VII collagen dimers, their NC-1 domains reside in the lamina densa as well as the superficial Bowman's layer. The intermediate lamina fibroreticularis itself, where the collagenous parts of the type VII collagen molecule reside, therefore has little gold labeling. An epithelial cell is seen above the basement membrane (top); the stroma is seen beneath the basement membrane (bottom). Bar 10 μm . **(B)** Inset. The lamina densa is intensely gold-labeled. **(C)** Schematic diagram of epithelial anchorage to the stroma (Adapted from Soma T, Nishida K, Yamato M, et al. *J Cataract Refract Surg.* 2009; 35: 1251-1259. Note the location of the NC-1 globuli of type VII collagen in C, depicted as black ovals, corresponding to the gold labels in A and B.



Supporting information Figure 6. Western blot of retinal substrates. Western blot of human (23-year-old female and 64-year-old male, pooled) retinal substrate. Monoclonal primary antibody (LH7.2). Both the 290 kDa and 145 kDa bands appear, although the latter only faintly. Negative control showed no bands. *For isolation of collagens see: Van Deemter M, Pas H, Kuijer R, et al. Invest Ophthalmol Vis Sci. 2009; 50:4552-4560.*



Supporting information Figure 7. Western blot of retinal substrates; pepsin digestion. Western blot of human (23-year-old female and 64-year-old male, pooled) retinal substrate. Monoclonal primary antibody (LH7.2). After one hour of digestion at 37°C with pepsin at a final concentration of 1 mg/ml (P+), no bands appeared, in contrast to omitting pepsin addition (P-). *For isolation of collagens see: Van Deemter M, Pas H, Kuijer R, et al. Invest Ophthalmol Vis Sci. 2009; 50:4552-4560.*



SUPPORTING INFORMATION VIDEO 1. Confocal microscopy imaging session presented as video. Retinal whole mount, from outer part of nerve fiber layer through inner part of inner plexiform layer. The polyclonal anti-type VII collagen antibody (green) labels intracellular vesicles. Vesicles within the same clusters may label with monoclonal anti-GFAP antibodies (red), indicating co-localization of both proteins within one vesicle or co-occurrence of both types of vesicles within one cell type. In the nerve fiber layer (first 2 seconds) GFAP labels glial filaments in a horizontal plane. The filaments then meander deeper into the retina. The GFAP positive vesicles can be distinguished from transversely 'cut' filaments. Cell nuclei are blue (DAPI).

This file is accessible through <https://doi.org/10.1371/journal.pone.0145502.s010>.

REFERENCES

1. Sakai L, Keene D, Morris N, Burgeson R. Type VII collagen is a major structural component of anchoring fibrils. *J Cell Biol.* 1986; 103:1577-1586.
2. Keene D, Sakai L, Lunstrum G, Morris N, Burgeson R. Type VII collagen forms an extended network of anchoring fibrils. *J Cell Biol.* 1987; 104:611-621.
3. Brody I. The keratinization of epidermal cells of normal guinea pig skin as revealed by electron microscopy. *J Ultrastruct Res.* 1959; 2:482-511.
4. Palade G, Farquhar M. A special fibril of the dermis. *J Cell Biol.* 1965; 27:215-224.
5. Leigh I, Purkis P, Bruckner-Tuderman L. LH7.2 monoclonal antibody detects type VII collagen in the sublamina densa zone of ectodermally-derived epithelia, including skin. *Epithelia.* 1987; 1:17-29.
6. König A, Bruckner-Tuderman L. Epithelial-mesenchymal interactions enhance expression of collagen VII in vitro. *J Invest Dermatol.* 1991; 96:803-808.
7. Wetzels R, Robben H, Leigh I, Schaafsma H, Vooijs G, Ramaekers F. Distribution patterns of type VII collagen in normal and malignant human tissues. *Am J Pathol.* 1991; 139:451-459.
8. Kawanami O, Ferrans V, Roberts W, Crystal R, Fulmer J. Anchoring fibrils. A new connective tissue structure in fibrotic lung disease. *Am J Pathol.* 1978;92(2):389-410.
9. Laguens R. Subepithelial fibrils associated with the basement membrane of human cervical epithelium. *J Ultrastruct Res.* 1972; 41:202-208.
10. Baker K, Anderson S, Romanowski E, Thoft R, SundarRaj N. Trigeminal ganglion neurons affect corneal epithelial phenotype. Influence on type VII collagen expression in vitro. *Invest Ophthalmol Vis Sci.* 1993; 34:137-144.
11. Paulus W, Baur I, Liszka U, Drlicek M, Leigh I, Bruckner-Tuderman L. Expression of type VII collagen, the major anchoring fibril component, in normal and neoplastic human nervous system. *Virchows Arch.* 1995; 426:199-202.
12. Bächinger H, Morris N, Lunstrum G, Keene D, Rosenbaum L, Compton L, et al. The relationship of the biophysical and biochemical characteristics of type VII collagen to the function of anchoring fibrils. *J Biol Chem.* 1990; 265:10095-10101.
13. Kenyon K. Recurrent corneal erosion: pathogenesis and therapy. *Int Ophthalmol Clin.* 1979; 19:169-195.
14. Gipson I, Spurr-Michaud S, Tisdale A. Anchoring fibrils form a complex network in human and rabbit cornea. *Invest Ophthalmol Vis Sci.* 1987; 28:212-220.
15. Tisdale A, Spurr-Michaud S, Rodrigues M, Hackett J, Krachmer J, Gipson I. Development of the anchoring structures of the epithelium in rabbit and human fetal corneas. *Invest Ophthalmol Vis Sci.* 1988; 29:727-736.
16. Tuori A, Uusitalo H, Burgeson R, Terttunen J, Virtanen I. The immunohistochemical composition of the human corneal basement membrane. *Cornea.* 1996; 15:286-294.
17. Ponsioen T, van Luyn M, van der Worp R, van Meurs J, Hooymans J, Los L. Collagen distribution in the human vitreoretinal interface. *Invest Ophthalmol Vis Sci.* 2008; 49:4089-4095.
18. Ponsioen T, van Luyn M, van der Worp R, Pas H, Hooymans J, Los L. Human retinal Müller cells synthesize collagens of the vitreous and vitreoretinal interface in vitro. *Mol Vis.* 2008; 14:652-660.
19. Balasubramani M, Schreiber E, Candiello J, Balasubramani G, Kurtz J, Halfter W. Molecular interactions in the retinal basement membrane system: a proteomic approach. *Matrix Biol.* 2010; 29:471-483.

20. Johnson M. How should we release vitreomacular traction: surgically, pharmacologically, or pneumatically? *Am J Ophthalmol.* 2013; 155:203-205. e1.
21. Kahl F, Pearson R. Ultrastructural studies of experimental vesiculation. II. Collagenase. *J Invest Dermatol.* 1967; 49:616-631.
22. Pas H, Kloosterhuis G, Heeres K, van der Meer J, Jonkman M. Bullous pemphigoid and linear IgA dermatosis sera recognize a similar 120-kDa keratinocyte collagenous glycoprotein with antigenic cross-reactivity to BP180. *J Invest Dermatol.* 1997; 108:423-429.
23. Laemmli U. Cleavage of structural proteins during the assembly of the head of bacteriophage T4. *Nature.* 1970; 227:680-685.
24. Purkinje J. *Bericht über die Naturforscherversammlung zu Prag im Jahre 1837* (cited by Catola G, Achúcarro N. Über die Entstehung de Amyloidkörperchen in Zentralnervensystem. *Virchow's Archiv für Pathologisch Anatomie und Physiologie und für Klinische Medizin.* 1906; 184:454-469.
25. Steele H, Kinley G, Leugtenberger C, Lieb E. Polysaccharide nature of corpora amylacea. *AMA Arch Pathol.* 1952; 54:94-97.
26. Robitaille Y, Carpenter S, Karpati G, DiMauro S. A distinct form of adult polyglucosan body disease with massive involvement of central and peripheral neuronal processes and astrocytes: a report of four cases and a review of the occurrence of polyglucosan bodies in other conditions such as Lafora's disease and normal ageing. *Brain.* 1980; 103:315-336.
27. Woodford B, Tso M. An ultrastructural study of the corpora amylacea of the optic nerve head and retina. *Am J Ophthalmol.* 1980; 90:492-502.
28. Kubota T, Naumann G. Reduction in number of corpora amylacea with advancing histological changes of glaucoma. *Graefes Arch Clin Exp Ophthalmol.* 1993; 231:249-253.
29. Kubota T, Holbach L, Naumann G. Corpora amylacea in glaucomatous and non-glaucomatous optic nerve and retina. *Graefes Arch Clin Exp Ophthalmol.* 1993; 231:7-11.
30. Song W, Zukor H, Liberman A, Kaduri S, Arvanitakis Z, Bennett DA, et al. Astroglial heme oxygenase-1 and the origin of corpora amylacea in aging and degenerating neural tissues. *Exp Neurol.* 2014; 254:78-89.
31. Kaur C, Sivakumar V, Yong Z, Lu J, Foulds W, Ling E. Blood-retinal barrier disruption and ultrastructural changes in the hypoxic retina in adult rats: the beneficial effect of melatonin administration. *J Pathol.* 2007; 212:429-439.
32. Ramirez J, Triviño A, Ramirez A, Salazar J, Garcia Sanchez J. Immunohistochemical study of human retinal astroglia. *Vision Res.* 1994; 34:1935-1946.
33. Selmaj K, Pawlowska Z, Walczak A, Koziolkiewicz W, Raine C, Cierniewski C. Corpora amylacea from multiple sclerosis brain tissue consists of aggregated neuronal cells. *Acta Biochim Pol.* 2008; 55:43-49.
34. Singhrao S, Neal J, Newman G. Corpora amylacea could be an indicator of neurodegeneration. *Neuropathol Appl Neurobiol.* 1993; 19:269-276.
35. Meng He H. Localization of blood proteins thrombospondin1 and ADAMTS13 to cerebral corpora amylacea. *Neuropathology.* 2009; 29:664-671.
36. Singhrao S, Neal J, Piddlesden S, Newman G. New immunocytochemical evidence for a neuronal/ oligodendroglial origin for corpora amylacea. *Neuropathol Appl Neurobiol.* 1994; 20:66-73.
37. Singhrao S, Morgan B, Neal J, Newman G. A functional role for corpora amylacea based on evidence from complement studies. *Neurodegeneration.* 1995; 4:335-345.

38. Triviño A, Ramírez J, Salazar J, Ramírez A. Human retinal astroglia. A comparative study of adult and the 18 month postnatal developmental stage. *J Anat.* 2000; 196:61-70.
39. Lesnik Oberstein SY. Ganglion cell neurites in human idiopathic epiretinal membranes. *Br J Ophthalmol.* 2008; 92:981-985.
40. Bu SC, Kuijer R, van der Worp RJ, Huiskamp EA, Renardel de Lavalette VW, Li XR, Hooymans JM, Los LI. Glial cells and collagens in epiretinal membranes associated with idiopathic macular holes. *Retina.* 2014; 34:897-906.
41. Bruckner Tuderman L, Schnyder U, Winterhalter K, Bruckner P. Tissue form of type VII collagen from human skin and dermal fibroblasts in culture. *Eur J Biochem.* 1987; 165:607-611.
42. Smith L, Sakai L, Burgeson R, Holbrook K. Ontogeny of structural components at the dermal-epidermal junction in human embryonic and fetal skin: the appearance of anchoring fibrils and type VII collagen. *J Invest Dermatol.* 1988; 90:480-485.
43. Woodley D, Burgeson R, Lunstrum G, Bruckner-Tuderman L, Reese M, Briggaman R. Epidermolysis bullosa acquisita antigen is the globular carboxyl terminus of type VII procollagen. *J Clin Invest.* 1988; 81:683-687.
44. Gipson I, Spurr-Michaud S, Tisdale A. Hemidesmosomes and anchoring fibril collagen appear synchronously during development and wound healing. *Dev Biol.* 1988; 126:253-262.
45. Briggaman R, Dalldorf F, Wheeler CJ. Formation and origin of basal lamina and anchoring fibrils in adult human skin. *J Cell Biol.* 1971; 51:384-395.
46. Wasano K, Yamamoto T. Microthread-like filaments connecting the epithelial basal lamina with underlying fibrillar components of the connective tissue in the rat trachea. A real anchoring device? *Cell Tissue Res.* 1985; 239:485-495.
47. Villone D, Fritsch A, Koch M, Bruckner-Tuderman L, Hansen U, Bruckner P. Supramolecular interactions in the dermo-epidermal junction zone: anchoring fibril-collagen VII tightly binds to banded collagen fibrils. *J Biol Chem.* 2008; 283:24506-24513.
48. McMillan J, Akiyama M, Shimizu H. Epidermal basement membrane zone components: ultrastructural distribution and molecular interactions. *J Dermatol Sci.* 2003; 31:169-177.
49. Tidman M, Eady R. Ultrastructural morphometry of normal human dermal-epidermal junction. The influence of age, sex, and body region on laminar and nonlaminar components. *J Invest Dermatol.* 1984; 83:448-453.
50. Ockleford C, McCracken S, Rimmington L, Hubbard A, Bright N, Cockcroft N, et al. Type VII collagen associated with the basement membrane of amniotic epithelium forms giant anchoring rivets which penetrate a massive lamina reticularis. *Placenta.* 2013; 34:727-737.



3

Chapter 3

Type VII collagen in the Human Accommodation System: Expression in Ciliary Body, Zonules and Lens Capsule

Bart Wullink^{1,2}

Hendri H Pas³

Roelofje J Van der Worp^{1,2}

Martin Schol¹

Sarah F Janssen^{4,5}

Roel Kuijer^{2,6}

Leonoor I Los^{1,2}

¹ Department of Ophthalmology, University Medical Center Groningen, University of Groningen Groningen, the Netherlands

² W.J. Kolff Institute, Graduate School of Medical Sciences, University of Groningen, Groningen, the Netherlands

³ Department of Dermatology, University Medical Center Groningen, University of Groningen, Groningen, the Netherlands

⁴ Department of Ophthalmology, VU Medical Center, Amsterdam, the Netherlands

⁵ Department of Clinical Genetics, Academic Medical Center, Amsterdam, the Netherlands

⁶ Department of Biomedical Engineering, University Medical Center Groningen, University of Groningen, Groningen, the Netherlands

ABSTRACT

Purpose: To investigate intraocular expression of COL7A1 and its protein product type VII collagen, particularly at the accommodation system.

Methods: Eyes from 26 human adult donors were used. COL7A1 expression was analyzed in ex vivo ciliary epithelium by microarray. Type VII collagen distribution was examined by Western blot analysis, immunohistochemistry and immuno-electron microscopy.

Results: COL7A1 is expressed by pigmented and non-pigmented ciliary epithelia. Type VII collagen is distributed particularly at the strained parts of the accommodation system. Type VII collagen was associated with various basement membranes and with ciliary zonules. Anchoring fibrils were not visualized.

Conclusion: Type VII collagen distribution at strained areas suggests a supporting role in tissue integrity.

INTRODUCTION

Type VII collagen (Col VII) is renowned as the major component of anchoring fibrils.¹ It is essential for epithelium-to-stroma anchorage in skin, mucosa and cornea.^{2,3} Although predominantly expressed in skin, Col VII is estimated to comprise a mere 0,001% of the total skin collagen content.⁴ Yet, the relevance of such levels of Col VII expression is clinically evidenced in severe dystrophic epidermolysis bullosa, where patients lack functional Col VII (i.e. anchoring fibrils). Their skin blisters readily at small amounts of friction, damaging their epithelial basement membranes at each event. Such repetitive wounding is accompanied by severe and extensive scar formation, mutilating deformations and recurrent infections. Patients succumb to skin cancer or sepsis often before age 35.^{5,6} Extraocular manifestations are well documented, and encompass mainly corneal and conjunctival (both surface ectoderm) erosions accompanied by scar formation, symblepharon, pannus, etc.⁶ Intraocular manifestations are only mentioned in rare case reports, where no clinical or histological abnormalities are found,⁷ or are limited to lens (also surface ectoderm) sclerosis.⁷⁻⁹ Interestingly, however, retinal COL7A1 gene expression was recently established (FANTOM5 consortium¹⁰). Moreover, its protein product was demonstrated at the vitreoretinal junction^{11,12} and inner layers of the normal retina,^{12,13} although no anchoring fibrils were visualized. Anchoring fibrils, however, are reported to be far more numerous at basement membrane zones of mechanically strained tissues.^{2,14,15} In order to investigate the characteristics of intraocular Col VII further, we explored the accommodation system. We observed COL7A1 expression at the pigmented and non-pigmented ciliary epithelia, and Col VII protein at the ciliary body and zonules.

MATERIALS AND METHODS

Samples

Ethics Statement: Eyes were provided by the Euro Cornea Bank, Beverwijk (<http://www.eurotissuebank.nl/corneabank/>), the Netherlands. In the Netherlands, the usage of donor material is provided for by the Organ Donation Act (WOD: Wet op de orgaandonatie). In accordance with this law, donors provide written informed consent for donation, with an opt-out for the usage of leftover material for related scientific research. Specific requirements for the use in scientific research of leftover material originating from corneal grafting have been described in an additional document formulated by the Ministry of Health, Welfare, and Sport, and the BIS foundation

(Eurotransplant; Leiden, July 21, 1995; 6714.ht). The current research was carried out in accordance with all requirements stated in the WOD and the relevant documents. Approval of the local medical ethics committee was not required, since the data were analyzed anonymously. Skin tissue was obtained from a cosmetic surgery procedure, after written informed consent of the patient and approval by the institutional review board.

We analyzed eyes from a total of 26 human donors (age 35 - 83 years, mean age 63.7 years), which were without known ophthalmic pathology (Table 1). In general, corneas had been removed for transplantation purposes. All eyes were fixed, frozen or processed within 48 hours post mortem.

Embedding

Eleven eyes were embedded in paraffin or resin as described previously.¹² For light microscopy, the anterior parts of four eyes were positioned in 2% agarose, prior to paraffin embedding and sectioned at 3-4 μm (Leica RM2265 Microtome, Heidelberg, Germany). For electron microscopy, the anterior parts of three eyes were washed, dehydrated, pre-infiltrated and embedded in T8100 resin (Technovit 8100, Heraeus Kulzer, Wehrheim, Germany). Areas of interest were sawn out, trimmed and sectioned at 100 nm thickness (Ultracut type 701, Reichert-Jung, Vienna, Austria). Three eyes and a skin sample were not fixed, but mounted in optimal cutting temperature compound (Tissue-Tek, Sakura Finetek Europe, Alphen aan den Rijn, The Netherlands), snap frozen in isopentane propane in liquid nitrogen, and cut in 7-10 μm thick sections (Leica CM3050 S Cryostat).

TABLE 1. Donor characteristics.

Assay	Embedding	Age	Gender	Cause of Death	Comorbidity	Fixative
IHC	paraffin	83	female	cerebrovascular accident	polymyalgia rheumatica	2% PF
		65	male	cardial	bladder cancer	2% PF
		64	male	cardial		2% PF
		78	female	cerebrovascular accident		2% PF
	cryo	67	female	malignancy		none
		68	male	malignancy		none
		83	male	cardial		none
		35*	female	N/A (control, abdominal skin)	obesity	none
		T8100	78	male	lung cancer	
	69		female	cerebrovascular accident		2% PF
	66		male	cardial		2% PF
	35		male	cardial		2% PF
	iTEM	T8100	56	male	cardial (suicide)	
77			male	cardial	atrial fibrillation	2% PF
78			female	cardial (asystole)	vascular disease	2% PF
Western blot		63	male	trauma		none
		78	female	cerebrovascular accident		none
		44	female	suicide	intoxication	none
		56	female	malignancy		none
Gene expression	cryo	39	male	cardial		none
		48	female	cardial		none
		56	male	aortic dissection		none
		58	male	cardial		none
		68	male	cerebrovascular accident	hypertension	none
		70	female	cardial		none
		73	male	cardial		none

PF paraformaldehyde; * skin sample only; iTEM immuno-electron microscopy; IHC immunohistochemistry.

Immunohistochemistry

Paraffin, T8100 and cryosamples were processed as described previously.¹² In short, sections from four paraffin embedded eyes were deparaffinized with xylene followed by ethanol rehydration steps. After washing, a protease K (IHC Select kit, Chemicon/Millipore, Billerica, MA, USA) dilution of 1:5 in PBS was added for 15 minutes to unmask epitopes. After washing, endogenous peroxidases were blocked (0.3% H₂O₂/PBS for 30 minutes). Non-specific binding of antigens was prevented (3% BSA/PBS for 30 minutes). Primary anti-Col VII antibodies (**Sup info Table 1**) were allowed to incubate (1:100 in PBS for 1 hour). These comprised two monoclonal antibodies, designated mAb(12)(LH7.2, Abcam) and mAb(14)(clone 32, EMD Milipore) and two polyclonal antibodies, designated pAb(16)(anti-tissue type Col VII, Calbiochem) and pAb(72)(polyclonal LH7.2, a kind gift from dr. Alex Nyström, University of Freiburg). After thorough washing in PBS, sections were incubated in corresponding horseradish conjugated secondary antibodies (rabbit-anti mouse and goat-anti-rabbit, DAKO, Glostrup, Denmark) (1:500 in PBS for 1 hour). Sections were washed, then stained using 3-amino-9-ethylcarbazole (AEC Staining Kit, Sigma-Aldrich, St. Louis, MO, USA) and counterstained with hematoxylin. For signal enhancement, an avidin/biotin labeling kit was used (Vectastain Elite ABC kit, Vector Labs, Burlingame, CA, USA), according to the manufacturer's instructions. A HC DMR microscope (Leica) was used to analyze the samples. All proceedings were performed at room temperature. In negative control sections incubation with primary antibodies was omitted.

Immuno-electron microscopy

Sections from T8100 embedded eyes were mounted on 150 mesh 0,6% formvar coated nickel grids. For antigen retrieval, samples were incubated in 0.05% trypsin (Gibco, Paisley, Schotland) in 0.1 M Tris-buffer (pH 7.8) containing 0.1% CaCl₂, for 15 minutes at 37°C. The sections were washed in 0.2 M phosphate buffer, incubated in 0.1 M citric acid (pH 3.0) for 30 minutes at 37°C, and washed again. In order to block nonspecific binding of the primary antibody, sections were incubated in PBS containing 2% BSA-c (Aurion, Wageningen, The Netherlands) and 2% goat serum, for 30 minutes at room temperature. Sections were then incubated in primary antibody pAb(16) (1:100) in a 1% BSA-c/PBS buffer, initially for 2 hours at 37°C, then at room temperature overnight. Afterwards, the sections were washed, and incubated with gold-labeled anti-rabbit IgG (goat-anti-rabbit, Gold Colloid 6 nm, Aurion; 1:200) for 1 h. The samples were washed in ultrapure water, fixed in 2% glutaraldehyde for 2 minutes, silver-enhanced according to kit protocol (R-Gent SE-LM Silver enhancement kit, Aurion) for 10 minutes at room temperature, and washed again with ultrapure water. Then, they were contrasted by

applying methylcellulose-uranyl acetate (9:1) at 4°C for 15 minutes, after which the solution was removed. The samples were allowed to dry for at least 15 minutes, and were analyzed in a CM100 BioTwin TEM (Philips, Eindhoven, the Netherlands) using iTEM software (ResAlta Research Technologies, Golden, CA, USA) and a Morada 11 MP TEM camera (Olympus Soft Imaging Solutions GmbH, Münster, Germany).

Antibody epitope mapping

The antibodies mAb(12), mAb(70)(US Biological, Swampscott, MA, USA) and pAb(72) target Col VII at its amino terminus (NC-1), while mAb(14) targets the collagenous domain towards the amino-terminal end. In order to assess the target epitopes of pAb(16), this antibody was mapped by a third party commercial laboratory (PEPperPRINT, Heidelberg, Germany)(**Sup info Figure 1**).

Western blotting

Seven bulbi (three pairs pooled for pAb(16), one bulbus for mAb(14)) were microscopically dissected in cooled 90% glycerol (diluted in 1% EDTA/PBS). Their anterior segment was isolated by cutting through the pars plana of the ciliary body circumferentially. The vitreous was dissected close to the anterior hyaloid, the iris was bluntly removed by forceps. The anterior segment was stretched and fixed on a clear silicone layer by insect pins. The zonules and lens capsule were contrasted with MembraneBlue-Dual dye (DORC, Zuidland, The Netherlands). The zonules were cut closely to the inner limiting membrane (ILM), minimizing contamination by ILM and ciliary epithelium. After opening of the capsular bag and removing the lens, visible lens fibers were flushed out. Traces of iris pigment that stuck to the anterior lens capsule were removed with Q-tips. Then, the pars plicata of the ciliary body was isolated from remaining retinal and choroidal fragments. Excess fluids were removed by centrifugation (1,000 rpm for 2 min). Tissues were homogenated by turaxing in 0,5% triton X100 in Tris-buffered saline. Some samples were subjected to bacterial type VII collagenase (high purity grade, Sigma; 30 units for 1h at 37°C) or pepsin (vortexing 5 min at room temperature, 4mg/ml pepsin in 0.5 M acetic acid at ¼ sample volume; Sigma) digestion prior to sample buffer incubation. Sample buffer, SDS-PAGE and Western blotting were performed as described earlier.¹² Briefly, nitrocellulose membranes were blocked with 2% fat free milk and incubated overnight in mAb(14) or pAb(16) (**Sup info Table 1**). The membranes were incubated in corresponding secondary antibodies (goat-anti-mouse or goat-anti-rabbit; Jackson ImmunoResearch, West Grove, PA, USA),

washed, incubated in tertiary alkaline phosphatase conjugated antibodies (rabbit-anti-goat-AP, Jackson) for 1 hour each, and developed with NBT/BCIP (BioRad). All steps were performed at RT. In controls, the primary antibody was omitted.

Gene expression

In order to assess COL7A1 expression in pigmented epithelium (PE) and non-pigmented epithelium (NPE), gene expression level data were provided by Janssen et al.¹⁶ Data were derived from their total dataset, including the unpublished remainder of their selection of top 10% relevant PE and NPE genes. In short, PE and NPE cells from seven snap frozen donor samples were separately collected through laser dissection microscopy. Then, RNA isolation, amplification, labeling and hybridization against 44xk Agilent microarrays was performed. Gene expression data was analyzed with R and the knowledge database Ingenuity.¹⁶

RESULTS

IHC and iTEM; polyclonal antibody

By light microscopy, pAb(16) labeling was observed at the ciliary zonules, stromal fibroblasts, and the basement membranes of PE and blood vessels. The zonules showed anti-Col VII labeling along their entire span (**Figure 1, 2**). Through that labeling, zonules could be traced to fibrillar structures at the NPE layer (**Figure 1A, 2A**). Labeling of the PE basement membrane was sharply delineated from pars plana (**Figure 1A**) to pars plicata. However, at the bases of the ciliary processes (**Figure 1B**), the area in between the PE basement membrane and that of nearby blood vessels labeled broadly (i.e. **Figure 1B, 2B**). Such labeling around blood vessels diminished rapidly towards the tips of the ciliary processes, where the sharp delineation returned (**Figure 1C**). The lens and lens capsule remained unlabeled (**Figure 1D**). At higher magnification however, small intracapsular structures were seen at the antero- and postequatorial capsule, where they corresponded to zonules (**Figure 2C, D**). They disappeared towards the anterior and posterior poles. The basal lamina of the posterior iris PE was slightly labeled, posteriorly more so than anteriorly. The iris stroma showed almost no labeling. Lens fibers showed some faint background labeling (on rare occasion), and were considered 'unlabeled' (**Figure 1D**).

By ITEM, labeling was confirmed. The zonules, including their NPE origin and capsular insertions, were labeled, as was the basement membrane of PE. No anchoring fibrils could be distinguished (**Figure 3, 4**). The basement membrane of the PE labeled moderately throughout its entire thickness (**Figure 3E, G**).

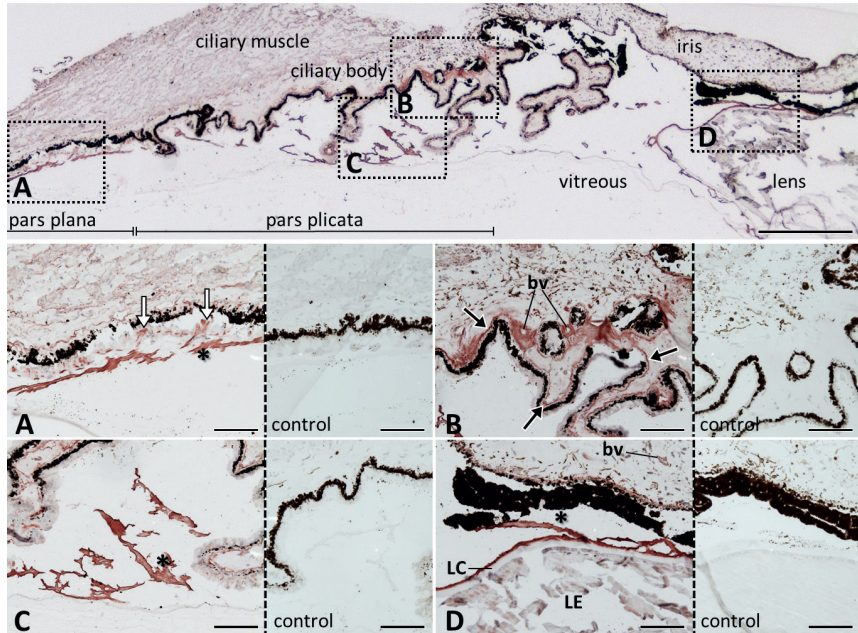


FIGURE 1. Col VII labeling of the accommodation system; pAb(16). Overview, and regions of interest (**A-D**). Zonules(*) label intensely, as do their probable sites of origin at the non-pigmented epithelium layer (*white arrows*). (**B**) Linear labeling is observed at the basement membrane of the ciliary pigmented epithelium. At the bases of the ciliary processes, extensive labeling is observed around blood vessels (*black arrows*). (**D**) The lens (*LE*) and its capsule (*LC*) appear unlabeled, in contrast to zonules(*), iris blood vessels (*bv*) and the basement membrane of iris pigmented epithelium. Controls did not label. Scale bars *overview* 500 μ m; *A-D* 100 μ m.

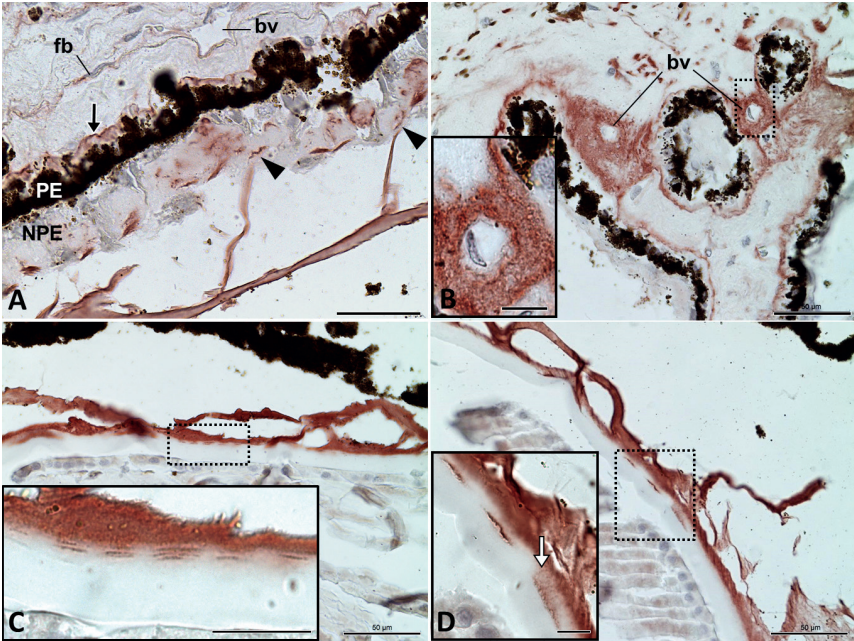


FIGURE 2. Col VII labeling of the ciliary body and zonules; pAb(16). Higher magnification of Figure 1. **(A)** Pars plana. The zonules connect to fibrillar structures (*arrowheads*) in the inner limiting membrane (*ILM*), which locally invaginates the non-pigmented epithelium (*NPE*). Apart from the fibrillar structures, the *ILM* does not label. Linear labeling is observed at the basement membrane (*black arrow*) of the pigmented epithelium (*PE*). Mostly, stromal fibroblasts (*fb*) display labeling, while small blood vessels (*bv*) do not. Bar 200 μm . **(B)** Pars plicata. The larger blood vessels, at the bases of the ciliary processes, label broadly in contrast to other blood vessels (*bv*). Bar 50 μm (inset; bar 10 μm). **(C, D)** Antero-equatorial lens capsule. Superficial intracapsular structures are labeled, at sites of zonular contact. Some fibrillar labeling is seen between a zonule contact point and an underlying intracapsular structure (*white arrow*). Scale bars 50 μm ; inset 10 μm .

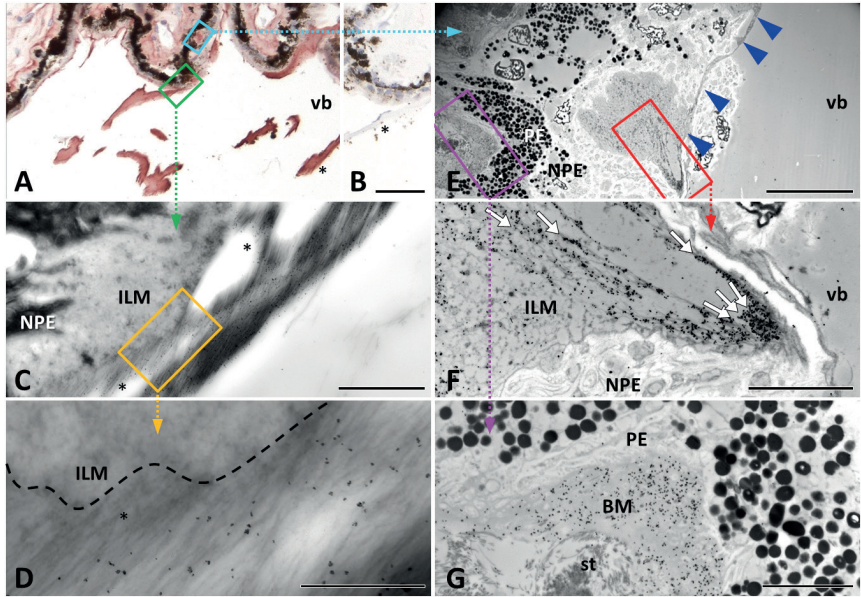


FIGURE 3. Col VII gold labeling of the zonules and basement membranes of pigmented and non-pigmented epithelium; pAb(16). (A) Light microscopic overview of regions of interest (E-G). (B) Negative control. (C) iTEM: Zonular fibers (*) are homogenously labeled (black dots). The inner limiting membrane (ILM) is not labeled. (D) A zonule adjacent to the ILM; no (fibrillar) zonule-ILM interactions are apparent. (E) Labeling at the basement membrane zone of the PE and at sites of zonular insertion (*in*) or ILM invagination into the NPE. Outside the invaginations, the ILM is a thin, practically unlabeled sheet (*arrowheads*). (F) Individual fibrils derive from the peripheral areas of the invaginated ILM and aggregate into a fiber (*white arrows*). (G) At this cutting angle, the gold labeled basement membrane (BM) of the pigmented epithelium (PE) appears broad. No anchoring fibrils are visualized between the BM and the subjacent unlabeled stroma (*st*). Scale bars B 50 μ m; C 20 μ m; D 5 μ m; E 5 μ m; F 2 μ m; G 1 μ m.

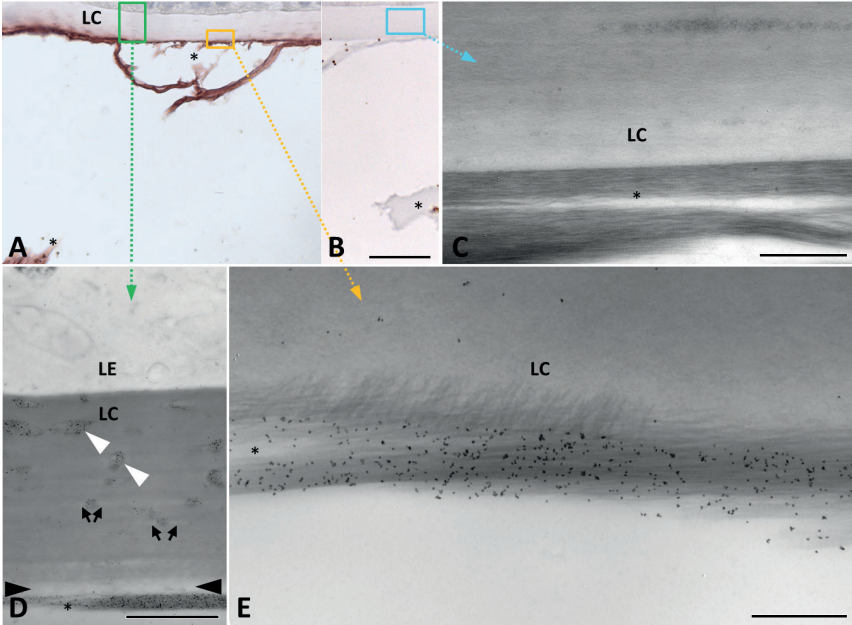


FIGURE 4. Col VII labeling of the zonules and their capsular insertions; pAb(16). (A) Light microscopic overview of regions of interest. The labeled intracapsular densities are most prominent underneath zonular attachments (*). (B) Negative control. (C) Negative control iTEM. (D) iTEM: Intracapsular densities also reside deep in the lens capsule (*white arrowheads*), the lens epithelium (LE) is unlabeled. A lucid layer is seen between zonules and lens capsule, at the antero-equatorial region (*black arrowheads*). The lens capsule has a striated aspect. Round linear densities are often flanked by an elongated area of lesser contrast (*small black arrows*). (E) iTEM: Perpendicular zonular fibers intermingle with the antero-equatorial lens surface, which is more lucent than its deeper parts. Scale bars B 50 μm ; C 2 μm ; D 5 μm ; E 1 μm .

At the capsular surface, some approximating zonules extended protruding fibrils, perpendicular to the zonular course and lens capsule surface (**Figure 4E**). Here, the assembled zonules ran parallel to the capsular surface, thus forming the zonular lamella. At areas without such perpendicular fibrils, a lucid unlabeled plane was seen between the zonules and lens capsule (**Figure 4D**, **Sup info Figure 2**). Intracapsular densities (or linear densities)¹⁷ were readily distinguishable from the lens capsular bulk by contrast density, but moreover since they were the only capsular structures that were labeled (**Figure 4D**). Although the labeled densities could indent the lens epithelial surface (**Sup info Figure 2B**), no actual intracellular labeling was seen. The intracapsular densities had round or elongated (linear) shapes. Their fibrillar aspect and labeling was less outspoken than that of zonules (**Figure 4C, D**). The round densities

had lucent envelopes, which was less distinct in the elongated variant (**Figure 4C, D, Sup info Figure 2B**). At the (antero-) equatorial lens capsule zonular fibrils mingled with the capsule at certain points (**Figure 4E**), but otherwise paralleled a lucent superficial capsular plane (**Sup info Fig. 2A, B**). No connections between zonules and intracapsular densities could be visualized convincingly, although on occasion faint intermediary fibrillar shapes could be discerned (**Sup info Fig. 2C**). The NPE and PE cells labeled negligibly, as did the collagenous stroma underneath the PE. In both IHC and iTEM, the vitreous cortex, the lens fibers and the lens epithelium remained unlabeled. Negative controls (IHC/iTEM) had no significant labeling or background. Results are summarized in **Table 2**.

TABLE 2. Summary of pAb(16) labeling intensities, semi-quantitative Col VII determination.

	Wb	IHC	iTEM
Ciliary body	+		
Stroma (fibroblasts)		+	+
Vascular BM		++	+
Pigmented epithelium BM		+++	++
Non pigmented epithelium BM (ILM)			-
Intercellular zonular origins		++	++
Zonules/lens capsule complex	+		
Zonules		+++	+++
Lens capsule			
Zonular membrane		-	-
Linear densities		++	++
Lens	-	-	-

BM basement membrane, + weak, ++ moderate, +++ intense labeling.

Antibody epitope mapping

Seven epitopes could be identified on the pAb(16) antibody with specific binding affinity for Col VII. The three epitopes, with the best signal-to-noise ratio (E-value), had affinity for the collagenous triple helical domain of Col VII. Of the four remaining epitopes, two epitopes would target NC-1 peptide sequences in the fibronectin (FN3) domain and two in the Von Willebrand factor (vWFA) domain (**Sup info Figure 1**).

IHC and iTEM; confirmation antibodies

In order to confirm our immunohistochemical results obtained by pAb(16) in ocular tissues, a comparison to other validated antibodies was made in cryosections of skin (**Sup info Figure 3**) and ciliary body (**Figure 5**). All antibodies labeled the dermal-epidermal basement membrane zone specifically. In cryosections of ocular tissue, the labeling of the pAb(16) antibody was partially reproduced by the other antibodies. The zonular fragments that survived cryosectioning were stained faintly, and only by the pAb(16) antibody. Intracapsular densities were not discernible. Avidin-biotin signal enhancement often resulted in basement membrane labeling. Evaluation by iTEM could not be performed, since none of the comparison antibodies proved able to label T8100 skin positive control sections adequately.

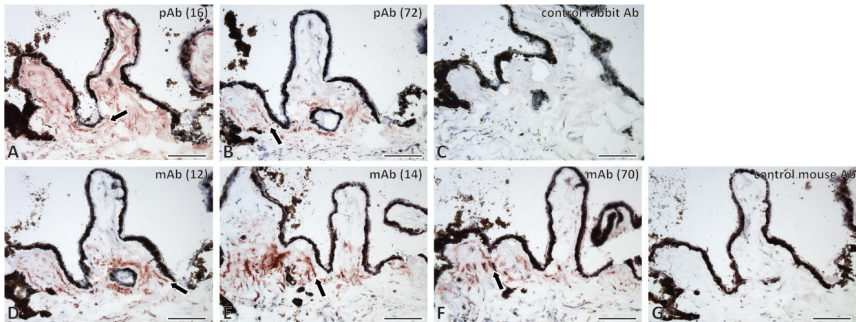


FIGURE 5. Anti-Col VII antibody comparison on unfixed ciliary body cryosections. The five antibodies (**A**, **B** monoconals; **D-F** polyclonals) label at the bases of the anterior ciliary processes, whereas the signal is more reduced at the posterior processes. The extensive labeling by the pAb(16) antibody is partially reproduced by the other antibodies. Here, pAb(16) gives more background labeling than in the paraffin sections (*see Figs. 1,2*). There is some longitudinal staining which indicates basement membrane associated staining (*arrows*). The few zonular fragments that remained after sectioning were stained faintly by the pAb(16) antibody, but not by the other antibodies. The linear densities in the lens capsule were not stained. Negative controls (**C** for mouse monoconals, **G** for rabbit polyclonals) showed no signals. Scale bars 100 μ m.

Western blotting

Col VII could be demonstrated in accommodation system lysates by mono- and polyclonal antibodies (**Figure 6**). Although Col VII was not easily extracted from cornea control tissue, a limited collagenase digestion of the crude lysate showed a 290 kDa

signal. Tissue type Col VII could be detected in zonules/lens capsule complex and ciliary body lysates, although a brief pepsin treatment of the crude lysate was needed for mAb(14) detection.

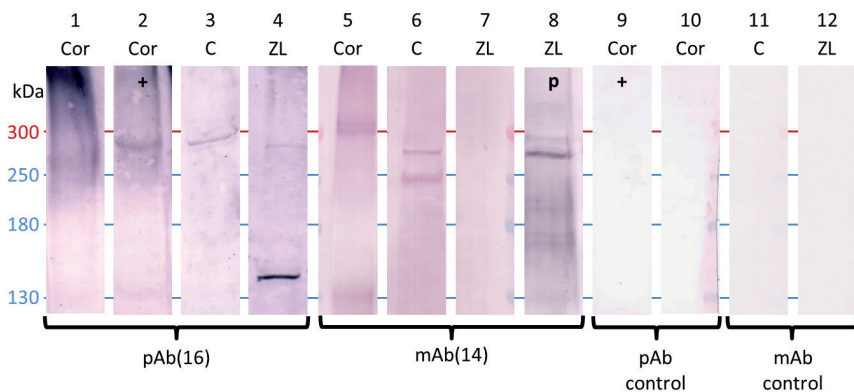


FIGURE 6. Western blots of accommodation system tissue lysates, with several antibodies against type VII collagen. (Lanes 1-4) pAb(16), no clear bands are seen in cornea lysates (*Cor*), which serve as a positive control, but high molecular weight aggregates (i.e. anchoring fibrils) are suspected given the dark smear at the top. Limited collagenase digestion (+) of cornea lysates clears the dark smear and results in a band around 290 kDa. This band is also detected in ciliary body (*C*) and zonule/lens capsule (*ZL*). Zonule/lens capsule lysates also show a strong band around 145 kDa. **(Lanes 5-8)** mAb(14), in another lysate batch, cornea lysates show a signal around 320 kDa, the ciliary body lysate around 290 and 250 kDa, whereas the zonula/lens capsule lysate only shows bands at 290 and 170 kDa after limited pepsin digestion (*p*) (compare *lane 7* to *lane 8*). **(Lanes 9-12)** negative controls, samples show no bands.

Gene expression

COL7A1 is equally expressed in PE and NPE at 'low' levels (compared to the total dataset), as indicated by a 'log₂ transformed absolute expression level' (**Table 3**).¹⁶ These data can be found in the GEO database (GSE37957).

TABLE 3. Gene expression levels of COL7A1 in microdissected PE and NPE.

Expression level*	Expression value
Very low/absent	<5,2955
Low	5,2955-9,0730
Moderate	9,0730-13,5714
High	>13,5714

Gender	Age	PE	NPE
male	39	7,408657	7,279606
female	48	8,004639	7,525126
male	56	7,219921	7,166875
male	58	7,767476	8,096206
male	68	7,685123	7,914225
female	70	7,21064	NA
male	73	7,596791	7,847934

*The mean gene expression values of the epithelia after normalization range from 2.09 to 18.88 (log2 transformed absolute expression levels). Janssen et al.¹⁶ published the selected 'highly expressed genes' group, which mean expression levels ranged from 13.70 to 18.88. COL7A1 expression in ciliary epithelia is around 7 to 8, which corresponds to a 'low' expression level (compared to the total dataset). Description: mRNA, Homo sapiens collagen, type VII, alpha 1 (COL7A1), (epidermolysis bullosa, dystrophic, dominant and recessive). SystematicName: NM_000094. Age at enucleation, *PE* pigmented epithelium, *NPE* nonpigmented epithelium.

DISCUSSION

This study establishes Col VII expression in accommodation system tissues. Col VII is mainly immunolocalized at the zonules, and around the blood vessels at the bases of ciliary processes. COL7A1 mRNA is expressed in human PE and NPE cells, at low levels.

The zonules are 'woven' by the NPE during organogenesis,¹⁸ when fine zonular fibers originate at the intercellular spaces of the NPE,¹⁹ aggregate into zonules and then transverse the ILM. With aging, the ILM is infolded into those intercellular spaces,¹⁹ which corresponds to the 'invaginations' we currently describe. Upon their lens capsule penetration, the zonules resolve into broadly fanning microfibrils,²⁰ which anchor to 'poorly defined structures'^{21, 22} near the epithelial cells. This anchoring fashion withstands the repetitive mechanical strain of accommodation.²¹ By Col VII labeling, we

underline that the zonules penetrate the lens capsule, transverse intracapsularly, and represent the 'linear densities' (**Sup info Figure 2A**) of the anterior and equatorial lens capsule.¹⁷ Col VII might support the microfibrillar interaction at either zonular terminus.

Zonules were labeled by pAb(16) in cryo and paraffin slides, but not by the other antibodies. Since monoclonal antibodies were able to detect Col VII by Western blot, Col VII epitopes might be unavailable when embedded within the zonular matrix, or due to steric hindrance of the antibodies. Since pAb(16) has several binding sites for Col VII, such restrictions may apply to a lesser extent, thus possibly explaining different staining patterns. In order to assess the origin of zonular Col VII, we obtained microarray data from ex vivo NPE and PE cells. Their COL7A1 mRNA expression profiles, combined with the data from Western blots, add to our IHC results. Our hypothesis of a possible role of Col VII in the accommodation system is therefore supported. The low levels of COL7A1 expression at detectable Col VII protein amounts suggest a low turnover (e.g. in comparison to skin²³).

The demonstration of Col VII at ciliary stromal cells, PE and blood vessels might relate to the repetitive mechanical strain these tissues are subjected to. The contact points between PE and the blood vessels at the ciliary base, for example, are intensely labeled. The ciliary epithelia need a rich vasculature for their active secretory functions. Unaided, such vascular accommodation might diminish the structural tenacity of the processes. Interestingly, accommodation system histopathology has not been reported in Col VII deficient patients.^{7,8}

By Western blot, the intense zonular IHC labeling appears to be due to the presence of NC-1 globuli. Although isolation of the relative minute quantities of Col VII from any extracellular matrix can be complicated due to its firm embedding therein, mAb(14) was able to detect a full length Col VII (290 kDa) signal in zonular/lens capsule lysates. However, none of the mAbs was able to target zonules in sections successfully, in contrast to ciliary body and cornea. Thus, the IHC/iTEM results obtained with pAb(16) could not be completely reproduced with other antibodies. We have tried to validate pAb(16) in various ways. The pAb(16) is frequently used in Col VII investigations, and does not show significant cross-reactivity to Col VII deficient human¹² or mouse tissues²⁴ or keratocytes²⁵.

Interestingly, convincing anchoring fibrils were not visualized, although some looped shapes of thin fibrils were situated in between anti-Col VII labeled structures (**Sup info Figure 2C**). Still, the function of Col VII might be established indirectly, through determination of interacting proteins. Proteomic studies have detected Col

VII in human ciliary body,¹¹ ILM,^{11, 26} retinal blood vessel,¹¹ and bovine zonule (Col VII fragment C9JBL3_HUMAN²⁷) samples, but the established dermal Col VII interactors (i.e. type I and IV collagen and laminin 332) were detected incompletely (ciliary body,^{28, 29} zonule,²⁷ lens capsule¹¹). Interactions of Col VII and fibrillin, the main component of zonules and part of a tissue mechanosensing complex,³⁰ have not been documented.

In order to address the potential functions of intraocular Col VII further, the discrepancy between Col VII labeling in the absence of anchoring fibrils would be supported by identifying the functional ocular Col VII interactor isotypes and possibly by thorough ophthalmological examination of rDEB patients.

Acknowledgments

We would like to thank the Euro Cornea Bank for supplying donor eyes, Behrouz Zandieh-Doulabi from VU University Amsterdam for his scientific assistance, the UMCG Microscopy & Imaging Centre for their equipment, and the UMCG Department of Plastic Surgery for supplying control tissue.

SUPPORTING INFORMATION

SUPPORTING INFO TABLE 1. Antibody characteristics.

Primary antibody	Specificity	Clonality	Host	Isotype	Company	Catalogus no.	Antibody Registry no.	Lot no.
Collagen, type VII	NC1 & 3H*	Polyclonal	Rabbit	IgG	Calbiochem (Merck/ Millipore)	234192	AB_211739	D00111036 D00050046 D00145113 D00168593 D00173199 2694891
Collagen, type VII	NC1**	Polyclonal LH7.2	Rabbit					
Collagen, type VII	NC1	Monoclonal LH7.2	Mouse	IgG1	Abcam	ab6312	AB_305415	GR158908 GR317324 856867
Collagen, type VII	3H***	Monoclonal II-32	Mouse	IgG1	Chemicon (Merck/ Millipore)	MAB2500	AB_94355	2890767 LV1797191
Collagen, type VII	NC1****	Monoclonal 2q633	Mouse	IgG1	US Biological	C7510-66A	not available	L7011163
β -actin		Polyclonal	Rabbit		Abcam	ab8227	AB_2305186	
CK-18		Monoclonal	Mouse		Abcam	ab668	AB_305647	
CK-19		Monoclonal	Mouse		Abcam	ab7754	AB_306048	

Hyperlinks are partially available. * this study (epitope mapping); ** kind gift from dr. Alexander Nyström from the Department of Dermatology, Medical Center - University of Freiburg, Germany; *** personal communication Merck; targets the amino-terminal (dashesheets not corrected for Col VII polarity shift in 1991 by Parente MG et al. Same antibody as 'NC-1 mAb' from Ref 1 and Ref 2; **** personal communication US Biologics; targets the amino-terminal (dashesheets were also not corrected for Col VII polarity shift). Same antibody as 'LH7.2 mAb' from Lapierre JC, Hu L, Iwasaki T, et al. *J Dermatol Sci*. 1994; 8:145-150 and Tanaka T, Takahashi K, Furukawa F, et al. *Br J Dermatol*. 1994; 131:472-476.

Methods and materials (PEPperPrint)

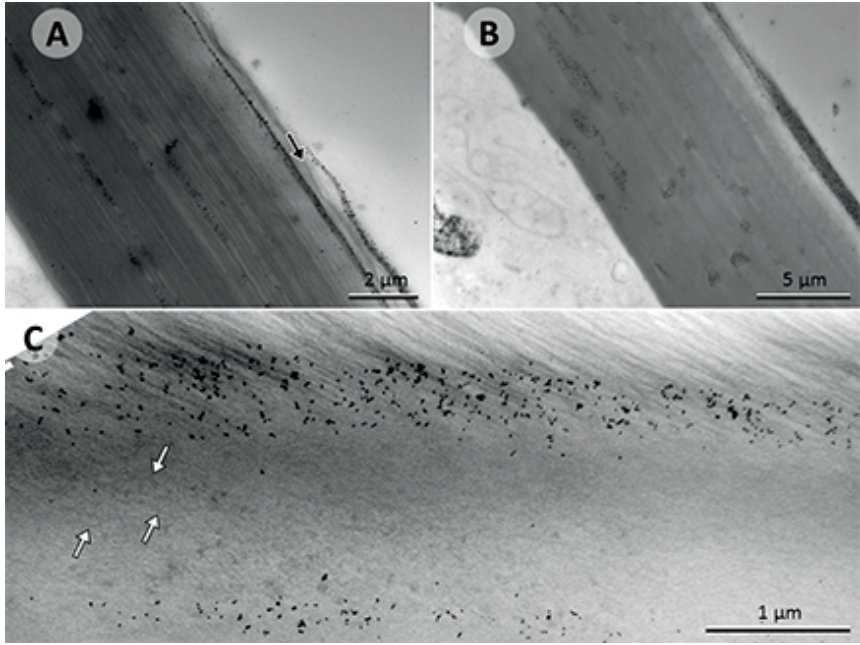
Microarray Content:	The sequence of human type VII collagen was elongated by neutral GSGSGG linkers to avoid truncated peptides. The elongated antigen sequence was translated into 10 and 15 amino acid peptides with peptide-peptide overlaps of 9 and 14 amino acids. The resulting peptide collection was split in two different peptide microarrays with 2,949 different 10 aa and 2,944 different 15 aa peptides printed in duplicate (5,898 and 5,888 peptide spots, respectively); both microarrays were framed by Flag (DYKDDDDKAS, 158 spots) and HA (YPYDVPDYAG, 158 spots) control peptides.
Sample:	Rabbit Polyclonal IgG Antibody (Merck Cat. 234192)
Washing Buffer:	PBS, pH 7.4 with 0.05% Tween 20 (3x1 min after each assay)
Blocking Buffer:	Rockland blocking buffer MB-070 (30 min before the first assay)
Incubation Buffer:	Washing buffer with 10% blocking buffer
Assay Conditions:	Antibody concentrations of 1 µg/ml and 10 µg/ml in incubation buffer; incubation for 16 h at 4°C and shaking at 140 rpm
Secondary Antibodies:	Sheep anti-rabbit IgG (H+L) DyLight680; 45 min at RT and a dilution of 1:5000 in incubation buffer
Control Antibody:	Monoclonal anti-HA (12CA5)-DyLight800; 45 min at RT and a dilution of 1:2000 in incubation buffer
Scanner:	LI-COR Odyssey Imaging System; scanning offset 0.65 mm, resolution 21 µm, scanning intensities of 7/7 (red = 700 nm/green = 800 nm)
Microarray Data:	Microarray Data Wullink (PEP201558111).xlsx
Microarray Identifier:	001080_02 (15 amino acid peptides), 001080_03 (10 amino acid peptides)

Experimental and data Analysis

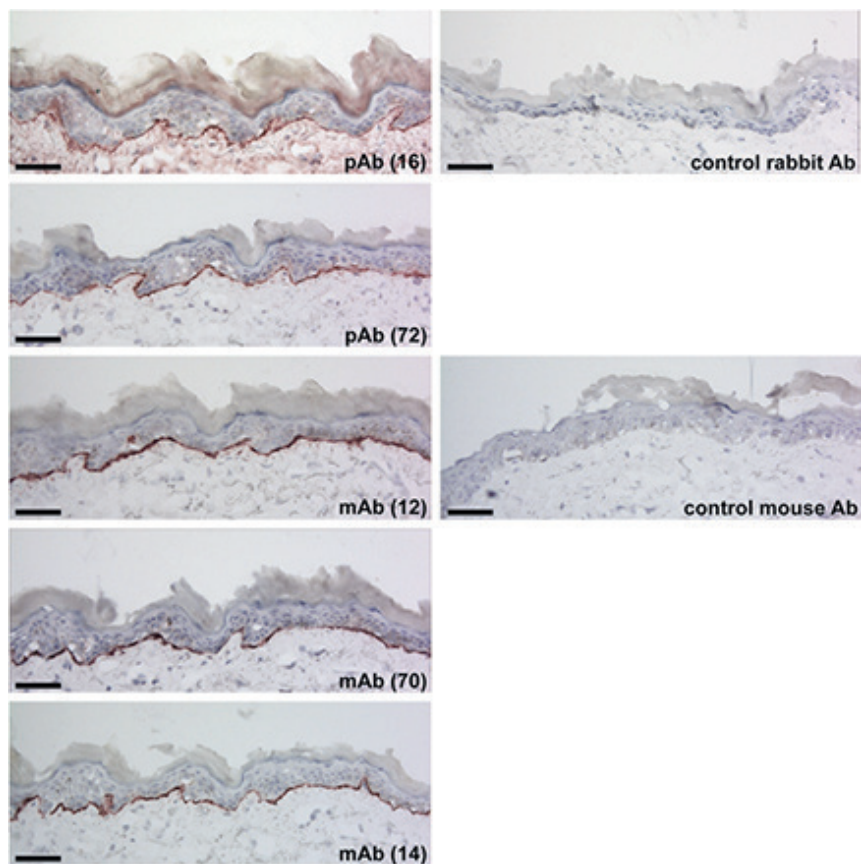
After 15 min pre-swelling in standard buffer and 30 min in blocking buffer, both human type VII collagen microarrays were initially incubated with the secondary antibody sheep anti-rabbit IgG (H+L) DyLight680 at a dilution of 1:5000 in the presence of the control antibody monoclonal anti-HA (12CA5)-DyLight800 at a dilution of 1:2000 for 45 min at room temperature to analyze background interactions with the collagen-derived peptides. Subsequent incubation of both peptide microarrays with the rabbit polyclonal IgG antibody at concentrations of 1 µg/ml and 10 µg/ml was followed by staining with the secondary antibody sheep anti-rabbit IgG (H+L) DyLight680 in the presence of the monoclonal anti-HA (12CA5)-DyLight800 control antibody and read-out at scanning intensities of 7/7 (red/green). HA control peptides were simultaneously stained as internal quality control to confirm the assay quality and to facilitate grid alignment for data quantification.

Quantification of spot intensities and peptide annotation were based on 16-bit gray scale tiff files that exhibit a higher dynamic range than 24-bit colorized tiff files; microarray image analysis was done with PepSlide® Analyzer and summarized in Excel file Microarray Data Wullink (PEP201558111).xlsx. A software algorithm breaks down fluorescence intensities of each spot into raw, foreground and background signal (see "Raw Data" tabs), and calculates the standard deviation of median foreground intensities (see "Mapping Summary" tab). Spots with a deviation of 40% were zeroed to yield corrected averaged foreground intensities. Based on corrected averaged median foreground intensities, intensity maps were generated and binders in the peptide maps highlighted by an intensity color code with red for high and white for low spot intensities.

We further plotted averaged spot intensities of the assays with the antibody sample against the elongated human type VII collagen sequence from the N- to the C-terminus to visualize overall spot intensities and signal-to-noise ratios (see "Intensity Plot" tab). For a better data overview, the baselines of the intensity plots were leveled and main responses annotated next to the corresponding signal. The intensity plots were correlated with peptide and intensity maps as well as with visual inspection of the microarray scan to identify the epitopes of the rabbit polyclonal IgG antibody. In case it was not clear if a certain amino acid contributed to antibody binding, the corresponding letters were written in gray.



SUPPORTING INFORMATION FIGURE 2. (A) The superficial plane of the lens capsule appears fibrillar (*black arrow*), but is more lucent and practically unlabeled compared to over/underlying zonules and intracapsular densities. (B) A deeper intracapsular density indents the lens epithelium surface, but intracellular gold labeling is not seen. (C) Some fine, looping fibrils can be distinguished in between the labeled structures of zonule and underlying intracapsular densities (*white arrows*). Scale bars A 2 μm, B 5 μm, C 1 μm.



SUPPORTING INFORMATION FIGURE 3. Anti-Col VII antibody comparison on skin cryosections. All anti-Col VII antibodies stain the dermal-epidermal basement membrane specifically. Scale bars 50 μm .

REFERENCES

1. Sakai LY, Keene DR, Morris NP, Burgeson RE. Type VII collagen is a major structural component of anchoring fibrils. *J Cell Biol.* 1986; 103:1577-1586.
2. Keene DR, Sakai LY, Lunstrum GP, Morris NP, Burgeson RE. Type VII collagen forms an extended network of anchoring fibrils. *J Cell Biol.* 1987; 104:611-621.
3. Gipson IK, Spurr-Michaud SJ, Tisdale AS. Anchoring fibrils form a complex network in human and rabbit cornea. *Invest Ophthalmol Vis Sci.* 1987; 28:212-220.
4. Bruckner-Tuderman L, Schnyder UW, Winterhalter KH, Bruckner P. Tissue form of type VII collagen from human skin and dermal fibroblasts in culture. *Eur J Biochem.* 1987; 165:607-611.
5. Mittapalli VR, Madl J, Löffek S, et al. Injury-driven stiffening of the dermis expedites skin carcinoma progression. *Cancer Res.* 2016;76: 940-951.
6. Fine JD, Mellerio JE. Extracutaneous manifestations and complications of inherited epidermolysis bullosa: part I. Epithelial associated tissues. *J Am Acad Dermatol.* 2009; 61:367-384.
7. Destro M, Wallow IH, Brighthill FS. Recessive dystrophic epidermolysis bullosa. *Arch Ophthalmol.* 1987; 105:1248-1252.
8. Motley WW, Vanderveen DK, West CE. Surgical management of infantile cataracts in dystrophic epidermolysis bullosa. *J AAPOS.* 2010; 14:283-284.
9. Papathanassiou M, Petrou P, Papalexis G, Theodossiadis P. Intraoperative complication during phacoemulsification in patient with epidermolysis bullosa. *J Cataract Refract Surg.* 2011; 37:198-200.
10. Lizio M, Harshbarger J, Shimoji H, et al. Gateways to the FANTOM5 promoter level mammalian expression atlas. *Genome Biol.* 2015; 16:22.
11. Uechi G, Sun Z, Schreiber EM, Halfter W, Balasubramani M. Proteomic view of basement membranes from human retinal blood vessels, inner limiting membranes, and lens capsules. *J Proteome Res.* 2014; 13:3693-3705.
12. Wullink B, Pas HH, Van der Worp RJ, Kuijjer R, Los LI. Type VII collagen expression in the human vitreoretinal interface, corpora amylacea and inner retinal layers. *PLoS ONE.* 2015; 10:e0145502.
13. Ponsioen T, van Luyn M, van der Worp R, van Meurs J, Hooymans J, Los L. Collagen distribution in the human vitreoretinal interface. *Invest Ophthalmol Vis Sci.* 2008; 49:4089-4095.
14. Tidman MJ, Eady RA. Ultrastructural morphometry of normal human dermal-epidermal junction. The influence of age, sex, and body region on laminar and nonlaminar components. *J Invest Dermatol.* 1984; 83:448-453.
15. Banks WJ, Bale E, White FH. Morphometric studies of the epidermal-dermal junction in the rat ear: some effects of experimental friction on epidermis and anchoring fibrils. *J Anat.* 1984; 139:425-435.
16. Janssen SF, Gorgels TG, Bossers K, et al. Gene expression and functional annotation of the human ciliary body epithelia. *PLoS ONE.* 2012; 7: e44973
17. Hogan MJ, Alverado JA, Wedell JE. *Histology of the human eye: an atlas and textbook.* 1st ed. Philadelphia, Saunders; 1971:p649.
18. Hanssen EE, Franc S, Garrone R. Synthesis and structural organization of zonular fibers during development and aging. *Matrix Biol.* 2001; 20:77-85.
19. Raviola G. The fine structure of the ciliary zonule and ciliary epithelium. With special regard to the organization and insertion of the zonular fibrils. *Invest Ophthalmol.* 1971; 10:851-869.

- 20.** Cain SA, Morgan A, Sherratt MJ, Ball SG, Shuttleworth CA, Kieley CM. Proteomic analysis of fibrillin-rich microfibrils. *Proteomics*. 2006; 6:111-122.
- 21.** Hiraoka M, Inoue K, Ohtaka-Maruyama C, et al. Intracapsular organization of ciliary zonules in monkey eyes. *Anat Rec (Hoboken)*. 2010; 293:1797-1804.
- 22.** Streeten BW. The zonular insertion: a scanning electron microscopic study. *Invest Ophthalmol Vis Sci*. 1977; 16:364-375.
- 23.** Kühl T, Mezger M, Hausser I, et al. Collagen VII half-life at the dermal-epidermal junction zone: implications for mechanisms and therapy of genodermatoses. *J Invest Dermatol*. 2016; 136:1116-1123.
- 24.** Wenzel D, Bayerl J, Nyström A, Bruckner-Tuderman L, Meixner A, Penninger JM. Genetically corrected iPSCs as cell therapy for recessive dystrophic epidermolysis bullosa. *Sci Transl Med*. 2014; 6:264ra165 (Table S3).
- 25.** Dayal JH, Cole CL, Pourreyyon C, et al. Type VII collagen regulates expression of OATP1B3, promotes front-to-rear polarity and increases structural organisation in 3D spheroid cultures of RDEB tumour keratinocytes. *J Cell Sci*. 2014; 127:740-751.
- 26.** Balasubramani M, Schreiber EM, Candiello J, Balasubramani GK, Kurtz J, Halfter W. Molecular interactions in the retinal basement membrane system: a proteomic approach. *Matrix Biol*. 2010; 29:471-483.
- 27.** De Maria A, Wilmarth PA, David LL, Bassnett S. Proteomic analysis of the bovine and human ciliary zonule. *Invest Ophthalmol Vis Sci*. 2017; 58:573-585.
- 28.** Zhang P, Kirby D, Dufresne C, et al. Defining the proteome of human iris, ciliary body, retinal pigment epithelium, and choroid. *Proteomics*. 2016; 16:1146-1153.
- 29.** Goel R, Murthy KR, Srikanth S, et al. Characterizing the normal proteome of human ciliary body. *Clin Proteomics*. 2013; 10:9.
- 30.** Cook JR, Carta L, Bénard L, et al. Abnormal muscle mechanosignaling triggers cardiomyopathy in mice with Marfan syndrome. *J Clin Invest*. 2014; 124:1329-1339.



4

Chapter 4

Type VII Collagen in the Ocular Vasculature

Bart Wullink, MD^{1,2,*}

Hendri H. Pas, PhD³

Roelofje J. Van der Worp, BAS^{1,2}

Theo van Kooten, PhD^{2,4}

Leonoor I. Los, PhD^{1,2}

¹ Department of Ophthalmology, University Medical Center Groningen, University of Groningen, Groningen, the Netherlands

² W.J. Kolff Institute, Graduate School of Medical Sciences, University of Groningen, Groningen, the Netherlands

³ Department of Dermatology, University Medical Center Groningen, University of Groningen, Groningen, the Netherlands

⁴ Department of Biomedical Engineering, University Medical Center Groningen, University of Groningen, Groningen, the Netherlands

* b.wullink@umcg.nl

Submitted to Retina

ABSTRACT

Background: Type VII collagen (Col VII) is an anchoring protein that is crucial in maintaining tissue integrity of surface epithelia, such as skin, mucosa and cornea. Recently, this protein was discovered intraocularly, in the accommodation system and at the vitreoretinal interface. Interestingly, the intraocular vasculature at these sites also demonstrated a marked anti-Col VII labeling. Previous studies, however, suggested that this anchoring protein was not a part of perivascular matrices. We aimed to validate the presence of perivascular Col VII in the human eye.

Methods: We have analyzed the vasculature of several tissues (donor eyes of varying ages (n=44), umbilical cords (n=6), hypodermal vasculature samples (n=7), renal artery samples (n=4), skin samples (n=2)) for Col VII presence with several techniques using antibodies against Col VII.

Results: We were able to demonstrate Col VII at the vasculature of the retina, optic nerve, ciliary body and choroid, where it resides between the inner sheath of the endothelial basement membrane and the outer GFAP envelope of the glial cells. Col VII was also detected at the vasculature of the extra-ocular control tissues, except in skin. Anchoring fibrils, the accepted mode of tissue anchorage by Col VII molecules, could not be visualized at the intraocular vasculature.

Conclusions: The presence of intraocular vascular Col VII was validated, although immunolocalization alone is insufficient evidence to implicate a typical 'dermal' anchoring function. The perivascular Col VII distribution in the retina appears to be associated with mural cells. Future analysis of Col VII deficient donor tissues might provide more substance to the function of perivascular Col VII.

INTRODUCTION

Anchoring fibrils are specialized sub-epidermal aggregates of type VII collagen (Col VII), which secure dermal and corneal epithelia to their underlying stroma. Therefore, deficiency of Col VII (and thus of functional anchoring fibrils) leads to the debilitating bullous disorder *severe dystrophic epidermolysis bullosa* (RDEB). Accordingly, Col VII is considered to be a 'dermal' protein. However, a number of studies have shown evidence for the presence of Col VII at extradermal sites including intraocular tissues such as the neuroretina and ciliary body.^{1,2} Surprisingly, prominent immunolabeling was seen at the blood vessels of unfixed tissues, which was validated by Western blotting, gene expression profiles and proteomics.^{2,3,4} The immunolocalization of Col VII at vascular tissues has been reported by others as well, but the validity of these observations is not generally accepted. These studies (**Table 1**) were mostly not directed at determining whether Col VII was present in blood vessels, but such information could be derived from their data. Tissues were grossly grouped in skin/mucosa/epithelial basement membranes, (chor)amnion tissue, blood vessels in any tissue, and muscular/heart/myofibroblasts. Many studies use similar techniques and antibodies, most of which are used on fixed cryosections.

To date, the immunolabeling patterns of Col VII at perivascular tissues (e.g. umbilical cord, choroid plexus, pelvis fascia, or glioma) were granular or punctuate in appearance, while the 'dermal' pattern is typically linear.⁵⁻⁹ Some authors speculated that such a punctuate immunolabeling pattern might represent an anchoring fibril network that differs from that of skin or cornea.¹⁰ Some clinical evidence for a role of Col VII in vascular tissues may be found in the fact that Col VII deficient patients may suffer from cardiomyopathies and aortic dilation, both with an onset at young age.^{11,12} This might indicate a primary ultrastructural vascular disorder related to a reduced presence of Col VII. Alternatively, it has been suggested that any (cardio)vascular pathologies that might develop in these patients are secondary to chronic anaemia.¹¹ In order to validate the presence of perivascular Col VII, we analyzed intraocular tissues, and compared those with selected extraocular vascular tissues. We were able to demonstrate the presence of Col VII at the vasculature of the retina, optic nerve, ciliary body and choroid. In addition, Col VII could be demonstrated at the vasculature of the umbilical cord, abdominal aorta, renal artery and hypodermis. Anchoring fibrils could not be demonstrated at any of these sites.

TABLE 1. Overview of several studies that address Col VII immunolabeling at blood vessels.

Reference	Embedding	Prefixation	Method	Antibody designation:			Labeling of Skin or mucosa	Labeling of vasculature yes/no
				in reference study	in other studies	in current study		
Hessle et al. (1984) ²⁰	cryo	acetone	IF	NP161	NP161		+	no
Leigh & Purkis et al. (1985) ^{**21}	cryo*	acetone*	IF	LH7.2	LH7.2	mAb(12)	+	no
Pallier et al. (1985) ²²	cryo, pre-TEM	none*	IF, TEM	H3a	H3a		+	no
Burgeson et al. (1985) ²³	cryo	acetone*	IF	antibody	NP161		+	no
Lunstrum et al. (1986) ²⁴	cryo	acetone*	IF	anti-type VII	NP185*		+*	n/a
				NP161	NP161		+	n/a
				pAb VII (Lu)	pAb	pAb(16)	+	n/a
Sakai et al. (1986) ²⁵	cryo, pre-TEM	acetone	ELISA	anti-NP32	NP32	mAb(14)	+	no*
				anti-NP161	NP161		+	no*
				anti-type VII	NP185		+	no
Heagerty et al. (1986) ¹⁴	cryo, TEM	acetone*, Karnovsky	IF, TEM, ELISA	LH7.2	LH7.2	mAb(70)	+	n/a
Lunstrum et al. (1987) ¹⁰				NP185	NP185		n/a	n/a
				NP76	NP76*		n/a	n/a
				pAb VII (Lu)	pAb	pAb(16)	n/a	n/a
				NP32	NP32	mAb(14)	n/a	n/a
				NP161	NP161		n/a	n/a
Keene et al. (1987) ²⁶	pre	none*	TEM	mAb/VII	NP185		+	n/a

TABLE 1. Continued.

Reference	Embedding	Prefixation	Method	Antibody designation:			Labeling of Skin or mucosa	Labeling of vasculature yes/no
				in reference study	in other studies	in current study		
Bruckner-Iudermann et al. (1987) ²⁷				mAb161	NP161		n/a	n/a
				pAb VII (Lu)	pAb	pAb(16)	+	n/a
Leigh et al. (1987) ²⁸	cryo, pre-TEM	unfixed & acetone/methanol	IF, IHC-P0, TEM	pAb VII (BT)	pAb	pAb(16)	+	n/a
				LH7.2	LH7.2	mAb(12)	+	no*
Yoshiike et al. (1988) ²⁹	cryo, pre-TEM	none*	TEM	pAb VII (BT)	pAb	pAb(16)	+	n/a
				H3a	H3a		+	n/a
				EBA-2*	L3D*		+	n/a
Woodley et al. (1988) ³⁰	cryo	acetone*	IF	MAb to NC1	NP161		+	no
				EBA-1	H3a		+	no
Kirkham et al. (1989) ³¹	cryo	acetone*	IHC-P0	LH7.2	LH7.2		+	no
	paraffin	routinely fixed	IHC-P0	LH7.2	LH7.2		-	no
Wetzels et al. (1989) ³²	cryo	acetone	IF, IHC-P0	LH7.2	LH7.2	mAb(12)	n/a	no
Wetzels et al. (1991) ³³	cryo, paraffin	acetone, PF*	IHC-P0	LH7.2	LH7.2		+	no
Wetzels et al. (1992) ¹⁸	cryo	acetone	IHC-P0	LH7.2	LH7.2	mAb(12)	n/a	granular
Ryynänen et al. (1993) ⁵	cryo	ethanol	IF	L3D	L3D		n/a	yes
Visser R (thesis) (1993) ³⁴	cryo, paraffin	10% formalin, or 2.5% PF	IF, IHC-AP	LH7.2	LH7.2	mAb(12)	n/a	no**
				NP76	NP76		n/a	no

TABLE 1. Continued.

Reference	Embedding	Prefixation	Method	Antibody designation:			Labeling of skin or mucosa	Labeling of vasculature yes/no
				in reference study	in other studies	in current study		
Lapierre et al. (1993a) ³⁵			ELISA	clone I, 185	NP185		n/a	n/a
			ELISA	LH7.2	LH7.2		n/a	n/a
Lapierre et al. (1993b) ³⁶			ELISA	H3A	H3a		n/a	n/a
			ELISA	L3D	L3D		n/a	n/a
Paulus et al. (1995) ⁷	cryo	acetone	IHC-AP	LH7.2	LH7.2		+	yes
				pAb VII (BT)	pAb	pAb(16)	+	yes
Tuori et al. (1996) ³⁷	cryo	acetone, chloroform	IF, IHC-PO	Mab (II, 32)	NP32	mAb(14)	n/a	no**
Virtanen et al. (1996) ¹⁹	cryo	acetone	IF	mAb II, 32	NP32	mAb(14)	n/a	no
Lohi et al. (1996) ³⁹	cryo	acetone	IF	161-6	NP161		n/a	no**
				NP-185	NP185		n/a	no**
Lohi et al. (1998) ⁴⁰	cryo	acetone	IHC-AP	mAb NP 32	NP32	mAb(14)	n/a	yes
Radziszewski et al. (2005) ⁸	cryo	zamboni	IF	C6805 mAb	LH7.2	mAb(12)	n/a	yes
Chi et al. (2010) ³⁸	cryo	none*	IF	LH7.2	LH7.2		+	yes (linear)
				L3d	L3D		+	yes (linear)
				EBA antisera			+	yes (linear)

Col VII labeling could either have been demonstrated (+), not mentioned (n/a) or absent (-). Fixatives are not always mentioned, but due to their group, standard procedures were likely (*presumed) to have been applied. In some study figures, blood vessels are reported to be negative, although weak labeling delineating blood vessels is recognizable (**). A/M acetone methanol 1:1, IHC immunolabeling with peroxidase labels (PO) or alkaline phosphatase (AP), IF immunofluorescence. Zamboni fixative phosphate buffered picric acid-formaldehyde, pre-embedding tissue incubation with antibodies prior to fixation and embedding. Polydonals from Lunstrum and Bruckner-Tuderman were prepared independently, but should be comparable to pAb(16). LH7.2, the Z0653 clone and C6805 should be identical. For the sake of completion, polyclonal antibodies are divided in heritage (Lu from Lunstrum group, BT from Bruckner-Tudermann group)

MATERIALS AND METHODS

Tissues

Ethics Statement: Eyes were provided by the Euro Cornea Bank, Beverwijk (<http://www.eurotissuebank.nl/corneabank/>), the Netherlands. In the Netherlands, the usage of donor material is provided for by the Organ Donation Act (WOD: Wet op de orgaandonatie). In accordance with this law, donors provide written informed consent for donation, with an opt-out for the usage of leftover material for related scientific research. Specific requirements for the use in scientific research of leftover material originating from corneal grafting have been described in an additional document formulated by the Ministry of Health, Welfare, and Sport, and the BIS foundation (Eurotransplant; Leiden, July 21, 1995; 6714.ht). The current research was carried out in accordance with all requirements stated in the WOD and the relevant documents. The vascular donor material was obtained after written informed consent of the patients. Its collection was approved by the institutional review board.

A total of 44 human eyes from 33 donors (15 men and 18 women) with ages varying between 22 and 83 years (mean donor age 63.8 years) and without known ophthalmic pathology were obtained after cornea removal (**Sup info Table 1**). All eyes were processed within 48 hours post mortem. Other vascular tissue samples included 6 umbilical cords (dissected into segments), hypodermal blood vessels from 7 panniculectomies (including 2 skin samples), and 4 samples of residual renal arteries from kidney transplantations.

Embedding

Eyes (n=4), umbilical cord segments (n=6), hypodermal blood vessels (n=7), renal arteries, and skin samples (n=2) were washed, mounted in optimal cutting compound OCT (Tissue-Tek; Sakura Finetek Europe, Alphen aan den Rijn, The Netherlands) and frozen in liquid nitrogen. Additionally, 12 eyes were embedded in paraffin (n=6 for 3-amino-9-ethylcarbazole staining, n=6 for immunofluorescence). Five eyes were embedded in T8100 resin (Technovit 8100; Heraeus Kulzer, Wehrheim, Germany) for light microscopic (n=3) or immunoelectron microscopic analysis (n=2, post-embedding)¹. One eye was embedded in epon resin for pre-embedding immunolabeling.¹ Four retinæ were dissected and briefly fixed (2% paraformaldehyde, 20 minutes). They were incubated in 1% Triton X-100/dH₂O (10 minutes) and washed extensively to remove loose retinal pigment epithelia fragments. These samples were then incubated in 3% H₂O₂/PBS for 72 hours, which reduced autofluorescence of the remaining pigment

epithelium. After a 24 hour incubation in 5% fatty acid free BSA/PBS blocking buffer they were labeled, washed and whole-mounted in antifading solution (AF100, Citifluor Ltd., London, UK) onto glass slides.

Immunohistochemistry (light microscopy)

Cryo, paraffin and resin samples were cut and processed as described previously.² In short, cryosections of about 10 µm thickness were cut using a cryomicrotome (CM3050 S Cryostat; Leica Microsystems, Wetzlar, Germany). Sections either remained unfixed, or were incubated in acetone or acetone/methanol for 10 minutes and air-dried. Any endogenous peroxidases were blocked by 0.3% H₂O₂/PBS incubation (30 minutes). The nonspecific binding of antigens was prevented by 3% BSA/PBS incubation (30 minutes). The primary anti-Col VII antibodies were allowed to incubate (1:100 in PBS for 1 hour). These comprised three monoclonal antibodies and three polyclonal antibodies, of which the details are given in **Table 2**.

TABLE 2. Anti-type VII collagen antibodies used in this study.

Primary antibody	Clone	Specificity	Host	Isotype	Company	Catalogue no.	Antibody Registry no.
pAb(16)		NC1 & 3H	Rabbit	IgG	Calbiochem (Merck/ Millipore)	234192	AB_211739
pAb(72)		NC1	Rabbit		Nyström et al.		
pAb(57)		NC1	Rabbit	IgG	Acris Antibodies	AP02276PU-S	AB_1618167
mAb(12)	LH7.2	NC1	Mouse	IgG1	Abcam	ab6312	AB_305415
mAb(14)	II-32	NC1	Mouse	IgG1	Chemicon (Merck/ Millipore)	MAB2500	AB_94355
mAb(70)	2Q633	NC1	Mouse	IgG1	US Biological	C7510-66A	n/a

pAb polyclonal antibody, *mAb* monoclonal antibody, *NC1* non-collagenous domain 1, *3H* collagen triple helical domain. The pAb(72) is a kind gift from dr. Alexander Nyström from the Department of Dermatology, Medical Center - University of Freiburg, Germany. The sequence with which pAb(72) was generated corresponds to a part of the NC-1 domain that was described to contain the LH7.2 epitope. It was tested against various purified ECM proteins and tissue lysates, and reacts with Col VII specifically.¹³

Then, sections were washed, incubated (1:500 in PBS, 1 hour) in corresponding horseradish conjugated secondary antibodies (DAKO, Glostrup, Denmark), and washed again. The sections were stained using 3-amino-9-ethylcarbazole (AEC Staining Kit; Sigma- Aldrich, St. Louis, MO, USA) and counterstained with hematoxylin. For signal enhancement, an avidin/biotin labeling kit (Vectastain Elite ABC kit; Vector Labs, Burlingame, CA, USA), was also used (according to the manufacturer's instructions) on cryo, paraffin and T8100 sections. Paraffin sections were cut at 3-4 µm thickness

(Leica RM2265 microtome), deparaffinized with xylene, and rehydrated by ethanol. For paraffin sections, antigen retrieval was achieved by protease K (IHC Select kit; Chemicon/Millipore) incubation, at a dilution of 1:5 in PBS for 15 minute period at 37°C. T8100 sections were cut at around 1 μm thickness. For resin sections, antigen retrieval was achieved by incubation in 0.05% trypsin (Gibco, Paisley, Scotland) in 0.1 M Tris-buffer (pH 7.8), containing 0.1% CaCl for 15 minutes at 37°C. Then, sections were washed in 0.2 M phosphate buffer and incubated in 0.1 M citric acid (pH 3.0) for 30 minutes at 37°C. An HC DMR microscope (Leica) was used to evaluate the samples. All procedures were carried out at room temperature (RT) unless stated otherwise. The negative control sections were not incubated in primary antibodies.

Immunofluorescence

Paraffin sections and retinal whole-mounts were used for double staining experiments. For sections, nonspecific binding of the primary antibodies was countered by incubation in 2% fatty acid free BSA (Sigma-Aldrich) in PBS for 30 minutes. The samples were incubated in primary antibodies (pAb(16), and either anti-glial fibrillary acidic protein (GFAP; mainly astrocytes, but also active Müller cells) mouse monoclonal (Sigma-Aldrich) or anti-smooth muscle actin (A2547, Sigma-Aldrich) 1:100 in 1%BSA/PBS, for 1 hour. The latter two antibodies were chosen to roughly determine the boundaries of Col VII locations at the vasculature. The sections were incubated in corresponding tetramethyl rhodamine isothiocyanate (TRITC, Sigma; 1:500) and fluorescein isothiocyanate (FITC, Dako; 1:500) antibodies for 45 minutes. Nuclei were visualized with 4', 6'-diamino-2-phenylindole solution (DAPI, Sigma; 1:5000). For whole-mounts, these incubations were each performed for 24 hours at 4°C. In control samples, the primary antibodies were omitted. A Leica TCS Sp2 confocal microscope was used in combination with corresponding imaging software (Leica LAS AF/LCS).

Immunoelectron microscopy

T8100 and epon sections of about 100 nm thickness (UltraCut E microtome, Reichert-Jung, Heidelberg, Germany) were used for immunoelectron electron microscopy. For T8100 post-embedding, sections were mounted on 150-mesh, 0.6% formvar-coated nickel grids. Antigen retrieval was achieved by trypsin, as mentioned. Nonspecific binding of the primary antibody was prevented by incubation in 2% BSA-c (Aurion, Wageningen, The Netherlands)/0.15% glycine/2% goat serum in PBS, for 30 minutes. Sections were incubated in a 1:100 primary pAb(16) antibody/PBS dilution for 2 hours at 37°C, then overnight at RT. After washing, samples were incubated in secondary gold-labeled antibody (Gold Colloid 5 nm, British Biocell International, Cardiff, UK;

1:200) for 1 hour at RT. Samples were fixed in 2% glutaraldehyde for 2 minutes after which silver enhancement (R-gent enhancer kit protocol, Aurion, 1:1) was performed for 10 minutes, according to the manufacturer's protocol. Samples were contrasted by methylcellulose-uranyl acetate (9:1) for 15 minutes at 4°C.

For epon pre-embedding, tissue blocks of 2x2 mm were dissected from one eye. They were fixed in 2% paraformaldehyde for 2 hours, washed in 0.1% NaBH₄ with 6.8% sucrose in phosphate buffer, and incubated in 5% BSA and 5% goat serum overnight to prevent nonspecific binding. The sample was incubated in a pAb(16) dilution of 1:100 in PBS overnight at RT. After thorough washing, the sample was incubated in secondary goat-anti-rabbit ultra-small gold-labeled antibody (Gold Colloid 2 nm, British Biocell International; 1:200) overnight. After thorough washing, the sample was fixed in 2% glutaraldehyde for 30 minutes, washed in 0.1M cacodylate buffer, and contrasted using 1% OsO₄. A 5 minute silver enhancement step was performed at RT. The samples were washed, dehydrated in ethanol (50%-100%) and propylene oxide, and mounted in epon. In control sections, the pAb(16) was omitted. All steps were performed at 4°C unless stated otherwise.

Western blot

From a total of 24 eyes, the sclera, choroid, retina, iris, ciliary body, lens, lens capsule, optic nerve, and vitreous bodies were dissected, pooled (n= 3 - 8 per pool) and homogenized. Segments of 6 umbilical cords, 7 hypodermal blood vessels, 4 renal arteries and 2 skin samples were dissected. Samples were cryogenically homogenized and solubilized in lysis buffer (CellLytic, Sigma-Aldrich). Homogenates were centrifuged at 13,000 rpm for 10 min at 4°C. The supernatants were either incubated in collagenase (60 units/ml; bacterial type VII collagenase, high purity grade, Sigma-Aldrich) or directly mixed with sample buffer (containing SDS and β-mercapto-ethanol) and then incubated at 37°C for 60 minutes. Alternatively, some samples were turraxed in sample buffer, or cryogenically homogenized and solubilized in sample buffer. Sample buffer, SDS-PAGE, and Western blotting proceedings were previously described.¹ For SDS-PAGE, 5 - 7.5% percent slab gels and a 72 mm wide 2D gel comb in a Bio-Rad Mini Protean II electrophoresis apparatus (Bio-Rad, Hercules, CA, USA) were used. The slabs were blotted to nitrocellulose membranes (Mini Protean II blotting unit, Bio-Rad) with 22 mM Tris (pH 8.3), 0.05% SDS, 168 mM glycine, and 20% methanol as a transfer buffer. The membranes were blocked in 2% fat-free milk for 1 hour, then incubated in primary antibodies pAb(16)(1:500), or a 1:1 mixture of the LH7.2 antibodies mAb(12) and mAb(70) (1:500 each). After incubation overnight, the membranes were washed with Tris-buffered saline containing 0.05% Tween-20. Corresponding secondary antibodies

(Jackson ImmunoResearch, West Grove, PA, USA; 1:1000) were added. After 1 hour of incubation, the membranes were washed and incubated with alkaline phosphatase conjugated tertiary antibodies (Jackson ImmunoResearch; 1:500) for another hour. After washing with Tween/ Tris-buffered saline and alkaline phosphatase buffer (100 mM Tris-HCl, 100 mM NaCl, and 5 mM MgCl₂, pH 9.5), the blot was developed with NBT/BCIP (BioRad, Hercules, CA, USA). Incubation and washing steps were performed at RT. In negative controls, the primary antibody was omitted.

RESULTS

Immunolabeling

The vasculature of retina, optic nerve, ciliary body, choroid, umbilical cord, abdominal aorta and renal artery (**Figures 1- 6; Sup info Figure 1**) were labeled by several anti-Col VII antibodies when assessed by microscopy. The unfixed cryosections were labeled more intensely than paraffin or T8100 sections. Also, polyclonal antibodies labeled more readily than monoclonal antibodies, and would therewith adequately label fixed tissues.

In order to validate the Col VII immunolabeling by pAb(16) at the ciliary body² and retinal¹ vasculature in paraffin sections, we compared the labeling patterns of pAb(16) to that of other anti-Col VII antibodies in unfixed cryosections (**Figure 1**). In each of these sections, some blood vessels would clearly label, while others would show only focal or no clear labeling (**Figure 1**). Then, as comparison to the ocular tissues, we analyzed the vascular labeling patterns of other vascularized tissues that were easily accessible, namely large (arteria renalis) and small blood vessels (from hypodermis). First, however, umbilical cord tissues were obtained to serve as positive controls. The umbilical cord is known to have both a dermis-like Col VII labeling pattern at the amnion BM, but was also reported to contain Col VII expressing endothelial cells in its vein.⁵ As expected, the epithelial basement membrane as well as the amnionic 'anchoring rivets' of the umbilical cords labeled intensely (**Figure 2**).^{5,6} Labeling was also seen in the umbilical arteries and vein (**Figure 3**), as well as in the renal artery (and abdominal aorta)(**Sup info Figure 1**). The hypodermal vasculature samples could not be sectioned appropriately due to unstable cryoembedding of the fatty matrix in the hydrophilic OCT compound. The vasculature of skin remained unlabeled (not shown).

The ocular vasculature was labeled by polyclonal antibodies in cryo and paraffin sections. Labeling was observed at the optic nerve head, at both the central retinal

artery and vein, as well as the smaller blood vessels (**Figure 4, Sup info Figure 2**). The labeling of tangentially cut blood vessels showed a striated aspect (**Sup info Figure 3**). In paraffin sections, the choroidal blood vessels were labeled in both immunofluorescence and AEC analysis (**Figure 4, Figure 5, Sup info Figure 4**). Unfortunately, the autofluorescent¹⁵ ECM protein elastin coincided with the vascular basement membranes of interest. This autofluorescent interference was bypassed by switching to AEC analysis, which showed labeling in the immediate proximity of the elastin fibers, but not of the fibers themselves (**Sup info Figure 5**). Immunofluorescence analysis of retinal paraffin sections showed no interference of elastin at the retinal vasculature (**Sup info Figure 6**). In retinal wholemounts, especially the larger blood vessels were labeled extensively for Col VII, while many smaller blood vessels were only weakly labeled or not at all (**Sup info Video 1**). The labeling showed a fibrillar aspect, mostly circling around the blood vessel walls, but clearly confined within the 'outer layer' of anti-glial cells (GFAP) labeling (**Figure 6A**). Furthermore, the Col VII labeling did not colocalize with myofibroblasts (α -SMA labeling), but rather seemed to exist mostly outside the α -SMA labeled envelope (**Figure 6B**).

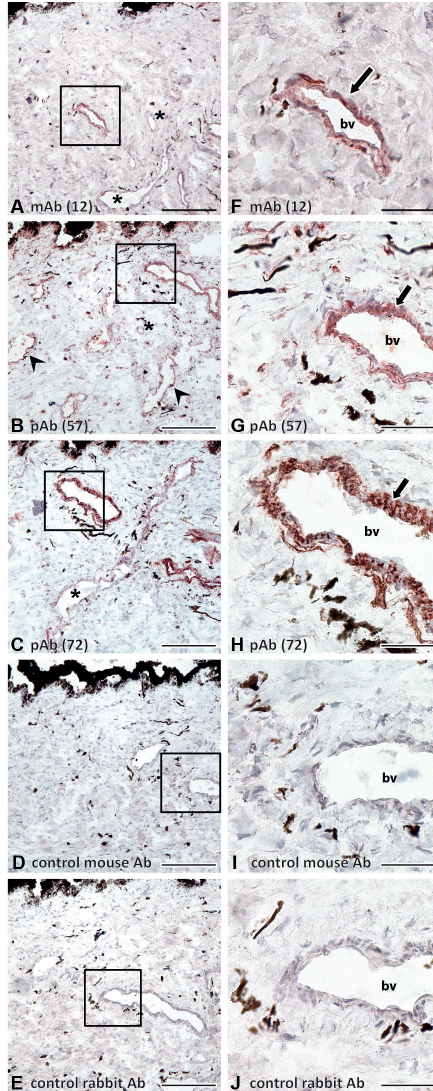


FIGURE 1. Col VII labeling at the ciliary body vasculature. Unfixed cryosections, pars plicata region, base of ciliary process, cut in a coronal plane. (A-E) Overviews of local blood vessels (bv), with corresponding insets (F-J). Various antibodies label (AEC, red) the walls of some blood vessels clearly (black arrows), whereas other blood vessels are labeled partially (arrowheads) or minimally (asterisks). The higher magnifications in the insets show clear labeling at the blood vessel walls (black arrows). Negative control sections of the monoclonal (D, I) and polyclonal (E, J) antibodies remained unlabeled. Some target antigen signals were amplified by an avidin/biotin complex labeling (B, C, G, H). Antibodies A-B mAb(12); C-D pAb(57); E-F pAb(72). Scale bars overview 200 μ m; inset 50 μ m.

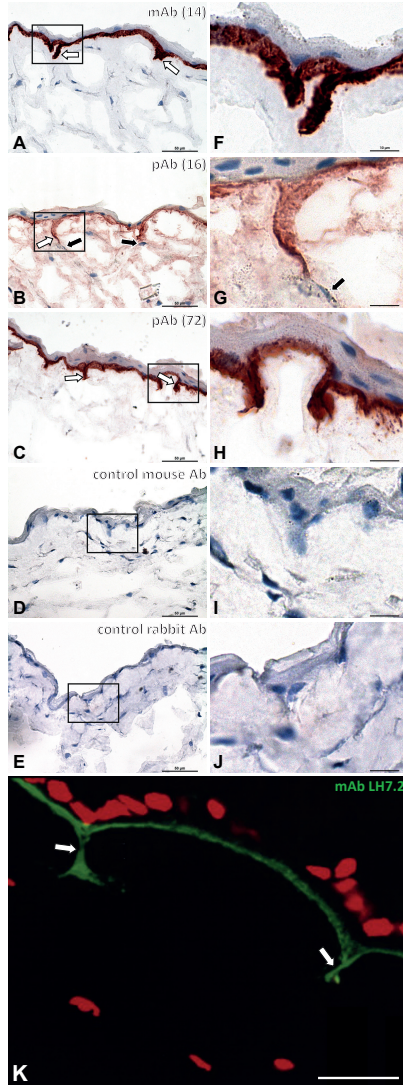


FIGURE 2. Col VII labeling at the superficial umbilical cord. Unfixed cryosections. (A-E) Overview of epithelial basement membrane with subepithelial 'anchoring rivets' (white arrows), with corresponding magnifications (F-J). Various antibodies label the epithelial basement membrane and the subepithelial rivets (AEC, red) in A-H, as was demonstrated previously (K, LH7.2 labeling in green and nuclear labeling in red; adapted from Ref 6). The labeled rivets protrude toward underlying fibroblasts (black arrows in B and G). Higher magnifications show clear labeling of the rivets, with some diffuse background staining of only the pAb(16) antibody. Negative control sections of the monoclonal (D,I) and polyclonal (E,J) antibodies remain unlabeled. Antibodies: A,F mAb(14), B,G pAb(16), C-H pAb(72). Scale bars overview 50 μ m; magnifications 10 μ m; K 25 μ m.

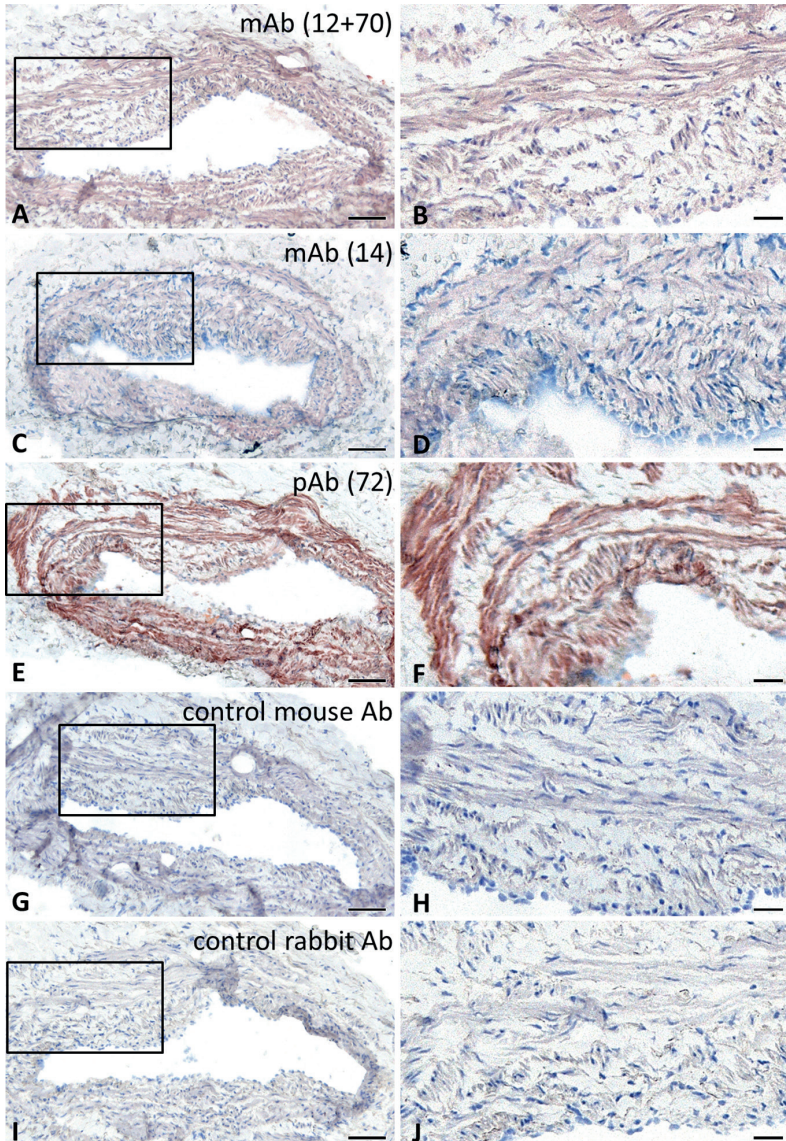


FIGURE 3. Col VII labeling at an umbilical cord vein. Unfixed cryosections. (A-D) Monoclonal and (D, E) polyclonal Col VII antibodies label at the blood vessel wall (AEC, red). The mAb(12+70) antibody labels at low intensity (C, D). Negative control sections for monoclonal (E) and polyclonal (F) antibodies remain unlabeled. Some vasa vasora (white arrows) can be appreciated, which appear to label at a similar intensity as the blood vessel walls. Antibodies A-B mAb(14); C-D mAb(12+70); E-F pAb(72). Scale bars A, C, E, I 50 μ m; B, D, F, H, J 25 μ m.

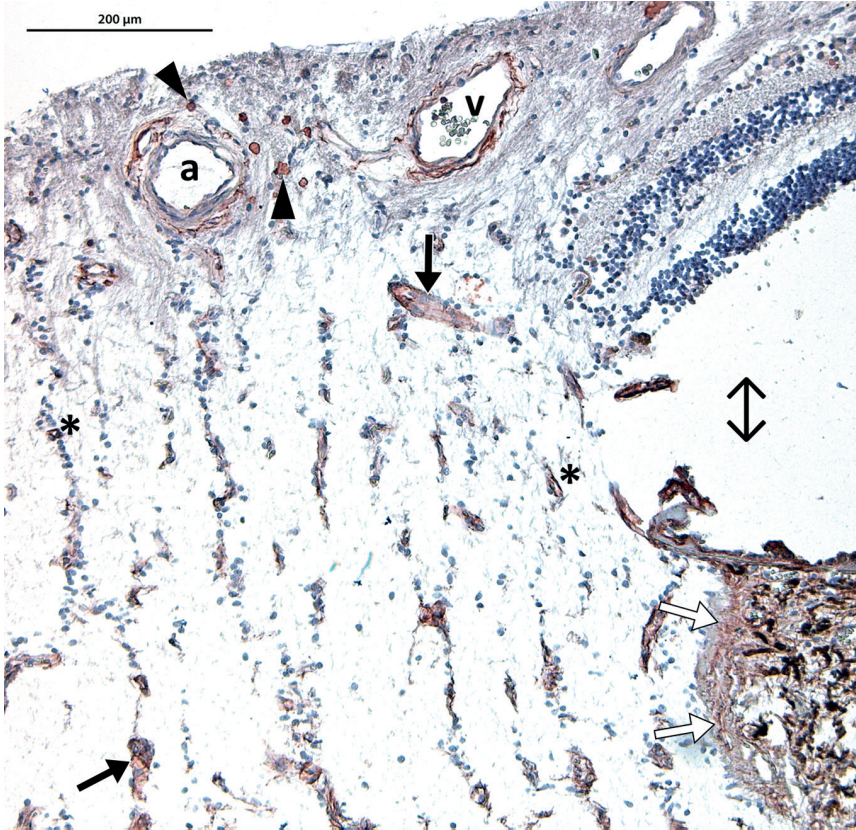


FIGURE 4. Col VII labeling of vasculature at the optic nerve head. Paraffin section, pAb(16). The larger blood vessels of the central retinal vasculature are labeled (AEC, red); (a) central retinal artery, (v) central retinal vein. Smaller blood vessels in the optic nerve head are labeled as well (asterisks). Some blood vessels are cut tangentially, which then show striated labeling along their trajectory (*black arrows*). In the lower right corner, the highly vascular choroid membrane is intensely labeled as well (*white arrows*). *Arrow heads* show corpora amylacea, ⇕ artificial detachment due to embedding. Scale bar 200 μ m.

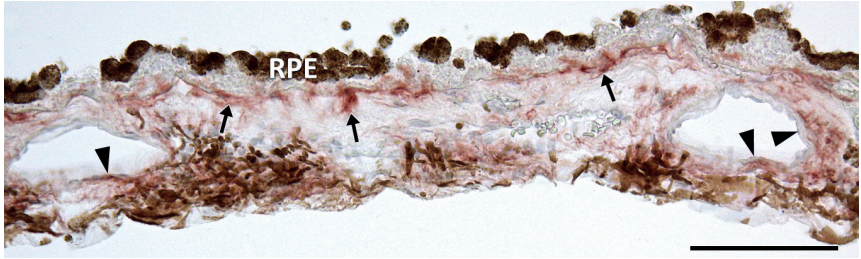


FIGURE 5. Col VII labeling at the choroid. Paraffin section, pAb(16). Col VII labeling (AEC, red) at the choriocapillaris (arrows) and larger choroidal blood vessels (arrowheads). Pigmented tissues appear brown. Scale bars 100 μ m.

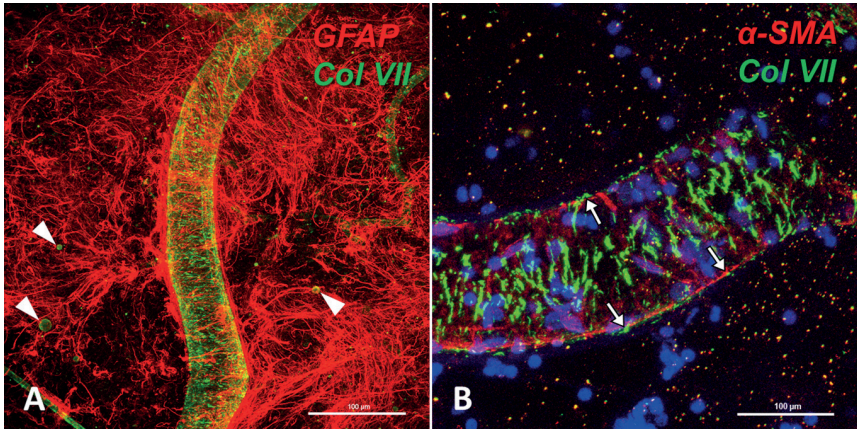


FIGURE 6. Dual fluorescence labeling of retinal vasculature. Unfixed retinal whole mounts, pAb(16). (A) Retinal blood vessels are labeled by Col VII (green) antibodies. This labeling does not colocalize with GFAP (red). Col VII appears to be located underneath the GFAP labeling. Corpora amylacea (arrow heads) are also Col VII positive. (B) Col VII does not colocalize with smooth muscle actin (α -SMA, red), but is encircling most of the α -SMA labeled structures (white arrows). Scale bars 100 μ m.

Immunoelectron microscopy

Immunoelectron microscopy of retinal blood vessels after pre-embedding labeling shows labeling of Col VII at the blood vessel outer walls, and around perivascular cellular basement membranes (**Figure 7**). In post-embedding labeling of the ciliary body, such labeling is extended to the basement membranes and around mural cells (**Figure 8**), and to a lesser extent, the stroma between ciliary blood vessels and pigmented epithelium.

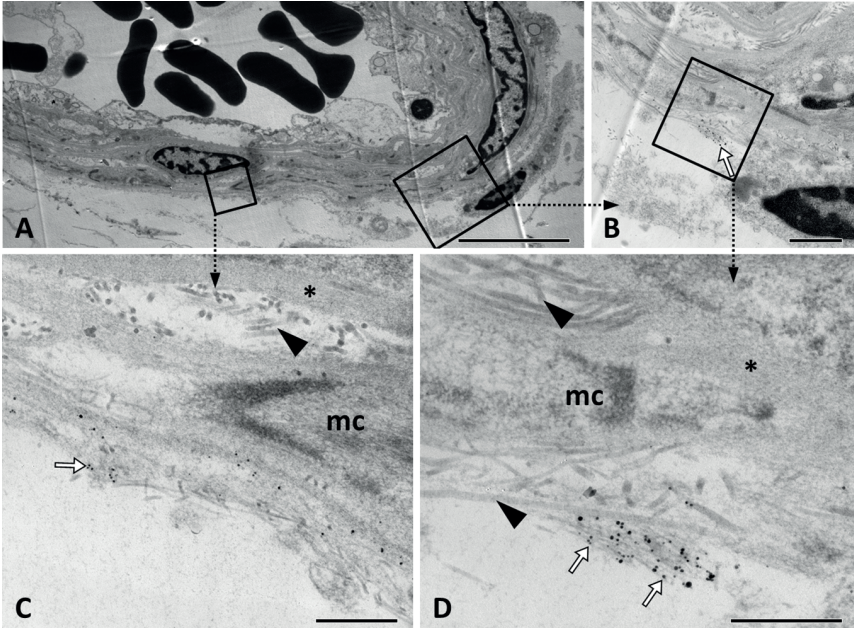


FIGURE 7. Blood vessel at the posterior retina. Epon, pre-embedding, pAb(16). (A) Overview, and magnifications at regions of interest (B-D). Gold labeling at small fibrils of the outer layer (white arrows). Silver enhancement of the nanogold particles resulted in varying diameters of the gold labels. No labeling is seen intracellularly (mc mural cell) at the mural cells inner basement membrane (*), or at the larger extracellular collagen fibers (arrowheads). Scale bars A 5 μ m; B 1 nm; C and D 500 nm.

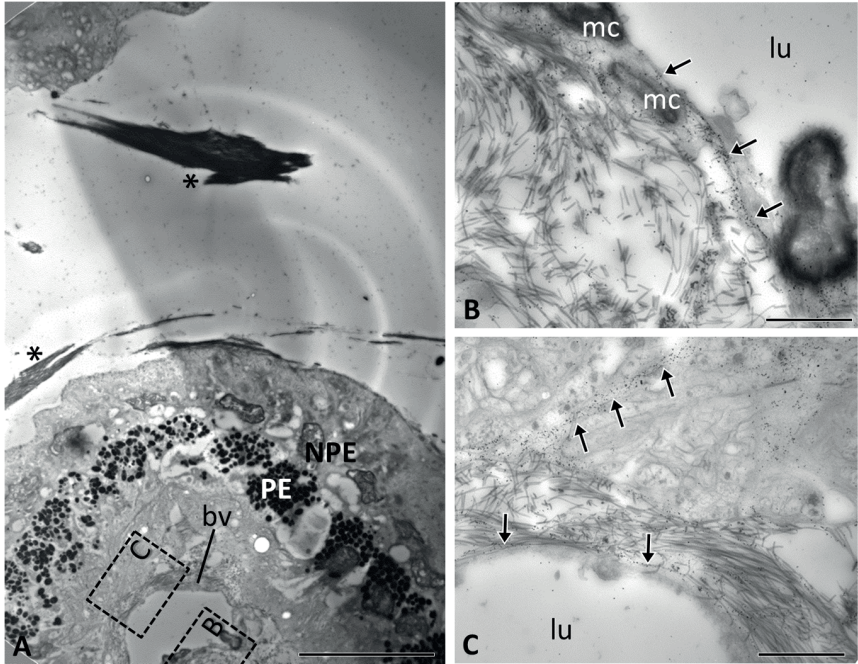


FIGURE 8. Ciliary body, post-embedded in T8100, pAb(16). (A) Overview of a tip of a ciliary process containing a small blood vessel (*bv*) underneath its pigmented epithelium (*PE*). In regions of interest (**B, C**) gold labeling (*black arrows*) is seen at the basement membranes surrounding two mural cells (*mc*) and blood vessel (*lu*) walls. Some labeling is seen at the large stromal fibers. Scale bars A 20 μm ; B and C 2 μm . *NPE* non pigmented epithelium, * zonules.

Western blotting

By Western blotting, Col VII could be demonstrated in several ocular tissues (**Figure 9, 10**). Mostly, the 145 kDa band corresponding to the NC-1 globular domain could be identified, while sometimes heavier products were seen. Cryogenic crushing appears to help release the NC-1 domain from the tissues. Signals from NC-1 targeting antibodies could be augmented further by collagenase incubation. Negative control sections did not show any bands (**Figure 10; Sup info Figure 7**). For isolating Col VII, liquid nitrogen homogenization and Cellytic lysis buffer both appear more effective than turraxing in sample buffer.

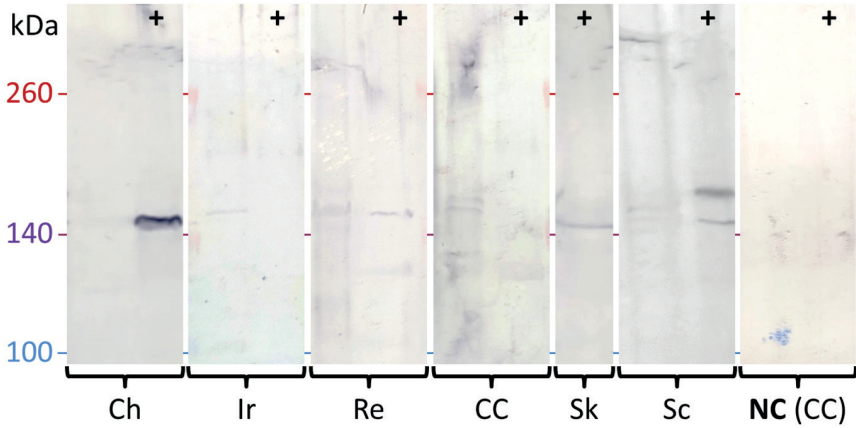


FIGURE 9. Western blot of isolated ocular tissue lysates, pAb(16). Samples subjected to collagenase digestion are indicated by (+). Collagenase digestion results in increased signals of the 145 kDa band, corresponding to the non-collagenous NC-1 domain. In this run, signals in iris (*Ir*) and retinal (*Re*) lysates are weak compared to those of ciliary body (*CC*) and choroid (*Ch*).

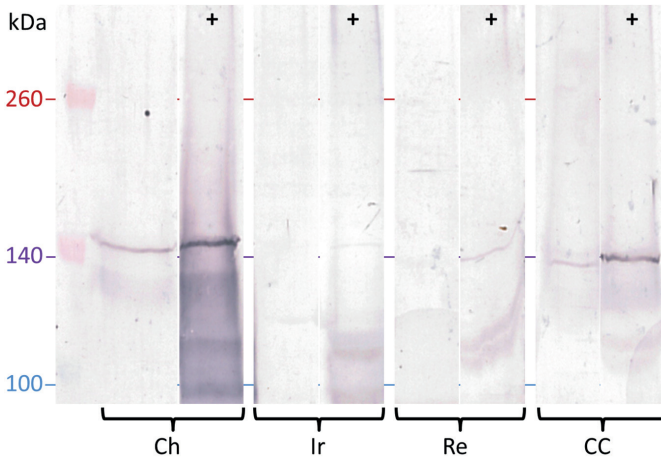


FIGURE 10. Western blot of isolated ocular tissue lysates, pAb(16). Samples subjected to collagenase digestion are indicated by (+). Collagenase treated skin lysate (*Sk*, positive control), shows the 145 kDa band corresponding to the NC-1 domain of Col VII. Most tissue lysates show this 145 kDa band, sometimes even without collagenase addition, which is suggestive of autolysis. Sclera lysate (*Sc*) shows >290 kDa products (aggregates) which are reduced to 145 kDa by collagenase. In iris lysate (*Ir*), the faint 145 kDa band completely disappears after collagenase treatment, in contrast to choroid (*Ch*), sclera (*Sc*) and retina (*Re*) lysates, in which the 145 kDa is augmented after collagenase treatment. Ciliary body (*CC*) lysate signal appears weak in this run. Negative control of ciliary body lysate shows no bands (*NC*).

In lysates of whole umbilical cord segments, a 145 kDa band (typical for the NC-1 domain of Col VII) appeared, as well as a clear 125 kDa band (corresponding to the P1 fragment of Col VII).¹⁵⁻¹⁷

(**Figure 11A**). Isolated umbilical vessels show the same labeling pattern as does isolated amnion (**Figure 11B**). Adult hypodermal vasculature and renal artery lysates give similar bands (**Figure 11A, C**). In contrast, choroid lysate may show multiple bands (**Sup info Figure 7**), or a single 145 kDa (**Figures 9, 10**) or 125 kDa (**Figure 11**) band. This is probably related to the sample volume and, more importantly, the freshness of the tissues.

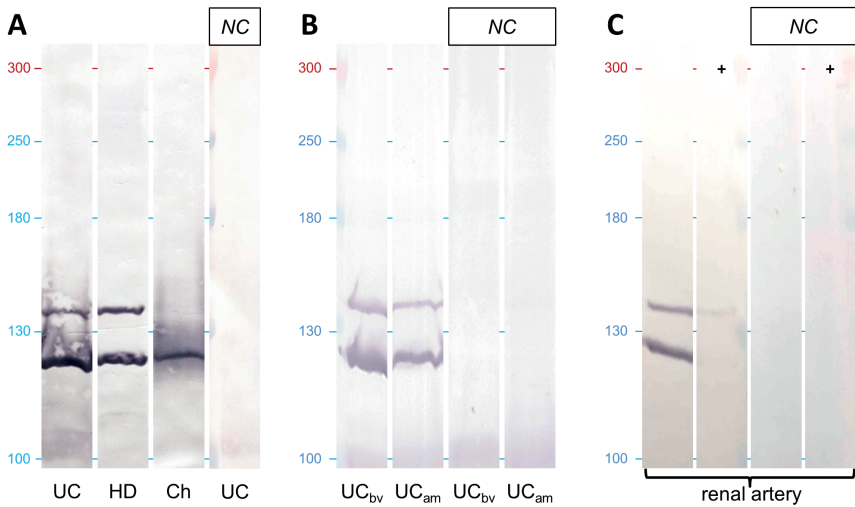


FIGURE 11. Western blots of vascular tissue lysates, mAb(12 + 70), Cellytic. (A) The positive control tissue, the umbilical cord lysates (*UC*) show bands at 145 kDa and 125 kDa, as do lysates from isolated hypodermal vasculature (*HD*). Choroid lysates show bands at 125 kDa, while umbilical cord negative control (*NC*) shows no bands. (B) Isolated umbilical blood vessels (UC_{bv} = arteries and vein, pooled) and isolated amnion (UC_{am}) lysates show both 145 and 125 kDa bands, while their negative controls do not. (C) Similar bands are seen in renal artery lysates without incubation, which disappear with (+) collagenase incubation.

DISCUSSION

Col VII could be demonstrated at most vascularized ocular and non-ocular tissues, by immunohistochemistry, -fluorescence, -electron microscopy and -blotting. By immunohistochemistry and -electron microscopy, Col VII was observed from the sub-endothelial layer throughout the blood vessel wall and perivascularly where it was associated with mural cells.

The perivascular labeling of Col VII in ciliary body, retina, optic nerve head and choroid sections as well as in the non-ocular tissues (aorta, renal artery and umbilical cord vessels) was validated by the corresponding amnion (positive control) labeling. We tried to pinpoint the perivascular location of Col VII more thoroughly in paraffin and resin sections, but we were dependent on polyclonal antibodies. The required fixation procedures would not allow for the use of monoclonals, since this persistently resulted in rudimentary staining. The perivascular Col VII labeling was compared to other vasculature associated proteins, GFAP and α -SMA, using immunofluorescence in retinal sections and wholemounts. This showed that Col VII localizes between the subendothelial basement membrane and the outer GFAP envelope of the glial cells.

Within a same section, some retinal vessels would label more intensely for Col VII than others. Such differences are not completely understood, but may in part be attributed to differences in blood vessel composition, based on e.g. regional differences or size. For example, perivascular Col VII could be detected in the head and neck region, but not in the thymus.^{18, 19} Methodological differences between studies (i.e. fixation) may also affect detection, as some perivascular Col VII was successfully labeled in several unfixed epithelial tissues before.⁹ In contrast to acetone fixation, the Zamboni fixative (pH7.3) allowed for Col VII detection by monoclonal LH7.2 in the lamina basalis and adventitial layers of pelvic fascia vasculature.⁸ In our experience, the ability to label Col VII with monoclonals correlates strongly with tissue freshness, methods of fixation, and adequate antigen retrieval. Previously, we were unable to demonstrate Col VII by monoclonals in fixed paraffin sections by immunoperoxidase labeling, or to provide convincing labeling of IF sections.¹

By comparing some immunohistological studies on Col VII (**Table 1**) the methodological variations among investigators become clear. (Chor)amnion tissue labeling, for example, may result in infrequent, granular or strong (++) labeling, depending on methods and antibodies used, while skin/mucosa labeling generally shows no variation. The currently established monoclonal antibodies target the NC-1 domain of Col VII (**Figure**

12). However, the formation of monoclonal antibody-antigen complexes is thought to be significantly impeded by fixatives, and the epitopes of tissue Col VII are reportedly susceptible to strong detergents and denaturing agents. The application thereof may reduce the labeling potential of monoclonal antibodies.¹⁹

Comparatively, in our Western blots, adequate bands were not obtained by the use of a singular monoclonal antibody. However, when monoclonal antibodies from two different companies were mixed and applied in the usual concentration, clear bands would appear. Such bands corresponded to the 145 kDa NC-1 domain, or a 125 kDa band which probably corresponds to the P1 fragment of Col VII.¹⁵⁻¹⁷ The susceptibility of Col VII to collagenase was tested after non-enzymatic extraction from the tissues. Collagenase is known to cleave the collagen triple helix, and leave the globular NC-1 domain still accessible to monoclonal antibody binding. After collagenase incubation, antibodies that target the triple helix (as pAb(16) partially does) should therefore show bands of diminished intensity, while NC-1 targeting antibody band intensities should remain unaltered. Interestingly, the mAb(12+70) band of the renal artery lysate, faded. Moreover, choroid lysates showed mAb bands of 125 kDa, while pAb showed 145 kDa bands after collagenase digestion. In most of our samples, however, collagenase incubation would increase band intensity. For pAb(16), this might be explained by increased accessibility of the residual epitopes, or higher concentration of Col VII monomers out of higher order aggregates. It is unclear whether influences like autolysis or the resolution of multimer Col VII aggregates might sufficiently explain such diversity.

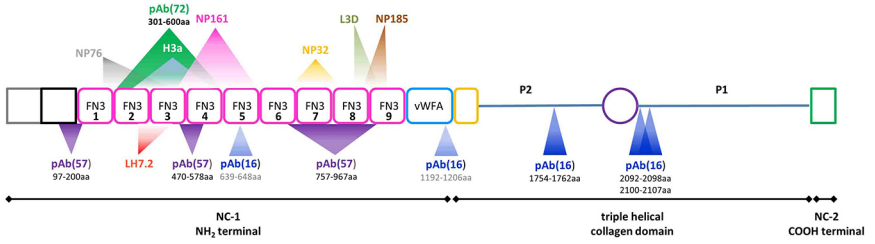
Generally, polyclonal antibodies are less affected by fixation, are often more sensitive due to their multiple potential epitope binding sites, and are regarded as less specific than monoclonals due to the potential cross-reactivity of the polyclonals. Our primary antibody pAb(16) was previously validated in our lab, and was shown to have epitopes on both the NC-1 domain and the triple helix. Western blotting with pAb(16), therefore, results in a relatively mild decrease of the 145 kDa bands in collagenase digested lysates since NC-1 epitopes could still be targeted by pAb(16), but not by mAb(12+70).¹
² The specificity of the pAb(16) antibody is underlined by the corresponding labeling patterns of the monoclonals and the polyclonal pAb(72) in umbilical cord control tissues.

In sections, no Col VII labeling was detected at the dermal vasculature, irrespective of fixation or antibodies used. We have not attempted to isolate dermal blood vessels for Western blot analysis. In contrast, the hypodermis vasculature could not be analyzed in sections, but showed clear Col VII presence in Western blots. No anchoring fibrils

were observed in any perivascular environment. Since anchoring fibrils are currently the only established functional anchoring mode of (aggregated) Col VII, we cannot determine the function of perivascular Col VII by our data alone. Future investigations on vascular tissues from RDEB donors, for example, might provide more substance for its function and clinical implications.

Our observation of a general presence of blood vessel associated Col VII from a number of ocular and non-ocular tissues is remarkable in view of the contradictory results reported in literature as summarized in **Table 1**. An important observation in our study was that successful immunolabeling with Col VII antibodies is much dependent on pretreatment of tissues, and is easily hindered by fixation procedures. This is particularly observed with the use of monoclonal antibodies. This observation in itself can explain that Col VII around blood vessels has been scarcely reported. In most previous studies, monoclonal antibodies have been used on fixed tissues. Maybe, as a consequence of such fixation, authors did not observe any labeling, fragmented labeling, or clear labeling in abnormal tissues only (e.g. fibrosis/neoplasms)(**Table 1**). Therefore, we advise to use monoclonal antibodies on unfixed cryosections in future exploratory studies on the presence of Col VII in tissues.

Figure 12: Simplified schematic representation of the reported locations of epitopes of anti-Col VII antibodies. In order to compare immunolabeling patterns that were reported in the literature of the past three decades, the antibodies that were used in those studies were reviewed. Several antibody designations were maintained in that time, and their origins not always clearly described. Sometimes, a(n) (co)author from a group that developed an antibody would later report original or additional characteristics. Such data was bundled into **Table 1**. In order to augment the interpretation of their study results, their methods and materials were regarded as well. Several authors have reported different results based on tissue fixation, embedding, method of antibody visualization and other antibody-epitope complex binding affection actions. Most antibodies are directed against a fibronectin-3 (*FN3*) motif on the NC-1 domain of the Col VII molecule. The polyclonal antibody pAb(16) is mainly directed against epitopes on the triple helical domain, although epitope mapping also showed some affinity against epitopes on the 5th FN3 domain and von Willebrand factor A domain (*vWFA*). LH7.2 is reportedly directed against an area at the 2nd and 3rd FN3 domain, while the polyclonal pAb(72) was designed to recognize an area spanning the 2nd to 4th FN3 domain. Decreased transparency of the triangles points or bases corresponds to increased certainty of epitope location.



Acknowledgements

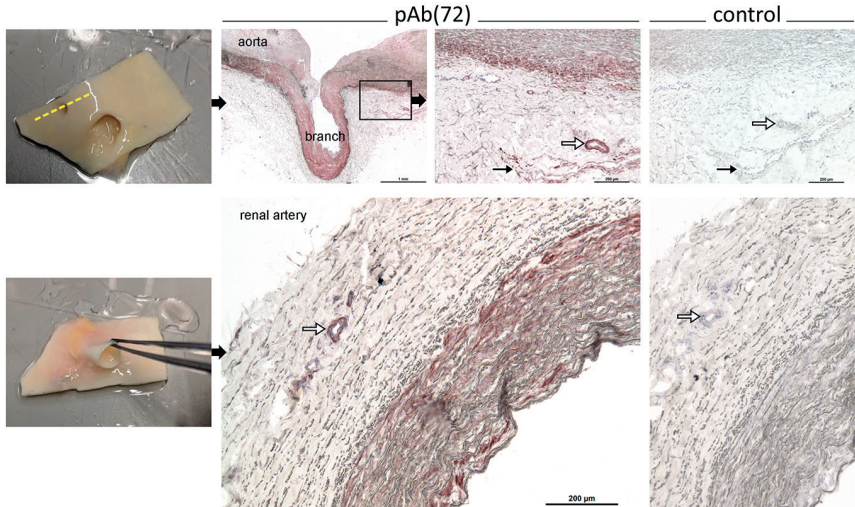
We would like to thank Alex Nyström, PhD (University of Freiburg, Freiburg im Breisgau, Germany) for his kind gift of polyclonal LH7.2 antibody; Wilfred den Dunnen, PhD, Rob Verdijk, PhD, and Gilles Diercks, PhD for their contribution to interpreting the data based on their anatomy/pathology expertise; UMCG Division of Transplantation Surgery, the Division of Obstetrics & Gynaecology, and the Euro Cornea Bank for supplying us with tissues.

SUPPORTING INFORMATION

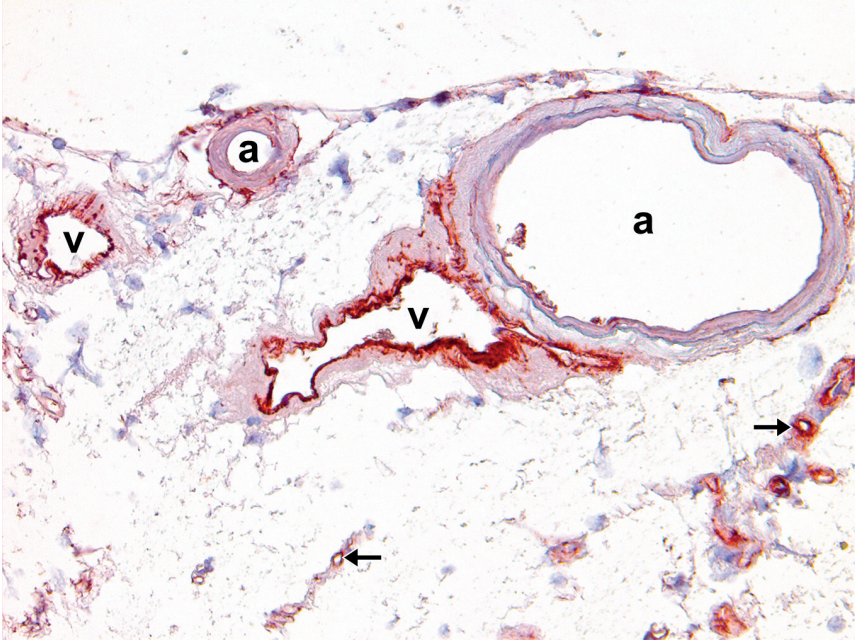
SUPPORTING INFORMATION TABLE 1. Donor characteristics.

Donors	Gender	Age	Cause of Death	OCT cryo	T8100 LM	T8100 post	epon pre	citifluor WM	paraffin AEC	Wb
74676	m	78	Malignancy		1					
77947	f	69	CVA		1					
97691	f	78	Cardial			1				
116727	f	63	Cardial						1	
120534	f	57	CVA					1		
120546	f	50	Malignancy					1		
120551	m	52	Malignancy					1		
125651	f	71	Cardial				1			
124042	f	73	Malignancy						1	
127435	f	65	Suicide							1
140379	f	83	CVA						1	
140385	m	65	Cardial						1	
140502	m	64	Cardial						1	
140521	f	78	CVA						1	
140846	f	48	Liver cirrhosis	1						
300589	m	44	Suicide							2
300594	f	56	Malignancy							2
300636	f	78	CVA							2
301414	f	67	Malignancy	1						
301417	m	68	Malignancy	1						
301418	m	83	Cardial	1						
301446	m	63	Trauma							2
301463	m	70	Respiratorial							2
301629	m	62	Cardial							2
301632	f	65	Cardial							2
301634	f	40	CVA							2
301641	f	76	Metabolic							2
301644	m	71	Malignancy							1
301835	m	66	Malignancy							2
301858	m	22	Cardial							2
303683	f	80	Malignancy					1		
305632	m	66	Cardial		1					
305633	m	35	Cardial			1				
33 donors				4	3	2	1	4	6	13
44 eyes				4	3	2	1	4	6	24

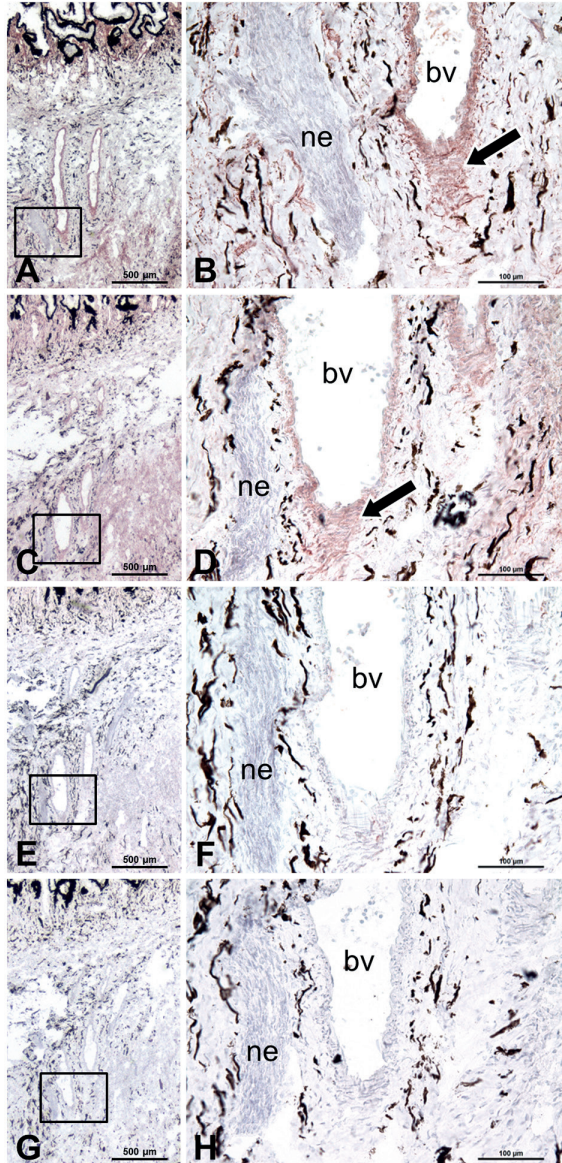
A total of 44 eyes of 33 donors were used for cryosections (*cryo*), light microscopy of resin samples (*LM*), post- or pre-embedding of resin samples for immunoelectron microscopy, whole mounting in antifading compound (*WM*), paraffin sections for peroxidase labeling (*AEC*), or SDS-PAGE/Western blotting (*Wb*); CVA cardiovascular accident.



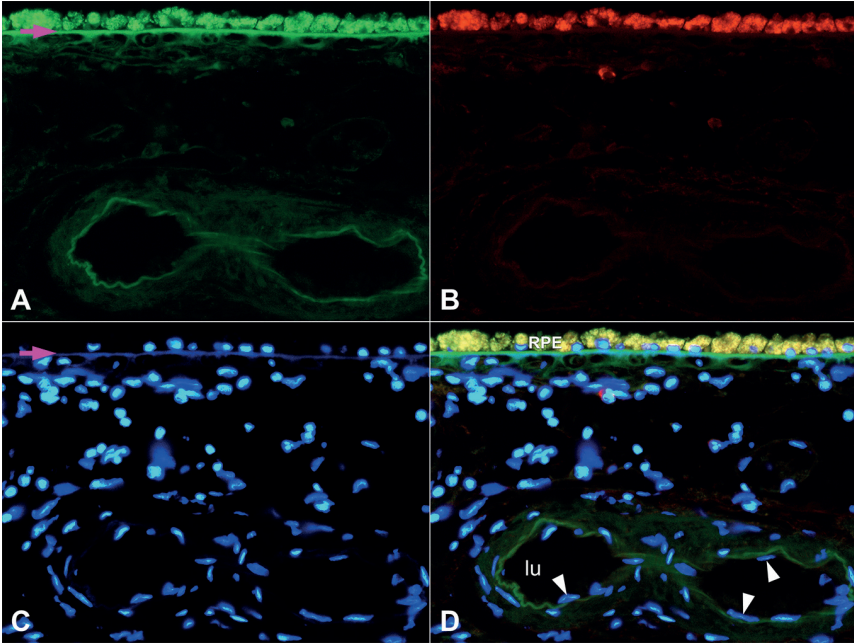
SUPPORTING INFORMATION FIGURE 1. Col VII labeling at the abdominal aorta and renal artery. Unfixed cryosections, pAb(72). **Top row:** a section through the abdominal aorta and a small aorta-to-renal artery branch (*yellow cutting line*) shows labeling mostly in the middle of the aortic and branch wall (AEC, red). Vasa vasora (*arrows*) stand out in the tunica externa of the aorta, especially in perpendicular sections (*white arrows*). Scale bars 1 mm and 100 μ m. **Bottom row:** the perpendicularly cut renal artery displays labeling mostly at the tunica media and at vasa vasora in the tunica externa. Negative controls show no labeling. Scale bar 200 μ m.



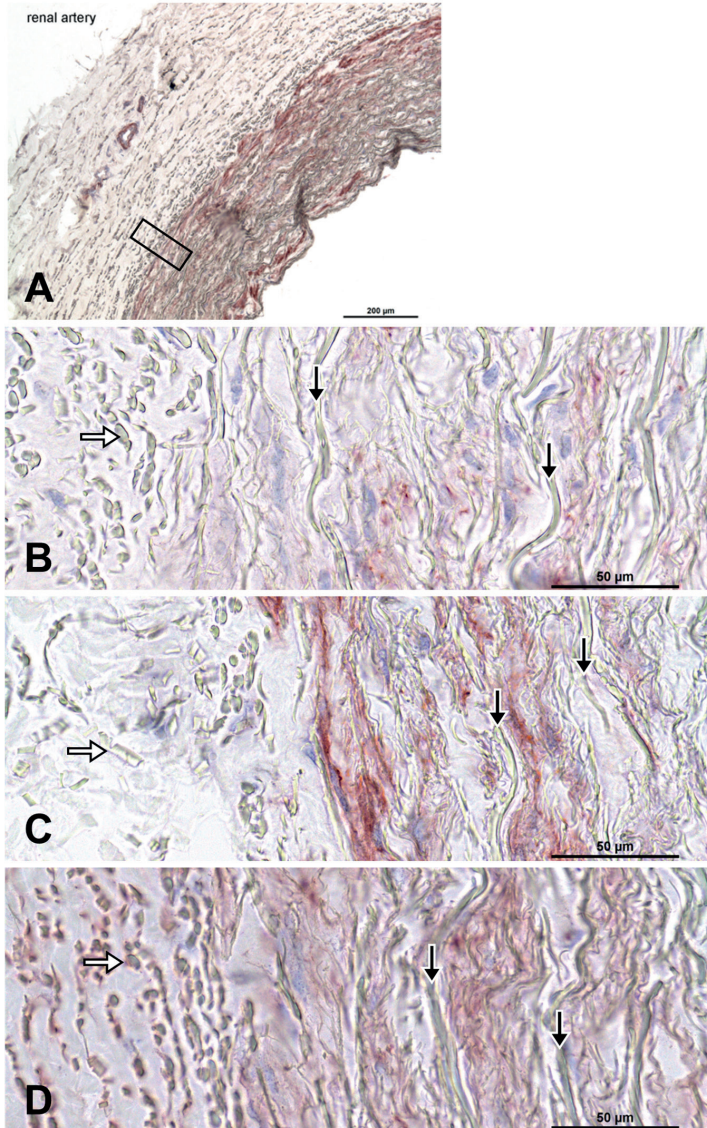
SUPPORTING INFORMATION FIGURE 2. Col VII labeling at the optic nerve head vasculature. Paraffin section, pAb(16), avidin/biotin enhancement. In this section, especially veins (v) and smaller blood vessels (*black arrows*) are labeled (AEC red). An artery (a) shows focal perivascular labeling. Scale bar 100 μ m.



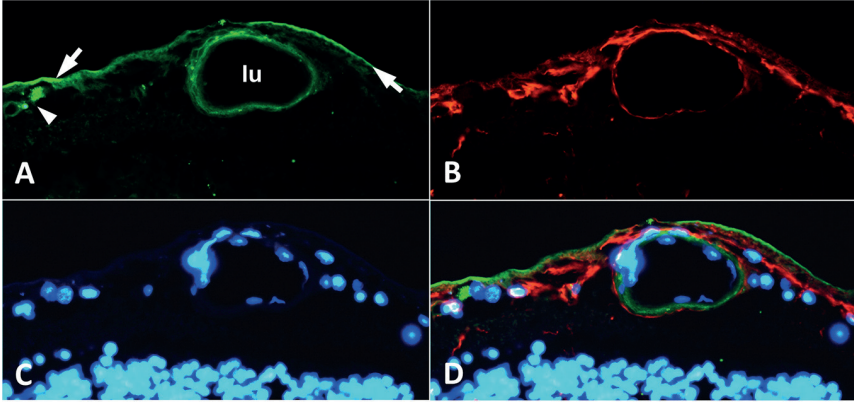
SUPPORTING INFORMATION FIGURE 3. Col VII labeling at the ciliary body vasculature. Unfixed cryosections, pars plicata region, cut in coronal plane. Overview (A, C, E, G) and corresponding magnifications (B, D, F, H) of ciliary blood vessel (bv) and nerve (ne). The antibodies mAb(12) (A,B) and pAb(72) (C, D) label the blood vessel wall (AEC, red), showing a striated aspect (black arrows). Negative control sections for mono- (E, F) and polyclonal (G, H) antibodies remain unlabeled. Scale bars overview 500 µm; magnifications 100 µm.



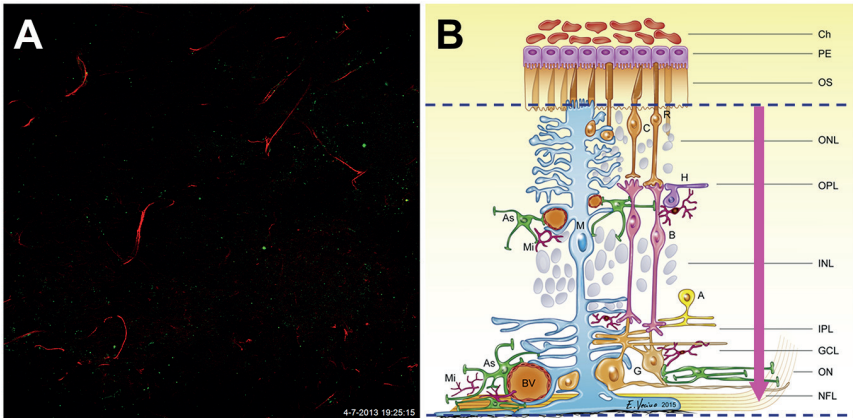
SUPPORTING INFORMATION FIGURE 4. Elastin and pigment autofluorescence at the choroidal membrane. Here some Col VII labeling (**A**, green) delineates the capillaries of the lamina choriocapillaris, directly under retinal pigmented epithelium (RPE). It also labels at larger vessels (*lu* lumen). In order to illustrate the scope of the expected elastin autofluorescence at Bruch's membrane (*pink arrows*), elastin autofluorescence was made visible by increasing the energy intensity in the blue channel (**C**, *DAPI*). In normal intensity settings, such as in the red channel, no autofluorescence is apparent at Bruch's membrane. Therefore, the signal of the normal intensity green channel is true; Col VII labeling occurs underneath Bruch's membrane, and surrounds the capillaries of the choriocapillaris. Autofluorescence of the RPE lipofuscin granules is seen especially in the green and red channels. In the merged image (**D**), some Col VII lining (green) can be seen underneath endothelial cells (*arrowheads*). GFAP did not label around choroidal blood vessels (**B**, red). Green pAb(16) (anti-Col VII marker), red GFAP (glial cell marker), blue DAPI (cell nucleus marker), paraffin section double labeling. Magnification x20.



SUPPORTING INFORMATION FIGURE 5. Transition area between tunica media and adventitia. Unfixed cryosections, renal artery, overview (A) labeled with pAb(72), and insets of high magnification (400x) labeled with mAb(14) (B), pAb(72) (C), and pAb(16) (D). None of the antibodies label elastin fibers (black arrows), although the pAb(16) antibody labels closely to (or perhaps around) perpendicularly cut elastin fibers (white arrows). The antibodies mAb(14) and pAb(72) do not label at such proximity. Scale bars overview 200 µm; magnifications 50 µm.



SUPPORTING INFORMATION FIGURE 6. Col VII and GFAP labeling at the retinal vasculature. Larger retinal blood vessels (*lu* lumen) show mural Col VII labeling (**A**, green, pAb(16)). GFAP (**B**, red) does not colocalize with Col VII. No elastin autofluorescence was seen at the retinal vasculature when increasing the energy intensity of the blue channel (**C**, DAPI). Additionally, a small ERM (*white arrows*), and corpora amylacea and vesicles (at *arrowhead*) are labeled by Col VII. The vascular Col VII labeling localizes closer to the lumen than the GFAP labeling (**D**, merged image). Paraffin section double labeling. Magnification x20.



SUPPORTING INFORMATION VIDEO 1. Dual fluorescence labeling of retinal vasculature. Unfixed whole mounts, pAb(16). (**A**) Confocal laser scanning microscopy assisted computer tomography through a retinal whole mount. First, some GFAP (red) labeling is seen around the smaller, Col VII (green) labeled blood vessels of outer retinal layers. Then glial cell coverage by GFAP drastically increases from around the inner plexiform layer (*IPL*) towards the nerve fiber layer (*NFL*), in approximation of larger blood vessels there. The video ends with Col VII labeled vesicle clusters around multiple perivascular cell nuclei (round dark cores of the green clusters). (**B**) schematic diagram of retinal organization, pink arrow shows direction of video/tomography. Adapted from Vecino E, Rodriguez FD, Ruzafa N, et al. *Prog Retin Eye Res.* 2016; 51:1-40.

REFERENCES

1. Wullink B, Pas HH, Van der Worp RJ, Kuijjer R, Los LI. Type VII collagen expression in the human vitreoretinal interface, corpora amylacea and inner retinal layers. *PLoS One*. 2015; 10:e0145502.
2. Wullink B, Pas HH, Van der Worp RJ, Schol M, Janssen F, Kuijjer R, Los LI. Type VII Collagen in the human accommodation System: Expression in ciliary body, zonules, and lens capsule. *IOVS*. 2018; 59:1075-1083.
3. Uechi G, Sun Z, Schreiber EM, Halfter W, Balasubramani M. Proteomic view of basement membranes from human retinal blood vessels, inner limiting membranes, and lens capsules. *J Proteome Res*. 2014;13:3693–3705.
4. Naba A, Clauser KR, Ding H, Whittaker CA, Carr SA, Hynes RO. The extracellular matrix: Tools and insights for the “omics” era. *Matrix Biol*. 2016; 49:10-24.
5. Ryynänen J, Tan EM, Hoffren J, Woodley DT, Sollberg S. Type VII collagen gene expression in human umbilical tissue and cells. *Lab Invest*. 1993; 69:300-304.
6. Ockleford C, McCracken S, Rimmington L, Hubbard A, Bright N, Cockcroft N, et al. Type VII collagen associated with the basement membrane of amniotic epithelium forms giant anchoring rivets which penetrate a massive lamina reticularis. *Placenta*. 2013; 34:727–737.
7. Paulus W, Baur I, Liszka U, Drlicek M, Leigh I, Bruckner-Tuderman L. Expression of type VII collagen, the major anchoring fibril component, in normal and neoplastic human nervous system. *Virchows Arch*. 1995; 426:199–202.
8. Radziszewski P, Borkowski A, Torz C, Bossowska A, Gonkowski S, Majewski M. Distribution of collagen type VII in connective tissues of postmenopausal stress-incontinent women. *Gynecol Endocrinol*. 2005; 20:121-126.
9. Chi CC, Wang SH, Prenter A, Cooper S, Wojnarowska F. Basement membrane zone and dermal extracellular matrix of the vulva, vagina and amnion: An immunohistochemical study with comparison with non-reproductive epithelium. *Australas J Dermatol*. 2010; 51: 243-247.
10. Lunstrum GP, Kuo HJ, Rosenbaum LM, Keene DR, Glanville RW, Sakai LY, et al. Anchoring fibrils contain the carboxyl-terminal globular domain of type VII procollagen, but lack the amino-terminal globular domain. *J Biol Chem*. 1987; 262:13706-13712.
11. Fine JD, Hall M, Weiner M, Li KP, Suchindran C. The risk of cardiomyopathy in inherited epidermolysis bullosa. *Br J Dermatol*. 2008; 159:677-682.
12. Ryan TD, Lucky AW, King EC, Huang G, Towbin JA, Jefferies JL. Ventricular dysfunction and aortic dilation in patients with recessive dystrophic epidermolysis bullosa. *Br J Dermatol*. 2016; 174:671-673.
13. Kühl T, Mezger M, Hausser I, Handgretinger R, Bruckner-Tuderman L, Nyström A. High Local Concentrations of Intradermal MSCs Restore Skin Integrity and Facilitate Wound Healing in Dystrophic Epidermolysis Bullosa. *Mol Ther*. 2015; 23:1368-1379.
14. Heagerty AH, Kennedy AR, Leigh IM, Purkis P, Eady RA. Identification of an epidermal basement membrane defect in recessive forms of dystrophic epidermolysis bullosa by LH 7:2 monoclonal antibody: use in diagnosis. *Br J Dermatol*. 1986; 115:125-131.
15. Chen M, Costa FK, Lindvay CR, Han YP, Woodley DT. The recombinant expression of full-length type VII collagen and characterization of molecular mechanisms underlying dystrophic epidermolysis bullosa. *J Biol Chem*. 2002; 277:2118-2124.
16. Titeux M, Pendaries V, Zanta-Boussif MA, Décha A, Pironon N, Tonasso L, et al. SIN retroviral vectors

- expressing COL7A1 under human promoters for ex vivo gene therapy of recessive dystrophic epidermolysis bullosa. *Mol Ther.* 2010; 18:1509-1518.
17. Bornert O, Kühl T, Bremer J, van den Akker PC, Pasmooij AM, Nyström A. Analysis of the functional consequences of targeted exon deletion in COL7A1 reveals prospects for dystrophic epidermolysis bullosa therapy. *Mol Ther.* 2016; 24:1302-1311.
18. Wetzels RH, van der Velden LA, Schaafsma HE, Manni JJ, Leigh IM, Vooijs GP, et al. Immunohistochemical localization of basement membrane type VII collagen and laminin in neoplasms of the head and neck. *Histopathology.* 1992; 21:459-464.
19. Virtanen I, Lohi J, Tani T, Sariola H, Burgeson RE, Lehto VP. Laminin chains in the basement membranes of human thymus. *Histochem J.* 1996; 28:643-650.
20. Hessle H, Sakai LY, Hollister DW, Burgeson RE, Engvall E. Basement membrane diversity detected by monoclonal antibodies. *Differentiation.* 1984; 26:49-54.
21. Leigh IM, Purkis PE. LH7:2 a new monoclonal antibody to a lamina densa protein. European Society for Dermatological Research, 15th Annual Meeting. *J Invest Dermatol.* 1985; 84:433-456. Abstract.
22. Paller AS; Queen LL, Woodley DT, Gammon WR, O'Keefe EJ, Briggaman RA. A mouse monoclonal antibody against a newly discovered basement membrane component, the epidermolysis bullosa acquisita antigen. *J. Invest Dermatol.* 1985; 84:215-217.
23. Burgeson RE, Morris NP, Murray LW, Duncan KG, Keene DR, Sakai LY; The structure of type VII collagen. *Ann N Y Acad Sci.* 1985; 460:47-57.
24. Lunstrum GP, Sakai LY, Keene DR, Morris NP, Burgeson RE. Large complex globular domains of type VII procollagen contribute to the structure of anchoring fibrils. *J Biol Chem.* 1986; 261:9042-9048.
25. Sakai LY, Keene DR, Morris NP, Burgeson RE. Type VII Collagen is a major structural component of anchoring fibrils. *J Cell Biol.* 1986; 103:1577-1586.
26. Keene DR, Sakai LY, Lunstrum GP, Morris NP, Burgeson RE. Type VII Collagen Forms an Extended Network of Anchoring Fibrils. *J Cell Biol.* 1987; 104:611-621.
27. Bruckner-Tuderman L, Schnyder UW, Winterhalter KH, Bruckner P. Tissue form of type VII collagen from human skin and dermal fibroblasts in culture. *Eur J Biochem.* 1987; 165:607-611.
28. Leigh I, Purkis P, Bruckner-Tuderman L. LH7.2 monoclonal antibody detects type VII collagen in the sublamina densa zone of ectodermally-derived epithelia, including skin. *Epithelia.* 1987; 1:17-29.
29. Yoshiike T, Woodley DT, Briggaman RA. Epidermolysis bullosa acquisita antigen: relationship between the collagenase-sensitive and -insensitive domains. *J Invest Dermatol.* 1988; 90:127-133.
30. Woodley D, Burgeson R, Lunstrum G, Bruckner-Tuderman L, Reese M, Briggaman R. Epidermolysis bullosa acquisita antigen is the globular carboxyl terminus of type VII procollagen. *J Clin Invest.* 1988; 81:683-687.
31. Kirkham N, Gibson B, Leigh IM, Price ML. A comparison of antibodies to type VII and type IV collagen laminin and amnion as epidermal basement membrane markers. *J Pathol.* 1989; 159:5-6.
32. Wetzels RH, Holland R, van Haelst UJ, Lane EB, Leigh IM, Ramaekers FC. Detection of basement membrane components and basal cell keratin 14 in noninvasive and invasive carcinomas of the breast. *Am J Pathol.* 1989; 134:571-579.
33. Wetzels R, Robben H, Leigh I, Schaafsma H, Vooijs G, Ramaekers F. Distribution patterns of type VII collagen in normal and malignant human tissues. *Am J Pathol.* 1991; 139:451-459.

- 34.** Visser R. *Basement membrane antigens in preneoplastic and neoplastic conditions (thesis)*. Maastricht, Universitaire Pers Maastricht; 1993: 81-84.
- 35.** Lapiere JC, Hu L, Iwasaki T, Chan LS, Peavey C, Woodley DT. Identification of the epitopes on human type VII collagen for monoclonal antibodies LH 7.2 and clone I, 185. *J Dermatol Sci*. 1994; 8:145-150.
- 36.** Lapiere JC, Woodley DT, Parente MG, Iwasaki T, Wynn KC, Christiano AM, Uitto J. Epitope mapping of type VII collagen. Identification of discrete peptide sequences recognized by sera from patients with acquired epidermolysis bullosa. *J Clin Invest*. 1993; 92:1831-1839.
- 37.** Tuori A, Uusitalo H, Burgeson RE, Terttunen J, Virtanen I. The immunohistochemical composition of the human corneal basement membrane. *Cornea*. 1996; 15:286-294.
- 38.** Lohi J, Leivo I, Tani T, Kiviluoto T, Kivilaakso E, Burgeson RE, et al. Laminins, tenascin and type VII collagen in colorectal mucosa. *Histochem J*. 1996; 28:431-440.
- 39.** Lohi J, Leivo I, Owaribe K, Burgeson RE, Franssila K, Virtanen I. Neoexpression of the epithelial adhesion complex antigens in thyroid tumours is associated with proliferation and squamous differentiation markers. *J Pathol*. 1998; 184:191-196.



5

Chapter 5

Recessive Dystrophic Epidermolysis Bullosa: type VII collagen deficiency is not associated with intraocular defects

Bart Wullink^{1,2}

José C. Duipmans³

Roelofje J. Van der Worp^{1,2}

Johanna M.M. Hooymans^{1,2}

Remco Stoutenbeek¹

Marcel F. Jonkman³

Leonoor I. Los^{1,2}

¹ Department of Ophthalmology, University of Groningen, University Medical Center Groningen, The Netherlands

² W.J. Kolff Institute, Graduate School of Medical Sciences, University of Groningen, The Netherlands

³ Center for Blistering Diseases, Department of Dermatology, University of Groningen, University Medical Center Groningen, The Netherlands

Submitted

ABSTRACT

Background: While many reports exist on the ocular surface defects that occur in recessive dystrophic epidermolysis bullosa (RDEB), not much is known about the intraocular status in these patients. Although the protein involved in this genetic defect, type VII collagen, is present in various intraocular tissues, its function remains unclear.

Objective: To establish whether intraocular structure and function are compromised in patients with type VII collagen deficiency.

Methods: We analyzed the RDEB literature that addressed ophthalmic findings, clinically examined RDEB patients, focussing on potential intraocular defects, and analyzed a pair of RDEB donor eyes for abnormalities by immunohistochemistry.

Results: The potential associations with cataract, accommodative dysfunction and detachments of tissues, as suggested in the literature, could not be substantiated. The poor visual performance of affected patients likely results from ocular surface scars and irregularities, which can not be refractively corrected in severely affected patients. Such surface irregularities also impeded reliable clinical testing of patients in computerized imaging systems.

Conclusion: We could not relate dermal type VII collagen deficiency to any intraocular defects.

INTRODUCTION

Inherited epidermolysis bullosa (EB) represents a group of hereditary bullous disorders which are primarily characterized by severe mechanical fragility of skin and mucosa, repeated development of blisters, and complicated wound healing.¹ Distinct molecular components from at least 20 genes can be at fault. These components are situated at specific ultrastructural levels in the skin (**Figure 1**). The molecular defect, therefore, translates to tissue cleavage at corresponding ultrastructural levels. Grossly, four subgroups are distinguished based on the level of cleavage: intraepidermal (EB simplex), lamina lucida (junctional EB), sublamina densa (dystrophic EB) level, or at multiple levels (Kindler).² Data from national EB registry studies seem to translate the relationship between the depth of these cleavage levels and their corresponding clinical findings: although all subgroups may have lethal subtypes, a deeper level of cleavage generally results in a more debilitating formation of scars.³⁻⁷ Indeed, given both dermal and extra-dermal (i.e. ocular) findings, the most debilitating EB type appears to be the dystrophic EB (DEB) variant, when inherited recessively (RDEB).^{2,7} As in RDEB, the dominantly inherited variant (DDEB) also results from tissue cleavage at the deepest level within the EB groups. Therefore, both DEB types show similar clinical findings. However, RDEB is typically much more severe than DEB because the corresponding functional molecular components, the anchoring fibrils, are not just poorly available but are lacking altogether.

In turn, the absence of anchoring fibrils results from impeded synthesis or bioavailability of the main component of the fibrils, type VII collagen (Col VII).⁸ Without these anchoring fibrils, blister formation readily occurs. In each such event, the epithelial basement membrane is either damaged, or is removed entirely from the dermis due to its adherence to the epidermal roof of the blister. Since epithelial cells need an intact basement membrane to execute their functions properly, the subsequent wound healing process is impaired.⁹ In reaction, extensive scar formation occurs, leading to debilitating deformations and mutilations. Surgical release is therefore required, often repeatedly.¹⁰ Moreover, many patients suffer constant pain and/or itch during the wounding/healing process. Severe, generalized RDEB therefore classifies as one of the most devastating genetically transmitted multiorgan diseases.²

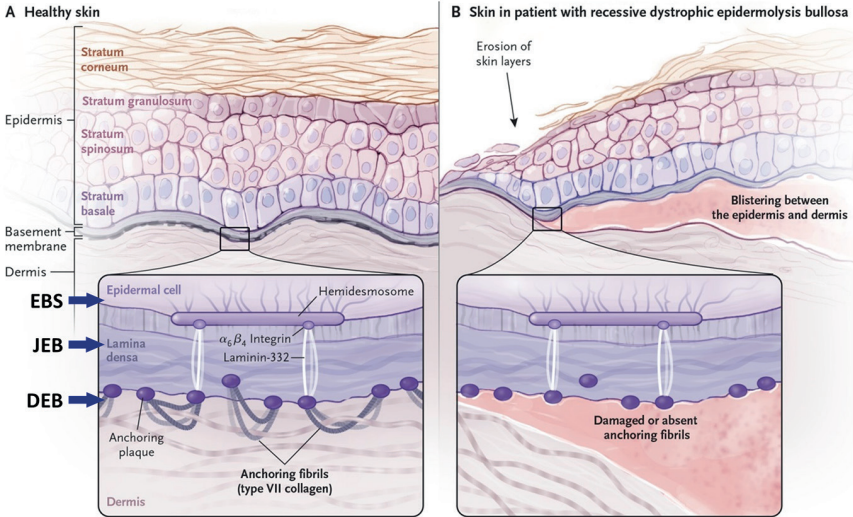


FIGURE 1. The epidermolysis bullosa subtype classification showing skin levels at which blisters develop.

This simplified representation of the basal epidermis and superficial dermis shows which level-specific proteins are at fault (**A**, purple arrows) per EB subtype; *EBS* simplex (basal), *JEB* junctional, and *DEB* dystrophic EB. In *DEB* (**B**), blistering occurs directly below the lamina densa, at the level of the anchoring fibrils. Adapted from Tolar J & Wagner JE. *N Engl J Med.* 2015; 372:382-384.

In EB, ocular surface tissues are often involved. Skin, cornea and conjunctiva are all ectodermal tissues, which share ultrastructural and biochemical similarities. Typically, corneal and conjunctival erosions develop, which provokes fibrotic wound healing in most types, leading to impaired vision. In *DEB*, such external eye involvement has been clearly established through various cohort studies, by Gans (USA 1979-1986; *DDEB* n=10; *RDEB* n=34), Lin (USA 1986-1991; *DDEB* n=17; *RDEB* n=61), Tong (UK 1980-1996; *DDEB* 28; *RDEB* n=72), Deplus (France 1991-1997; *DDEB* n=1; *RDEB* n=37) and Fine (USA 1986-2002; *DDEB* n=242; *RDEB* n=421).³⁻⁶ Their study data shows that despite a considerable phenotypic variability in *DEB*, several ocular symptoms can be considered 'common' (**Table 1**).¹¹

TABLE 1. Distribution of external eye findings per EB subtype.

		Frequency of Occurrence: Ocular Findings per EB subtype (%)																	
		EBS					JEB					DEB							
		Weber-Cockayne		Dowling-Meara		Koebner	Ogna	Herlitz		non-Herlitz			Pasinié & Cockayne-Touraine		Non-Hallopeau-Siemens, generalized other		Hallopeau-Siemens	RDEB Inversa	
		EBS, localized	EBS, generalized severe	EBS, generalized intermediate	EBS, generalized severe	EBS, generalized intermediate	Ogna	JEB, generalized severe	JEB, generalized intermediate	JEB, generalized intermediate	JEB, generalized intermediate	JEB, generalized intermediate	DDEB, generalized	RDEB, generalized intermediate	RDEB, generalized severe	RDEB, generalized severe	RDEB, generalized severe	RDEB, generalized severe	RDEB, generalized severe
		n = 1,092	n = 113	n = 96	n = 379	n = 40	n = 190	n = 424	n = 265	n = 139	n = 17								
Former nomenclature (Fine et al. 2004)		0.92	6.19	3.13	2.64	47.50	25.26	2.12	32.45	74.10	35.29								
Current nomenclature (Fine et al. 2014)		0.27	0.00	3.16	0.53	26.83	13.37	0.95	16.92	50.00	29.41								
		0.00	0.00	0.00	0.00	4.76	2.11	0.00	1.89	10.07	11.76								
		0.37	0.88	2.08	0.26	7.14	6.32	0.71	6.46	17.52	17.65								
		0.00	0.00	0.00	0.00	14.29	2.11	0.00	1.90	7.19	0.00								
		1.19	2.65	11.04	1.85	2.38	4.23	1.65	5.30	5.80	11.76								
		13.17	13.27	15.63	16.14	16.67	13.68	17.18	21.89	38.13	41.18								
		0.82	1.77	0.00	0.53	0.00	1.58	0.94	1.41	6.47	0.00								

Frequency of occurrence of ocular findings in bullous diseases, based on findings of 2748 patients. Current (EB classification <2014) and former nomenclature applied. Adapted from Ref7, with permission.

Interestingly, although skin defects are often recognised at birth, the earliest corneal involvement reported (to our knowledge) occurred 'only' at 4 months-of-age.⁴ Moreover, the cornea and conjunctiva are affected in a 'mere' 32-74% of the RDEB patients.⁷ Surgical releases also appear to be more often required in non-ocular surface tissues, e.g. hands and the oral cavity, than in ocular surface tissues.¹⁰ In Fine's series, impaired vision was described in 38% of the severe RDEB patients and blindness occurred in around 6.5%.⁷ It is unclear whether this could be contributed exclusively to corneal involvement or whether intraocular structures might have been involved as well.

Intraocular involvement is, altogether, scarcely covered in previous studies. The literature that was reviewed up to 1986 did not correlate any intra-ocular disorders to DEB¹². After that, some intraocular abnormalities were reported in DEB patients, but those were considered to be 'coincidental',^{4, 13-19} More recently however, expression of the Col VII encoded by *COL7A1* gene was demonstrated in retinal Müller cells.²⁰ Also, ciliary pigmented and non-pigmented epithelia transcribed *COL7A1*, while its protein product (Col VII) was immunolocated to the retinal basement membrane (ILM), retinal astrocytes, and the accommodation system tissues.²¹⁻²⁴ The function of Col VII at these sites remains unclear. Yet, some of these areas are accessible to clinical examination.

In the current study, we sought to gain more insight in the role of intraocular Col VII. Therefore, we 1.) analyzed the RDEB literature that addressed ophthalmic findings, and reviewed their data on both external eye and intraocular findings, 2.) clinically examined RDEB patients, focussing on potential intraocular defects, and 3.) analyzed a pair of RDEB donor eyes for abnormalities by immunohistochemistry.

MATERIALS AND METHODS

Literature search

PubMed was searched with the terms 'recessive dystrophic epidermolysis bullosa' and 'eye'. Studies that did not mention any ophthalmological examination outcomes were not included. Additional studies were added through assessing references.

Study approval

The clinical examination of patients and use of donor material was approved by the ethics committee of the University Medical Center of Groningen and conducted according to the declaration of Helsinki. Patients and donor provided informed consent for the use of clinical and histological data.

Patients and donor

Four clinical patients and one donor were enrolled. All suffered from generalized RDEB, as diagnosed by the supraregional referral center of the Benelux, the Center for Blistering Diseases, UMCG (**Table 2**).

TABLE 2. Patient and donor information.

Patient	Gender	Age	First COL7A1 mutation	Second COL7A1 mutation	RDEB phenotype	pAb(16)	mAb(12)	mAb(70)	SCC
EB1	m	32	c.1573C>T, p.Arg525X	c.6508C>T, p.Gln2170X	gen. intermediate	2+	1-2+	1-2+	multiple
EB2	m	20	c.344dupG, p.Asn116fs	c.6082G>A, p.Gly2028Arg	gen. intermediate	-	2+	2+	no
EB3	m	24	c.7828C>T, p.Arg2610X	c.7828C>T, p.Arg2610X	gen. severe	2-3+	1-2+	1-2+	no
EB4	f	25	c.3G>T, p.Met1?	c.4997dupG, p.Pro1668fs	gen. severe	1+	0	0	no
EB5*	m	22	c.3G>A, p.Met1?	c.353delG, insCCCCCTGCAA, p.Arg118fs	gen. severe	0	0	0	multiple

Characteristics on RDEB genetic defects and resulting phenotype. Staining intensities by immunofluorescent diagnostics with several anti-Type VII collagen antibodies: 'no staining (0+)' through 'staining intensity comparable to that of healthy skin (4+)'. SCC squamous cell carcinoma resulting from RDEB. Note: more information about the patients genotype can be accessed through the international database of dystrophic epidermolysis bullosa patients and COL7A1 mutations (<https://molgenis03.target.rug.nl>), by inserting mutation in searchbox. gen. generalized.

Clinical examinations

Clinical patients were reviewed during their routine visits for multidisciplinary checkup. None of them were currently suffering from additional ocular complaints, apart from already established ocular involvement. The examinations were carried out by experienced healthcare professionals in order to reduce examination time and patient

discomfort, while optimizing chances of noting subtle irregularities. All patient data were anonymized upon acquisition and stored electronically. The patients underwent basic ophthalmologic examinations (manual refraction, best-corrected visual acuity by Snellen chart, slit-lamp evaluation and funduscopy), but also accommodation (by push-up technique according to Donders), Scheimpflug imaging/partial coherence interferometry (Pentacam HR 70900, Oculus Optikgeräte GmbH, Wetzlar, Germany), optical coherence tomography (OCT HS100, Canon Europe Ltd, Middlesex, UK) and ultra-widefield scanning laser ophthalmoscope (Optos 200Tx, Marlborough, MA, USA) examinations. The maximal accommodation capabilities were measured because of the recently observed Col VII distribution at the zonules and ciliary body.²⁴ Since Col VII was shown to be diminished in keratoconus,²⁵⁻²⁸ Pentacam examinations might establish pre-clinical keratoconus in RDEB patients. OCT examinations could supply information on subtle macular abnormalities and Optos examinations on retinal abnormalities. We chose not to perform tonometry, since its outcome would be unreliable due to the corneal condition of our patients, as well as the lack of indication and risk of iatrogenic epithelial damage. Ocular hypertension was reported but once,¹³ without commenting on the anterior chamber status or probable cause.

Donor

The donor was a 22 year-old male patient with generalized severe RDEB, who suffered from metastasized squamous cell carcinoma. He was severely mutilated, and seldomly used steroids. His medical history reported recurrent cornea erosions (with photophobia) from 3 years of age, which had led to pannus formation and mild symblepharon in both eyes. His anterior chamber was never reported to contain any cells. Due to health issues he could not be enrolled in the clinical examinations of this study, but he visited our clinic a year earlier. By then, he suffered from lagophthalmus which had resulted in cicatricial ectropion and corneal haze. Intraocular disorders (i.e. cataract, phacodonesis, vitreous or retinal detachments) were never reported. His eyes were analyzed immunohistochemically by means of light microscopy (LM) and transmission-electron microscopy (TEM). One eye was subdivided coronally, one half for embedding in paraffin, and one half for freezing in optimal cutting temperature compound. The other eye was embedded in Technovit 8100. These proceedings were described previously.^{22, 42} In short, parts designated for paraffin and resin embedding were fixed in 2% paraformaldehyde, after cutting two small transcleral holes to facilitate penetration of fixatives and embedding media. The loss of vitreous was prevented by gently rotating the specimens during the washing, dehydration, and infiltration steps.

Sections of 3–4 μm thickness were cut. Cryosections were cut at 10 μm thickness. As a positive control, tissues from a 35 year-old male donor without known ophthalmologic pathology were used.

Immunohistochemistry

Several antibodies were used for IHC examination of the donor eye samples (**Sup info Table 1**).

RESULTS

Literature

The previous case reports on external eye findings in generalized RDEB describe patients ranging from 0.5 to 70 years old, but mostly pre-adults (7/11) (**Table 3**). In ten cases the best corrected Snellen visual acuities were given as ranging from hand movements to as good as 20/20. Not all studies reported on how (and whether) refraction was tested, although the corneal irregularities that were found would certainly have affected refraction outcomes. The case reports on internal eye findings in generalized severe RDEB describe patients ranging from 0.5 to 40 years old, mostly pre-adults (4/6) (**Table 4**). None of these studies reported on accommodation outcomes. Two studies reported on a shallow anterior chamber and several studies observed cataracts, both primary and secondary. Only four studies described a fundoscopic examination, in which no abnormalities were found. Imaging results were not mentioned in the severe cases.

TABLE 3. External eye findings reported in the literature and observed in the current study.

Year	Study	Age	Gender	RDEB	Eye	BCVA	BCVA- post OK	Refraction	External eye findings and remarks
2017	current	33 y	m	gen. intermediate	OD	20/63		S+2.50 C-3.50 x10°	General: photophobia, difficulty opening eyes during examination
	<i>EB1</i>				OS	20/63		S+1.00 C-4.00 x170°	Cornea: OS small bullae inferior, OU clouding & mild vascular ingrowth
	current	20 y	m	gen. intermediate	OD	20/25		S+2.00 C-2.00 x110°	General: no photophobia, no difficulty opening eyelids
	<i>EB2</i>				OS	20/25		S+1.00 C-1.00 x110°	Cornea: OU clouding, no vascular ingrowth, epithelium intact
current		25 y	m	gen. severe	OD	20/63		S-0.50 C-1.00 x170°	General: photophobia, difficulty opening eyes during examination, normal eyelids
	<i>EB3</i>				OS	20/200		S-1.00 C-1.50 x10°	Cornea: OD quiet appearance, OS ghost vessels, OU central subendothelial haze
current		30 y	f	gen. severe	OD	20/100		S+0.50 (spectacles)	General: photophobia, difficulty opening eyes during examination
	<i>EB4</i>				OS	20/100		S-2.50 (spectacles)	Cornea: OU quiet appearance, irregular surface, mild vascular ingrowth (old)
current		22 y	m	gen. severe	OD	20/50		n/a	General: cicatricial ectropion with lagophthalmus OU
	<i>EB5, donor</i>				OS	20/40		n/a	Cornea: haze, irregular epithelium, erosions
		17 y	f	gen. severe	OD	20/200	20/20 (18m)		General: OS possible mild amblyopia, OU extensive symblepharon limiting ocular mobility
2016	Medisinge	17 y	f	gen. severe	OD	HM	6/9 (3y)	S 0.00 C-2.50 x10°	Cornea: OU superficial opacification, anterior stromal neovascularization
					OS	CF	20/30 (18m)		Post-Op: diplopia, 35 prism diopter exotropia (resolved after therapy), no stereoacuity, cornea clear without neovascularization
2016	Medisinge	17 y	f	gen. severe	OD	HM	6/9 (3y)	S 0.00 C-2.50 x10°	General: OU astigmatism with posterior blepharitis & Meibomian gland dysfunction
					OS	6/24		S 0.00 C-2.00 x100°	Cornea: OU vascularization, scars, recurrent erosions. OD: bandage contact lens placement due to corneal infiltrate. results in melt > PKP

TABLE 3. Continued.

Year	Study	Age	Gender	RDEB	Eye	BCVA	BCVA- post OK	Refraction	External eye findings and remarks
2015	Huebner	49 y	f	gen. intermediate	OD 20/20 OS 20/20	20/20	soft contact lenses	soft contact lenses	Post-Op: OD posterior capsule opacity (1y) > laser capsulotomy General: no remarks reported
		70 y	f	gen. intermediate	OD 20/20 OS 20/25	20/20	soft contact lenses scleral lenses	soft contact lenses scleral lenses	Cornea: clear, with subepithelial blisters OU General: no remarks reported
2010	Motley	0.5 y	m	gen. severe	OD N/A OS N/A	N/A	S+1.00 (Post-Op) S+1.50 (Post-Op)	Scleral lenses	Cornea: subepithelial scars, irregular surface General: poor eye contact and nystagmus at age 6m due to dense cataracts, brisk/light orbicularis reaction Cornea: no apparent corneal or conjunctival fragility
2010	Thanos	11.5 y	m	gen. severe	OD 20/40 to HM OS 20/32	20/50	20/50	20/50	Post-Op: fixation and following targets, improvement of eye contact, no surface defects (24m) General: OD limbal stem cell deficiency
2006	Altın-Yaycıoğlu	12 y	f	gen. severe	OD 20/20 OS 20/80	20/80	20/30 (22w) 20/30 (22w)	S 0.00 C-3.50 x90°	Cornea: OD symblepharon, corneal vascularization, pannus, severe symblepharon (inability of active lid opening) Post-Op: clear cornea, stable surface, re-symblepharon (4m), re-symblepharon and pseudopterygium (12m) General: impeded motility eyelid OS, ocular pain Cornea: OU haze, symblepharon and superficial corneal vascularization OS Post-Op: (amniotic membrane) normal bulbar mobility, thinner corneal stroma with mild vascularization OS

TABLE 3. Continued.

Year	Study	Age	Gender	RDEB	Eye	BCVA	BCVA- post OK	Refraction	External eye findings and remarks
2005	Matsumoto	11 y	m	gen. severe	OD	20/200			General: OU conjunctivitis, but without follicles, scars or cicatricial changes. Grade 3 conjunctival metaplasia
					OS	20/30			Cornea: OD erosion, OS extensive keratopathy, blistering
1992	Sharkey	14 y	m	gen. severe	OD	CF		S+19.00 C-4.00 x90°	General: poor vision since early childhood, eyelids normal (on photo)
					OS	HM		unobtainable	Cornea: OU cornea plana & sclerocornea
1971	Hill	30 y	m	gen severe.	OD	20/70			General: scarring of eyelids, OU cicatricial ectropion, lagophthalmos
					OS	20/100			Cornea: superficial scarring
1987	Destro	40 y	f	gen. severe	OD	20/200		20/70	General: photophobia, lagophthalmos, dryness, pain, decreased vision, intraocular hypertension, chronic conjunctivitis OU, paracentral scotoma
					OS	20/200			Cornea: ulcerations without infiltration OD, diffuse subepithelial scarring, irregular astigmatism
									Intraoperative epithelial detachment

These data demonstrate the burden of ophthalmological disease in RDEB patients. Most of the severely affected RDEB patients are unable to wear contact lenses or glasses, since these may damage corneal epithelium and skin. Corneal irregularities and cylindrical deviations can therefore not be corrected. This visual debilitation adds to a reduced overall functionality. PKP penetrating keratoplasty, OU oculo uterque/both eyes.

TABLE 4. (Intra)ocular findings described in the literature and observed in the current study.

Year	Study	Age	Gender	RDEB	Eye	Maximum accommodation	ACD	Lens	Pentacam	Fundus	Optos	OCT
2017	current	33 y	m	rDEB ¹	OD	20 dpt (5 cm)	normal	normal	pachy center 930-1050 μm**	normal	normal***	two subtle RPE proliferations***
	EB1				OS	20 dpt (5cm)	normal	normal	pachy center 820-850 μm**	normal	normal***	two subtle RPE proliferations***
					OU	40 dpt (2,5 cm)			keratoconus: probably not			
	EB2	20 y	m	rDEB ¹	OD	5 dpt (20 cm)	normal	normal	pachy center 680 μm***	normal	normal***	normal aspect***
					OS	5 dpt (20 cm)	normal	normal	pachy center 650 μm***	normal	normal***	normal aspect***
					OU	6.67 dpt (15 cm)			keratoconus: no			
	EB3	25 y	m	rDEB	OD	10 dpt (10 cm)	normal	normal	pachy center 680 μm*	normal	normal***	normal aspect**
	miosis				OS	10 dpt (10 cm)	normal	normal	pachy center 600-660 μm*	normal	papilla leporina**	normal aspect**
					OU	20 dpt (5 cm)			keratoconus: undetectable			
	EB4	30 y	f	rDEB	OD	3.3 dpt (30 cm)	normal	normal	*	*	*	*
					OS	3.3 dpt (30 cm)	normal	normal	pachy center 790 μm.	*	normal***	normal**
					OU	5 dpt (20 cm)			keratoconus: anterior maps indicative			
	EB5	22 y	m	rDEB	OD		normal	normal	n/a	normal		

TABLE 4. Continued.

Year	Study	Age	Gender	RDEB	Eye	Maximum accommodation	ACD	Lens	Pentacam	Fundus	Optos	OCT
	(donor)											
2016	Koullis	17 y	f	rDEB	OD	normal	normal	normal	n/a	normal		
					OS	normal		normal		normal		
2016	Medsinge	17 y	f	rDEB	OD	shallow	OD: melt> lens aspiration + steroids> cataract	OD: melt> lens aspiration + steroids> cataract		normal		
					OS		lens involved in keratitis/melt > cataract					
2015	Huebner	49 y	f	rDEB ¹	OD	no remarks	no remarks	not reported	not reported	not reported		
					OS	no remarks	no remarks	not reported	not reported	not reported		
		70 y	f	rDEB ¹	OD	no remarks	no remarks	no remarks	no remarks	not reported		
					OS	no remarks	no remarks	no remarks	no remarks	not reported		
2010	Motley	6 m	m	rDEB	OD	no remarks	no remarks	posterior lentiglobus, trampoline, dense prim. cataract		no remarks		
					OS	no remarks	no remarks	posterior capsule open (OS), dense prim. cataract		normal (intraoperative)		
1994	Lin	2.5 y	f	DDEB				no remarks				
		17 y	f	DDEB				primary cataract OS (anterior polar at 17 months)				
		60 y	f	?				primary cataract OU				

TABLE 4. Continued.

Year	Study	Age	Gender	RDEB	Eye	Maximum accommodation	ACD	Lens	Pentacam	Fundus	Optos	OCT
1992	Sharkey	14 y	m	rDEB	OD		shallow	spontaneous resorption cataract OD, capsule intact				
					OS		shallow	mature cataract OS, capsule intact		not reported		
1971	Hill	30 y	m	rDEB	OD			cataract (systemic steroids)		normal		
1987	Destro	40 y	f	rDEB	OD			secondary cataract (steroids)				
					OS			secondary cataract (steroids)		normal		

The current case series study (n = 4) is supplemented with cases and larger cohort studies. Image quality: **** normal, *** fair, ** poor/unreliable measurement, and * very poor image quality/very unreliable measurement (limiting corneal surface/blinking/other). Sometimes examinations are not mentioned in the literature (not reported), although sometimes examinations probably did take place but the outcome was not reported (no remarks). ¹ RDEB of intermediate severity, ACD anterior chamber depth, RPE retinal pigment epithelium.

Our four cases (mean age 27.0 years, range 20-33 years) had best corrected visual acuities ranging from 20/200 to 20/40 vision (Table 3). Automated refraction on them was impossible because of cornea surface irregularities. Surface irregularities included mainly bullae, erosions, clouding, scars, and vascular ingrowth (**Table 3**). Automated imaging yielded unreliable results. Pentacam central corneal thickness measurements, for example, showed some extreme values (EB1: 930-1050 μm , normal: 550.5 \pm 35.5 μm).²⁹ Nevertheless, one patient (EB4) had reliable outcomes consistent with keratoconus, at least in one eye. Manual ophthalmological examinations were hindered by photophobia and limited physical flexibility of the patients during positioning.

In contrast to some intraocular findings in the literature, our severely affected patients did not have shallow anterior chambers, cataracts, or any irregularities concerning the lens capsule. Notably, none of our patients used any steroids which might have influenced cataract formation. The determination of accommodation values was also influenced by corneal irregularities, effectively causing multifocality in our patients (**Sup info Figure 1**). Fundoscopic examination, supplemented with Optos and OCT imaging, showed a papilla leporina (EB3), and two subtle RPE proliferations (EB1). No important intraocular abnormalities were found. During all examinations, the use of protective foam dressings¹⁶ was considered for each patient, but deemed unnecessary by both the patients themselves and our clinical nurse specialist. No skin or mucosal blisters developed during the examinations.

Autopsy and (immuno)histological examinations

Apart from dermal pathology, general donor autopsy revealed a cardiac compensatory hypertrophy, and an endocardial fibroelastosis (without aortic dilation³⁰). Histologically, the RDEB cornea and conjunctiva showed signs of degenerative and inflammatory pannus (**Figure 2**). Epithelial edema and erosions were evident, consistent with a typical bullous keratopathy. Bowman's layer was either displaced by additional connective tissue, or obliterated. Vascular ingrowth was seen at the paracentral cornea. Basement membrane doubling was seen mainly at the central cornea. Both pigmented and nonpigmented epithelial tissues contained numerous vacuoles, which might also have resulted from embedding procedures (**Sup info Figures 2, 3**). Intraocularly, there were no obvious tissue detachments apart from those typically seen in post mortem embedded tissues. In cryosections, the antibodies mAb(12) and (72) did not label any accommodation system structures of the RDEB donor, in contrast to a stromal tissue band in the ciliary body of the normal control tissue (**Figure 3**). In light microscopy resin sections, the pAb(16) antibody faintly labeled the basement membranes of ciliary blood vessels and pigmented epithelium of the RDEB donor, while

other anti-Col VII antibodies would not label these structures at all. By immunoelectron microscopy, the pAb(16) antibody labeling would show scarce labeling at the zonules and linear densities at the lens capsule (**Figure 4**). The normal donor tissues labeled as expected²⁴ at the corneal epithelial basement membrane, the basement membrane of the pigmented ciliary epithelium, the zonules and the linear densities that reside within the lens capsule.

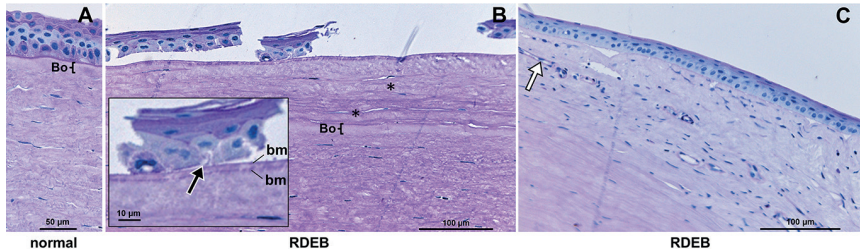


FIGURE 2. Light microscopic overview of RDEB donor cornea, PAS stain. (A) Normal donor cornea, (paracentral) without edema and with normal Bowman's membrane (*Bo*). The RDEB donor cornea (**B** central, **C** peripheral) shows signs of pannus, bullous keratopathy, pre-mortem edema (*black arrow*), vascular ingrowth (*white arrow*) and additional connective tissue (*) between the epithelium and Bowmans layer. In the central cornea, the epithelium is flattened and its basement membrane (*bm*) is doubled. In the peripheral cornea, Bowman's membrane lacks completely. Scale bars A 50 µm; B and C 100 µm; inset B 10 µm.

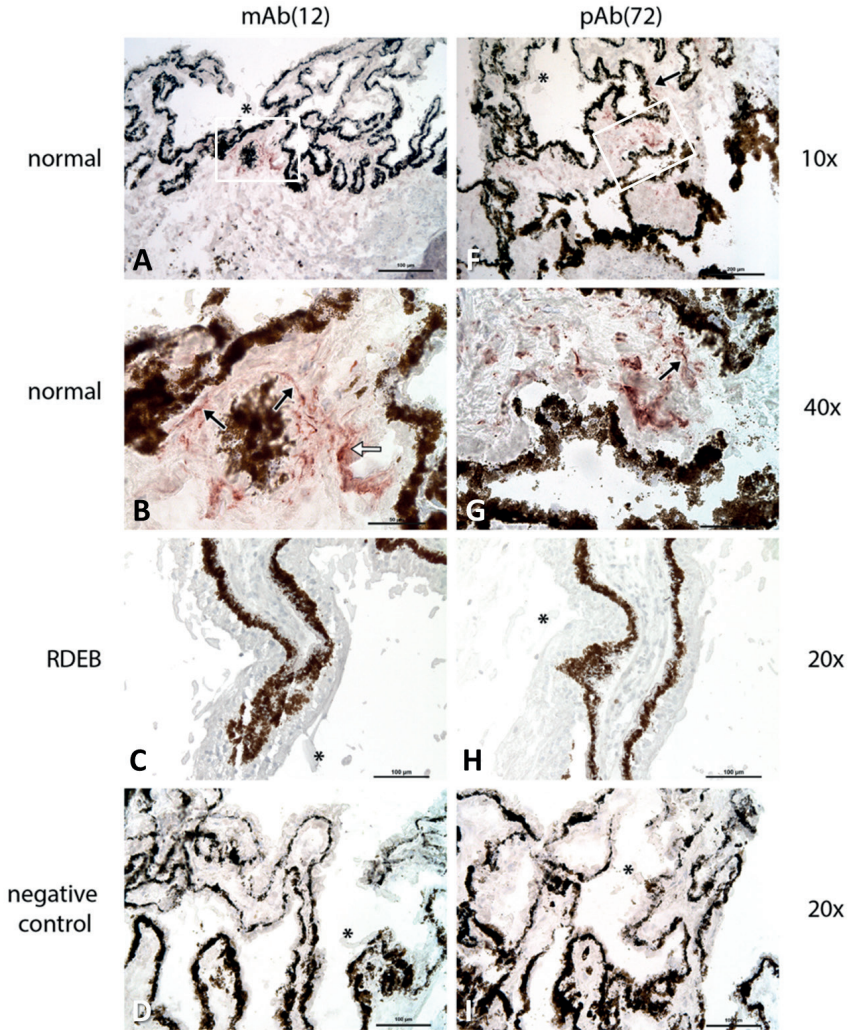


FIGURE 3. Col VII labeling at the ciliary body of a normal and an RDEB donor. Cryosections. In normal donor eyes, the monoclonal (**A, B**) and polyclonal (**F, G**) antibodies label at the stroma below the basement membranes of the pigmented ciliary epithelium (*black arrows*) and blood vessels (*white arrow*). The intermediate stroma in between two opposing basement membranes shows weak diffuse labeling. In contrast, these antibodies do not label at these locations in the RDEB donor eye (**C, H**) or in the negative control of normal donor eye tissue (**D, I**). In cryosections, no labeling was observed at the zonules (*). *cb* ciliary body; *pc* posterior chamber; *pro* ciliary process. Scale bars **A, C, D, H, I** 100 μ m; **B, G** 50 μ m; **F** 200 μ m.

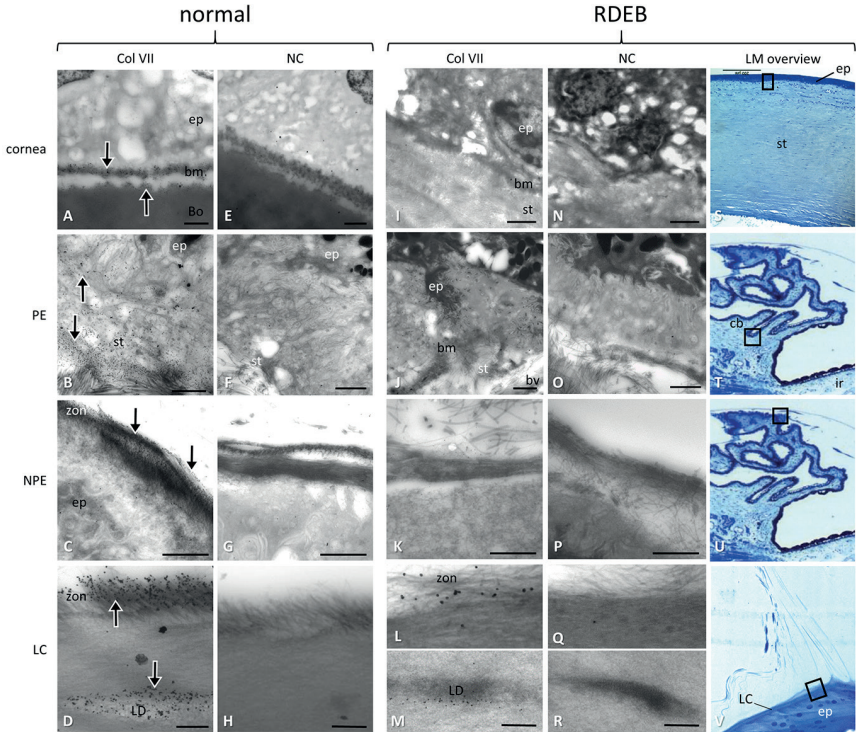


FIGURE 4. Col VII labeling in a normal and an RDEB donor. Immunoelectron microscopy. (**A-D, I-M**) labeling with pAb(16), their negative controls (**E-H, N-R**) and a light microscopic overview at the regions of interest with (**S-V**, toluidine blue). Normal donor tissue shows labeling at the basement membranes (*bm*, arrows) of the cornea (**A**) and the pigmented (**PE**) ciliary epithelium (**B**). At the PE, some labeling is observed at tiny fibrils surrounding large stromal (*st*) collagen fiber bundles. (**C**) At the non-pigmented epithelium (**NPE**), labeling is located at the superimposed zonules. (**D**) At the lenscapsule (**LC**), intense labeling is seen in zonules (*zon*) and linear densities (*LD*). In the RDEB donor, no labeling is observed at the basement membranes of cornea (**I**), pigmented (**J**) and non-pigmented epithelium (**K**), whereas only scarce labeling is seen at zonules (**L**) and linear densities associated with the lens capsula (**M**). The corresponding negative controls show no labeling or minimal background labeling. *bv* blood vessel; *cb* ciliary body; *ep* epithelium; *ir* iris; *LM* light microscopic. Scale bars **A-C, E-G, I-K, N-P, S-U** 2 μ m; **D, H, L, M, Q, R, V** 500 nm.

DISCUSSION

In the current study, we sought to gain more insight in the role of intraocular Col VII by analysing Col VII deficiency. We observed that previous studies on RDEB patients report primarily on external eye findings and that several case studies suggest a possible influence on intraocular tissues. In our case series, we find no intraocular irregularities that can directly be attributed to RDEB. Immunohistological analyses in an RDEB donor shows absence of Col VII in parts of the accommodation system that normally contain Col VII. Nonetheless, we can not correlate this to clinical dysfunction.

In our RDEB patients and in the literature, ocular surface problems and photophobia are a common finding which interfere with ophthalmological examinations. Corneal scarring results in an irregular corneal surface with haziness and irregular astigmatism, which often leads to diminished visual acuity. Mellado et al. (2018) measured the best-corrected visual acuities (BCVA) in the EB subtypes. Only 46.8% of the 31 investigated RDEB patients were found to have a BCVA of more than 0.1, in contrast to 78.6% in junctional EB patients (n=7).³¹ Unfortunately, many RDEB patients do not tolerate the wearing of (scleral) contact lenses or spectacles, so refractive corrections cannot be made. Their poor visual acuity, painful corneal erosions, evaporative dry eyes and cicatricial conditions contribute to a low quality of life. Some of these corneal impediments might be alleviated by cornea, amnion or limbal stem cell transplantation stabilizing the corneal surface and improving visual acuity.^{18, 19, 32, 33} Several authors reported that Col VII distribution is diminished in keratoconus.²⁵⁻²⁸ The one measurement in our case series that was deemed interpretable showed an anterior cornea profile suggestive of keratoconus. Because of the limited number of patients and reliable measurements, this finding can be no more than a possible indication of a higher susceptibility for keratoconus in RDEB patients.

The anterior chambers were of normal depth in our case series, as reported in most studies. Only two RDEB case studies reported shallow anterior chambers.^{15, 18}

We did not observe any lens irregularities in our case series. In contrast, cataract was reported in 7 out of 11 patients described in eight DEB studies (**Table 3**, mostly recessive DEB, generalized, severe). This difference may be explained by a reporting bias, since case reports tend to describe pathology and thus there is under reporting of normal findings. Also, at least some reported cataracts seem to be coincidental, because of their congenital, post-infectious, post-surgical or steroid-use associated nature.^{13, 14, 18} Primary lens capsule opacifications have been described at 6 months of age, while the

posterior capsule of another 7 month old RDEB patient was found to be open prior to cataract surgery.^{4, 15, 16} Lin et al. (1994), however, suggested that intraocular structures would be affected only through secondary complications of ocular surface damage.⁴ Thus, the crystalline lens, although embryologically a purely ectodermal structure like the epidermis, would not be involved in the RDEB process. Because of these contradictory reports, we cannot exclude the possibility of an association between Col VII deficiency and cataract formation.

The abnormal accommodative measurements found in our study, are probably caused by corneal irregularities and do not give an adequate impression of the performance of the lens-zonular-ciliary body system. Pentacam and slitlamp investigations did not show any irregularities in this complex. It is thus unclear whether the lack of Col VII in the ciliary body and reduced labeling of the zonules and linear densities in the RDEB donor, as observed by immuno-TEM, have any clinical significance. In both clinical and IHC examinations, no zonular defects were noted.

Fundoscopy examination and Optos imaging of our patients did not reveal any disorders that could be directly related to Col VII deficiency. A papilla leporina was revealed in one patient. We regard this as a coincidental finding, unrelated to the Col VII depositions found in the neuroretina.²² Also, the subtle RPE proliferations are probably coincidental. Fundoscopy examination, as part of routine examination, might have been performed in many of the described cases, but few report on their outcomes. This probably means that during those examinations no apparent disorders were seen, i.e. all parameters were considered to be within normal limits. Alternatively, the examinations may have been limited to the anterior segment of the eye, or the imaging results were deemed of inadequate quality.

Interestingly, immunoelectron microscopic investigations showed specific gold labeling at the ciliary zonules and linear densities of the RDEB donor, albeit in severely diminished amounts. This residual labeling indicates that the RDEB donor did either have minute amounts of intraocular Col VII, or that the polyclonal antibody used detects epitopes of Col VII in absence of the full length molecule.²⁴ In addition, not all patients with a dermal Col VII deficiency demonstrate a direct ocular involvement, implicating an incomplete genotype-phenotype correlation.³¹ Moreover, a RDEB mouse model showed a Col VII content of 58% in corneas, in contrast to 10% in skin, in corresponding wild-type tissues.³⁴

Regarding ocular findings, studies typically describe patients that visit their clinic because of active ophthalmological conditions, while our case series consisted of

patients that visited our hospital for routine multidisciplinary checkup. Although the latter might suggest a milder ophthalmological phenotype, the genotype and dermatological phenotype in our case series were severe. Our case series participated with dedication, despite their impediments by wheelchair-boundedness and multiorgan involvement related small body sizes.

In conclusion, despite immunolocalization of Col VII at several intraocular sites in normal control tissues, no important intraocular defects could be established in dermally Col VII deficient patients.

Acknowledgements

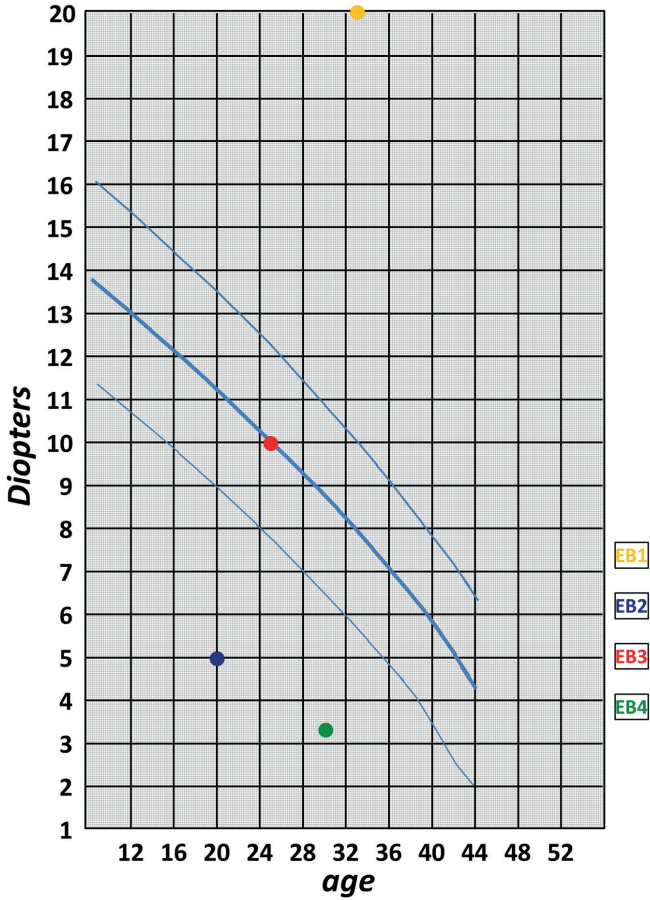
The authors thank Rob Verdijk from LUMC/Erasmus MC for his scientific assistance, the University Medical Center Groningen (UMCG) Microscopy and Imaging Centre for use of their equipment.

SUPPORTING INFORMATION

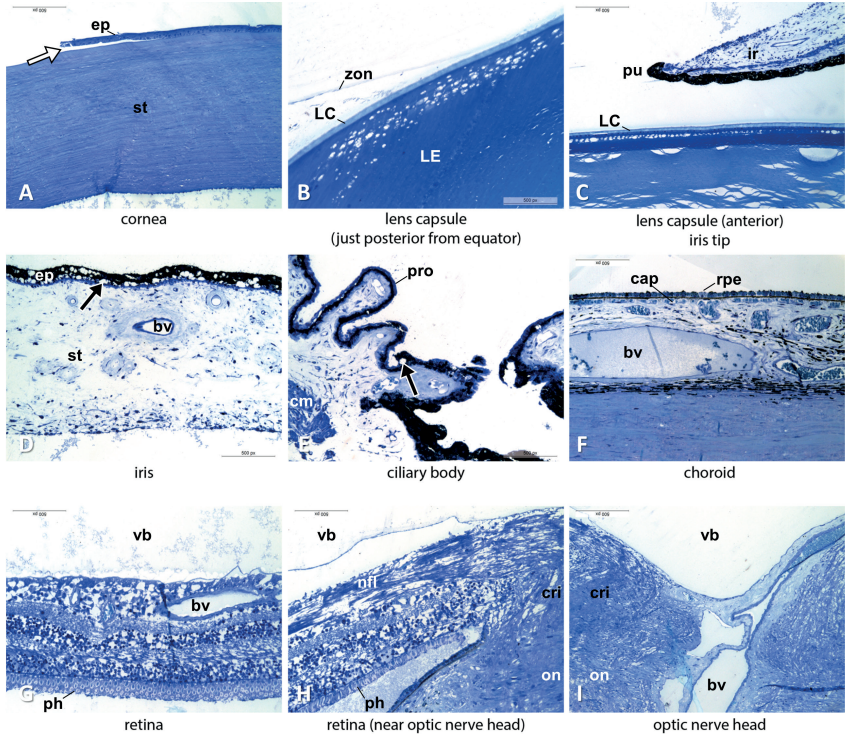
SUPPORTING INFORMATION TABLE 1. Primary anti-type VII collagen antibodies used in this study.

Antibody	Specificity	Clonality	Host	Isotype	Company	Cat.	Ab Registry
pAb(16)	NC1 & 3H ¹	Polyclonal	Rabbit	IgG	Calbiochem (Merck/ Millipore)	234192	AB_211739
pAb(72)	NC1 ²	Polyclonal	Rabbit				
mAb(12)	NC1	Monoclonal LH7.2	Mouse	IgG1	Abcam	ab6312	AB_305415
mAb(14)	NC1 ³	Monoclonal II-32	Mouse	IgG1	Chemicon (Merck/ Millipore)	MAB2500	AB_94355
mAb(70)	NC1 ⁴	Monoclonal 2q633	Mouse	IgG1	US Biological	C7510-66A	n/a

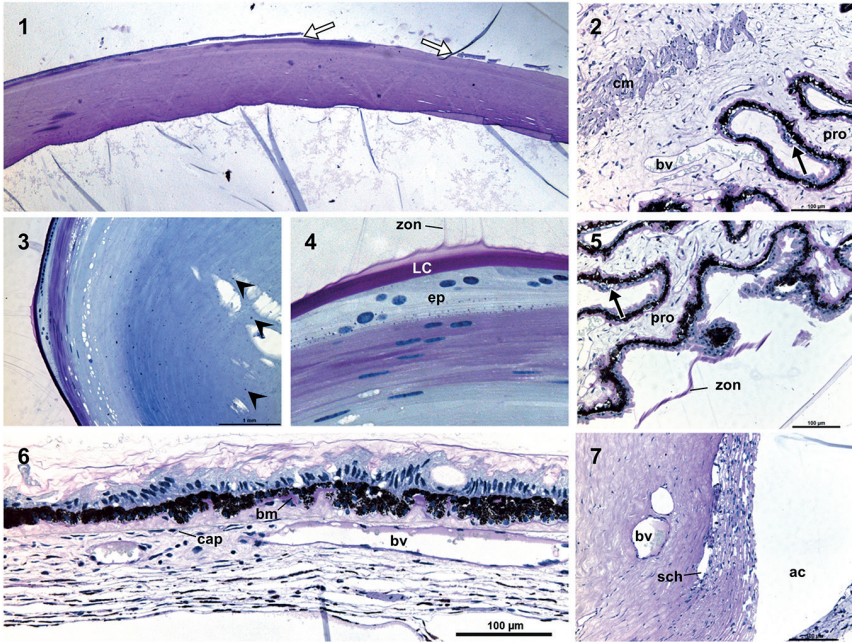
Adapted from Ref 24. Specificity for epitopes as established ¹by Wullink et al. (2018); ²by Kühl T et al. *J Invest Dermatol.* 2016; 136:1116-1123, as kind gift from dr. Alexander Nyström from the Department of Dermatology, Medical Center - University of Freiburg, Germany; ³through personal communication with Merck: targets the amino-terminal (note datasheets not corrected for Col VII polarity shift 1991) = NC-1 mAb from Ref 8 and Keene DR, Sakai LY, Lunstrum GP, et al. *J Cell Biol.* 1987; 104:611-621; ⁴ personal communication US Biologics: targets the amino-terminal (datasheets not corrected for Col VII polarity shift 1991) = LH7.2 mAb from Lapiere JC, Hu L, Iwasaki T, et al. *J Dermatol Sci.* 1994; 8:145-150 and Tanaka T, Takahashi K, Furukawa F, et al. *Br J Dermatol.* 1994; 131:472-476. *Cat.* catalogue number; *Ab* Antibody Registry database.



SUPPORTING INFORMATION FIGURE 1. Graph from Duane (1922), adapted. Accommodation values of four clinical RDEB patients. Monocular diopeters (*D*) are presented as colored dots, the blue lines correspond to the normal range of accommodation values per year of age in the normal population. Each patient had identical accommodation values for both eyes (L=R). Two patients were far below the normal reference values, one patient had an extremely high value. Abnormal values were probably influenced by corneal irregularities.



SUPPORTING INFORMATION FIGURE 2. Light microscopic overview of RDEB donor tissues. Toluidin blue stain, T8100 resin. Most intraocular tissues appear to be without significant defects. The cornea, however, shows a typical corneal erosion/blister (*white arrow*). The lens capsule appears to be attached and intact. The iris and ciliary body epithelia showed numerous vacuoles (*black arrows*). *bm* basement membrane; *Bo* Bowman's membrane; *bv* blood vessel; *cap* choriocapillaris; *cm* ciliary muscle; *pro* ciliary process; *ep* epithelium; *LC* lens capsule; *LE* crystalline lens; *nfl* nerve fiber layer; *on* optic nerve; *ph* photoreceptors; *pu* pupil; *RPE* retinal pigment epithelium; *st* stroma; *vb* vitreous body; *zon* zonule. Magnification x20.



SUPPORTING INFORMATION FIGURE 3. Light microscopic overview of RDEB donor tissues. PAS stain, T8100 resin. (1) The cornea shows multiple erosions (*white arrows*). (2) The ciliary body epithelium shows numerous vacuoles (*black arrow*). (3) In the deep lens fiber layer, multiple nuclei (*arrowheads*) are situated. (4) The zonules appear to attach themselves normally at the equatorial lens capsule and (5) ciliary body. (6) The choroid and (7) trabecular system do not show any striking irregularities. *ac* anterior chamber; *bm* basement membrane; *bv* blood vessel; *cap* choriocapillaris; *ep* epithelium; *cm* ciliary muscle; *LC* lens capsule; *pro* ciliary process; *sch* Schlemm's canal; *zon* zonule. Magnification 1 x10; 4 x40; Scale bars 2, 5, 6, 7 100 μ m; 3 1 mm.

REFERENCES

1. Fine JD, Bruckner-Tuderman L, Eady RA, et al. Inherited epidermolysis bullosa: Updated recommendations on diagnosis and classification. *J Am Acad Dermatol.* 2014; 70:1103-1126.
2. Fine JD. Inherited epidermolysis bullosa. *Orphanet J Rare Dis.* 2010; 5:12.
3. Gans LA. Eye lesions of epidermolysis bullosa. Clinical features, management, and prognosis. *Arch Dermatol.* 1988; 124:762-764.
4. Lin AN, Murphy F, Brodie SE, Carter DM. Review of ophthalmic findings in 204 patients with epidermolysis bullosa. *Am J Ophthalmol.* 1994; 118:384-390.
5. Tong L, Hodgkins PR, Denyer J, et al. The eye in epidermolysis bullosa. *Br J Ophthalmol.* 1999; 83:323-326.
6. Deplus S, Bremond-Gignac D, Blanchet-Bardon C, Febrarro JL, Gaudric A. Review of ophthalmologic complications in hereditary bullous epidermolysis. Apropos of 40 cases. *J Fr Ophthalmol.* 1999; 22:760-765.
7. Fine JD, Johnson LB, Weiner M, et al. Eye involvement in inherited epidermolysis bullosa: experience of the National Epidermolysis Bullosa Registry. *Am J Ophthalmol.* 2004; 138:254-262.
8. Sakai LY, Keene DR, Morris NP, Burgeson RE. Type VII Collagen is a major structural component of anchoring fibrils. *J Cell Biol.* 1986; 103:1577-1586.
9. Van Agtmael T, Bruckner-Tuderman L. Basement membranes and human disease. *Cell Tissue Res.* 2010; 339:167-188.
10. Terrill PJ, Mayou BJ, McKee PH, Eady RA. The surgical management of dystrophic epidermolysis bullosa (excluding the hand). *Br J Plast Surg.* 1992; 45:426-434.
11. Varki R, Sadowski S, Uitto J, Pfenndner E. Epidermolysis bullosa. II. Type VII collagen mutations and phenotype-genotype correlations in the dystrophic subtypes. *J Med Genet.* 2007; 44:181-192.
12. Holbrook KA. Extracutaneous epithelial Involvement in inherited epidermolysis bullosa. *Arch Dermatol.* 1988; 124:726-731.
13. Destro M, Wallow IH, Brightbill FS. Recessive Dystrophic Epidermolysis Bullosa. *Arch Ophthalmol.* 1987; 105:1248-1252.
14. Hill JC, Rodrigue D. Cicatricial ectropion in epidermolysis bullosa and in congenital ichthyosis: its plastic repair. *Can J Ophthalmol.* 1971; 6:89-97.
15. Sharkey JA, Kervick GN, Jackson AJ, Johnston PB. Cornea plana and sclerocornea in association with recessive epidermolysis bullosa dystrophica. Case report. *Cornea.* 1992; 11:83-85.
16. Motley WW 3rd, Vanderveen DK, West CE. Surgical management of infantile cataracts in dystrophic epidermolysis bullosa. *J AAPOS.* 2010; 14:283-284.
17. Huebner S, Baertschi M, Beuschel R, Wyss M, Itin P, Goldblum D. Use of therapeutic contact lenses for the treatment of recurrent corneal erosions due to epidermolysis bullosa dystrophica. *Klin Monbl Augenheilkd.* 2015; 232:380-381.
18. Medsinghe A, Gajdosova E, Moore W, Nischal KK. Management of inflammatory corneal melt leading to central perforation in children: a retrospective study and review of literature. *Eye (Lond).* 2016; 30:593-601.
19. Koulisis N, Moysidis SN, Siegel LM, Song JC. Long-term follow-up of amniotic membrane graft for the treatment of symblepharon in a patient with recessive dystrophic epidermolysis bullosa. *Cornea.* 2016; 35:1242-1244.

20. Ponsioen TL, van Luyn MJ, van der Worp RJ, Pas HH, Hooymans JMM, Los LI. Human retinal Müller cells synthesize collagens of the vitreous and vitreoretinal interface in vitro. *Mol Vis*. 2008; 14:652-660.
21. Janssen SF, Gorgels TG, Bossers K, et al. Gene expression and functional annotation of the human ciliary body epithelia. *PLoS One*. 2012; 7:e44973.
22. Wullink B, Pas HH, Van der Worp RJ, Kuijer R, Los LI. Type VII collagen expression in the human vitreoretinal interface, corpora amylacea and inner retinal layers. *PLoS One*. 2015; 10: e0145502.
23. Uechi G, Sun Z, Schreiber EM, Halfter W, Balasubramani M. Proteomic view of basement membranes from human retinal blood vessels, inner limiting membranes, and lens capsules. *J Proteome Res*. 2014; 13:3693-3705.
24. Wullink B, Pas HH, Van der Worp RJ, et al. Type VII collagen in the human accommodation system: expression in ciliary body, zonules, and lens capsule. *Invest Ophthalmol Vis Sci*. 2018; 59:1075-1083.
25. Zimmermann DR, Fischer RW, Winterhalter KH, Witmer R, Vaughan L. Comparative studies of collagens in normal and keratoconus corneas. *Exp Eye Res*. 1988; 46:431-442.
26. Kenney MC, Nesburn AB, Burgeson RE, Butkowski RJ, Ljubimov AV. Abnormalities of the extracellular matrix in keratoconus corneas. *Cornea*. 1997; 16:345-351.
27. Tuori A, Uusitalo H, Burgeson RE, Terttunen J, Virtanen I. The immunohistochemical composition of the human corneal basement membrane. *Cornea*. 1996; 15:286-294.
28. Greene CA, Kuo C, Sherwin T. Aberrant patterns of key epithelial basement membrane components in keratoconus. *Cornea*. 2017; 36:1549-1555.
29. Schlatter B, Beck M, Frueh BE, Tappeiner C, Zinkernagel M. Evaluation of scleral and corneal thickness in keratoconus patients. *J Cataract Refract Surg*. 2015; 41:1073-1080.
30. Ryan TD, Lucky AW, King EC, Huang G, Towbin JA, Jefferies JL. Ventricular dysfunction and aortic dilation in patients with recessive dystrophic epidermolysis bullosa. *Br J Dermatol*. 2016; 174:671-673.
31. Mellado F, Fuentes I, Palisson F, Vergara JI, Kantor A. Ophthalmologic approach in epidermolysis bullosa: a cross-sectional study with phenotype-genotype correlations. *Cornea*. 2018; 37:442-447.
32. Jones SM, Smith KA, Jain M, Mellerio JE, Martinez A, Nischal KK. The frequency of signs of meibomian gland dysfunction in children with epidermolysis bullosa. *Ophthalmology*. 2016; 123:991-999.
33. Thanos M, Pauklin M, Steuhl KP, Meller D. Ocular surface reconstruction with cultivated limbal epithelium in a patient with unilateral stem cell deficiency caused by epidermolysis bullosa dystrophica Hallopeau-Siemens. *Cornea*. 2010; 29:462-464.
34. Chen VM, Shelke R, Nyström A, et al. Collagen VII deficient mice show morphologic and histologic corneal changes that phenotypically mimic human dystrophic epidermolysis bullosa of the eye. *Exp Eye Res*. 2018; 175:133-141.



6

Chapter 6

General discussion

The aim of this thesis was to increase the understanding of the characteristics and role of Col VII in the intraocular environment by studying its distribution, origins, and -if possible- its function. In this chapter, the data of our studies are integrated into the current knowledge on Col VII, the implications of our findings are discussed and some future perspectives that may further increase our understanding of this protein are given.

1.0 SIMILARITIES AND DISSIMILARITIES OF COL VII LABELING: INTRAOCULAR VS. SKIN

1.1 Labeling pattern dissimilarities

The interpretation of the distribution of intraocular Col VII would be simplified if its characteristics, such as labeling pattern and fibril formation, would be similar to that in skin. Our studies have shown that there are similarities in the characteristics in both tissues, but also differences.

1.2 Linear labeling in the intraocular environment

We were able to demonstrate Col VII at various intraocular BM zones. The labeling at the non-pigmented epithelium of the ciliary body showed a continuous linear pattern directly below the epithelial BM, in correspondence with the Col VII distribution in skin. This was especially the case at the ciliary body, in which the labeling would follow both the flat contours of the tissue (*pars plana*), as well as the protruding tissues (*pars plicata*). Based on mRNA analysis, the Col VII at this BM is expected to be derived from adjacent epithelial cells, as is the case with keratinocytes in skin.

The basement membrane of the lens (*lens capsule*) also showed a crisp linear Col VII labeling pattern at its stromal side (*vitreous*), but is in that regard not fully comparable to the situation in skin. The linear labeling pattern of the lens capsule, namely, is caused by the labeling of the ciliary zonules that envelope the lens capsule. Then again, these zonules are primarily made up of fibrillin, which is also a resident of the direct subbasal environment of the skin. At the posterior pole, the BM of the retina (*inner limiting membrane*) showed minute labeling, which was only visible in TEM analysis. Despite the small amount of anti-Col VII gold labeling that was found at this area, the gold labels would often be found embedded in the BM, and followed a linear pattern. It would of course be reasonable to assume that the linearity of this pattern could be derived from differences in the penetration of the tissues of vitreous and ILM, and

that a less penetrable ILM would result in collections of gold labels predominantly at its vitreous side. Such linear patterns, however, were also obtained in post-embedded labeling. Another theoretical explanation for the linearity found at these BMs could be the difference in electrical charge between e.g. the ILM and the surrounding tissues. Such a difference could lead to preference of the metallic labeling to the ILM, even in post-embedded sections. Our study controls ruled out these theoretical possibilities.

Many labeling patterns of (intraocular) vascular tissues could be considered to be linear. Apart from the many pattern discontinuities, blood vessels also showed circumferential anti-Col VII labeling patterns that were uninterrupted. Of course, pattern varieties are common to immunohistological analysis, especially when various vascular tissues and techniques are compared. For example, immunofluorescent studies of retinal whole mounts would show an almost 'digitated' labeling at the blood vessel walls, a pattern that might also be regarded as a highly interrupted linearity. At high magnification of blood vessels in TEM analysis, the linearity of gold label distribution would often be less pronounced than in peroxidase-labeled paraffin sections analyzed by light microscopy.

1.3 Non-linear labeling in the intraocular environment: the retina

In the superficial retina, small clustered vesicles were labeled. Such a pattern is reminiscent of the labeling observed in keratinocyte and fibroblast cell cultures and is different from the common linear labeling observed in skin sections. If Col VII was to support the fragile neural tissue in a similar fashion as in skin, a continuous deposition of Col VII (i.e. anchoring fibrils) would be distributed along the mesenchymal (i.e. vitreous) side of the basement membrane. By iTEM analysis, such specific labeling was observed in sparse numbers. Looped anchoring fibrils were not observed. The vesicles might resemble a means of Col VII transport toward the vitreoretinal interface. Their location suggests that they are associated with retinal ganglion cells, but their colocalization with GFAP suggests an association with astrocytes or activated Müller cells. In contrast to ganglion cells, astrocytes and Müller cells may synthesize Col VII and/or other ECM proteins.¹⁻⁴

Alternatively, the possibility of compartmentalization of diffusely distributed retinal Col VII into vesicles, either for storage or degradation (i.e. phagocytosis of Col VII debris and storage into corpora amylacea), was also considered. Both Müller cells and astrocytes are capable of phagocytosis, in contrast to retinal ganglion cells.^{1,5} Müller cells span the entire thickness of the retina, but have their nucleus in the inner nuclear layer. Astrocytes are relatively small, and may be distributed throughout the retina. Since the vesicles

were always distributed perinuclearly, we deemed an association with astrocytes more likely. Moreover, corpora amylacea are believed to be of astrocytic origin.⁶ Astrocytes may store redundant or residual proteins.⁷ A direct association between the vesicles and corpora amylacea could not be made, since neither entity was observed in close proximity to the other. The vesicles are therefore more likely to be associated with Col VII synthesis than phagocytosis or storage. Potentially, the Col VII content of the vesicles might be deployed to function locally, at the vitreoretinal interface, or both. Additionally, Col VII might support glial cell-to-blood vessel interaction, since astrocytes and Col VII apparently envelope blood vessels at the superficial retina layers.

1.4 Non-linear labeling in the intraocular environment: ciliary body

A more broad anti-Col VII labeling was seen in the ciliary body, at sites where the BM of the pigmented epithelium would approximate the walls of blood vessels. The labeling appeared strong and specific, with mainly broad, sharply delineated boundaries. Outside those boundaries, some diffuse stromal background labeling was observed. On occasion, the blood vessel walls would show wisps of fine fibers traversing into the stroma.

The single BM of either pigmented epithelium or blood vessel alone could probably not account for the broadness of this pattern. Based on the location of this broader labeling, an association with hyaline degeneration (corresponding to Hogans⁸ 'BM-like material') must be considered, since most of our donors were of age. The BMs in elderly donors are also known to duplicate or broaden at times. Probably, the first phenomenon would not result in such labeling intensity, and the second would show two or more lines (conform the BM of the pigmented epithelium). How Col VII molecules would take part in either the physiological or degenerative processes, or by which mechanism Col VII would be deployed to produce such a broad labeling remains unexplained. We suspect that the mechanical stress of the accommodation system is at least partly accountable for deposition of Col VII. Interestingly, the blood vessels of the retina show distinct lines and do not share the broader pattern of their ciliary counterparts in donors of corresponding age.

1.5 Non-linear labeling in the intraocular environment: zonules

One of the most intriguing findings of our studies was the intense, diffuse and specific labeling of the ciliary zonules. As thin fibers, the zonules were seen to originate between the non-pigmented ciliary epithelial cells, then converge between the stromal apices of these cells at the junction with the vitreous, and then 'pour' out from between the

epithelial cells into the vitreous as zonular fibers. These extracellular fibers transduce forces from the ciliary muscle to the lens capsule. A flexible anchoring protein that could support the zonular fiber architecture through its connections to other extracellular matrix components should be useful. Then, after having traversed the vitreous, the zonule-associated Col VII might also support the incorporation of the zonules into the lens capsule, by interacting with the capsule's main component, Col IV. Although some collagen types are associated with zonular fibers, the presence of Col VII has never been reported previously. In our studies, the zonules would label in all analytical techniques used (TEM, IF, LM, Wb), and in all embedding media (paraffin, T8100, cryo), but only with pAb(16). The sensibility and specificity of pAb(16) is discussed later on.

2.0 (DIS)SIMILARITIES OF COL VII CHARACTERISTICS

2.1 Intraocular vs. skin

There are more differences between the Col VII characteristics of the intraocular environment and the skin outside of their labeling patterns. Despite the Col VII labeling at various intraocular tissues, no corresponding anchoring fibrils could be demonstrated. Such a discrepancy is not easily explained by the current dermatological literature, and would probably be regarded as antibody cross-reactivity (i.e. false-positivity). In order to adequately validate the presence of Col VII, any indirect evidence for such a claim would need to be strong. The use of only one antibody or analytical method would not be adequate, since Col VII is a novel find in most of the examined tissues. Therefore, more evidence was gathered in support of our hypothesis.

2.2 Anti-Col VII labeling in the (visual) absence of anchoring fibrils

Our means to detect anchoring fibrils was validated by their demonstration in our control tissues of skin and cornea. Depending on the methods used, light microscopic evaluation would show labeling by most anti-Col VII antibodies (including monoclonals) at intraocular BMs, around stromal components, or cells plausibly capable of collagen synthesis. These observations were supported by several other analytical techniques (Wb, RT-PCR, etc). Unfortunately, our monoclonal antibodies would not perform well in resin sections in general, so absent gold labeling in iTEM sections was not deemed to be representative or contributory. Still, the fine collagen fibrils that were labeled by pAb(16), did not match the general morphology (size, shape, banding pattern) of typical stromal fibrils (e.g. Col I, II, III, V). They also were explicitly more recognizable (i.e. coarser) than the Col IV fibers of the lamina densa network. Cross-reactivity of other,

adjacent collagens was therefore unlikely. At the vitreoretinal interface, such gold labeling was located in between the lamina densa and stroma, in agreement with skin and cornea.

2.3 The visual 'absence' of anchoring fibrils in skin: spatial distribution

Even when anchoring fibrils are known to exist in a tissue, early dermal studies have advocated that these fibrils may be difficult to discern. In literature, a multitude of technical difficulties which could impede detection by TEM were put forward (see chapter 2). On the other hand, some authors felt so confident in detecting anchoring fibril by their morphology, that they comparatively quantified their numbers per age group and gender.⁹ Reportedly, the visual detection of anchoring fibrils in cornea tissue is more difficult than in skin, possibly due to a smaller abundance of anchoring fibrils *in toto*, or otherwise due to a different orientation of the fibrils (parallel to the BM in skin vs. perpendicular to BM in cornea).^{10,11} This last suggestion could imply that in cornea the linear type is dominant to the more clearly recognizable looping type. Despite clear Col VII immunoreactivity in several other tissues and cell cultures, no actual anchoring fibrils have ever been demonstrated in tissues other than skin and cornea (to our knowledge).

2.4 The visual 'absence' of anchoring fibrils in skin: size and temporal distribution

The difficulty of reliably identifying anchoring fibrils may be reflected by the inconsistencies in the reports on their characteristics. In cornea, the average penetration depth of anchoring fibrils into the stroma was measured at $0.60 \mu\text{m} \pm 1 \mu\text{m}$ (max $2.05 \mu\text{m}$), with anchoring fibril widths up to $0.15 \mu\text{m}$ [10Gipson 1987].¹⁰ Others reported a length of $1.5 \mu\text{m}$ and a width of $27.5 \text{ nm} \pm 3.9 \text{ nm}$, and found the fibrils leaving Bowman's layer in parallel pairs perpendicular to the ocular surface crossing the anterior stromal lamellae.¹² Corneal anchoring fibrils become visible at 26 weeks of gestation, but their differentiation from anchoring filaments and stromal fibers was already very difficult.¹³ Others found the corneal anchoring fibrils to become notable at 13 weeks of gestation, and measured a stromal penetration of $0.54 \pm 0.01 \mu\text{m}$.¹⁴ Col VII immunofluorescence by monoclonals could be observed in wounded (keratectomy) rabbit cornea's at 48 hours of healing, but anchoring fibrils were not visible until 4 weeks post-injury.¹¹ So, during gestation and after injury, Col VII (or some of its epitopes) may be detected in the temporary absence of notable anchoring fibrils. A transient expression of Col VII was reported in the endometrium, as part of the menstrual cycle. Instead of the common uninterrupted linear labeling at its epithelial

BM, the linearity was reduced to focal labeling in the proliferative phase. Therefore, Col VII was thought to play a role in dealing with the intrauterine shear forces that occur transiently in the menstrual cycle. Focal expression would exist when these forces were relatively low. Alternatively, the temporal distribution was suggested be part of a yet undetermined regulatory function of Col VII.¹⁵

2.5 The visual ‘absence’ of anchoring fibrils: a hypothesis

In our studies, most donors were adults or elderly without known ophthalmologic disorders. The discrepancies of the anchoring fibril characteristics in the aforementioned reports probably lie, at least partly, in the difficulty of their visualization. Whether that is because methods and experience vary, or that there might be unexplained variations in anchoring fibril characteristics (orientation, size, amount) remains unclear. We cannot rule out that individual Col VII fibers, or sparsely aggregated anchoring fibrils, might also be present and functional, which would also explain the variances found in our own investigations. Perhaps there are phenomena that occur differently in the intraocular (or extradermal) environment, such as the *in vivo* stabilization of mature anchoring fibrils by transglutaminase cross-links.¹⁶ Otherwise, there may be differences in the conformation of the epitopes that are targeted by our antibodies, which may not label intact Col VII molecules, but instead correspond to parts or physiological fragments thereof. By analogy, restin and endostatin are small parts of the collagen types XV and XVIII, respectively. They are domains of the intact molecules, and are considered to have anti-angiogenic or perhaps tumorigenic characteristics when detached. Mutations of these collagen types result in eye and microvessel phenotypes.^{17, 18} It is unknown whether the NC-1 or the helical domain of Col VII could be proteolytically cleaved off in a similar fashion to produce an autonomously functional protein. If so, it would certainly help to explain some of our results, especially the intense labeling of the zonules.

3.0 INDIRECT EVIDENCE OF COL VII LABELING VALIDITY

3.1 Antibody validation

The visual absence of anchoring fibrils might also be explained by the absence of Col VII altogether. Of course, we have validated our results carefully, but we should keep the possibility of potentially false-positive reactions in mind, which are inherent in immunohistochemical experiments. The most obvious of those immunoreactions

would be a false-positive labeling of the zonules, since the pAb(16) labeled them intensely while the monoclonals did not. For this reason, the pAb(16) antibody underwent thorough validation.

3.2 The specificity and sensitivity of the main antibody, pAb(16)

Because pAb(16) is a polyclonal antibody, collagen experts might have some doubt in accepting any results that are obtained by the use of this antibody alone. Polyclonality, namely, might mean more potential epitopes, including erratic ones on other unintentionally targeted proteins, especially when these proteins have highly comparable parts such as the collagenous Gly-X-Y repeats. Also, the pAb(16) antibody was not engineered through recombination. Instead, it is a classically derived IgG, raised against full length purified, human placenta extracted Col VII, which was injected into a rabbit host. According to the manufacturers datasheet, the pAb(16) does not cross-react with fibronectin or types I-IV or VI collagen [Datasheet]. As in any other subject of analytical processes, antibodies must be validated thoroughly, by demonstrating minimal cross-reactivity and batch variability and thus optimizing applicability for the corresponding analytical methods.¹⁹ It is recommended to only use those antibodies that have been defined down to the level of the DNA sequence that produces them, and which are manufactured in engineered 'recombinant' cells.²⁰ Pilot studies by our group have confirmed that human primary non-pigmented epithelial cells are capable of Col VII synthesis *in vitro*. This was validated by IHC, ELISA and Western blot analysis with commercially available monoclonal LH7.2 antibodies. Because the intensely pAb(16) labeled ciliary zonules derive from these cells, the labeling validity of this antibody was further supported. The steadfast results and applicability range of the pAb(16) antibody in the various analytical methods, together with the results of the epitope mapping survey convinced us of the reliability of this antibody.

3.3 Validity of pAb(16) in literature

The use of polyclonal antibodies is widespread in Col VII literature. In particular, the pAb(16) antibody in particular is well used by experts in the field.²¹⁻²⁹ None of these authors has reported any cross-reactivity, or other concerns about (the results from) this antibody. Unfortunately, we were unable to determine the exact origin of pAb(16), i.e. whether it shares a similar clonality as the polyclonals used since the first Col VII investigations (Table 1 in chapter 4).

3.4 Reproducibility of labeling with pAb(16)

We have tested the reproducibility of the immunohistochemical (IHC) results of the pAb(16) antibody in skin and ocular tissues in our own lab. We found that this antibody produced very reproducible labeling patterns time and again. A polyclonal antibody from another company, pAb(15) (Abcam) gave identical results, although both companies might have sold the same antibody under different names. Different batches from Calbiochem (n=7) gave identical results per analytical method (IHC on paraffin and cryo, Western blots, iTEM).

4.0 RULING OUT CROSS-REACTIVITY

4.1 Potential cross-reactivity with protein fibers adjacent to Col VII

We have validated the pAb(16) labeling results of skin sections by our lab (biomedical engineering) in a different lab, which was then performed by other technicians (dermatology UMCG), and with their own pAb(16) batch. The results of these labeling procedures were identical to ours.

4.2 Cross-reactivity of pAb(16) in a case of RDEB?

Despite the accumulated validity of the pAb(16), a possible cross-reaction with pAb(16) was observed a skin biopsy sample of a 'completely' Col VII deficient (non-Dutch, but European) infant. The infant was known to suffer from severe RDEB due to a homozygotism for a (*c.1637-240_3252del4061*) mutation in the COL7A1 gene (NM_000094.3), very similar to a reported case.³⁰ This mutation would result in a disruption of the RNA splicing, which would probably introduce a premature stopcodon and impede synthesis of Col VII protein. However, intronic mutations may produce several splice products, some of which might be in-frame and still result in synthesis of some form of Col VII protein. At the time of the biopsies, it was unclear what mutant COL7A1 mRNA would form. The infant was (phenotypically) doing spectacularly well, despite no LH7.2 or pAb(16) labeling was detected at common microscope settings (**Figure 1A**)(score: 0 out of 4). Sporadically, thin anchoring fibrils were observed, but only in the first year. Unfortunately, within a few months, the infant deceased after a sudden rapid deterioration, reflective of the severity of its RDEB genotype. Accidentally, it was noted that in the corresponding skin sections, long threadlike structures would become visible when the detection signal was severely augmented (**Figure 1**). Morphologically, these threads resembled fibrils of the elastic type, which

are notorious for their autofluorescent characteristics. Usually, such fluorescence is not encountered in such close proximity to Col VII, so it was deemed worthwhile to rule out cross-reactivity, or (re)confirm their autofluorescence. There are three candidate fiber types in skin: elastin, elanin, and oxytalan. The fibril's location and shape were most reminiscent of oxytalan (**Figure 2 & 3**).

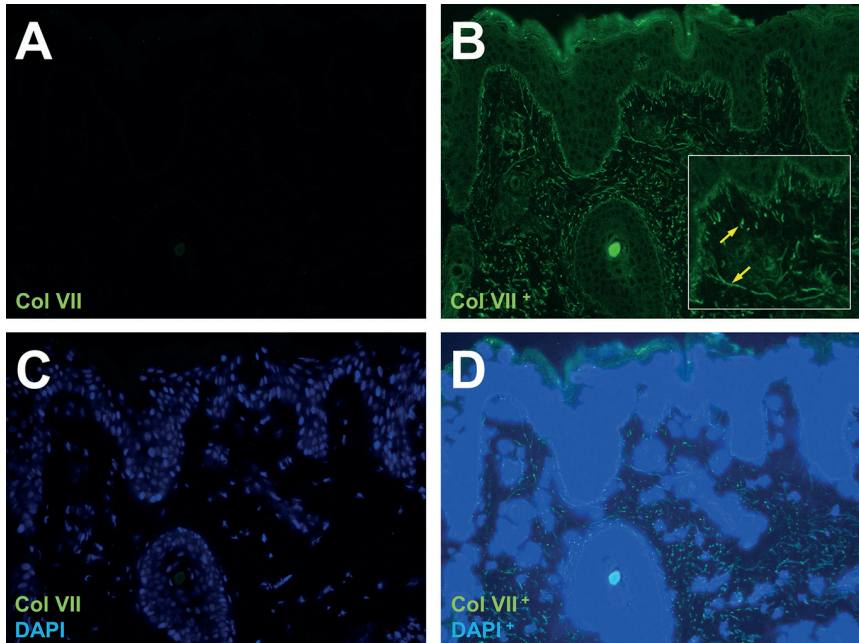


FIGURE 1. Immunofluorescence of Col VII and DAPI in skin sections of an infant RDEB patient. A.) In customary settings, the dermal-epidermal basement membrane is not labeled with pAb(16), as is expected. B.) When the signal is enhanced to the level of recognizable background structures, fibrils (yellow arrows) below the BM and in the stroma would stand out. C.) Customary setting overlay with DAPI and pAb(16). D.) Signal enhanced overlay with DAPI and Col VII as comparison to the amount of signal enhancement is needed for image B).

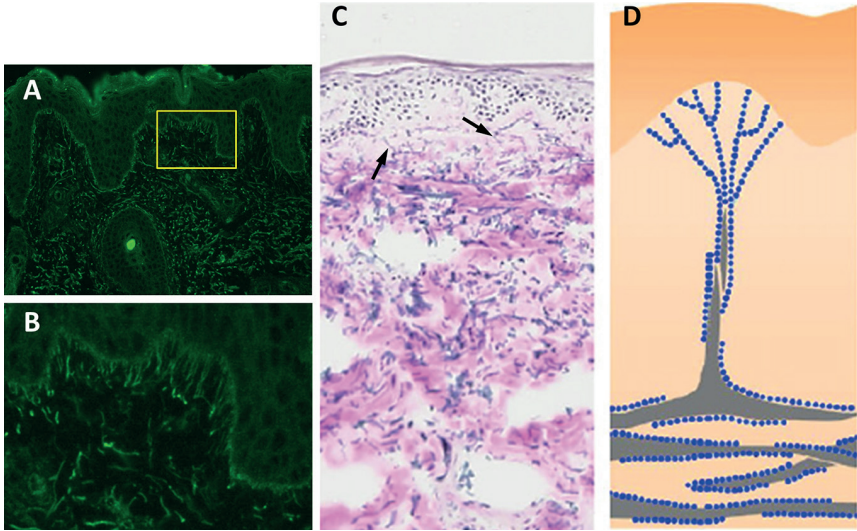


FIGURE 2. Extracellular components in young adult skin. A.) Autofluorescence in enhanced signal from Figure 1. The yellow box indicates the inset of B.) and the aspect and location of sub-basal elastic fibers. C.) Section stained with Miller's elastic stain, in which oxytalan fibers (*black arrows*) run downwards from the subbasal lamina to meet other fibers in the reticular dermis D.) Adapted from Naylor AE, Watson RE, Sherratt MJ. *Maturitas*. 2011; 69:249-256.

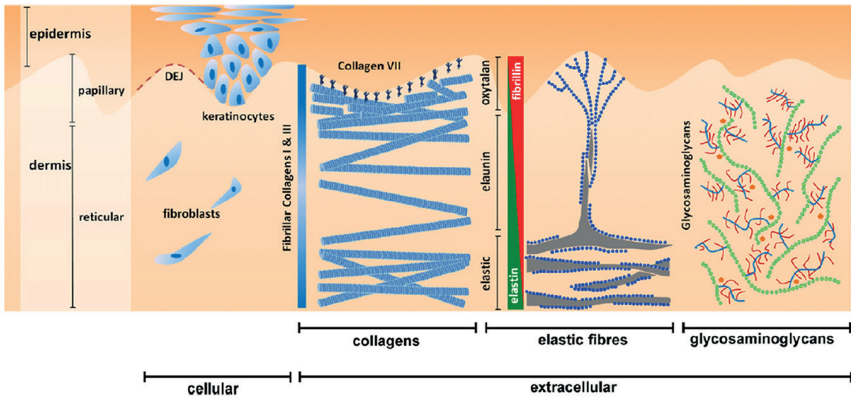


FIGURE 3. Schematic representation of extracellular components in young adult skin. As Col VII, the elastic fibers originate in the subbasal lamina. Elastic fibers are complex structures that contain elastin as well as microfibrils.³⁵ Here, these elastic fibers are considered to be fibrillin rich, and to a lesser extent elastin (and elauinin). But, as shown, elauinin and elastin are generally deposited more deeper in the stroma than Col VII. The localization of oxytalan thus correlates with that of Col VII, and the subbasal fibers seen in enhanced immunofluorescent signal images might be explained by autofluorescence of these oxytalan fibers. Adapted from Naylor AE, Watson RE, Sherratt MJ. *Maturitas*. 2011; 69:249-256.

4.3 pAb(16) does not cross-react with oxytalan

Oxytalan fibrils are fibrillin-rich microfibrils that, like Col VII, run perpendicular to the epidermis. In infants, the oxytalan fibers appear as ‘roots’³¹ (**Figure 2**). The elastin components in such fibers may be notoriously sticky and autofluorescent, a double hindrance in immunofluorescence studies.³² In a previous Col VII investigation of the rabbit cornea, such ‘roots’ might have labeled with monoclonal antibodies. The authors observed a ‘discontinuous beaded line of (immuno)localization along the basal cell surface’. The source was, however, attributed to anchoring plaques¹⁴ instead of the ‘roots’. We found that such rooted fibrils might also show in normal skin when labeled with monoclonals, as long as the signal is sufficiently augmented (**Figure 4**). We thus concluded that the faint rooted pattern could be sufficiently explained by autofluorescence, instead of actual pAb(16) cross-reactivity.

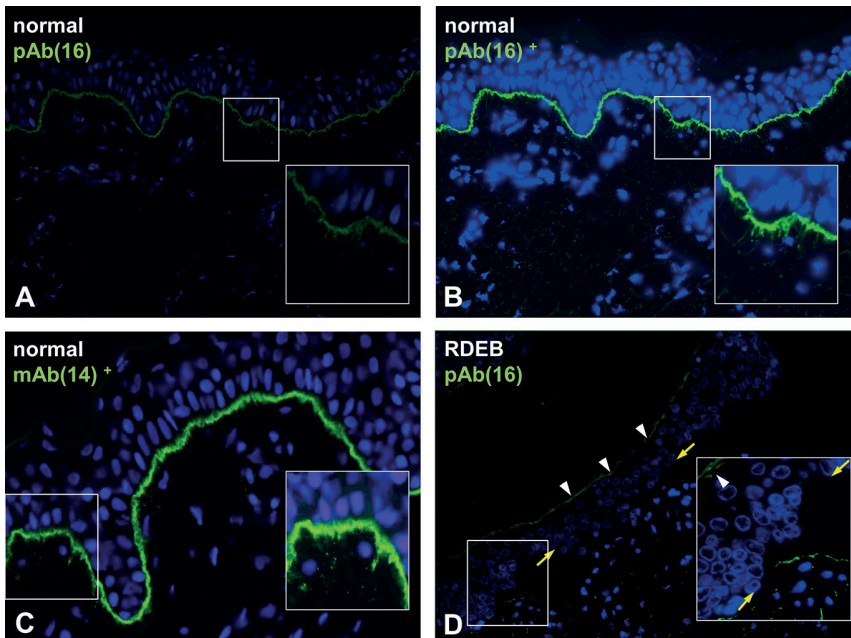


FIGURE 4. Comparison of oxytalan fibers by monoclonal mAb(14) and polyclonal pAb(16) antibodies. A.) Healthy donor labeled with polyclonals with custom signal settings. Normal skin sections may also show oxytalan fibers with polyclonal (B), as well as monoclonal antibodies (C). D.) Complete Col VII deficiency in a severe RDEB skin biopsy section. The dermal-epidermal basement membrane does not label at all (between yellow arrows), although some deeper elastic fibers show autofluorescence, as does the stratum corneum (white arrowheads). The autofluorescence of both structures is well known. Magnifications A-D $\times 10$; C 20 \times .

4.4 pAb(16) does not cross-react with elastin

Such autofluorescence, or potential cross-reactivity, was also encountered in immunofluorescence analysis of vascular tissues. We have used immunofluorescence on cryosections readily, since these section types provided the most effective presentation of tissue epitopes, enabling the labeling with most of our monoclonal antibodies. In cryosections, our antibodies would label at the vascular walls, in close proximity to the elastin fibers. These elastic fibers primarily function as an elastic reservoir, which distributes any mechanical stress evenly throughout the wall onto the sturdy collagen fibers. As a result, elastin appears side-by-side to the adjacent collagens, although in sections both fiber types do not precisely overlap one another.³³ The differentiation between such matrix fibrils may be difficult in cryosections, because of the poor morphology in cryosections (compared to paraffin or resin). In order to interpret the Col VII labeling correctly, and to differentiate between any false-positive labeling of elastin or autofluorescence thereof, these two influences needed to be nullified. By substitution to peroxidase/AEC labeling (**Figure 5**), any influence of autofluorescence in the cryosections was bypassed. The recombinant pAb(72) anti-Col VII antibody would label similarly as pAb(16), and thus close to elastin fibrils. The distinct hyaline, or glass-like appearance (**SI Fig. 5 in chapter 4**) of elastin could now easily be differentiated from collagen fibrils. In TEM studies, elastin was observed in the larger vessels of the retina, mainly those close to the ILM, where elastin would mingle with the collagens of the outer vascular BMs.³⁴ Elastin appears amorphous in TEM studies,³⁵ and could therefore be differentiated from the perivascular fibrils/fibers that were targeted by our antibodies. In the vascular lysates, and Western blots thereof, we do not expect an important influence of elastin. After cross-linking in the ECM, elastin cannot be dissociated anymore, and can only be extracted and purified by removing all other tissue components.^{32, 35, 36} Our lysates would not likely contain enough soluble elastin to interfere with our signals or interpretations. We agree that collagens, such as Col VII, appear side-by-side with elastin at vascular tissues. We also believe our antibodies have genuinely targeted Col VII perivascularly.

Interestingly, some speckled perivascular Col VII labeling was recently observed in the subepidermis, in proximity to Col IV and elastin. Hayakawa et al. (2017) hypothesized that Col VII may not be deposited around blood vessels for any mechanical stabilization, but for use in some other, unknown pathway. Because their Col VII labeling did not colocalize with their vascular markers (CD31, against endothelial cells), the authors ultimately abandoned their hypothesis.³³

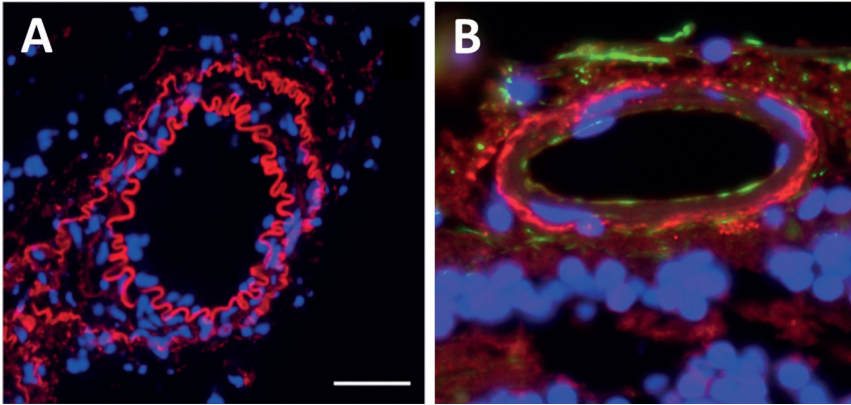


FIGURE 5. Immunofluorescent aspect of blood vessels. **A.)** Cryosection of a mouse renal artery. Elastin is selectively stained by a dye (red, Alexa Fluor 633), appearing as specific as an actual anti-elastin labeling would. The staining shows elastin's location and shape similarities, which might interfere with the interpretation of Col VII labeling. **B.)** Cryostat section of a human retinal vessel. This anti-Col VII labeling by pAb(16) (red) demonstrates the similarities with elastin labeling (and thus also the location of potential elastin autofluorescence) at such magnifications. In blood vessel walls, elastin typically adopts an undulating pattern. Blue DAPI nuclear staining. Green GFAP glial cells labeling. Scale bar 40 μm . *A, adapted from Halabi CM, Mecham RP. Methods Cell Biol. 2018; 143:207-222.*

4.5 pAb(16) does not cross-react with fibrillin

The cross-reactivity with oxytalan in skin was now ruled out, but there remained the unexplained intense pAb(16) labeling of the ciliary zonules. The zonules are regarded as oxytalan fibers, microfibrils that are made up primarily by fibrillins and lack elastin.^{37, 38} An interaction between microfibrils and collagens was previously suggested. Local collagens might influence microfibril bundle packing and integration into the lens capsule.³⁹ In that study, the presence of Col VII was not investigated. Proteomic studies of zonular lysates, as well as immunohistochemical studies, could not (convincingly) demonstrate zonular Col VII. Any cross-reactivity of pAb(16) to the three most abundant glycoproteins in the human zonulome (fibrillin-1, LTBP2 and MFAP2), is unlikely. An immunofluorescence study of the accommodation system showed their corresponding labeling patterns to be dissimilar from ours.⁴⁰

5.0 THE INTERPRETATION OF COL VII IMMUNOLABELING RESULTS

The intraocular milieu expresses COL7A1 and synthesizes Col VII, while anchoring fibrils are visibly absent. This combination is suggestive of an alternate conformational mode of Col VII, that does not entice apparent lateral aggregation. For example, our antibodies might have targeted epitopes on Col VII molecules or fragments which lack the interaction sites/formations for aggregation. Such a hypothesis could be addressed by using all the validated antibodies at hand of which the target epitope(s) on the Col VII molecule are (roughly) known, and to compare their labeling patterns in serially cut immuno-TEM (iTEM) sections, or perform co-localization studies that could affirm or rule out the presence of intact Col VII molecules. Unfortunately, other antibodies than pAb(16) did not work well in post-embedding for iTEM. Perhaps the epitopes of anti-Col VII monoclonals are damaged or destroyed by the fixation and embedding procedure, which apparently occurs easily in the presence of strong detergents or reducing agents.³³ Pre-embedding studies with monoclonal antibodies were performed in earlier stages of data collection for this thesis. Because of tissue penetration difficulties, and the sudden unavailability of fresh donor materials after an adjustment in Dutch legislation, pre-embedding and cryo-TEM analysis were forsaken.

6.0 INTERMOLECULAR INTERACTIONS OF COL VII

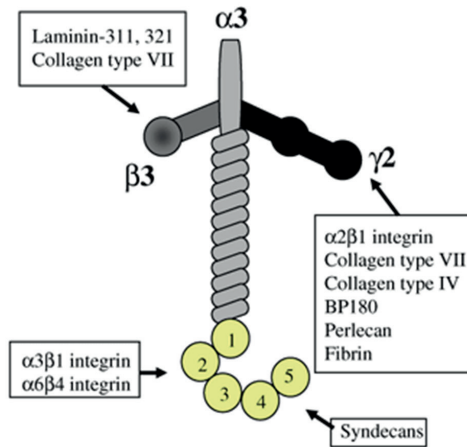
6.1 Basement membrane proteins associated with Col VII

As anchoring fibril component, Col VII needs to interact with other BM zone proteins to effectively incorporate into (and function at) the BM. In the absence of visible anchoring fibrils, we might still establish a potential anchoring function of Col VII (i.e. by unaggregated fibrils) at the intraocular tissues indirectly. We would have to demonstrate the presence of proteins that Col VII usually interacts with. Of course, we should take into account that such intermolecular interactors might differ per tissue, or even per BM region within a tissue. In dermal BM anchoring, Col VII interacts with Col IV, laminin-332 and fibronectin through its NC-1 domain.⁴¹⁻⁴³ We chose to investigate the presence of laminin-332 first.

6.2 Intermolecular interaction of Col VII with laminin

Laminin is a heterotrimeric protein composed of an α -, β -, and γ -chain combination. Each of these chains has its genetic variants (five α , four β , two γ chain types). A laminin isoform is described by its combination of these chains, for example laminin- $\alpha3\beta3\gamma2$,

or simply laminin-332. Not all theoretical chain combinations are encountered in practice, since only 16 laminin isoforms have been recognized. All of the Col VII-laminin interactions have been attributed to laminin-332 at the upper lamina densa, by its $\beta 3$ chain arm and to a lesser extent through its $\gamma 2$ chain arm.⁴¹ Some affinity of the NC-1 for laminin-311 was also observed, but a mutual affinity to the NC-1 domain was only demonstrated by laminin-332.^{41, 43, 44}



Laminin-332

FIGURE 6. The structure of laminin-332. Each chain has its own receptors and ECM proteins binding sites. Adapted from Sugawara K, Tsuruta D, Ishii M, et al. *Exp Dermatol.* 2008; 17:473-480.

In a pilot iTEM study, we have failed to colocalize laminin-332 with Col VII. By using a monoclonal anti-laminin $\alpha 3$ chain antibody (N-20, Santa Cruz, SC16583), we were unable to demonstrate laminin-332 convincingly. Given the technical difficulties previously experienced with monoclonal antibodies for iTEM in general, we abandoned this path. We were able to obtain (raw and unpublished) gene expression profiles of the non-pigmented and pigmented ciliary epithelium.⁴⁵ These data showed that these epithelia express both COL7A1 and the genes of the laminin-332 subchains. Their expression levels make the translation into these proteins likely, but does not prove such protein synthesis to actually occur. Our pAb(16) antibodies, however, labeled readily at these epithelia. Further evidence for laminin-332 presence was collected through a literature search.

TABLE 1. Gene expression profile of Col VII and laminin-332 at the ciliary body.

Expression level	Expression value
Very low/absent	<5,30
Low	5,31-9,07
Moderate	9,08-13,57
Highest	>13,58

ProbelName	GeneName	SystematicName	FeatureNum	PE												NPE															
				39Jr		48Jr		56Jr		58Jr		68Jr		70Jr		73Jr		39Jr		48Jr		56Jr		58Jr		68Jr		70Jr		73Jr	
				M	F	M	F	M	F	M	F	M	F	M	F	M	F	M	F	M	F	M	F	M	F	M	F	M	F		
A_23_P144071	COL7A1	NM_000094	43739	7,41	8,00	7,22	7,77	7,69	7,21	7,60	7,28	7,53	7,17	8,10	7,91	7,85	7,41	8,00	7,22	7,77	7,69	7,21	7,60	7,28	7,53	7,17	8,10	7,91	7,85		
A_24_P179569	LAMA3	NM_000227	11091	4,79	5,43	4,45	4,88	4,36	4,79	4,81	4,86	5,57	4,97	5,20	4,68	5,10	4,79	5,43	4,45	4,88	4,36	4,79	4,81	4,86	5,57	4,97	5,20	4,68	5,10		
A_23_P89780	LAMA3	NM_198129	18290	10,20	11,77	10,88	10,95	10,48	11,26	10,29	10,26	11,75	10,59	10,96	10,69	11,34	10,52	10,20	11,77	10,88	10,95	10,48	11,26	10,29	10,26	11,75	10,59	10,96	10,69	11,34	
A_24_P687302	LAMA3	NM_198129	18482	5,88	6,73	6,59	5,97	5,80	6,16	6,65	6,73	6,92	7,61	6,36	5,53	6,40	6,63	5,88	6,73	6,59	5,97	5,80	6,16	6,65	6,73	6,92	7,61	6,36	5,53	6,40	
A_23_P86012	LAMB3	NM_001017402	35139	6,57	7,04	6,25	6,41	6,80	6,13	6,30	6,75	7,29	6,57	6,23	6,21	6,60	6,60	6,57	7,04	6,25	6,41	6,80	6,13	6,30	6,75	7,29	6,57	6,23	6,21	6,60	
A_23_P160968	LAMC2	NM_018891	19735	7,65	9,55	NA	8,66	5,97	9,02	7,97	7,70	9,16	8,10	8,49	6,33	8,18	NA	7,65	9,55	NA	8,66	5,97	9,02	7,97	7,70	9,16	8,10	8,49	6,33	8,18	
A_23_P201636	LAMC2	NM_005562	36548	9,90	11,58	10,39	11,57	9,03	10,89	9,89	9,97	11,30	10,34	11,16	NA	10,88	10,09	9,90	11,58	10,39	11,57	9,03	10,89	9,89	9,97	11,30	10,34	11,16	NA	10,88	

The mean gene expression values of the epithelia after normalization range from 2.09 to 18.88 (log2 transformed absolute expression levels). Janssen et al. (2013) published the selected 'highly expressed genes' group, which mean expression levels ranged from 13.70 to 18.88. COL7A1 expression in ciliary epithelia is approximately 7 to 8, which corresponds to a 'low' expression level (compared with the total dataset). Description: mRNA, Homo sapiens collagen, type VII, alpha 1 (COL7A1) (epidermolysis bullosa, dystrophic, dominant and recessive). Systematic Name: NM_000094. Age at enucleation. Non-pigmented (NPE) and pigmented ciliary epithelium (PE).

6.3 Immunohistochemical demonstrations of ocular laminin in literature

The individual $\alpha 3/\beta 3$ -chains of laminin-332 have been demonstrated at the BMs of cornea, limbus, conjunctiva and the blood vessels of those tissues. Except from the blood vessels, Col VII was similarly demonstrated in that study.⁴⁶ Another study had demonstrated laminin-332 at Bruch's membrane, at which we now show presence of Col VII (**Figure 5 in chapter 4**).⁴⁷ The presence of either Col VII or laminin-332 in blood vessels is not commonly accepted (**Table 2**). Some evidence for the presence of laminin-332 at blood vessels was recently put forward, at the vasculature that provides for enamel formation.⁴⁸

TABLE 2. Reactivity of various monoclonal antibodies at ocular surface tissue basement membranes.

Antibody	Cornea	Limbus	Conjunctiva	Blood vessels
Laminin-1 (pAb)	+	+	+	+
$\alpha 1$ -chain	+/-	+	+	+
$\alpha 2$ -chain	-	+	-	-
$\alpha 3$ -chain	+	+	+	-
$\beta 1$ -chain	+/-	+	+	+
$\beta 2$ -chain	-	+	+	+
$\beta 3$ -chain	+	+	+	-
$\gamma 1$ -chain	+/-	+	+	+
Laminin-5	+	+	+	-
Collagen IV	-	+	+	+
Collagen VII	+	+	+	-
Fibronectin (pAb)	+	+	+	+

+ positive reaction, +/- reaction varied, - negative reaction. PC polyclonal antibody. Note the absent labeling of Col VII and laminin-332 at blood vessels. Adapted from Tuori A, Uusitalo H, Burgeson RE, Terttunen J, Virtanen I. *Cornea*. 1996; 15:286-294.

6.4 Detection of interacting proteins to Col VII by IHC: limitations

Detection of BM components by IHC may sometimes fail, where alternative methods succeed. For a time, even Col IV was thought to be absent from the central cornea, because it could not be demonstrated by IHC, despite several epitope unmasking procedures.^{49, 50} Positive mRNA detection and Western blots contradicted such absence of Col IV, which stimulated further investigations by different antibodies and (unmasking) techniques.⁵¹ Today, each of the Col IV chains has been demonstrated in

the human cornea, also by IHC.^{46, 51, 52, 53} Likewise, Col VII (and laminin-332) could not be demonstrated in lens capsule sections while we detected Col VII in both sections and lysates.⁵⁴ Conversely, some studies were unable to detect COL7A1 mRNA in lysates of whole human eyes altogether, while we have demonstrated COL7A1 mRNA and, correspondingly, Col VII presence by several techniques including IHC.⁵⁵ The outcome of multiple analytical techniques can complement individual investigations such as IHC. An additional tool for identifying ECM protein components (i.e. Col VII) may be found in proteomics, either for ruling out false-negative or false-positive results.

6.5 Detection of interacting proteins to Col VII by proteomics

Proteomics is the large scale study of proteins, usually by liquid chromatography-mass spectrometry (**LC-MS/MS**). LC-MS/MS is designed to simplify the identification and quantification of the proteins that are extracted from biological tissues. It may be very sensitive. For example, proteomic analysis could detect near-all Col IV subchains (6 chains, 3 locations, 1 chain absent = 17 out of 18 hits) at all three basic layers of the cornea, where IHC failed (idem, but 5 chains absent = 13 out of 18 hits).^{53, 56} By proteomics, multiple laminins could also be detected. The entire laminin-332 combination was found in the corneal epithelium, where anchoring fibrils are located.⁵⁶ The Col VII-binding subunits $\beta 3$ and $\gamma 2$ were found in the endothelium, while COL7A1 was detected at the adjacent Descemet's membrane.^{56, 57} To our knowledge, Col VII has never been demonstrated by IHC at the cornea endothelium. Elastin and fibrillin-1 were not detected in the cornea in these studies.

A potential pitfall in proteomic analysis is that not all of the corneal proteins, especially the stromal collagens, are equally soluble in SDS.⁵⁶ This means that it might not be possible to adequately resolve such proteins by SDS-PAGE, prior to LC-MS/MS or Western blotting. By proteomic quantification, these authors estimated that collagens account for about 50% of the total proteins in the stroma layer, 30% in the endothelium layer and only about 2% in the epithelium layer. At the epithelium, the concentration of Col VII should be highest due to the presence of anchoring fibrils and relative little presence of other collagens. The authors detected Col VII in both the epithelium and the stroma. They explain the presence of Col VII in both layers by an imperfect separation prior to tissue homogenization (i.e they scraped off the epithelium with a knife, but probably also shavings of the Col VII rich BM/Bowman's layer complex). Still, their outcome proves that detection of Col VII -even in the collagen rich stromal lysates- is possible by LC-MS/MS. This outcome is in agreement with our investigations, since we are also able to detect Col VII in our Western blots. Based on IHC labeling intensities however, the tissues that we wanted to proteomically analyze, were likely

to contain much less Col VII than tissues with i.e. an established anchoring fibril layer. Because zonules showed intense labeling in our IHC analysis, a literature search for collagens in the zonular proteome was conducted.

TABLE 3. The presence of collagens and laminins in corneal tissues, as detected by proteomics.

Name	Epithelium	Stroma	Endothelium	Name	Epithelium	Stroma	Endothelium
alpha-1(I) chain	X	X	X	alpha-2(I) chain	X	X	X
alpha-1(II) chain	X	X	X	alpha-2(IV) chain		X	X
alpha-1(III) chain	X	X	X	alpha-2(IX) chain		X	
alpha-1(IV) chain	X	X	X	alpha-2(V) chain	X	X	X
alpha-1(IX) chain			X	alpha-2(VI) chain	X	X	X
alpha-1(V) chain	X	X	X	alpha-2(VIII) chain		X	X
alpha-1(VI) chain	X	X	X	alpha-2(XI) chain		X	
alpha-1(VII) chain	X	X	X	alpha-3(IV) chain	X	X	X
alpha-1(VIII) chain		X	X	alpha-3(V) chain	X	X	
alpha-1(X) chain		X		alpha-3(VI) chain	X	X	X
alpha-1(XI) chain	X	X	X	alpha-4(IV) chain	X	X	X
alpha-1(XII) chain	X	X	X	alpha-5(IV) chain	X	X	X
alpha-1(XIV) chain	X	X	X	alpha-5(VI) chain		X	
alpha-1(XIX) chain			X	alpha-6(IV) chain	X		X
alpha-1(XVI) chain	X	X		Laminin subunit alpha-3	X		
alpha-1(XVII) chain	X	X		Laminin subunit alpha-5			X
alpha-1(XVIII) chain	X	X	X	Laminin subunit beta-1	X		X
alpha-1(XXI) chain		X		Laminin subunit beta-2			X
alpha-1(XXIII) chain		X		Laminin subunit beta-3	X	X	X
alpha-1(XXIV) chain		X	X	Laminin subunit gamma-1		X	X
alpha-1(XXVII) chain	X	X	X	Laminin subunit gamma-2	X	X	X
alpha-1(XXVIII) chain		X					

Many collagens and laminins may be detected in each LC-MS/MS analysis, sometimes even in small amounts. Proteomics may be a helpful tool in supplying additional evidence for the detection of proteins (or excluding presence thereof) when epitopes are masked or otherwise unavailable. Adapted from Dyrland TF, Poulsen ET, Scavenius C, et al. *J Proteome Res.* 2012; 11:4231–4239.

6.6 Detection of collagens in zonules by proteomics

Proteomic investigations of the human and bovine ciliary zonules failed to detect Col VII.^{39,40} Collagens were found, and represented a minor protein group in comparison to e.g. fibrillin-1. Within this minority, the collagens types II(α 1), XI(α 1), and V(α 2, α 3) were dominant.⁴⁰ These authors found purifying human zonules much more difficult than their bovine counterpart. Interestingly, a Col VII chain fragment with human homology (C9JBL3) was found in the bovine samples.⁴⁰

Despite the sensitivity of mass spectrometry, the proteins are severely disrupted in the process, by all kinds of buffers and enzymes, prior to being digested by trypsin. Then, the amino acid sequences that are detected by the mass spectrometer must be identified, and significantly match the matrixome database in order to count as 'hit'. It is possible that in these studies, Col VII is either not sufficiently extracted, or digested beyond recognition, or otherwise left undetectable because of its potential scarcity. Many enzyme treatments may be tried out in order to optimize the yield of a protein of interest, but trypsin is usually found to be the most effective.³⁹ Tissues may be subjected to collagenase treatment (prior to trypsin), with an unknown effect on Col VII detection. In order to prove any positive detection of a protein by LC-MS/MS, Western blot analysis is used as subsequent, supportive addition. As discussed earlier, most Western blots of intraocular tissues showed outcomes in agreement with IHC results.

6.7 Detection of retinal Col VII and its interacting proteins by proteomics

The proteome of collagens and laminins was also investigated in BMs of human retinas (ILM), retinal blood vessels and lens capsules (**Table 4**).⁵⁸ Empirically, the values in the table have shown linearity to absolute protein abundance ($r^2 > 0.9$). This means that Col VII protein is detected at these BMs, but in minute amounts compared to e.g. most type IV collagen isoforms. The retinal blood vessel lysates that have been processed for SDS-PAGE and LC-MS/MS, respectively, apparently have proteomically detectable amounts of Col VII.

6.8 Immunohistochemical exploration of blood vessels: an anchoring complex?

Immunohistochemically, Col VII and the laminin chains α 3 and β 3 (γ 2 was not done) were demonstrated at the colonic mucosa, but not at its blood vessels.⁵⁹ Short segments of Col VII labeling were demonstrated between the corneal/limbal BM and the underlying blood vessels, a pattern that corresponded to 'accumulations of BM-like material with pockets of anchoring fibrils embedded in the thickened BM'.⁶⁰ Such BM thickening and/or duplication is often seen at the BM zones of older donors.

Alternatively, the authors suggest that the limbal basal cells sporadically synthesize Col VII and other BM components, leaving isolated islands of BM in the stroma.⁶⁰ Otherwise, it is commonly accepted that the BMs of blood vessels do not display all of the dermal anchoring complex components.

TABLE 4. Relative quantitative levels of proteins were determined using intensity-based absolute quantitation (iBAQ) algorithm.

Gene Names	iBAQ BV1			iBAQ ILM			iBAQ LC1		
	1	2	3	1	2	3	1	2	3
COL1A1	7	43	465	0	23	0	0	94	0
COL1A2	9	101	927	0	5	0	0	494	0
COL3A1	7	32	154	0	0	0	0	11	1
COL4A1	8544	251730	26039	1199	2984	145	99742	63017	63419
COL4A2	6930	299880	31421	958	2464	33	83136	49682	71461
COL4A3	472	38853	7213	26079	62460	21192	9228	11073	14160
COL4A4	240	10763	2154	16183	25476	7096	4125	3717	4148
COL4A5	401	23793	1459	9958	28477	4205	8725	5666	8575
COL4A6	0	11478	0	11	0	0	2459	0	1104
COL5A1	1.8	765	35	54	83	2	553	96	245
COL5A2	3,9	446	57	10	4	0	239	26	154
COL5A3	0	10	1	0	0	0	0	5	0
COL7A1	0	1	1	24	3	4	3	2	0
LAMA;LAMA1	1.6	82	4	143	641	192	1	89	0
LAMA2;LAMM	134	12	140	180	202	46	0	1015	0
LAMA3;LAMNA	4.0	5	35	0	0	0	0	65	0
LAMA4	57	81	194	5	0	5	0	164	3
LAMA5	2068	36274	16871	8213	14455	7251	5449	33611	9109
LAMB1	51	2217	13	2	0	637	1519	204	212
LAMB2;LAMC1	4321	28450	16632	21802	20543	7030	11037	48156	4690
LAMB2;LAMS	4536	44636	30983	27566	31938	14471	9496	40507	9081

The iBAQ values are obtained from the LC-MS data by averaging (*) the signal intensity of the detected ions for a given protein by the number of theoretically detectable ions for that protein. (1,2,3) lists the matrisomal proteins identified with their iBAQ values for each of the nine BM samples. *Adapted from Ref 58.* Values were divided by 1.000 and rounded off for convenience.

7.0 TRANSLATION OF INTRAOCULAR COL VII DETECTION: CLINICAL IMPLICATIONS

In our studies, we have demonstrated Col VII protein at various locations. Because anchoring fibrils are apparently absent, and even the intermolecular components needed for an anchoring complex such as in skin are inconsistently reported, it remains unclear whether the presence of Col VII at the determined localizations might perform (or contribute to) an anchoring role. The logical way to deduce such a function would be to investigate any occurring defects when Col VII is dysfunctional or absent. Such functional absence occurs in patients suffering from severe recessive dystrophic epidermolysis bullosa. Therefore, we sought to investigate this patient group for defects, with special interest in the previously determined Col VII-positive locations. Interestingly, the RDEB donor eyes did not show any convincing intraocular defects by (immuno)histochemical analysis. Also, the clinically investigated RDEB-patients were found to have no apparent irregularities in their intraocular anatomy. The lack of apparent irregularities might be explained by several hypotheses.

1.) Other proteins may compensate for the dysfunctional Col VII, even in the total absence of Col VII. Theoretically, that would mean that other intramolecular bonds successfully maintain tissue integrity. Such is the case in laminin-332 deficiency: although the absence of laminin-332 in skin is lethal, other tissues/organs appear not to be significantly affected. This phenomenon suggests a compensation rescue by other laminins.^{48, 61} Another example is Col IV(α 5)-chain deficiency (Alport syndrome), where the ECM is significantly altered, but the deficiency is thought to be functionally balanced by increased synthesis and deposition of Col VII.⁶²

2.) Col VII might not play any significant anchoring role in intraocular tissues. In turn, this suggests that Col VII may perform some other role, since nature would not deposit Col VII there for naught. Recently, it was suggested that Col VII is a member of a unique innate immune-supporting multi-protein complex against bacterial colonization in the spleen and lymph nodes. Col VII would specifically bind and sequester the innate immune activator cochlin in the lumen of lymphoid conduits, enabling the activation of innate immune cells in the skin. That study also showed that Col VII is expressed by lymphoid stromal cells.⁶³ The presence of Col VII around intraocular blood vessels might therefore indicate an unknown, but comparable, purpose. However, no clear signs of intraocular inflammation were observed in the RDEB donor sections.

Another role of intraocular Col VII might be found in its potential ECM manipulation and cell signaling pathways, which is currently investigated in squamous cell carcinogenesis. The role of Col VII in this process is, however, context and tissue dependent since Col VII appears to be upregulated in some tumour types and downregulated in others. Furthermore, it is believed that Col VII supplementation would increase the migration and invasion of carcinogenic keratinocytes in culture⁶⁴ (and thus be pro-carcinogenic) while, in contrast, Col VII suppresses TGF- β signaling and angiogenesis through binding of $\alpha 2$ integrin⁶⁵ (and thus be anti-carcinogenic). When squamous cells lose their differentiation (i.e. become malignant), their deposition of Col VII deteriorates first, only after which Col IV deterioration follows. The poorly differentiated cells may then still synthesize Col VII, but are unable to deposit it extracellularly, and metastasis is at hand.⁶⁶ To date, the importance of basement membranes and the role of their components in angiogenesis and tumor invasion to metastasis are well known,⁶⁷ but any such role of Col VII at intraocular or vascular basement membranes is yet to be determined.

3.) Perhaps the friction in the eye is unlike that of skin. In skin, the amount of friction is believed to influence the expression of Col VII, if such a linear deduction may be made from the amount of anchoring fibrils observed. Mechanobullous defects in RDEB patients occur especially by friction exerted perpendicular to the skin (i.e. shear stress by rubbing), in contrast to compressional/tensional stress (i.e. skin impression). In RDEB, ocular surface defects are thought to -at least partially- result from repeated abrasions after friction or minor trauma, generally paralleling the extent of the skin affection. In comparison to older literature, the corneas of our RDEB cohort and recent literature appear to be spared, relative to their skin.⁶⁸ Of course, corneas are subjugated to less mechanical stress than skin in general, but a relation to improved (availability of) lubricants that wet and minimize the repeated surface friction may also be made. The forces at the accommodation system are exerted in a moist environment, and probably predominantly consist of tension -and to a lesser extent compression- forces. A deficiency in Col VII might therefore not result in destabilized tissues.

4.) Col VII may be a representational late, non-functional marker of sclerosis, hyalinization, or even fibrosis. In renal tissues, for example, Col VII is not considered to be a normal component of glomeruli. It is expressed only in obvious glomerular scar formation or sclerosis. Then, its incorporation into anchoring fibrils proves a prerequisite to restore and maintain the stability and integrity of the BM zone, which is instrumental in healing.^{69, 70} Hyaline degeneration might partially account for the thickness of the

BM-like depositions, i.e. at the ciliary body blood vessels that broadly labeled for Col VII. Most of our donors were over 50 years of age. However, young donors demonstrated a similar intraocular and perivascular Col VII immunoreactivity.

8.0 FUTURE AIMS

Given the specific immunoreactivity of anti-Col VII labeling in intraocular tissues, in absence of typical anchoring fibrils, it would be tempting to speculate that any anchoring fibrils there are too thin to be detected. In turn, that would mean that either the molecular structure of intraocular Col VII is different from that of skin, so that lateral aggregation does not occur, or that some other components that are needed for such aggregation are not available in the eye. Alternatively, we might have detected only parts of the Col VII molecule, and no anchoring fibrils (of any form) are present. This would suggest an alternative function of Col VII that is yet to be determined.

An unexplained relation exists between RDEB patients and concurrent cardio(vascular) defects, as was discovered in our RDEB donor, as well as in others.⁷¹ It is strange that the two rare clinical entities of RDEB and non-ischemic cardiomyopathy occur simultaneously. Up to 18% of patients with RDEB, shows evidence for a dilated aortic root. Although their association has been appreciated for at least 25 years, a common pathological mechanism has not yet emerged.^{71,72} It was suggested that even if Col VII was shown to have no direct role in the heart at all, its presence might still serve as a major modifier of factors that regulate cardiovascular remodeling and function.⁷¹ Therefore, further investigations towards ECM modulation, cell signaling, and/or other potential bioactive functions of Col VII and its NC-1 domain could elucidate more of its anchoring and non-anchoring functions.

Therapeutic options for the management of RDEB have been reviewed recently but will not be discussed here, since they do not concern the intraocular environment.⁷³

REFERENCES

1. Ponsioen TL, van Luyn MJ, van der Worp RJ, Pas HH, Hooymans JM, Los LI. Human retinal Müller cells synthesize collagens of the vitreous and vitreoretinal interface in vitro. *Mol Vis.* 2008; 14:652-660.
2. Hirano S, Yonezawa T, Hasegawa H, Hattori S, Greenhill NS, Davis PF, et al. Astrocytes express type VIII collagen during the repair process of brain cold injury. *Biochem Biophys Res Commun.* 2004; 317:437-443.
3. Alitalo K, Bornstein P, Vaheri A, Sage H. Biosynthesis of an unusual collagen type by human astrocytoma cells in vitro. *J Biol Chem.* 1983; 258:2653-2661.
4. Wang DD, Bordey A. The astrocyte odyssey. *Prog Neurobiol.* 2008; 86:342-367.
5. Qu J, Wang D, Grosskreutz CL. Mechanisms of retinal ganglion cell injury and defense in glaucoma. *Exp Eye Res.* 2010; 91:48-53.
6. Ramirez JM, Triviño A, Ramirez AI, Salazar JJ, Garcia-Sanchez J. Immunohistochemical study of human retinal astroglia. *Vision Res.* 1994; 34:1935-1946.
7. Meng H, Zhang X, Blaivas M, Wang MM. Localization of blood proteins thrombospondin1 and ADAMTS13 to cerebral corpora amylacea. *Neuropathology.* 2009; 29:664-671.
8. Hogan MJ, Alverado JA, Wedell JE. *Histology of the Human Eye: An Atlas and Textbook.* 1st ed. Philadelphia, Saunders; 1971:260-319.
9. Tidman MJ, Eady RA. Ultrastructural morphometry of normal human dermal-epidermal junction. The influence of age, sex, and body region on laminar and nonlaminar components. *J Invest Dermatol.* 1984; 83:448-453.
10. Gipson IK, Spurr-Michaud SJ, Tisdale AS. Anchoring fibrils form a complex network in human and rabbit cornea. *Invest Ophthalmol Vis Sci.* 1987; 28:212-220.
11. Gipson IK, Spurr-Michaud S, Tisdale A, Keough M. Reassembly of the anchoring structures of the corneal epithelium during wound repair in the rabbit. *Invest Ophthalmol Vis Sci.* 1989; 30:425-434.
12. Binder PS, Rock ME, Schmidt KC, Anderson JA. High-voltage electron microscopy of normal human cornea. *Invest Ophthalmol Vis Sci.* 1991; 32:2234-2243.
13. Alvarado J, Murphy C, Juster R. Age-related changes in the basement membrane of the human corneal epithelium. *Invest Ophthalmol Vis Sci.* 1983; 24:1015-1028.
14. Tisdale AS, Spurr-Michaud SJ, Rodrigues M, Hackett J, Krachmer J, Gipson IK. Development of the anchoring structures of the epithelium in rabbit and human fetal corneas. *Invest Ophthalmol Vis Sci.* 1988; 29:727-736.
15. Visser R. *Basement membrane antigens in preneoplastic and neoplastic conditions (thesis).* Maastricht, Universitaire Pers Maastricht; 1993: 81-84.
16. Chung HJ, Uitto J. Type VII collagen: the anchoring fibril protein at fault in dystrophic epidermolysis bullosa. *Dermatol Clin.* 2010; 28:93-105.
17. Zaferani A, Talsma DT, Yazdani S, Celie JW, Aikio M, Heljasvaara R, et al. Basement membrane zone collagens XV and XVIII/proteoglycans mediate leukocyte influx in renal ischemia/reperfusion. *PLoS One.* 2014; 9:e106732.
18. Mutolo MJ, Morris KJ, Leir SH, Caffrey TC, Lewandowska MA, Hollingsworth MA, et al. Tumor suppression by collagen XV is independent of the restin domain. *Matrix Biol.* 2012; 31:285-289.

19. Baker M. Antibody anarchy: A call to order. *Nature*. 2015; 527:545-551.
20. Bradbury A, Plückerthun A. Reproducibility: Standardize antibodies used in research. *Nature*. 2015; 518:27-29.
21. Wenzel D, Bayerl J, Nyström A, Bruckner-Tuderman L, Meixner A, Penninger JM. Genetically corrected iPSCs as cell therapy for recessive dystrophic epidermolysis bullosa. *Sci Transl Med*. 2014; 6:264ra165.
22. Nyström A, Velati D, Mittapalli VR, Fritsch A, Kern JS, Bruckner-Tuderman L. Collagen VII plays a dual role in wound healing. *J Clin Invest*. 2013; 123:3498-3509.
23. Nyström A, Buttgereit J, Bader M, Shmidt T, Ozcelik C, Hausser I, et al. Rat model for dominant dystrophic epidermolysis bullosa: glycine substitution reduces collagen VII stability and shows gene-dosage effect. *PLoS One*. 2013; 8:e64243.
24. Kühn T, Mezger M, Hausser I, Guey LT, Handgretinger R, Bruckner-Tuderman L, et al. Collagen VII half-life at the dermal-epidermal junction zone: implications for mechanisms and therapy of genodermatoses. *J Invest Dermatol*. 2016; 136:1116-1123.
25. Kretz M, Siprashvili Z, Chu C, Webster DE, Zehnder A, Qu K, et al. Control of somatic tissue differentiation by the long non-coding RNA TINCR. *Nature*. 2013; 493:231-235.
26. Elfert SC. *Correlation between triple helix stability of collagen VII and skin fragility in dystrophic epidermolysis bullosa (thesis)*. Freiburg (im Breisgau), University of Freiburg; 2009; 1-96.
27. Breitenbach JS, Rinnerthaler M, Trost A, Weber M, Klausegger A, Gruber C, et al. Transcriptome and ultrastructural changes in dystrophic epidermolysis bullosa resemble skin aging. *Aging (Albany NY)*. 2015; 7:389-411.
28. Villone D, Fritsch A, Koch M, Bruckner-Tuderman L, Hansen U, Bruckner P. Supramolecular interactions in the dermo-epidermal junction zone: anchoring fibril-collagen VII tightly binds to banded collagen fibrils. *J Biol Chem*. 2008; 283:24506-24513.
29. Titeux M, Pendaries V, Zanta-Boussif MA, Décha A, Pironon N, Tonasso L, et al. SIN retroviral vectors expressing COL7A1 under human promoters for ex vivo gene therapy of recessive dystrophic epidermolysis bullosa. *Mol Ther*. 2010; 18:1509-1518.
30. Kern JS, Loeckermann S, Fritsch A, Hausser I, Roth W, Magin TM, et al. Mechanisms of fibroblast cell therapy for dystrophic epidermolysis bullosa: high stability of collagen VII favors long-term skin integrity. *Mol Ther*. 2009; 17:1605-1615.
31. Naylor EC, Watson RE, Sherratt MJ. Molecular aspects of skin ageing. *Maturitas*. 2011; 69:249-256.
- 32.) Halabi CM, Mecham RP. Elastin purification and solubilization. *Methods Cell Biol*. 2018; 143:207-222.
33. Hayakawa T, Hirako Y, Teye K, Tsuchisaka A, Koga H, Ishii N, et al. Unique mouse monoclonal antibodies reactive with maturation-related epitopes on type VII collagen. *Exp Dermatol*. 2017; 26:811-819.
- 34.) Chen K, Weiland JD. Discovery of retinal elastin and its possible role in age-related macular degeneration. *Ann Biomed Eng*. 2014; 42:678-84.
35. Wagenseil JE, Mecham RP. Vascular extracellular matrix and arterial mechanics. *Physiol Rev*. 2009; 89:957-989.
36. Jackson DS, Cleary EG. The determination of collagen and elastin. *Methods Biochem Anal*. 1967; 15:25-76.
37. Mecham R, Davis E. Extracellular matrix assembly and structure. In: Yurchenco P, Birk D, and Mecham R, eds. *Elastic fiber structure and assembly*, New York, Academic Press; 1994:281-314.

- 38.** Jensen SA, Handford PA. New insights into the structure, assembly and biological roles of 10-12 nm connective tissue microfibrils from fibrillin-1 studies. *Biochem J.* 2016; 473:827-838.
- 39.** Cain SA, Morgan A, Sherratt MJ, Ball SG, Shuttleworth CA, Kiely CM. Proteomic analysis of fibrillin-rich microfibrils. *Proteomics.* 2006; 6:111-122.
- 40.** De Maria A, Wilmarth PA, David LL, Bassnett S. Proteomic Analysis of the Bovine and Human Ciliary Zonule. *Invest Ophthalmol Vis Sci.* 2017; 58:573-585.
- 41.** Chen M, Marinkovich MP, Veis A, Cai X, Rao CN, O'Toole EA, et al. Interactions of the amino-terminal noncollagenous (NC1) domain of type VII collagen with extracellular matrix components. A potential role in epidermal-dermal adherence in human skin. *J Biol Chem.* 1997; 272:14516-15422.
- 42.** Lapiere JC, Chen JD, Iwasaki T, Hu L, Uitto J, Woodley DT. Type VII collagen specifically binds fibronectin via a unique subdomain within the collagenous triple helix. *J Invest Dermatol.* 1994; 103:637-641.
- 43.** Burgeson RE, Lunstrum GP, Rokosova B, Rimberg CS, Rosenbaum LM, Keene DR. The structure and function of type VII collagen. *Ann NY Acad Sci.* 1990; 580:32-43.
- 44.** Chen M, Marinkovich MP, Jones JC, O'Toole EA, Li YY, Woodley DT. NC1 domain of type VII collagen binds to the beta3 chain of laminin 5 via a unique subdomain within the fibronectin-like repeats. *J Invest Dermatol.* 1999; 112:177-183.
- 45.** Janssen SF, Gorgels TG, Bossers K, Ten Brink JB, Essing AH, Nagtegaal M, et al. Gene expression and functional annotation of the human ciliary body epithelia. *PLoS One.* 2012; 7:e44973.
- 46.** Tuori A, Uusitalo H, Burgeson RE, Terttunen J, Virtanen I. The immunohistochemical composition of the human corneal basement membrane. *Cornea.* 1996; 15:286-294.
- 47.** Aisenbrey S, Zhang M, Bacher D, Yee J, Brunken WJ, Hunter DD. Retinal pigment epithelial cells synthesize laminins, including laminin 5, and adhere to them through alpha3- and alpha6-containing integrins. *Invest Ophthalmol Vis Sci.* 2006; 47:5537-5544.
- 48.** Wazen RM, Viegas-Costa LC, Fouillen A, Moffatt P, Adair-Kirk TL, Senior RM, et al. Laminin γ 2 knockout mice rescued with the human protein exhibit enamel maturation defects. *Matrix Biol.* 2016; 52-54:207-218.
- 49.** Cleutjens JP, Havenith MG, Kasper M, Vallinga M, Bosman FT. Absence of type IV collagen in the centre of the corneal epithelial basement membrane. *Histochem J.* 1990; 22:688-694.
- 50.** Ishizaki M, Westerhausen-Larson A, Kino J, Hayashi T, Kao WW. Distribution of collagen IV in human ocular tissues. *Invest Ophthalmol Vis Sci.* 1993; 34:2680-2689.
- 51.** Kabosova A, Azar DT, Bannikov GA, Campbell KP, Durbeej M, Ghohestani RF. Compositional differences between infant and adult human corneal basement membranes. *Invest Ophthalmol Vis Sci.* 2007; 48:4989-4999.
- 52.** Ljubimov AV, Burgeson RE, Butkowsky RJ, Michael AF, Sun TT, Kenney MC. Human corneal basement membrane heterogeneity: topographical differences in the expression of type IV collagen and laminin isoforms. *Lab Invest.* 1995; 72:461-473.
- 53.** Merjava S, Liskova P, Sado Y, Davis PF, Greenhill NS, Jirsova K. Changes in the localization of collagens IV and VIII in corneas obtained from patients with posterior polymorphous corneal dystrophy. *Exp Eye Res.* 2009; 88:945-952.
- 54.** Saika S, Kawashima Y, Miyamoto T, Okada Y, Tanaka SI, Ohmi S, et al. Immunolocalization of prolyl 4-hydroxylase subunits, alpha-smooth muscle actin, and extracellular matrix components in human lens capsules with lens implants. *Exp Eye Res.* 1998; 66:283-294.

55. Wistow G, Bernstein SL, Wyatt MK, Behal A, Touchman JW, Bouffard G, et al. Expressed sequence tag analysis of adult human lens for the NEI/Bank Project: over 2000 non-redundant transcripts, novel genes and splice variants. *Mol Vis.* 2002; 8:171-184.
56. Dyrlund TF, Poulsen ET, Scavenius C, Nikolajsen CL, Thøgersen IB, Vorum H, et al. Human cornea proteome: identification and quantitation of the proteins of the three main layers including epithelium, stroma, and endothelium. *J Proteome Res.* 2012; 11:4231-4239.
57. Poulsen ET, Runager K, Risør MW, Dyrlund TF, Scavenius C, Karring H, Praetorius J. Comparison of two phenotypically distinct lattice corneal dystrophies caused by mutations in the transforming growth factor beta induced (TGFB1) gene. *Proteomics Clin Appl.* 2014; 8:168-177.
58. Uechi G, Sun Z, Schreiber EM, Halfter W, Balasubramani M. Proteomic view of basement membranes from human retinal blood vessels, inner limiting membranes, and lens capsules. *J Proteome Res.* 2014;13:3693-3705.
59. Lohi J, Leivo I, Tani T, Kiviluoto T, Kivilaakso E, Burgeson RE, et al. Laminins, tenascin and type VII collagen in colorectal mucosa. *Histochem J.* 1996; 28:431-440.
60. Gipson IK. The epithelial basement membrane zone of the limbus. *Eye (Lond).* 1989; 3:132-140.
61. Adair-Kirk TL, Griffin GL, Meyer MJ, Kelley DG, Miner JH, Keene DR, et al. Keratinocyte-targeted expression of human laminin $\gamma 2$ rescues skin blistering and early lethality of laminin $\gamma 2$ deficient mice. *PLoS One.* 2012; 7:e45546.
62. Giannakakis K, Massella L, Grassetti D, Dotta F, Perez M, Muda AO. Type VII collagen in Alport syndrome. *Nephrol Dial Transplant.* 2007; 22:3501-3507.
63. Nyström A, Bruckner-Tuderman L. Injury- and inflammation-driven skin fibrosis: The paradigm of epidermolysis bullosa. *Matrix Biol.* 2018; 68-69:547-560.
64. Pourreyron C, Chen M, McGrath JA, Salas-Alanis JC, South AP, Leigh IM. High levels of type VII collagen expression in recessive dystrophic epidermolysis bullosa cutaneous squamous cell carcinoma keratinocytes increases PI3K and MAPK signalling, cell migration and invasion. *Br J Dermatol.* 2014; 170:1256-1265.
65. Martins VL, Caley MP, Moore K, Szentpetery Z, Marsh ST, Murrell DF, et al. Suppression of TGF β and Angiogenesis by Type VII Collagen in Cutaneous SCC. *J Natl Cancer Inst.* 2015; 108:djv293.
66. Visser R. *Basement membrane antigens in preneoplastic and neoplastic conditions (thesis).* Maastricht, Universitaire Pers Maastricht; 1993: 57-67.
67. Sherwood DR. Cell invasion through basement membranes: an anchor of understanding. *Trends Cell Biol.* 2006; 16:250-256.
68. Jones SM, Smith KA, Jain M, Mellerio JE, Martinez A, Nischal KK. The Frequency of Signs of Meibomian Gland Dysfunction in Children with Epidermolysis Bullosa. *Ophthalmology.* 2016; 123:991-999.
69. Onetti Muda A, Ruzzi L, Bernardini S, Teti A, Faraggiana T. Collagen VII expression in glomerular sclerosis. *J Pathol.* 2001; 195:383-390.
70. Hopkinson I, Anglin IE, Evans DL, Harding KG. Collagen VII expression in human chronic wounds and scars. *J Pathol.* 1997; 182:192-196.
71. Ryan TD, Ware SM, Lucky AW, Towbin JA, Jefferies JL, Hinton RB. Left ventricular noncompaction cardiomyopathy and aortopathy in a patient with recessive dystrophic epidermolysis bullosa. *Circ Heart Fail.* 2012; 5:e81-82.

72. Ryan TD, Lucky AW, King EC, Huang G, Towbin JA, Jefferies JL. Ventricular dysfunction and aortic dilation in patients with recessive dystrophic epidermolysis bullosa. *Br J Dermatol*. 2016; 174:671-673.

73. Rashidghamat E, McGrath JA. Novel and emerging therapies in the treatment of recessive dystrophic epidermolysis bullosa. *Intractable Rare Dis Res*. 2017; 6:6-20.



7

Chapter 7

Summary

Chapter 1 (General introduction) describes the aims and outline of this thesis.

This thesis characterizes Col VII in the intraocular environment, by immunohistochemical, -fluorescence, -blotting and -electron microscopy. Collagen type VII (Col VII) is an anchoring protein, which is typically reserved for securing dermal and mucosal epithelial basement membranes to their underlying stroma. The anchoring function is achieved by anchoring fibrils, which are lateral aggregates of Col VII molecules. These fibrils loop from and to the basement membrane, hereby entrapping stromal fibers. Non-looping anchoring fibrils have also been observed, which are thought to bind directly to the stromal fibrils. Recently, expression of Col VII was discovered in the retina, although it is unclear whether Col VII also functions as an anchoring protein here. The main goal is to elucidate more of the characteristics of intraocular Col VII, and possibly deduce its function in the intraocular milieu.

Chapter 2 describes the investigation of Col VII at the vitreoretinal interface. Previously, Col VII was observed in structures at the superficial layers of the retina, as well as in Müller cell cultures. The retinal structures exist in two variants: within corpora amylacea and in small clustered vesicles. Both variants occur mainly in the ganglion cell layer and the inner plexiform layer. Because the corpora amylacea have an astrocytic origin, and the vesicles colocalized with the glial cell markers, we associate astrocytes with the synthesis and storage of retinal Col VII. Electron microscopic analysis shows the presence of Col VII epitopes at the inner limiting membrane, which was validated by Western blots. Col VII was thus found at the transition between epithelia and mesenchyme, as is common in skin. Anchoring fibrils, however, are not observed, so an anchoring function could not be dedicated to the Col VII presence.

Chapter 3 addresses the presence of Col VII in the tissues of the accommodation system. In skin, the number of anchoring fibrils present varies per skin region, and is essentially related to the amount of mechanical stress that a region copes with. More mechanical stress means more anchoring fibrils. Since Col VII is the major component of anchoring fibrils, any intraocular Col VII expression (apart from the retina) would most likely be present at mechanically stressed tissues. The accommodation system is subject to such mechanical stress, and was therefore explored for Col VII presence by several immunohistochemical techniques. Col VII was demonstrated at the basement membranes of the ciliary body epithelia and at adjacent blood vessels, the ciliary zonules and the lens capsule. Although Col VII was observed at structures that would theoretically benefit from the support of anchoring fibrils, no actual anchoring fibrils were observed. This chapter also describes the validation of our main antibody.

Chapter 4 further explores the distribution and characteristics of the Col VII that was observed at intraocular blood vessels. Retinal and uveal samples are analyzed and compared to extraocular blood vessels using several immunohistochemical techniques. Col VII is observed at the blood vessels of most of these tissues, except those in skin. Retinal whole mount immunofluorescence double labeling suggests that the perivascular Col VII distribution is associated with pericytes.

Chapter 5 reports on potential intraocular defects that may be found in Col VII deficient patients, hereby reviewing the available literature. The regions in which Col VII was previously observed are investigated clinically (n=4 patients) and immunohistochemically (n=1 donor). No apparent defects were noted that could be related to Col VII deficiency. Recurrent ocular surface defects contribute to scar formation, which leads to patient multifocality and -subsequently- hinders diagnostics by automated imaging systems.

Chapter 6 (General discussion) reviews our obtained data in the light of relevant literature. Our main antibody pAb(16) is reviewed, its potential cross-reactivity ruled out, and its validity confirmed. At various intraocular tissues (BM of pigmented epithelium, retinal blood vessels, inner limiting membrane, lens capsule) our Col VII labeling has shown some resemblance to that of skin: a linear labeling pattern. In other intraocular tissues (zonules, intraretinal deposits, tissue around ciliary blood vessels), the labeling was consistently non-linear, namely vesicular or diffuse. An additional disparity to skin is that anchoring fibrils were not detected in any intraocular tissue. Other investigators have reported that anchoring fibrils (especially the non-looped variant) may not easily be detected in general, but we hypothesize that the impeded visualization might also be explained by their restraint to laterally aggregate. As anchoring fibrils appear to be absent despite our validated Col VII immunolocalization, alternative explanations for the observed Col VII presence are discussed. The absence of intraocular defects in Col VII-deficient patients could be explained by a compensatory role of Col VII-supporting proteins, and the absence of anchoring fibrils either by an immune-supporting role of Col VII, a biological signaling modality of Col VII in angiogenesis/tumorigenesis, or a role of Col VII as a marker of sclerosis.



8

Chapter 8

Samenvatting (Nederlands)

Hoofdstuk 1 (algemene introductie) beschrijft de rationale achter dit proefschrift.

Dit proefschrift probeert de eigenschappen van Col VII, zoals het in het intraoculaire milieu voorkomt, verder in kaart te brengen met behulp van immunohistochemie, -fluorescentie, -blotting en -electron microscopie. Collageen type VII (Col VII) is een ankerewit, dat normaliter de basaalmembranen van dermale weefsels vasthecht aan de stromale onderlaag. Deze verankering komt tot stand door ankerfibrillen. Dit zijn structuren die ontstaan door laterale aggregatie van de Col VII moleculen, waarbij beide uiteinden van de aggregaten vastgrijpen in de bovenliggende basaalmembraan. De lussen die zo ontstaan 'vangen' stromale vezels, waardoor het epitheliale basaalmembraan aan het stroma wordt vastgehecht. Er bestaan ook directe verbindingen tussen ankerfibrillen en de stromale vezels, die bijdragen aan het vasthechten. Recent onderzoek wees uit dat de retina Col VII tot expressie brengt. Het is alleen onduidelijk of Col VII ankerfibrillen vormt in het intraoculaire milieu, of anderszins een hechtende functie heeft. Het voornaamste doel is om meer eigenschappen van intraoculair Col VII te achterhalen, en -indien mogelijk- een uitspraak te kunnen doen over de functie van Col VII in het intraoculaire milieu.

Hoofdstuk 2 beschrijft het onderzoek naar Col VII op de grenslaag van retina naar glasvocht. Eerdere onderzoeken van onze groep hebben aangetoond dat Col VII in bepaalde structuren in de oppervlakkige lagen van de retina voorkomt, als ook in retinale Müller celculturen. De retinale structuren lijken in twee verschillende varianten voor te komen, namelijk als corpora amylacea en als kleine, geclusterde vesikels. Beide varianten komen vooral voor in de ganglioncellaag, en in de binnenste plexiforme laag daaronder. Omdat corpora amylacea een astrocytaire oorsprong hebben, en ook de vesikels aankleuren met antilichamen tegen astrocyten, associëren we dit celtype met het produceren en opslaan van het retinale Col VII. Met elektronenmicroscopie tonen we aan dat Col VII in kleine hoeveelheden aanwezig is onder het basaalmembraan van de vitreoretinale grenslaag. Deze bevindingen werden gevalideerd door middel van Western blots. In de huid wordt Col VII normaliter ook op een dergelijke overgang van epitheel naar mesenchym gevonden. Onze bevindingen komen in die zin overeen met de literatuur. Ankerfibrillen werden echter niet gezien, dus kon er geen vasthechtende functie aan het Col VII worden toegekend.

Hoofdstuk 3 behandelt de aanwezigheid van Col VII in de weefsels van het accommodatiesysteem. In de huid lijkt het aantal ankerfibrillen per lichaamsregio te verschillen. Hun aantallen hangen samen met de hoeveelheid mechanische belasting die een lichaamsregio van buitenaf ontvangt. Hoe meer een regio belast wordt, hoe meer ankerfibrillen er aanwezig zijn om die belasting te verwerken. Omdat Col VII het

hoofdbestandsdeel is van de ankerfibrillen, verwachtten we dat áls Col VII voorkomt in intraoculaire weefsels (buiten de retina), dat hoogstwaarschijnlijk zal zijn in weefsels die mechanisch worden belast. De aanwezigheid van Col VII werd daarom onderzocht in het accommodatiesysteem, met behulp van verscheidene immunohistochemische technieken. Col VII werd aangetoond in de epitheliale basaalmembranen van het corpus ciliaire, rondom bloedvaten, in de zonula en in het lenskapsel. Maar, alhoewel deze structuren theoretisch baat zouden hebben bij ondersteuning van ankerfibrillen, werd Col VII niet gezien in deze typische conformatie. Dit hoofdstuk beschrijft ook de validatie van het voornaamste antilichaam uit onze studies.

Hoofdstuk 4 gaat verder in op de verdeling en eigenschappen van Col VII, dat eerder werd gezien bij intraoculaire bloedvaten. Retinale en uveale weefsels worden nu onderzocht en vergeleken met extraoculaire bloedvaten, middels verschillende immunohistochemische technieken. Col VII wordt aangetoond in de bloedvaten van de meeste van deze weefsels, behalve in die van de huid. Retina's werden in hun volledige dikte onderzocht middels immunofluorescentie microscopie met dubbel-labeling. Hieruit blijkt dat retinale pericyten mogelijk betrokken zijn bij de aanwezigheid van het perivasculaire Col VII.

Hoofdstuk 5 beschrijft het onderzoek naar eventuele intraoculaire afwijkingen in Col VII deficiënte patiënten, waarbij ook de beschikbare literatuur wordt betrokken. De locaties waarin Col VII eerder werd gevonden worden verder onderzocht; klinisch in een viertal Col VII deficiënte patiënten, en immunohistochemisch in één donorpatiënt. Er worden geen belangrijke intraoculaire afwijkingen gevonden. De littekenvorming die in deze groep patiënten de uitwendige weefsels van het oog aantast, blijkt voor (refractieve) multifocaliteit te zorgen, waardoor de metingen door geautomatiseerde diagnostische apparatuur niet betrouwbaar zijn.

Hoofdstuk 6 (Algemene discussie) vergelijkt onze bevindingen met de bestaande literatuur. Ons belangrijkste antilichaam ondergaat een verdere kritische beoordeling, betreffende de kans op eventuele vals-positieve aankleuringen en betrouwbaarheid. In ogenschouw blijken verscheidene intraoculaire weefsels (zoals het basaalmembraan van het gepigmenteerde ciliaire epitheel, retinale bloedvaten en het vitreoretinale basaalmembraan) doorgaans aan te kleuren volgens het bekende dermale patroon: lineair. Andere weefsels (zoals zonula, de intraretinale structuurtjes, en het gebied rondom ciliaire bloedvaten) kleuren niet volgens dit patroon aan, maar als vesikels of diffuus. De intraoculaire omstandigheden lijken verder te verschillen van die in de huid, omdat er geen ankerfibrillen worden gezien. Andere onderzoekers beschreven al dat ankerfibrillen in het algemeen moeilijk waar te nemen kunnen zijn; daarnaast

veronderstellen wij ook dat de ankerfibrillen niet goed zichtbaar zijn omdat zij wellicht niet lateraal aggregeren. Indien zou blijken dat er -ondanks de aanwezigheid van Col VII- daadwerkelijk geen ankerfibrillen aanwezig zijn (terecht-negatief), worden de mogelijke verklaringen daarvoor (uit de literatuur) besproken. Zo zou de afwezigheid van intraoculaire afwijkingen in Col VII deficiënte patiënten verklaard kunnen worden met een functionele compensatie door Col VII-ondersteunende eiwitten, en de afwezige ankerfibrillen door een immunologische-gemedieerde functie van Col VII, een biologische signaalfunctie in angiogenese of tumorgenese, of als een bijkomende factor in sclerose.

DANKWOORD

Vooraf aan de te volgen betuiging van lof wens ik de rationale achter dit boek uit de doeken te doen.

In mijn derde jaar geneeskunde werd ik benaderd door Dirk Ponsioen. Hij en zijn onderzoeksgroep zochten een gemotiveerde 4e jaar geneeskundestudent die kon helpen met het oplossen van wat vraagstukken die waarschijnlijk zouden blijven liggen als hij zijn eigen promotie had afgerond. Ik was nog geen 4^e jaars, maar kennelijk enthousiast genoeg. Mijn vader, als eerste academicus van zijn familie, was ook gepromoveerd en had daar als medicus nooit spijt van gehad. Als kind was ik altijd al geïnteresseerd in experimenten (badproducten mengen in bad om te kijken wat er gebeurde, de eerste scheikunde-experimenten kit, de biologie in de achtertuin). Daarnaast vond ik klussen, repareren en ontwerpen (elektra, hout, hutten) ook geweldig. Het doen van een wet-lab onderzoek, zoals die nu afgerond is, bleek een goede mengvorm van beide. Tijdens een cursus Loopbaantraining in 2016, die als onderdeel van de persoonlijke verrijking werd aangeboden als promovendus aan de RuG, werd onderzocht hoe tevreden de deelnemers waren over hun huidige baan, aan de hand van verschillende vragen en determinanten. Er werd onderstreept hoezeer het werken, aan het project dat voor u ligt, mij aansprak. Ik zou niet kunnen zeggen hoeveel dagen 'werk' er in dit project is gestoken. Ik weet ook niet of ik hetzelfde pad had bewandeld als ik a priori had geweten hoeveel tijd het gekost zou hebben, maar ik heb er achteraf geen spijt van. Waarschijnlijk kan dat verklaard worden omdat ik dit project ook zie als een stukje levensvulling, in de zin dat het een microscopisch stukje bijdraagt aan het vooruithelpen van de mens, door onze kennis te vergroten. Ja, het cliché 'ik heb geen dag gewerkt, alleen maar gehobbyd' is mogelijk van toepassing. Toch, de tijdsinvestering is ten koste gegaan van investeringen in vrienden, familie en andere interesses. Want, op papier heb ik wellicht 4 jaar echt fulltime aan het project gewerkt, maar mijn eerste entry in een labjournaal was eind 2007. Als men de kleur van de roos wegdenkt uit de berekening zou men dus ook kunnen stellen dat het project 2019-2007= 12 kalenderjaren heeft geduurd, afgerond naar boven voor extra drama ;-). Tegenwoordig moeten promotietrajecten in 3-4 jaar behaald worden, waarbij er wellicht een bepaald regime opgelegd kan worden binnen een reeds lopend onderzoekstraject, waarin de promovendus slechts een afgebakend stukje doet en daardoor weinig in de pap te brokkelen heeft inzake de invulling en ontwerp van zijn/haar 'eigen' thesis.

Daarom, op de eerste plaats van dank, mijn copromotor dr. Leonie Los. Ik ben je dankbaar omdat je me vrij liet in het project, dat ik zo mijn eigen gang heb mogen gaan, mits dat goed onderbouwd kon worden. Het zou veel efficiënter zijn geweest als je, net als de huidige standaard, je eigen ideeën, ontwerpen en inrichting daarvan had willen vasthouden. Het is volkomen waarschijnlijk dat je als onderzoeksgroep veel méér kunt publiceren (lees produceren) als je elke promovendus een forse overlap geeft met je eigen onderzoekstraject en dat van andere promovendi, zodat zij technieken kunnen uitwisselen, meer zinvol overleg kunnen hebben, als tweede auteur op papers kunnen komen, en efficiënter gebruik kunnen maken van het ingehuurd personeel. Het siert je als leidinggevende dat je dit zo hebt kunnen invullen, ondanks ongetwijfeld de toenemende publicatiedruk die onderzoekers tegenwoordig kennen. Dit project wat we samen hebben voltooid is een losstaande satelliet tussen de hemellichamen van dermatologie, celbiologie, oogheelkunde, pathologie en biomedical engineering. De congressen die we over collagene bezochten gingen vooral over orthopedie, de oogheelkundige congressen gingen over de kliniek, de biologische en biomedical engineering congressen gingen over bacteriën en cellen. De type VII collageenonderzoeken gaan vrijwel uitsluitend over dermato(patho)logie. Her en der konden we, samen met Corien van der Worp-Flobbe, gelukkig wel ideeën opdoen. Leonie, je deur stond altijd open, er was altijd ruimte voor debat, je was vliegensvlug met corrigeren van teksten, waarin eindeloze 'd's en 't's aangepast moesten worden indien in Nederlands geschreven, en alle keren dat je gedacht moet hebben 'wat is dit nu weer voor een raar idee', je mijn idee vrijwel altijd een kans gunde.

Corien van der Worp-Flobbe, wat hebben we intens samengewerkt! Toen ik de eerste stapjes in het lab zette hield jij, als analiste, mijn hand vast. Vrijwel alle technieken die beschreven zijn in dit boek (met daarnaast een nog groter deel dat niet in dit boekje terecht zijn gekomen) heb ik van jou geleerd. De dynamiek die we hadden was echt leuk, omdat we in aanpak en ideeën nogal eens wisselden en fantastisch koppig konden zijn. Als ik in de stress zat met een experiment kon ik je altijd bellen voor advies, als ik een ingrediënt niet kon vinden wist jij raad. We hebben ook lief en leed gedeeld, zelfs betreft privé situaties. Dank je wel voor je gigantische inzet.

Dr. Hendri Pas, met regelmaat kwam ik bij je binnen gelopen om adviezen te vragen over experimentele opzetten of de interpretatie van Western blots. We hadden vrij diepe gedachtewisselingen over allerlei zaken aangaande Col VII. Ondanks dat je bureau vol lag met stapels werk, wilde je toch gelegenheid voor dergelijke overlegjes maken.

Samen met dr. Roel Kuijer en dr. Theo van Kooten hebben we vele overlegmomenten gehad. Zij deelden hun werkkamer, met eveneens een deur die ver open stond. Toen Roel stopte met zijn werk als onderzoeker en begeleider in het project, nam Theo dat stuk over. De invulling van experimenten, de uitvoering daarvan en het corrigeren van mijn teksten kwamen voor een belangrijk deel door jullie bijdrage.

Dank voor je begeleiding, prof. dr. Anneke Hooymans. Bij de voortgang van dit project heb je belangrijk bijgedragen aan het uiteindelijke afronden van het project. Je hebt op prettige wijze de Duimschroeven des Tijds wat aangedraaid, wat wel echt nodig was om de laatste fase tot spoedige afronding te laten komen.

Dear dr. Shaochong Bu, my type VI collagen specialist friend, what wonderful time we had when feeling sorry for ourselves when another experiment had failed. I admire the way in which you were able to complete your thesis, given your circumstances of that time.

Medewerkers van de Biomedical Engineering BME, voor tips, trucs, gebruik van materialen en gezelligheid van alledag.

Dank voor de praktische bijdragen en datacollectie: Liesbeth van Schie (paranimf), Martin Schol, en Mohammad Timraz.

Zonder onderzoeksmaterialen zou dit boekje überhaupt niet tot stand zijn gekomen, dus dank aan de medewerkers van de Euro Tissue Bank Beverwijk voor het jarenlang suppleren van donorogen. Helaas kwam er aan deze toestroom in 2013 een einde, wegens een nieuwe interpretatie van de Wet op Orgaandonatie.

Dank ook aan de wetenschappelijke bijdragen van: dr. Alexander Nyström voor het suppleren van antilichamen, maar ook gedachtewisselingen over de biochemische eigenschappen van Col VII; dr. Peter van den Akker, dr. Marjon Pasmooij, dr. Marieke Bolling, MANP Josée Duipmans, medewerkers lab dermatologie en prof. dr. Marcel Jonkman (†14-01-2019) voor jullie dermatologische en genetische inbreng; dr. Wilfred den Dunnen, dr. Gilles Diercks en dr. Rob Verdijk voor jullie 'pathologische' inbreng; prof. dr. Ruud Bank en dr. Willy Halfter voor moleculaire en collageneuze inbreng; het UMCG Microscopy and Imaging Center, en Marjolein Blaauboer, Cor Semeins en Behrouz Zandieh Doulabi van het Academisch Centrum Tandheelkunde Amsterdam (ACTA 11^e verdieping) voor het gebruik maken van jullie instrumenten; (oud)medewerkers van de Medische Biologie (2007-2010) voor jullie begeleiding in de beginfase.

Alle AIOS, afdelingshoofd en waarnemend opleider prof. dr. Nomdo Jansonius, opleider dr. Jan Willem Pott, en stafleden der afdeling Oogheelkunde UMCG: dank voor jullie support, maar ook geduld, met name gedurende het laatste jaar onderzoek wat samenviel met het eerste jaar van mijn opleiding. Het combineren van twee opleidingen was niet eenvoudig, zeker niet na 6 jaar uit de kliniek te zijn geweest , met daarnaast een roerige periode. Medeonderzoekers van het Laboratorium Experimentele Onderzoeken LEO, dank voor jullie gezelligheid en kameraadschap, maar ook voor de rust indien dat nodig was ;-) In het bijzonder dr. Ronald Bierings, dr. Lianne Nibroug-Vinke en dr. Wietse Wieringa voor jullie wijsheden, persoonlijke bijdragen aan de ontwikkeling van een promovendus en jullie humor. Fenna, dank voor het leveren van doorgaans onvindbare artikelen en de laatste nieuwtjes.

Elies, dank aan jou en je familie dat jullie er voor me waren in een moeilijke tijd, waarin de begrafenis van mijn vader, mijn broer Freek, het verloren gaan van mijn ouderlijke huis, en mijn auto-ongeluk elkaar in kort tempo opvolgden. Ik ben blij dat je de gelegenheid die je kreeg om in Amsterdam te werken en te promoveren maximaal hebt weten te benutten, ondanks de omstandigheden van toen.

Dank aan mijn Redders en de medewerkers van het BWC Beverwijk, voor het redden van mijn leven en daarom weliswaar niet-wetenschappelijke, maar kritieke bijdrage dit project af te ronden. Daarnaast: alle medewerkers die bijdroegen aan mijn revalidatie.

Aan mijn vrienden uit Zutphen en Groningen (Stylloos, JC Sjeik en studie), dit boek is de reden waarom jullie mij de afgelopen jaren veel minder vaak, minder lang, en mogelijk minder beschonken hebben gezien hebben dan wenselijk was. Probeer het boek desalniettemin niet als onderzetter te gebruiken, tafelpootverhoger of erger. Gelukkig heb ik de belangrijkste gebeurtenissen in jullie leven wel actief meegemaakt, en andersom ook. Nu het boek af is, hoop ik dat we weer meer gelegenheid krijgen elkaar vaker en langer te zien.

Lieve pap, en broer Freek junior, ik had dit moment graag met jullie willen delen. Op deze manier, en middels een stelling, delen we toch nog een beetje. Lieve zussen en hun gezinnen, ik hoop jullie na vandaag ook vaker te kunnen zien!

Lieve mams en Aart, Jochem en Media, dank voor jullie steun in het tot stand komen van dit boekje. Afspraken die verzet of niet gemaakt konden worden omdat ik moest werken, mijn celkweken eten moest geven, of het typewerk wat af moest... jullie accepteerden deze sprongen die horen bij mijn matig ontwikkeld plannend vermogen

wat gecombineerd werd met de onvoorspelbare grillen van fundamenteel onderzoek, teneinde mij de ruimte te geven die ik op dat moment nodig had. Mams, dank voor je onvoorwaardelijke steun en zuurkoolschotels die me op de been hielden ;-)

Mijn allerliefste Suus, wat een geluk heb ik met jou. En wat waardeer ik je geduld in de laatste weken van de afronding van dit project, waarbij zelfs flink geknaagd werd aan onze weekenden samen. Je steunt me al ruim 2 jaar met heel je hebben en houden (zuurkoolschotel-donaties inclusief) en dat voelt geweldig. Naast ons privéleven kan ik zelfs klinische ervaringen met je uitwisselen en blokken we samen voor de toetsen. We beleefden daarnaast fijne momenten van rust met je fantastische familie. Binnenkort kunnen wij samen eindelijk vaker op vakantie, daar kijk ik naar uit. Maar eerst mag ik je nog mijn paranimf noemen!

CURRICULUM VITAE

Bart Wullink was born on 2nd October 1980 in Ermelo. He lived his childhood in a residential 'farmhouse' in the green outskirts of Voorst, Gelderland. His secondary school education was at the Baudartius College in Zutphen, after which he moved to Groningen. In 2001, he enrolled in the University of Groningen, firstly for Business administration, but in 2004 for Medicine. In the third year of Medicine, he was contacted by dr. Dirk Ponsioen, after which he joined the ophthalmology research group of dr. Leonie Los, at the University Medical Center Groningen (head prof. dr. JMM Hooymans). At first, he followed the current collagen research line of that time, but was allowed to pursue his interests: the characteristics of Type VII collagen. His internships were followed in the University Medical Center Groningen, the Nij Smellinghe hospital of Drachten, and the Martini hospital of Groningen. During these internships, he managed to conduct some of the research of this thesis. His master's degree was obtained in 2012, after which he was able to pursue the investigation of Type VII collagen fully. In 2013 however, the investigations were interrupted, but could be resumed nearly two years later. On the 1st of April 2018, his training for ophthalmologist started (head prof. dr. NM Jansonius, supervisor dr. JWR Pott), during which he finished the work on this thesis.



